UNIVERSITY OF CALIFORNIA SAN DIEGO

Oxygen dependence of visual physiology and behavior in marine invertebrate larvae and its ecological implications

A dissertation submitted in partial satisfaction of the requirements for the degree Doctor of Philosophy

in

Oceanography

by

Lillian R. McCormick

Committee in charge:

Professor Lisa A. Levin, Chair
Professor Dimitri Deheyn
Professor Todd Martz
Professor Nicholas Oesch
Professor Frank Powell
Professor Martin Tresguerres

2019

The Dissertation of Lillian R. McCormick is approved, and it is acceptable in quality and in form for publication on microfilm and electronically:

_____

_____

_____

_____

_____

_____
Chair

University of California San Diego

2019

DEDICATION

To C.W. Moran, for your endless love, support, and patience. I can't wait for our next chapter.

To my family, thank you for bringing me up around the natural world and supporting me every step of the way.

EPIGRAPH

“The cure for everything is salt water: sweat, tears, and the sea."

- Isak Dinesen

TABLE OF CONTENTS

LIST OF TABLES

Chapter 2

Chapter 5

Chapter 6

LIST OF FIGURES

Chapter 1

Chapter 2

Chapter 3

Chapter 4

Chapter 6

Chapter 7

ACKNOWLEDGMENTS

This dissertation would not have been possible without the support of many people. First and foremost, I would like to express extreme gratitude to my adviser and committee chair, Dr. Lisa Levin. From the first day I met Lisa, she has been nothing but enthusiastic about my project, despite it being on the outskirts of her normal range of science. She has been incredibly willing to let me stubbornly pursue my interests, and has been very supportive, responsive, and patient through the entirety of my dissertation. Her kindness is unparalleled, and she has always pushed me to be the best scientist I can be. Lisa took a chance on me, and for that I am very grateful.

I would like to thank my committee for their thoughtful discussion and advice on my dissertation. Dimitri Deheyn has always welcomed me into his lab, encouraged me to pursue side projects tangential to my dissertation, and always asks thought-provoking questions that improve my research. Todd Martz has provided so much expertise on integrating marine sensors into my research, and his sensor technology course was where I first developed the first model of the SeapHOx deLUX. Nick Oesch was extremely receptive to me conducting electrophysiology on marine invertebrates in his traditionally mammalian lab, and has been such an incredibly valuable resource for all aspects of my dissertation. Frank Powell has been an excellent source of knowledge on oxygen science and physiology, and always asks extremely productive questions. Martin Tresguerres has read sections of my research since taking Marine Physiology in my first quarter of graduate school and always encourages me to make the most realistic and insightful interpretations. I was very lucky to have a very diverse range of expertise on my committee, and it definitely made this dissertation stronger.

I was very privileged to have people encouraging me to conduct research in my undergraduate degree, and Joel Thompson, David Hastings, and Jonathan Cohen helped me take me first steps into the research world. Jonathan Cohen has provided mentorship since 2008, gave me my first research technician position, and was always open to giving me advice on vision science during my graduate career; I am very grateful.

One of my favorite parts about the Scripps community has been being involved with the scientific diving and boating program. A very large thank you to Christian McDonald, Brett Pickering, Ashleigh Palinkas, Rich Walsh, and Phil Zerfoski. Rich Walsh has been such a fabulous source of knowledge and creative solutions, and has become a very good friend. He has helped an incredible amount with designing the SeapHOx setup, deployment, and diving maintenance, in addition to always helping me be a better and safer diver. Phil Zerofski has been such an incredible resource and has supported my research in more ways than I can describe. From his tireless zooplankton collections to our impromptu conversations about the marine environment and its animals, my dives and interactions with Phil will be some of my favorite memories. My time at Scripps would have been very different without all of you.

I have been lucky to find a dive buddy that sticks with me even through bad weather and cold water. Isa Arzeno has been so instrumental to the maintenance and field work of the SeapHOx deLUX, completing almost every single SeapHOx dive with me over the past 4 years, and has become a very supportive friend in the process. I was lucky enough to be invited to help her with her dissertation research in the Seychelles in 2016, and that is the trip that solidified our friendship. I want to acknowledge all of my other dive buddies over the years, including Matthew Costa, Mohammad Sedarat, Beverley French, Abby Cannon, Maddie Harvey, in addition to Rich Walsh and Phil Zerfoski.

I do not have much expertise with marine sensors, and the Martz Lab has been instrumental in the development and maintenance of the SeapHOx. Ellen Briggs re-wrote the code to accommodate the PAR sensor, and Taylor Wirth has been so much help over the last four years in trouble-shooting issues, taking care of the instrument, and educating me on all things SeapHOx. I want to acknowledge Melissa Carter for providing the sea spider the SeapHOx has been mounted on. Additionally, a big thank you to Emily Bockmon, who spent time out of her post-doc to help me modify and recreate the MSEAS for use in my experiments.

Additionally, I want to thank William Gilly and Perrin Teal at Hopkins Marine Lab and Stanford for sending me *D. opalescens* egg capsules from Monterey. Pichaya Lertvilai also collected some *O. bimaculatus* eggs that were used for this research.

I am very grateful for all of the support from the graduate and financial offices at Scripps; they work tirelessly behind the scenes to enable students to concentrate on research. Thank you so much to Gilbert Bretado, Shelley Weisel, Maureen McGreevy, Maureen McCormick, Hanna Choe, Adrielle Wei, and Minerva Nelson for helping me navigate the complex world of university and grant funding, budgeting, and a lot of reimbursements.

My dissertation work would not have been possible without the financial support from many organizations. These include a National Science Foundation Graduate Research Fellowship Program award (DGE-1144086) that funded my first three years as a graduate student, a Mia J. Tegner grant from Scripps, a Frontiers of Innovation Scholars Program award, two Charles H. Stout Foundation grants, a National Science Foundation Bio-Oce grant (OCE-1829623), a P.E.O. Scholar Award, and to the Scripps Institution of Oceanography education office.

I would also like to thank the current and past members of the Levin lab including my amazing office mate and friend, Jen Le, Olívia Periera, Oliver Ashford, Andrew Mehring, Erik Sperling, Natalya Gallo, Kirk Sato, Mike Navarro, Christina Frieder, Carlos Niera, Guillermo Mendoza, and of course, Jennifer Gonzalez. Jen G. has provided so much support and advice on all of the small things that are so essential to making science work as smoothly as possible.

My time at Scripps would not have been the same without my wonderful Biological Oceanography cohort: Matthew Costa, Jessica C. Garwood, Ben Whitmore, Regina Guazzo, Bellineth Valencia, AJ Schlenger, and Josh Jones; we all struggled together and supported each other through the process. I want to thank the people who have supported me in the process of my graduate career; the UCSD Triathlon, UCSD Cycling team, and SDBC cycling communities provided a welcome physical distraction from the stress of graduate school, and I made some wonderful friends in the process. I have always looked up to the amazing powerhouse women I am friends with, and Molly Shuman-Goodier, Rachel Rubin, Bailey Kennett, Jen Galvin, Katie Denman, Esther Walker, Kat Ellis, and Katherine Nadler have provided so much encouragement and support throughout the years.

I was taught to respect and love the environment from a young age, and I want to thank my amazing parents for creating an environment that let me be me, encouraged me to follow my interests, and have supported me in every way possible. My pup Seamus is always happy and never fails to make me smile and feel loved. Last, and most definitely not least, I want to express my extreme gratitude towards my partner, C.W. Moran. He has supported me from the minute I told him I was accepted at Scripps until the final days of my dissertation, and has always found the right thing to say. My dissertation has not been without its ups and

downs, and he has helped me navigate this with more patience and encouragement than I can put into words. Thank you.

Chapter 2, in full, is a reprint of the material as it appears in **McCormick, L. R.** and L. A. Levin. 2017. Physiological and ecological implications of ocean deoxygenation for vision in marine organisms. Philosophical Transactions of the Royal Society A 375: 20160322. http://dx.doi.org/10.1098/rsta.2016.0322. The dissertation author was the primary investigator and author of this material.

Chapter 3, in full, is a reprint of the material as it appears in **McCormick, L.R.,** Levin, L. A. and N.W. Oesch. 2019. Vision is highly sensitive to oxygen availability in marine invertebrate larvae. Journal of Experimental Biology 222:10. DOI: 10.1242/jeb.200899. The dissertation author was the primary investigator and author of this material.

Chapter 4, in part, is in preparation for submission for publication. The dissertation author was the primary investigator and author of this material. **McCormick, L. R.**, Levin, L. A., and N. C. Wegner. Comparing critical oxygen limits for metabolism and vision in cephalopod paralarvae.

Chapter 5, in part, is in preparation for submission for publication. The dissertation author was the primary investigator and author of this material. **McCormick, L. R.**, Levin, L. A., and N. W. Oesch. Oxygen sensitivity of phototaxis behavior in highly visual cephalopod paralarvae.

Chapter 6, in part, is in preparation for submission for publication. The dissertation author was the primary investigator and author of this material. **McCormick, L. R.**, Gangrade, S., Garwood, J. C., Wirth, T., Martz, T. R. and L. A. Levin. Defining a suitable

"luminoxyscape" to evaluate changing light requirements under oxygen-limitation in visual marine organisms.

VITA

2011 Bachelor of Science, Marine Science, Eckerd College

2015 Master of Science, Marine Biology, Scripps Institution of Oceanography, University of California San Diego

2019 Doctor of Philosophy, Oceanography, Scripps Institution of Oceanography, University of California San Diego

PUBLICATIONS

McCormick, L. R., Levin, L. A., and N. W. Oesch. 2019. Vision is highly sensitive to oxygen availability in marine invertebrate larvae. Journal of Experimental Biology 222:10. DOI: 10.1242/jeb.200899

McCormick, L. R. and L. A. Levin. 2017. Physiological and ecological implications of ocean deoxygenation for vision in marine organisms. Philosophical Transactions of the Royal Society A 375:20160322. http://dx.doi.org/10.1098/rsta.2016.0322

Cohen, J. H., **McCormick, L. R.** and S. M. Burkhardt. 2014. Effects of dispersant and oil on Survival and Swimming Activity in a Marine Copepod. Bulletin of Environmental Contamination and Toxicology 92(4):381-7 DOI 10.1007/s00128-013-1191-4

McCormick, L. R. and J. H. Cohen. 2012. The pupil light reflex of the Atlantic brief squid, *Lolliguncula brevis*. Journal of Experimental Biology 215:2677-2683. DOI 10.1242/jeb.068510

ABSTRACT OF THE DISSERTATION

Oxygen dependence of visual physiology and behavior in marine invertebrate larvae and its ecological implications

by

Lillian R. McCormick

Doctor of Philosophy in Oceanography

University of California San Diego, 2019

Professor Lisa A. Levin, Chair

Many invertebrates undergo a planktonic larval stage, during which they have a deeper distribution during the day (to 80 m), and then ascend to the surface at night. Those migrating in regions with eastern boundary currents, such as the Southern California Bight, are exposed to large gradients of both oxygen and irradiance with depth in the ocean, in addition to seasonal variability. Marine larvae of visual species rely on sophisticated eyes for prey capture, predator avoidance, and vertical migration; this vision is very oxygen demanding. The critical early life stages of marine invertebrates can be vulnerable to changes in ocean conditions, and stress from oxygen loss could compromise optimal visual function, fitness,

and survival. This research evaluated the effects of reduced oxygen partial pressure (pO_2) on visual physiology, metabolism, and visual behavior in larvae of animals with "fast" vision, including cephalopods and arthropods, and the potential consequences for their distributions in the ocean. A decrease in pO_2 from 21 kPa (surface ocean pO_2) to ~ 3 kPa caused retinal function to decline by 60-100% in larvae of the market squid *Doryteuthis opalescens*, the two-spot octopus *Octopus bimaculatus*, the graceful rock crab *Metacarcinus gracilis*, and the tuna crab *Pleuroncodes planipes*. Temporal resolution was impaired at 3.8 kPa in *D. opalescens* but not in *P. planipes.* Oxygen effects on retinal function occurred at higher pO_2 (22, 11.5 kPa) than the critical oxygen limit for metabolism (P_{crit}) (2.47, 0.48 kPa) for *D. opalescens* and *O. bimaculatus*, respectively, indicating visual effects are dissociated from general metabolic decline. Phototaxis behavior decreased with exposure to pO_2 that would cause 50% retinal function in the cephalopod larvae. To define available visual habitat for these larvae (the critical luminoxyscape), oxygen and light conditions were measured over various temporal and spatial scales using a custom-built sensor package deployed at 30 m depth in 2015-2017, and from hydrographic profiles taken between 1999 and 2017 in the Southern California Bight (CalCOFI). Oxygen and light during the seasonal upwelling periods and in the nearshore environment reached levels that alter visual function of these species. Future effects of ocean deoxygenation may manifest as impaired larval vision.

CHAPTER 1

Introduction

Lillian R. McCormick

Chapter 1. Introduction

The early life stage of marine invertebrates is a crucial bottleneck for survival and recruitment to the adult population. In many marine species, larvae (the early life stage in cephalopods and crabs) undergo a planktonic phase prior to settling on the seafloor (for benthic species) or changing morphologically and increasing their depth range (for pelagic species). Planktonic larvae are considered zooplankton, and generally feed on smaller zooplankton (such as copepods) or phytoplankton. Large zooplankton, including the larvae of cephalopods and crabs, vertically migrate over small spatial scales (usually within the upper 100 m of the ocean) to avoid visual predation by having a deeper daytime distribution and shallow night time distribution (Forward 1988, Cohen and Forward 2009), however true vertical and horizontal distributions of early life stages are not well known. As with fish larvae, the "first feeding" for marine invertebrate larvae is often crucial to determining their survival, and must occur within the first 24-48 hours of hatching in most species (Hunter 1981, Robin et al. 2014). Larvae of highly visual marine species (cephalopods, arthropods, and fish; McCormick and Levin 2017) rely on vision for diel vertical migration (Forward 1988), larval settlement (Crisp and Ritz 1973), prey capture (Chen et al. 1996, Robin et al. 2014), and/or predator avoidance (Charpentier and Cohen 2015), and are subject to the same environmental requirements for vision as adult organisms. In some cases, the tolerance limits for stressors (e.g., oxygen, temperature, pH, light, salinity) may be higher for early life stages than adults, increasing their vulnerabilities to changing ocean conditions (Przeslawski et al. 2015).

Oxygen and Light Requirements for Vision

Sensory reception, particularly vision, is an essential and metabolically demanding process for both vertebrates and invertebrates (Niven and Laughlin 2008). Oxygen is necessary for photoreceptors (the light-sensitive cells in the eye) to function. The retina, containing the photoreceptor cells, is the tissue with one of the highest metabolic demands in the vertebrate body (Anderson 1968, Waser and Heisler 2005, Wong-Riley 2010). In humans, exposure to 10% atmospheric oxygen decreases the sensitivity of the eye to light, and also changes color perception by affecting rods more than cones (Ernest and Krill 1971). Additionally, the ability of human eyes to respond to movement (temporal resolution) can be compromised during exposure to reduced oxygen (Fowler et al. 1993). In the marine environment, highly visual species have evolved sophisticated eyes with high light sensitivity and the spatial and temporal resolution to support their active, predatory life strategies; the tradeoff for these developed sensory systems are a much higher metabolic cost and increased oxygen requirements that can be challenging to maintain in an environment of highly variable oxygen and light conditions (Niven and Laughlin 2008, Warrant and Johnsen 2013). Oxygen thresholds in marine organisms are commonly represented as a metabolism-based metric, P_{crit}, which is the partial pressure of oxygen (pO_2) where the rate of oxygen consumption changes, usually indicating the onset of metabolic decline (Seibel 2011). Critical limits for oxygen should always be considered in context with the behavior and ecology of the organism (Seibel 2011), and thus visual effects of oxygen impairment can potentially occur at pO_2 above the P_{crit}.

Ocean Deoxygenation

Oxygen is introduced into the ocean as a product of photosynthesis and from mixing at

the surface, and removed from the water column by the respiration of plants, animals, and microbes (Baumann and Smith 2018). Climate-forced ocean warming creates stratification, which increases the outgassing of oxygen from the surface, decreases the mixing of oxygen from the surface to the ocean interior, and also decreases upwelling of nutrients, limiting photosynthesis and the production of oxygen (Keeling and Garcia 2002, Keeling et al. 2010). Increased stratification and reduced oxygen solubility in warmer waters are subsequently causing an expansion of oceanic oxygen minimum zones, mid-water features characterized by the lowest oxygen concentration (Stramma et al. 2008), and expanded oxygen loss over broad sections of the north and east Pacific, tropical, and subtropical oceans and the southern ocean (Stramma et al. 2010, 2012, Helm et al. 2011, Schmidtko et al. 2017, Levin 2018). Climate change is also exacerbating eutrophication and coastal hypoxia (Altieri and Gedan 2015). El Niño-Southern Oscillation (ENSO) events also can contribute to oxygen loss via effects on temperature and productivity (Turi et al. 2018). Globally, this has amounted to a 2% loss in oxygen content in the ocean (Schmidtko et al. 2017). However, upwelling areas, such as the Southern California Bight (SCB) are particularly concerning for oxygen loss (Nam et al. 2015), where intensified upwelling winds and strengthened undercurrents are exacerbating the problem, and significant oxygen declines (20-30% on the outer shelf) have already been recorded (Bograd et al. 2008, 2015, Sydeman et al. 2014).

The observed decline in oxygen concentration in the ocean has widespread effects on marine life (Breitburg et al. 2018), causing changes in physiology of marine organisms (Seibel 2011, Deutsch et al. 2015, Somero et al. 2015) and habitat compression (Gilly et al. 2013), which alter the distribution and ecological interactions of species (Ekau et al. 2010, Bertrand et al. 2011, Chu and Tunnicliffe 2015, Netburn and Koslow 2015). Mesopelagic

(midwater) species can experience compression of diurnal vertical migration depths corresponding to the distribution of hypoxic waters globally (Bianchi et al. 2013). Descriptions of habitat compression for billfish (Stramma et al. 2012), mesopelagic fish (Netburn and Koslow 2015), and krill (Seibel et al. 2016) have largely been premised on physiological constraints imposed by oxygen tolerances (such as critical oxygen limits for metabolism).

Spatial and temporal variability in oxygen and light conditions on upwelling margins

Both light and oxygen concentration exhibit strong gradients with depth in the ocean, particularly on highly productive margins with eastern boundary currents where the upwelling of low-oxygen water creates steep gradients at shallow depths (e.g. SCB). In the California margin, upwelling is caused by wind-driven surface currents and Ekman transport close to shore and wind-stress curl farther offshore, causing nutrient-rich, low oxygen, and low pH water at very shallow depths in the nearshore environment (Feely et al. 2008, Rykaczewski and Checkley 2008, Levin et al. 2015). The upwelling occurs seasonally in spring and summer when winds are directed towards the equator, but short-time scale (~1 week) variability is also present (Huyer 1983, Send and Nam 2012). Oxygen conditions also vary greatly on diel, event scale, and inter-annual time scales, such as with ENSO (Levin et al. 2015). For example, the daily range of oxygen at 7 m depth in nearshore La Jolla can be as large as 220 μmol kg^{-1} (Frieder et al. 2012).

Light (irradiance) can also vary on various temporal and spatial scales. Irradiance declines exponentially with depth, and wavelengths are selectively attenuated, which changes the spectral composition of the downwelling irradiance over vertical spatial scales (Jerlov

1951). The attenuation of irradiance in the water column can also depend on the amount of detritus and phytoplankton in the water and cloud cover, so variations can happen over time scales shorter than a diel cycle, in addition to seasonal changes (shorter lighted days during the winter in the Northern Hemisphere). There is also evidence that there was an increase in light attenuation (causing a shoaling in the depth of the euphotic zone) in the southern portion of the SCB between 1969 and 2007, primarily attributed to an increase in anthropogenic nutrient output and a longer residence time for phytoplankton (Aksnes and Ohman 2009).

Marine planktonic animals have been known to experience distribution constraints based on both oxygen (Bertrand et al. 2011, Bianchi et al. 2013, Netburn and Koslow 2015) and light (Røstad et al. 2016), but the interactions of these two stressors for visual organisms has not been described, and may be especially significant for the survival of highly visual marine larvae.

Larval development and distribution of the study species

Arthropods

The larvae of most arthropods undergo a planktonic stage, even if they become benthic as adults, and these possess a complex apposition compound eye used for phototaxis, the detection of prey, predator avoidance, and orientation (Cronin and Jinks 2001). Active arthropods (notably decapod crustaceans) rely on sensing light (in addition to salinity and temperature) for orientation in the water column, and are prone to horizontal transport by currents; some larvae must maintain specific depth distributions to enable current advection required for settlement (Shanks 1985, Epifanio and Cohen 2016).

The graceful rock crab, *Metacarcinus gracilis*, can be found from the intertidal zone to

depth of 175 m from Alaska to Baja California, Mexico. Females lay eggs during the late summer in the SCB, and after hatching development involves 5 zoeal stages and one megalopa stage (Ally 1975). Megalopae (Fig. 1A) are thought to have a daytime distribution of 30-60 m water depth and a nighttime distribution of 0-30 m depth (Wing et al. 1998).

The tuna crab/pelagic red crab, *Pleuroncodes planipes*, is a highly visual galatheid crab with both pelagic and benthic phases traditionally found along the shelf at water depths of 30-300 m from Baja California to Chile (Boyd 1960, Yannicelli et al. 2012). Both adult and larval *P. planipes* are very tolerant to low oxygen, and are commonly observed at pO_2 as low as 0.04 mL L^{-1} (~0.13 kPa at 11.1 °C and 34.8 salinity) (Yannicelli et al. 2013, Pineda et al. 2016, Seibel et al. 2018). Populations increase during El Niño years in the SCB (Boyd 1960, Longhurst 1968, Gomez-Gutierrez and Sanchez-Ortiz 1997) and this species has shown a recent increase in abundance in its northern range (i.e. SCB; McClatchie et al. 2016). The greatest abundance of early larval stages (Fig. 1B) are in January and February (Boyd 1960, 1967, McClatchie et al. 2016). All five larval stages vertically migrate (Boyd 1960).

Cephalopods

Embryonic visual development is vital to survival in the early life stages of cephalopods; the eyes are considered fully developed at the time of hatching in the larvae (which are often called “paralarvae” during their planktonic larval stage; Robin et al. 2014). Feeding must begin immediately because hatching embryos retain only a small volume of yolk reserve sufficient to get them to the first feeding time (Vidal et al. 2002). Hatching of cephalopod paralarvae primarily occurs at night, and positive phototactic behavior enables them to swim up to the food-rich surface waters before there is enough light for predators to

see them at the spawning grounds (Fields 1965).

The California market squid, *D. opalescens,* is distributed in the eastern Pacific Ocean from Baja, Mexico to British Colombia. Adults occur at depths of 15-200 m, but can be found as deep as 500 m (Fields 1965). The squid return to the continental shelf (nearshore) to spawn where they deposit benthic egg capsules. The benthic encapsulated embryos and hatched paralarvae experience highly variable oxygenation (Navarro et al. 2018). Adults are heavily fished, and this species has been one of the most profitable fisheries in southern CA (Sweetnam 2010). After hatching, paralarvae (Fig. 1C) vertically migrate daily through the upper water column (0-80m depth) and feed on zooplankton; larval abundances are greatest January-March (Fields 1965, Zeidberg and Hamner 2002, Van Noord and Dorval 2017).

The two-spot octopus, *O. bimaculatus* is a nearshore, coastal species found primarily in rocky reef habitats from northern California to Baja California, Mexico to a depth of 30 m. Females lay strands of small eggs on rocky substrate, with up to 20,000 total eggs in all strands (Ambrose 1981). After ~30 days, paralarvae hatch and show positive phototaxis, and are thought to vertically migrate over the same depth range as *D. opalescens* (Ambrose 1981). Paralarvae (Fig. 1D) are most abundant in the late summer and early fall (Ambrose 1988).

The Thesis: Introductory remarks

When I began work on this dissertation in 2013, I already had formulated the questions that would comprise the core structure of my thesis. My undergraduate research was examining the pupil light reflex and spectral responsivity in a nearshore coastal squid (McCormick and Cohen 2012), and after graduation, I worked as a research technician in a lab studying sensory ecology and behavior in zooplankton in response to toxic stressors

(Cohen et al. 2014). I also began working part time for a research group examining the effects of diel-cycling hypoxia on growth and development in several coastal fish species. Always seeing things as a visual ecologist, I began researching the effects of hypoxia on visual systems in cephalopods. Despite the large gradients in oxygen over time and with depth, I found relatively little information on the effects in marine organisms, but found that hypoxia and vision was very well studied in terrestrial organisms. As such, the overarching question of this thesis became, "Does low oxygen affect vision in marine organisms?" The objective of this thesis was to answer this question using a tiered approach, examining the manifestation of oxygen-impairment in visual physiology, behavior, and ecology.

Since there was relatively little information on the topic, I first examined what was known about oxygen effects on vision in marine organisms, and supplemented with information from the terrestrial environment. Chapter 2 is a review detailing the potential implications for reduced oxygen on vision in marine organisms. Chapter 2 is published in full as McCormick and Levin (2017).

Oxygen effects on vision would naturally first be expressed in a change in physiology in the animal. One experimental technique to measure visual responses is electrophysiology, where the electrical responses of visual cells to a light stimulus are recorded (Brown 1968). Chapter 3 measures the retinal responses to light and temporal resolution in larvae of the market squid, *D. opalescens*, the two spot octopus, *O. bimaculatus*, the slender crab, *M. gracilis*, and the tuna crab, *P. planipes* during exposure to reduced pO_2. Chapter 3 is published in full as McCormick et al. (2019).

Results of Chapter 3 raise the question of whether the thresholds for retinal function are simply a reading of general metabolic decline through the eyes, or whether the visual

effects of reduced pO_2 are mediated differently than declines in metabolism. To address this, Chapter 4 determines the critical oxygen limit for metabolism (P_{crit}) and metabolic rates for *D. opalescens* and *O. bimaculatus* paralarvae.

Animals have the capacity to experience stress or impairment without altering behavior, and it was important to determine whether impaired retinal function would alter visual behavior, and at what pO_2 conditions. One visual behavior important to marine organisms is phototaxis, defined as directed movement towards or away from light. Chapter 5 describes the effects of reduced pO_2 on the light requirements for phototaxis in *D. opalescens* and *O. bimaculatus* paralarvae and identifies critical thresholds for function.

After identifying oxygen and irradiance thresholds for retinal function, phototaxis behavior, and metabolism, it was important to determine whether the larvae may actually experience conditions that cause visual impairment within their habitat in the Southern California Bight. In Chapter 6, I propose the concept of a 'luminoxyscape' to describe the combinations of irradiance and oxygen that larvae would be exposed to, and determine to what extent the vision of larvae could potentially be constrained based on the oxygen and light thresholds determined in previous chapters.

The final chapter, Chapter 7, summarizes the results of oxygen effects on vision in marine invertebrate larvae, and predicts the implications for larval survival in light of ongoing ocean oxygen loss.

Literature Cited

Aksnes, D. L., and M. D. Ohman. 2009. Multi-decadal shoaling of the euphotic zone in the southern sector of the California Current System. Limnology and Oceanography 54:1272–1281.

Ally, J. R. R. 1975. A description of the laboratory-reared larvae of *Cancer gracilis* Dana, 1852 (Decapoda, Brachyura). Crustaceana 28:231–246.

Altieri, A. H., and K. B. Gedan. 2015. Climate change and dead zones. Global Change Biology 21:1395–1406.

Ambrose, R. F. 1981. Observations on the embryonic development and early post-embryonic behavior of *Octopus bimaculatus* (Mollusca: Cephalopoda). The Veliger 24:139–146.

Ambrose, R. F. 1988. Population dynamics of *Octopus bimaculatus*: influence of life history patterns, synchroneous reproduction and recruitment. Malacologia 29:23–39.

Anderson, B. 1968. Ocular effects of changes in oxygen and carbon dioxide tension. Transactions of the American Ophthalmological Society 66:423–74.

Baumann, H., and E. M. Smith. 2018. Quantifying metabolically driven pH and oxygen fluctuations in US nearshore habitats at diel to interannual time scales. Estuaries and Coasts 41:1102–1117.

Bertrand, A., A. Chaigneau, S. Peraltilla, J. Ledesma, M. Graco, F. Monetti, and F. P. Chavez. 2011. Oxygen: A fundamental property regulating pelagic ecosystem structure in the coastal southeastern tropical pacific. PLoS ONE 6:2–9.

Bianchi, D., E. D. Galbraith, D. A. Carozza, K. A. S. Mislan, and C. A. Stock. 2013. Intensification of open-ocean oxygen depletion by vertically migrating animals. Nature Geoscience 6:545–548.

Bograd, S. J., M. P. Buil, E. Di Lorenzo, C. G. Castro, I. D. Schroeder, R. Goericke, C. R. Anderson, C. Benitez-Nelson, and F. A. Whitney. 2015. Changes in source waters to the Southern California Bight. Deep Sea Research Part II: Topical Studies in Oceanography 112:42–52.

Bograd, S. J., C. G. Castro, E. Di Lorenzo, D. M. Palacios, H. Bailey, W. Gilly, and F. P. Chavez. 2008. Oxygen declines and the shoaling of the hypoxic boundary in the California Current. Geophysical Research Letters 35:L12607.

Boyd, C. M. 1960. The larval stages of *Pleuroncodes planipes* Stimson (Crustacea, Decapoda, Galatheidae). Biological Bulletin 118:17–30.

Boyd, C. M. 1967. The benthic and pelagic habitats of the red crab, *Pleuroncodes planipes*. Pacific Science 21:394–403.

Breitburg, D., L. A. Levin, A. Oschlies, M. Grégoire, F. P. Chavez, D. J. Conley, V. Garçon, D. Gilbert, D. Gutiérrez, K. Isensee, G. S. Jacinto, K. E. Limburg, I. Montes, S. W. A. Naqvi, G. C. Pitcher, N. N. Rabalais, M. R. Roman, K. A. Rose, B. A. Seibel, M. Telszewski, M. Yasuhara, and J. Zhang. 2018. Declining oxygen in the global ocean and coastal waters. Science 7240.

Brown, K. T. 1968. The electroretinogram: Its components and their origins. Vision Research 8:633-IN6.

Charpentier, C. L., and J. H. Cohen. 2015. Chemical cues from fish heighten visual sensitivity in larval crabs through changes in photoreceptor structure and function. The Journal of Experimental Biology 218:3381–3390.

Chen, D. S., G. Van Dykhuizen, J. Hodge, and W. F. Gilly. 1996. Ontogeny of copepod predation in juvenile squid (*Loligo opalescens*). Biological Bulletin 190:69–81.

Chu, J. W. F., and V. Tunnicliffe. 2015. Oxygen limitations on marine animal distributions and the collapse of epibenthic community structure during shoaling hypoxia. Global Change Biology 21:2989–3004.

Cohen, J. H., and R. B. J. Forward. 2009. Zooplankton diel vertical migration — A review of proximate control. Oceanography and Marine Biology: an Annual Review 47:77–110.

Cohen, J. H., L. R. McCormick, and S. M. Burkhardt. 2014. Effects of dispersant and oil on survival and swimming activity in a marine copepod. Bulletin of Environmental Contamination and Toxicology 92:381–387.

Crisp, D. J., and D. A. Ritz. 1973. Responses of cirripede larvae to light. I. Experiments with white light. Marine Biology 23:327–335.

Cronin, T. W., and R. N. Jinks. 2001. Ontogeny of vision in marine crustaceans. American Zoology 41:1098–1107.

Deutsch, C., A. Ferrel, B. Seibel, H.-O. Pörtner, and R. B. Huey. 2015. Climate change tightens a metabolic constraint on marine habitats. Science 348:1132–1136.

Ekau, W., H. Auel, H. O. Pörtner, and D. Gilbert. 2010. Impacts of hypoxia on the structure and processes in pelagic communities (zooplankton, macro-invertebrates and fish). Biogeosciences 7:1669–1699.

Epifanio, C. E., and J. H. Cohen. 2016. Behavioral adaptations in larvae of brachyuran crabs: A review. Journal of Experimental Marine Biology and Ecology 482:85–105.

Ernest, J. T., and A. E. Krill. 1971. The effect of hypoxia on visual function: psychophysical studies. Investigative Ophthalmology and Visual Science 10:323–328.

Feely, R. A., C. L. Sabine, J. M. Hernandez-ayon, D. Ianson, and B. Hales. 2008. Evidence for upwelling of corrosive continental "acidified" water onto the continental shelf. Science 1490:1–4.

Fields, W. G. 1965. The structure, development, food relations, reproduction, and life history of the squid *Loligo opalescens* Berry. State of California, Department of Fish and Game Fish Bulletin 131.

Forward, R. B. 1988. Diel vertical migration- Zooplankton photobiology and behavior. Oceanography and Marine Biology 26:361–393.

Fowler, B., J. Banner, and J. Pogue. 1993. The slowing of visual processing by hypoxia. Ergonomics 36:727–735.

Frieder, C. A., S. Nam, T. R. Martz, and L. A. Levin. 2012. High temporal and spatial variability of dissolved oxygen and pH in a nearshore California kelp forest. Biogeosciences 9:1–14.

Gilly, W. F., J. M. Beman, S. Y. Litvin, and B. H. Robison. 2013. Oceanographic and biological effects of shoaling of the oxygen minimum zone. Annual Review of Marine Science 5:393–420.

Gomez-Gutierrez, J., and C. A. Sanchez-Ortiz. 1997. Larval drift and population structure of the pelagic phase of *Pleuroncodes planipes* (Stimson) (Crustacea: Galatheidae) off the southwest coast of Baja California, Mexico. Bulletin of Marine Science 61:305–325.

Helm, K. P., N. L. Bindoff, and J. a. Church. 2011. Observed decreases in oxygen content of the global ocean. Geophysical Research Letters 38:1–6.

Hunter, J. R. 1981. Feeding ecology and predation of marine fish larvae. Pages 33–77 *in* R. Lasker, editor. Marine fish larvae; Morphology, ecology, and relation to fisheries.

Huyer, A. 1983. Coastal upwelling in the California Current system. Progress in Oceanography 12:259–284.

Jerlov, N. G. 1951. Optical studies of ocean water. Reports of the Deep-Sea Swedish Expedition 3:1–59.

Keeling, R. E., A. Körtzinger, and N. Gruber. 2010. Ocean deoxygenation in a warming world. Annual Review of Marine Science 2:199–229.

Keeling, R. F., and H. E. Garcia. 2002. The change in oceanic O_2 inventory associated with recent global warming. Proceedings of the National Academy of Sciences 99:7848–7853.

Levin, L. A. 2018. Manifestation, drivers, and emergence of open ocean deoxygenation. Annual Review of Marine Science 10:229–260.

Levin, L. A., K. K. Liu, K. C. Emeis, D. L. Breitburg, J. Cloern, C. Deutsch, M. Giani, A. Goffart, E. E. Hofmann, Z. Lachkar, K. Limburg, S. M. Liu, E. Montes, W. Naqvi, O. Ragueneau, C. Rabouille, S. K. Sarkar, D. P. Swaney, P. Wassman, and K. F. Wishner. 2015. Comparative biogeochemistry-ecosystem-human interactions on dynamic continental margins. Journal of Marine Systems 141:3–17.

Longhurst, A. R. 1968. Distribution of the larvae of *Pleuroncodes planipes* in the California Current. Limnology and Oceanography 13:143–155.

McClatchie, S., R. Goericke, A. Leising, T. D. Auth, E. Bjorkstedt, R. R. Robertson, R. D. Brodeur, X. Du, C. A. Morgan, F. P. Chavez, A. J. Debich, J. Hildebrand, J. Field, K. Sakuma, M. G. Jacox, M. Kahru, R. Kudela, C. Anderson, B. E. Lavaniegos, J. Gomez-Valdes, S. P. A. Jimenez-Rosenburg, R. Mccabe, S. R. Melin, L. M. Sala, M. D. Ohman, B. Peterson, J. Fisher, I. D. Schroeder, S. J. Bograd, E. L. Hazen, S. R. Schneider, R. T. Golightly, R. M. Suryan, A. J. Gladics, S. Loredo, J. M. Porquez, A. R. Thompson, E. D. Weber, W. Watson, V. Trainer, P. Warzybok, R. Bradley, and J. Jahncke. 2016. State of the California Current 2015-2016: Comparisons with the 1997-98 El Nino. California Cooperative Oceanic Fisheries Investigations Reports 57:1–57.

McCormick, L. R., and J. H. Cohen. 2012. Pupil light reflex in the Atlantic brief squid, *Lolliguncula brevis*. The Journal of Experimental Biology 215:2677–2683.

McCormick, L. R., and L. A. Levin. 2017. Physiological and ecological implications of ocean deoxygenation for vision in marine organisms. Philosophical Transactions of the Royal Society A 375.

McCormick, L. R., L. A. Levin, and N. W. Oesch. 2019. Vision is highly sensitive to oxygen availability in marine invertebrate larvae. Journal of Experimental Biology 222:1–11.

Nam, S., Y. Takeshita, C. A. Frieder, T. Martz, and J. Ballard. 2015. Seasonal advection of Pacific Equatorial Water alters oxygen and pH in the Southern California Bight. Journal of Geophysical Research: Oceans 120:2331–2349.

Navarro, A. M. O., P. E. Parnell, and L. A. Levin. 2018. Essential market squid (*Doryteuthis opalescens*) embryo habitat : A baseline for anticipated ocean climate change. Journal of Shellfish Research 37:601–614.

Netburn, A. N., and J. A. Koslow. 2015. Dissolved oxygen as a constraint on daytime deep scattering layer depth in the southern California current ecosystem. Deep Sea Research Part I: Oceanographic Research Papers 104:149–158.

Niven, J. E., and S. B. Laughlin. 2008. Energy limitation as a selective pressure on the evolution of sensory systems. The Journal of experimental biology 211:1792–804.

Van Noord, J. E., and E. Dorval. 2017. Oceanographic influences on the distribution and relative abundance of market squid paralarvae (*Doryteuthis opalescens*) off the Southern and Central California coast. Marine Ecology 38:e12433.

Pineda, J., W. Cho, V. Starczak, A. F. Govindarajan, H. M. Guzman, Y. Girdhar, R. C. Holleman, J. Churchill, H. Singh, and D. K. Ralston. 2016. A crab swarm at an ecological hotspot: Patchiness and population density from AUV observations at a coastal, tropical seamount. PeerJ 2016.

Przeslawski, R., M. Byrne, and C. Mellin. 2015. A review and meta-analysis of the effects of multiple abiotic stressors on marine embryos and larvae. Global Change Biology 21:2122–2140.

Robin, J., M. Roberts, L. Zeidberg, I. Bloor, A. Rodriguez, F. Briceño, N. Downey, M. Mascaró, M. Navarro, A. Guerra, J. Hofmeister, D. D. Barcellos, S. A. P. Lourenço, C. F. E. Roper, N. A. Moltschaniwskyj, C. P. Green, and J. Mather. 2014. Transitions during cephalopod life history: The role of habitat, environment, functional morphology, and behaviour. Advances in Marine Biology 67:361–437.

Røstad, A., S. Kaartvedt, and D. L. Aksnes. 2016. Light comfort zones of mesopelagic acoustic scattering layers in two contrasting optical environments. Deep-Sea Research Part I 113:1–6.

Rykaczewski, R. R., and D. M. Checkley. 2008. Influence of ocean winds on the pelagic ecosystem in upwelling regions. Proceedings of the National Academy of Sciences 105:1–6.

Schmidtko, S., L. Stramma, and M. Visbeck. 2017. Decline in global oceanic oxygen content during the past five decades. Nature 542:335–339.

Seibel, B. A. 2011. Critical oxygen levels and metabolic suppression in oceanic oxygen minimum zones. The Journal of experimental biology 214:326–336.

Seibel, B. A., B. E. Luu, S. N. Tessier, T. Towanda, and K. B. Storey. 2018. Metabolic suppression in the pelagic crab, *Pleuroncodes planipes*, in oxygen minimum zones. Comparative Biochemistry and Physiology Part - B: Biochemistry and Molecular Biology 224:88–97.

Seibel, B. A., J. L. Schneider, S. Kaartvedt, K. F. Wishner, and K. L. Daly. 2016. Hypoxia tolerance and metabolic suppression in oxygen minimum zone Euphausiids: Implications for ocean deoxygenation and biogeochemical cycles. Integrative and Comparative Biology:1–14.

Send, U., and S. Nam. 2012. Relaxation from upwelling: The effect on dissolved oxygen on the continental shelf. Journal of Geophysical Research: Oceans 117:1–9.

Shanks, A. L. 1985. Behavioral basis of internal-wave-induced shoreward transport of megalopae of the crab *Pachygrapsus crassipes*. Marine Ecology Progress Series 24:289–295.

Somero, G. N., J. M. Beers, F. Chan, T. M. Hill, T. Klinger, and S. Y. Litvin. 2015. What changes in the carbonate system, oxygen, and temperature portend for the Northeastern Pacific Ocean: A physiological perspective. BioScience 66:14–26.

Stramma, L., G. C. Johnson, J. Sprintall, and V. Mohrholz. 2008. Expanding oxygen-minimum zones in the tropical oceans. Science 320:655–659.

Stramma, L., E. D. Prince, S. Schmidtko, J. Luo, J. P. Hoolihan, M. Visbeck, D. W. R. Wallace, P. Brandt, and A. Körtzinger. 2012. Expansion of oxygen minimum zones may reduce available habitat for tropical pelagic fishes. Nature Climate Change 2:33–37.

Stramma, L., S. Schmidtko, L. A. Levin, and G. C. Johnson. 2010. Ocean oxygen minima expansions and their biological impacts. Deep Sea Research Part I: Oceanographic Research Papers 57:587–595.

Sweetnam, D. 2010. Review of selected California fisheries for 2009: Coastal pelagic finfish, market squid, red abalone, dungeness crab, Pacific herring, groundfish/nearshore live-fish, highly migratory species, kelp, California halibut, and sandbasses. California Cooperative Oceanic Fisheries Investigations Reports 51:14–39.

Sydeman, W. J., M. García-Reyes, D. S. Schoeman, R. R. Rykaczewski, S. A. Thompson, B. A. Black, and S. J. Bograd. 2014. Climate change and wind intensification in coastal upwelling ecosystems. Science 345:77–80.

Turi, G., M. Alexander, N. S. Lovenduski, A. Capotondi, J. Scott, C. Stock, J. Dunne, J. John, and M. Jacox. 2018. Response of O_2 and pH to ENSO in the California Current System in a high-resolution global climate model. Ocean Science 14:69–86.

Vidal, E. a G., F. P. DiMarco, J. H. Wormuth, and P. G. Lee. 2002. Optimizing rearing conditions of hatchling loliginid squid. Marine Biology 140:117–127.

Warrant, E. J., and S. Johnsen. 2013. Vision and the light environment. Current Biology 23:R990–R994.

Waser, W., and N. Heisler. 2005. Oxygen delivery to the fish eye: root effect as crucial factor for elevated retinal PO_2. The Journal of Experimental Biology 208:4035–47.

Wing, S. R., L. W. Botsford, S. V Ralston, and J. L. Largier. 1998. Meroplanktonic distribution and circulation in a coastal retention zone of the northern California upwelling system. Limnology and Oceanography 43:1710–1721.

Wong-Riley, M. 2010. Energy metabolism of the visual system. Eye and Brain 2:99–116.

Yannicelli, B., K. Paschke, R. R. González, and L. R. Castro. 2013. Metabolic responses of the squat lobster (*Pleuroncodes monodon*) larvae to low oxygen concentration. Marine Biology 160:961–976.

Zeidberg, L. D., and W. M. Hamner. 2002. Distribution of squid paralarvae, *Loligo opalescens* (Cephalopoda: Myopsida), in the Southern California Bight in the three years following the 1997-1998 El Niño. Marine Biology 141:111–122.

Figures

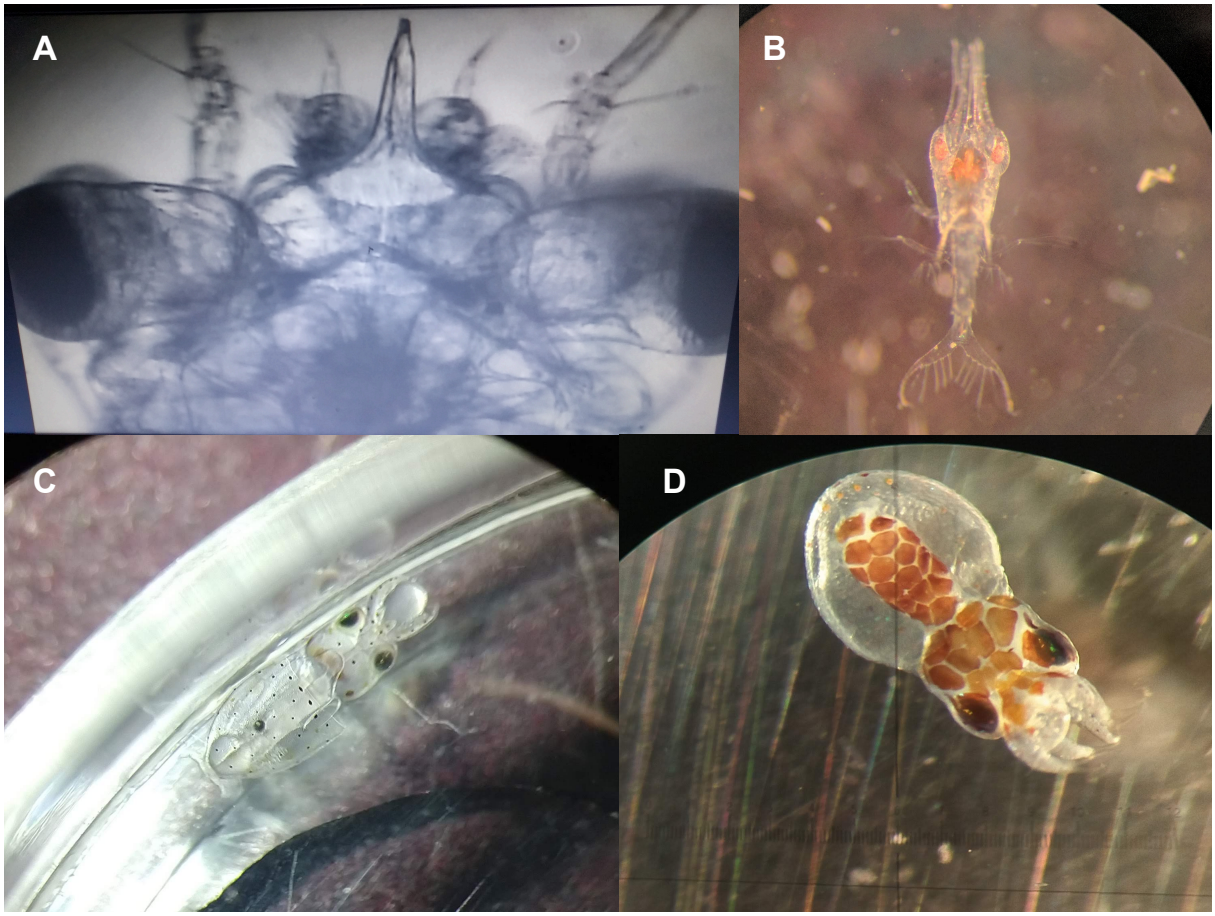

Figure 1.1. Larvae of the marine invertebrate species used in this study. Images show A) a *Metacarcinus gracilis* larvae (megalopa) under a microscope before experimentation, B) a *Pleuroncodes planipes* larva (Stage II), C) a recently hatched paralarva of *Doryteuthis opalescens*, and D) a paralarva of *Octopus bimaculatus.*

CHAPTER 2

Physiological and ecological implications of ocean deoxygenation for vision in marine organisms

Synopsis

This chapter is a review detailing the potential effects of low oxygen on vision in marine organisms. The differences in oxygen gradients in the marine environments are compared to those experienced in the terrestrial environment, and the challenges oxygenating visual systems underwater are discussed with relation to evolution of visual systems during oxygenation events and the morphology of visual structures. The possible physiological, behavioral, and ecological implications of oxygen-impaired vision are discussed in light of ocean deoxygenation and local oxygen loss, with special concern for highly visual marine species that may be especially at risk.

This chapter is presented as a paper. "Physiological and ecological implications of ocean deoxygenation for vision in marine organisms," was published as a review paper in *Philosophical Transactions of the Royal Society A* in 2017.

PHILOSOPHICAL TRANSACTIONS A

rsta.royalsocietypublishing.org

Review

Cite this article: McCormick LR, Levin LA. 2017 Physiological and ecological implications of ocean deoxygenation for vision in marine organisms. *Phil. Trans. R. Soc. A* **375**: 20160322. http://dx.doi.org/10.1098/rsta.2016.0322

Accepted: 18 May 2017

One contribution of 11 to a discussion meeting issue 'Ocean ventilation and deoxygenation in a warming world'.

Subject Areas:
oceanography

Keywords:
deoxygenation, ocean, hypoxia, vision, eye, habitat compression

Author for correspondence:
Lillian R. McCormick
e-mail: lrmccorm@ucsd.edu

Electronic supplementary material is available online at https://dx.doi.org/10.6084/m9.figshare.c.3816619.

THE ROYAL SOCIETY PUBLISHING

Physiological and ecological implications of ocean deoxygenation for vision in marine organisms

Lillian R. McCormick[1] and Lisa A. Levin[1,2]

[1]Integrative Oceanography Division, and [2]Center for Marine Biodiversity and Conservation, Scripps Institution of Oceanography, La Jolla, CA 92093-0218, USA

LAL, 0000-0002-2858-8622

Climate change has induced ocean deoxygenation and exacerbated eutrophication-driven hypoxia in recent decades, affecting the physiology, behaviour and ecology of marine organisms. The high oxygen demand of visual tissues and the known inhibitory effects of hypoxia on human vision raise the questions if and how ocean deoxygenation alters vision in marine organisms. This is particularly important given the rapid loss of oxygen and strong vertical gradients in oxygen concentration in many areas of the ocean. This review evaluates the potential effects of low oxygen (hypoxia) on visual function in marine animals and their implications for marine biota under current and future ocean deoxygenation based on evidence from terrestrial and a few marine organisms. Evolutionary history shows radiation of eye designs during a period of increasing ocean oxygenation. Physiological effects of hypoxia on photoreceptor function and light sensitivity, in combination with morphological changes that may occur throughout ontogeny, have the potential to alter visual behaviour and, subsequently, the ecology of marine organisms, particularly for fish, cephalopods and arthropods with 'fast' vision. Visual responses to hypoxia, including greater light requirements, offer an alternative hypothesis for observed habitat compression and shoaling vertical distributions in visual marine species subject to ocean deoxygenation, which merits further investigation.

This article is part of the themed issue 'Ocean ventilation and deoxygenation in a warming world'.

1. Introduction

(a) Global change

Ocean deoxygenation and eutrophication have become more prevalent over the last half century, primarily attributed to the effects of ocean warming [1–3] and the inputs of nutrients associated with growing human populations [4]. Oxygen is input into the ocean as a product of photosynthesis, from mixing at the surface and via thermohaline circulation, while it is removed from the water column by the respiration of plants, animals and microbes. Climate-forced ocean warming reduces oxygen solubility and creates stratification, which increases the outgassing of oxygen from the surface, decreases the mixing of oxygen from the surface to the deeper water column, and could also decrease nutrient inputs, limiting photosynthesis and the production of oxygen [5]. Globally, the ocean has experienced a 2% reduction in oxygen content since the 1960s [6]. This has been manifested as: expansion of oceanic oxygen minimum zones, mid-water features characterized by low oxygen concentrations [7]; expanded oxygen loss over broad sections of the east Pacific, tropical and subtropical oceans [8], and the Southern Ocean [9]; and exacerbated coastal hypoxia [10,11]. Of particular concern are upwelling areas (e.g. Southern California Bight [12]), where increased upwelling winds [13,14] and strengthened low-oxygen undercurrents [15] are intensifying the problem, and significant oxygen declines have already been recorded [15,16]. In many areas, ocean deoxygenation is accompanied by an increase in carbon dioxide and decrease in pH, linked to respiration [17–19].

The observed decline in oxygen concentration in the ocean has widespread effects on marine life, causing changes in the physiology of marine organisms [20–22] and habitat compression [23–25], which alter the distribution and ecological interactions of species [26–29]. For some mesopelagic species, Bianchi *et al.* [30] document major compression of diurnal vertical migration depths, with lower boundaries corresponding to the distribution of hypoxic (dissolved oxygen less than 60 µmol kg^{-1}) waters globally. Explanations of habitat compression for billfish [25], mesopelagic fish [31], euphausiid krill [32] and even benthic sea urchins [33] have largely been premised on physiological constraints imposed by limited oxygen tolerances. Here, we explore the possibility that ocean deoxygenation affects one of the most oxygen-demanding functions in marine organisms, vision, and examine both the physiological and ecological consequences.

(b) Oxygen requirements for vision

Vision is an essential and metabolically demanding sensory process for both terrestrial and marine organisms [34–36]. Oxygen is necessary for neurons and photoreceptors (light-sensitive cells in the eye) to function, and is used primarily in the oxidative phosphorylation process that releases energy to form the adenosine triphosphate (ATP) required for transport of ions out of cells against their electronic/concentration gradients in order to prime cells for reactivation [34,36,37]. As a result, oxygen requirements will be especially high in visual systems with high temporal resolution ('fast' vision), where there is an increased rate of these reactions [38]. Neurons use oxidative metabolism almost exclusively, instead of additional metabolism through glycolysis as found in other cells [39]. Consequently, visual cells, similar to brain cells, are dependent on oxygen and damage can occur even after only minutes without sufficient ATP [36,40]. In terrestrial vertebrates, the retina containing the photoreceptor cells is the tissue with the highest metabolic demand in the body [41–43]. Within the retina, the specific layer of photoreceptors in the eyes of mice was found to have an oxygen demand approximately two times greater than the other layers of the retina [44]. Retinal hypoxia has been linked to blindness and visual impairment in humans, and is involved in eye diseases, including retinal ischaemia and vein thrombosis, diabetes and glaucoma [45]. Numerous studies on humans have examined the function of the eye in high-altitude-flying pilots exposed to low oxygen and found deleterious effects [46–48], indicating that the effects of environmental oxygen concentration are as concerning as local hypoxia (i.e. in retina only). We note that animals possess visual systems with a range of structures. The majority

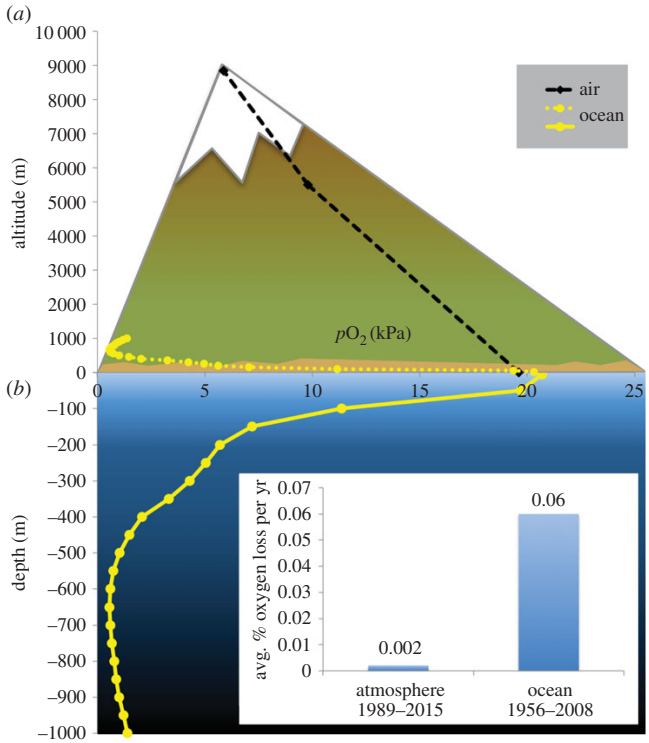

Figure 1. (*a*) Change in partial pressure of oxygen (pO_2) with altitude in air (black circles and dashed line) and with depth in the ocean (yellow circles and dotted line). (*b*) Ocean pO_2 data are shown over a 10-fold magnification in vertical distance in comparison to atmospheric data to display detail (yellow circles and solid line). Air estimates from sea level to the top of Mount Everest (8848 m) were determined using Peacock, 1998 [50]. Ocean pO_2 from the surface to 1000 m depth calculated from CTD (conductivity–temperature–depath) data recorded off southern California on 8 November 2015. Inset: average per cent oxygen loss in atmospheric and oceanic oxygen during the periods 1989–2015 [51] and 1956–2008 [52], respectively. (Online version in colour.)

of the approximately 2.2 million species of marine organisms [49] are without the thick retinal layer found in the vertebrate eye. However, most research studying oxygen effects on vision has targeted terrestrial vertebrates. Below, we present as many marine-specific and invertebrate examples as possible. These suggest that visual sensitivity to low oxygen is possible in most organisms and eye designs, but we acknowledge that the effects will vary among species and eye types.

(c) Vision and oxygen in marine organisms

Oxygen effects on vision are not as well documented in marine organisms, but may be significant given the much greater range of oxygen concentrations in the ocean in comparison to the atmosphere. In air, the percentage of oxygen remains constant at 20.9%, but at high altitudes the air pressure drops, causing the partial pressure of oxygen to decrease. This decrease is linear with altitude, and at 8848 m (the summit of Mount Everest) drops to 30% of the oxygen pressure found at sea level [50] (figure 1*a*). In comparison, the percentage saturation of oxygen in the core of the oceanic oxygen minimum zone off the coast of southern California (e.g. 8.4 µmol kg^{-1} O_2 at 650 m depth and 5.6°C) is a mere 2.75% of the oxygen pressure at the surface

(e.g. 226.3 µmol kg^{-1} O_2 at 5 m depth and 20.6°C) (figure 1*b*). Thus the ocean exhibits a much stronger gradient in oxygen over a much smaller vertical range than found on land (figure 1). In addition, oxygen concentrations in both the atmosphere and ocean have been steadily declining over the last few decades [1,16,51–53]. Oxygen at station P in the NE Pacific Ocean has declined by approximately 0.06% per year at the 26.5 isopycnal (constant potential density) since 1956 (0.67 µmol kg^{-1} yr^{-1} [52]); this rate of change is 30 times higher than the decrease in atmospheric oxygen (0.002% since 1989 [51]) (figure 1*b*, inset).

The high oxygen demands of vision in the marine environment are apparent when examining depth trends of metabolic rates and metabolic enzyme concentrations in marine organisms with eyes. Highly visual organisms, including fish, cephalopods and some arthropods, show large (up to 200-fold) metabolic declines with a minimum depth of occurrence [54–56]. The same trend is observed in enzyme activity for both aerobic metabolism (citrate synthase) and anaerobic metabolism (lactate and octopine dehydrogenase); highly visual fish and cephalopods residing in shallow areas of the ocean have much greater enzyme activity levels than their deeper-water counterparts [56]. These sharp declines are not observed in the metabolic rates or enzyme activity of other, less-visual pelagic organisms such as chaetognaths, pteropods or other gelatinous animals, or even in benthic fish, cephalopods or arthropods that have eyes with lower temporal resolution [54,56]. The visual interactions hypothesis [54] proposes that organisms in shallow water are highly mobile and rely on vision for frequent, high-speed predator–prey interactions, whereas the decrease in ambient light in the deep ocean reduces the need for fast vision and locomotion, and therefore reduces the metabolic needs of these organisms [54,56]. While this hypothesis includes locomotion as a key mechanism for changing metabolic rate, it also highlights the high metabolic demands of vision in marine organisms.

Eye tissues in marine organisms may therefore be highly sensitive to variations in oxygen. Despite the potential significance of this issue for visual physiology and ecology, very little research has been done to determine the full extent of the effects of low oxygen on vision in marine vertebrates and invertebrates. The specific concentration of oxygen at which eye tissues are affected is likely to be different for each species, depending on both the whole-body general metabolic demands and the complexity of their visual structures. Marine organisms have the unique challenge of regulating their internal oxygen pressure (pO_2) independent of external pO_2. The P_{crit} value, defined as the external partial pressure of oxygen below which the organism's metabolism is not able to regulate pO_2 independent of the environment [57–60], is a traditional metric used to define oxygen tolerances. However, these critical limits are most useful when they consider the specific physiological demands and ecological functions for a species [61], and the critical limit of pO_2 for visual function could be different from what is reflected in a metabolic metric such as P_{crit}. Because the eyes and associated structures require a high concentration of oxygen [41–43], 'visual hypoxia', or the oxygen concentration at which the eye is not receiving enough oxygen for normal visual function, may occur at a much higher level than traditional metabolic limits to environmental hypoxia. While this trend is suggested in existing studies [62], this hypothesis should be tested further.

The most basic requirement for an 'eye' is some form of directional photoreception (detection of light), accomplished through a photoreceptor cell. Modifications to the eye to improve its quality of detection include grouping additional photoreceptor cells and structures to achieve directionality, adding one or more lenses to form and focus an image, and/or having a pupil to control incoming light intensity [63]. Increased eye size and complexity may improve detection, but also could incur a higher oxygen demand [64]. Eyes are present to some extent in most marine animals [65], and the structure and capabilities are a reflection of both the function of vision in the organism's life history and the light quality of its environment. For example, in the marine realm, both sea stars and chitons possess light-detecting compound eyes in their bodies suitable to accomplish basic phototaxis (movement towards or away from light), despite not having traditionally structured eyes. In sea stars, these are located on modified tube feet at the end of each arm [66], and chitons have aragonite lenses over retinal photoreceptor cells built into the edges of each chitinous plate [67]. In contrast, cephalopods (the group containing squid, octopus and

cuttlefish) and marine vertebrates (fish, marine mammals, etc.) have a pair of sophisticated eyes with structure and complexity comparable to those in terrestrial vertebrates [63]. These patterns can be attributed to the differences in life history of each group; sea stars use vision for phototactic responses that allow them to return to the reef or detect shadows for hiding under rocks or coral [66], whereas squid and fish are highly active predators that require an image-forming eye to detect prey and respond to the rapid changes of movement by predators and prey [68].

The spectral sensitivities of eyes in marine species are also finely tuned to the light available in their environment [69]. There is exponential decay of visible light intensity with depth in the water column and there is also a change in the intensity of specific wavelengths (quality), with higher wavelengths (red light) disappearing very quickly and middle wavelengths attenuating slightly deeper, until the only available light in the mesopelagic realm is shorter-wavelength blue light [70]. Large fluctuations can occur with time of day, turbidity and biological production, where changes in the attenuation (disappearance) of light can occur with short-term events or over seasons [71]. As a result, organisms have evolved visual systems designed to function in the specific ranges of light, and theoretically oxygen, present in their environment, and it is likely that organisms will remain in that specific range to maintain full visual function. In the ocean, this corresponds to a particular range of water depths, and probably reflects both the physiological capabilities of the organism's visual system and that of their prey and predators.

Below, we review evidence for the potential negative effects of low oxygen on vision and visual behaviours in marine organisms and assess the likely implications for their physiology, behaviour and ecology under current and future ocean deoxygenation. We first examine the evolution of eyes with respect to historical atmospheric and ocean oxygenation events. We then discuss how different eye designs and oxygenation mechanisms of eyes in vertebrates and invertebrates may play a role in determining their vulnerability to hypoxia. Previous research is reviewed to discuss potential effects on visual physiology and morphology that may subsequently alter behavioural responses of species exposed to low oxygen and change ecological interactions. Finally, potential knowledge gaps are highlighted to help articulate effective research questions for the future.

2. Review

(a) Effects of oxygenation on evolution of vision and eye design

Eye evolution offers substantial evidence for the influence of oxygenation on vision. The oxygenation of the atmosphere and oceans has varied greatly over the past several billion years, with major increases in oxygenation occurring approximately 2.5–2 billion years ago (bya) and 545 million years ago (mya) [72] (figure 2). The coincident timing of eye evolution and oxygenation of the ocean support the theory that ocean oxygenation allowed for the evolution of specialized eyes, enabling fast vision (as seen in marine vertebrates (fish), cephalopods and some arthropods) (figure 2). Thorough reviews detailing each step of eye evolution and eye designs and structure [63,73–75] reveal that vision has evolved multiple times independently (such as in the fan worms, chitons and bivalves), that evolution rarely follows a strictly linear path and that more complex visual structures do not always indicate recent evolution [75,76].

A complex eye is beneficial because it allows for visual acuity, spatial resolution, temporal resolution, light detection and/or colour vision [63]. There are a variety of eye designs in marine organisms, and many do not fit the traditional definition of 'complex' as characterized by the vertebrate eye [68]. The specific benefits the eye provides, however, depend on its structure. Nilsson [75] classifies eyes into four classes of function and complexity. Class I eyes show basic non-directional photoreception, often consisting of one or two photoreceptor cells that detect light intensity to maintain circadian rhythms. Class II eyes can sense light direction and can also perform basic phototaxis. The photosensitive structures of classes I and II are considered the earliest origin of eyes, such as the eyespots found in the protists that have evolved over the last 1.5 billion years [77], such as the ocelli found in the dinoflagellates in genus *Warnowia* [78] or

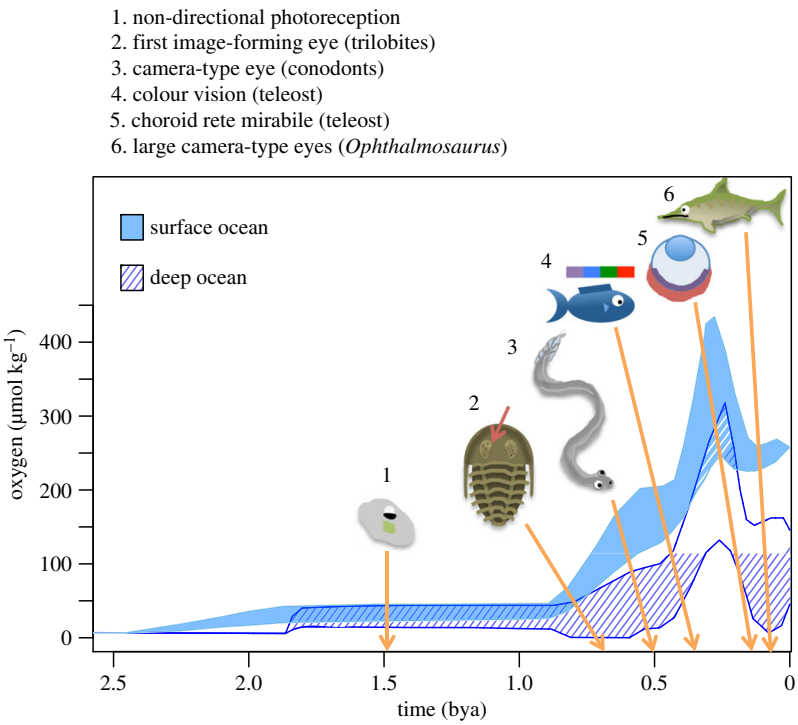

Figure 2. Evolution of ocean oxygenation and eye development. Timeline of ocean oxygenation in surface waters (light blue solid shading) and deep waters (dark blue striped shading), bounded by the minimum and maximum estimates, with key events in the evolution of eye designs added. Major steps (1–6) approach greater complexity, from basic non-directional photoreception to the development of image-forming compound and simple eyes and methods of oxygenation. Oxygen estimates modified from [72]. (Online version in colour.)

chitons [79]. An ocellus (plural ocelli) is a collection of one or more pigment cells each connected to photoreceptors, and is a primitive eye not containing any additional structures [68]. Eyespots and ocelli therefore do not have high oxygen requirements; these eye types evolved during the 'boring billion' (1.85–0.85 bya), when the atmosphere and ocean surface had a very low level of oxygen, but the deep ocean was still largely anoxic and there had been little expansion of metazoan life [72,80,81] (figure 2). Class III eyes are able to form a basic image (low-resolution vision) but have weak or no lens(es), and include the pit eye found in *Nautilus* and cup eyes in gastropod molluscs or cubozoan jellies. Class IV eyes are capable of high-resolution vision and include the camera-type eye found in fish and cephalopods [75]. Eye designs with advanced structures usually possess one to many lenses that enable the eye to focus light onto one to many photoreceptors, an aperture or migrating pigments in order to adjust the intensity of incoming light (e.g. pupil) and/or complex neural structures to transmit the electrical responses to light to the brain [68].

The large jump between class I, II and III vision (photoreceptive eyespot/ocellus or basic image-forming eye) and an eye with class IV vision (high spatial and temporal resolution capable of fast vision) that would have much higher oxygen requirements occurred around the time of the Cambrian Explosion approximately 545 mya [68]; the very first known image-forming eye was a compound eye observed in fossils from 543 mya in the trilobites [77,82]. This coincided with the end of the second and largest increase in the atmospheric and oceanic concentration of oxygen between 840 and 545 mya [72] (figure 2). Many of the animal body plans and groups

that are still present today developed during the Cambrian Explosion, and the evolution of large-bodied predators and carnivory as a feeding strategy are hypothesized to be linked to increased oxygen in the atmosphere and ocean; it has even been proposed that vision was the driving force behind predator evolution [83–85]. At this time, there was a diversification of eye designs in arthropods, molluscs, annelids and, about 25 million years later, chordates [77]. For example, the first camera-type eye was found in the conodonts (eel-like early ancestors of vertebrates) [85]. The more specialized compound eye, the reflecting superposition eye design in decapod crustaceans, is thought to have developed in the Devonian/Carboniferous period (419–358 mya) [86].

During the Carboniferous period (359–299 mya), oxygen in both the atmosphere and ocean showed a large increase, although the deep ocean also showed intermittent periods of anoxia [72]. Colour vision is also hypothesized to have evolved around this time (during 400–300 mya). Photoreceptors with opsins of at least two different wavelength sensitivities are required for colour vision, and the earliest marine forms were thought to be tetra-chromats, as seen in modern-day teleosts [87]. Adding photoreceptors of different sensitivities does not necessarily add to the oxygen demand of eyes, but each photoreceptor type may show a unique oxygen limitation (see §2c). The largest camera-type eyes, perhaps also with a greater oxygen demand, were found in *Ophthalmosaurus*, a deep-sea diving reptile with a body similar to a dolphin, approximately 165 mya, when the oxygen concentration in the deep ocean had finally increased to approximately 150 $\mu mol\, kg^{-1}$ [85].

While increases in ocean oxygen concentration may have allowed for the diversification of vision, severe declines in oxygenation could promote evolution of mechanisms for coping with low oxygen in the eye. For example, the choroid rete in fish, a vascularized organ that provides oxygenation to the eye (see §2b), is thought to have evolved approximately 200 mya [88], in the same general period as a sharp decline in oxygen in the surface ocean [72]. Defining the exact periods of evolution for each eye forms is difficult; the radiation of analogous or similar eye types is thought to have occurred multiple times over the course of evolution, even within phyla, attributable to convergent evolution under similar environmental pressures and visual requirements [68,77,89]. It is probable that the evolution of sophisticated visual systems and eye designs was limited by the available oxygen concentrations, as complex visual systems and their sophisticated neural wiring have greater oxygen requirements [38].

Therefore, an organism's eye design reflects its specific visual needs, and also the environmental characteristics to which the organism is exposed, such as light quality and quantity, and, theoretically, oxygen. For example, the superposition compound eye found in moths and many deep-sea crustaceans has an array of long lenses that act as telescopes separated by a 'clear zone' that effectively creates a large pupil and large receptors to increase the eye's sensitivity to light 10- to 1000-fold in comparison to other compound eye types. These are very efficient for low light vision, but have low temporal resolution and therefore cannot detect fast-moving objects or flashes [63]. Similarly, a single-chamber eye with a movable, spherical lens has high spatial and temporal resolution and the ability to stabilize during quick movements such as swimming, but has a reduced ability to detect images at very low light levels, and several layers of oxygen-demanding tissues [43]. Naturally, organisms possess the design that meets their specific visual requirements (e.g. a fast-moving, visual predator would possess a single-chamber lens eye rather than a superposition compound eye), but also must have the capability of supporting the metabolic requirements of the structure (eyes with high temporal resolution have higher metabolic requirements) [64]. A survey was completed of the existing literature to find oxygen tolerances for marine organisms (primarily using results from [90] and [91]) and match these values with the complexity of visual tasks required for each organism (classes I–IV [75]). Organisms that adopt higher-complexity visual tasks (e.g. class III or IV) also show higher oxygen limits (and therefore lower tolerance of low oxygen) (figure 3). Although such organisms may also be active predators whose mobility also creates high oxygen demand [84], this finding is consistent with the hypothesis that eyes with advanced visual structures and fast detection capabilities require more oxygen to function (specific to marine vertebrates, cephalopods and arthropods in the ocean).

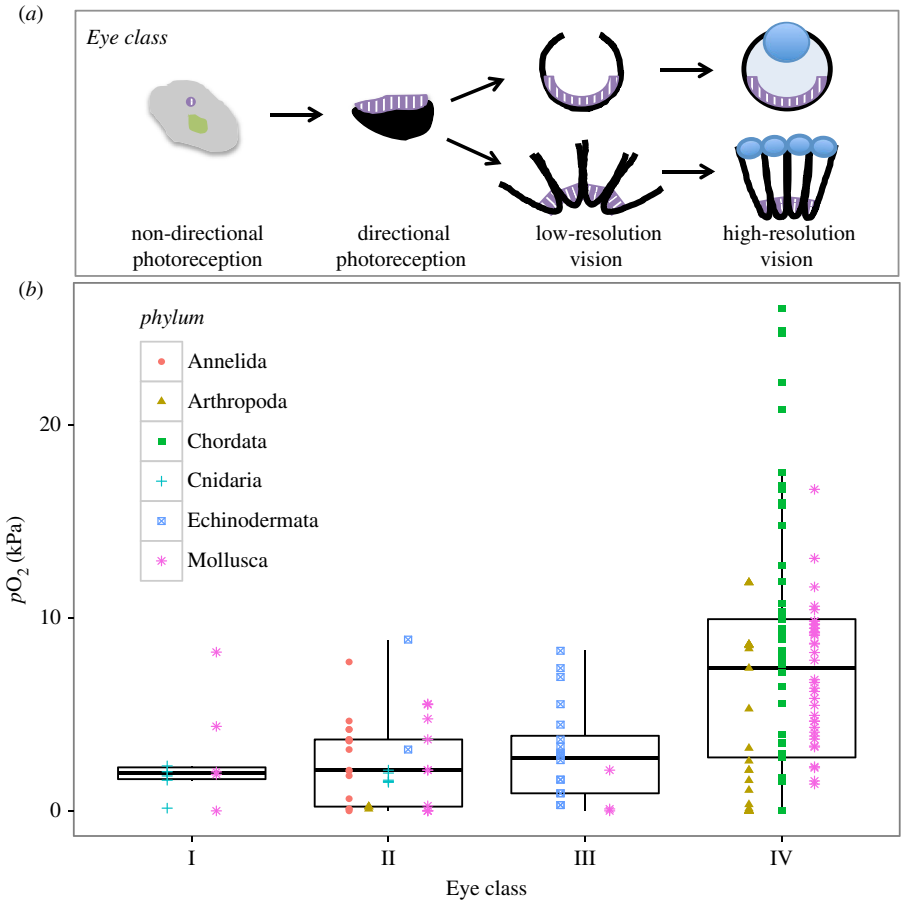

Figure 3. Oxygen tolerances as a function of visual complexity class. (*a*) Eye class (I–IV) increases in the complexity of visual structure and visual task capability. Adapted from [75]. (*b*) Oxygen tolerances (metabolic or behavioural) were obtained from [90] and [91] and then arranged by class of visual complexity as described by Nilsson [75]; details provided in electronic supplementary material. Boxes show mean values (dark midline) and first and third quartiles of oxygen tolerance data (lower and upper limits of box) for each eye class; all individual points are shown with symbols and colours designating phylum. (Online version in colour.)

(b) Mechanisms of eye oxygenation

The capability for supporting an advanced eye may be accomplished through specialized vasculature in and around the eye. General circulation required to carry oxygen to the eye may occur (i) within the haemolymph of organisms with an open circulatory system, (ii) with a combination of vessels and sinuses as found in arthropods and molluscs, or (iii) through a circulatory system such as vascularization in organisms like marine vertebrates or some polychaetes with full separate circulatory systems [92]. Organisms either can regulate their internal oxygen concentration over a range of environmental concentrations (oxygen regulators) or have metabolisms dependent on the environmental concentration of oxygen (oxygen conformers) [58].

Similarly, within the eye, a highly vascularized retina may contain local adaptations for oxygen efficiency that can buffer against external changes in conditions (e.g. an oxygen regulator), while

an organism with a full body sinus may exhibit a more direct or magnified response to oxygen variation (e.g. oxygen conformer). The structures of vasculature within organisms containing a closed circulatory system can be very diverse and involve extra-ocular vascularization, intra-ocular vascularization or a combination of both [77]. Some marine organisms have developed additional, specialized tissues or vasculature for oxygenating the eye. The choroid rete mirabile in fish is known as a tissue that supplies an increased oxygen pressure to the eye, and is similar in structure and function to the rete mirabile near the swim bladder [93]. This horseshoe-shaped organ surrounds the eye, and is larger and more developed in fish that show a higher partial pressure of oxygen in the eye and rely on vision, further implying the oxygenation function of the choroid rete [94]. The oxygen-concentrating mechanism was first attributed to the counter-current capillary exchange and presence of carbonic anhydrase [95,96], but has more recently been explained by a root effect (elevating pressure of oxygen by acidifying the blood) in the tissue [43,97]. Similarly, cephalopods possess an optic (ophthalmic) sinus adjacent to each eye and optic lobe, present even in developing embryos [98]. During development in some fishes, a transient set of blood vessels and capillaries cover the eye; this forms as early as 2 days post-fertilization in zebrafish embryos, and is replaced after retinal vasculature is developed at approximately 9 days post-fertilization [99]. For animals that require visual function, but in which haemoglobin is absent or very low, such as in some Antarctic fishes, more elaborate vasculature is developed in the eye to compensate [100–102]. Oxygenation in marine invertebrates with simpler eyes, and therefore potentially a lower visual metabolic demand, may involve physiological methods (see §2c) to enable oxygenation of visual cells or organs. Both the structure and design of the eye, and also the specific methods of oxygenation employed, may influence the response of the eye to low oxygen.

(c) Physiological responses of vision to hypoxia

The effects of low oxygen concentration on visual physiology could be an extremely important consequence of hypoxia, as physiological limits to visual function could then subsequently alter animal behaviour, distribution and species interactions. One consequence of visual hypoxia may be impaired photoreceptor function, potentially expressed as a change in sensitivity to light. While little research has been done in marine organisms, studies in vertebrates support this idea. High-altitude-flying pilots exposed to no supplemental oxygen (and therefore mild hypoxia) showed a significant reduction in night vision at a 10 000 ft (3048 m) elevation in comparison to pilots receiving 100% oxygen or 'normal' supplemental oxygen [46]. Additionally, the visual system of humans exposed to air with 10% oxygen had a higher threshold for light than in those exposed to air with the normal 21% oxygen concentration; essentially their eyes required a higher light level for visual detection of the same stimulus under hypoxia [103]. In the same study, colour vision sensitivity was also reduced during exposure to 10% oxygen, with a greater inhibition in cones (colour-sensitive receptors) than in the rods (low-light receptors); mammalian cones have approximately twice as many densely packed mitochondria as rods to produce the additional ATP required for cones in light [104–106].

Hypoxia appears to affect most photoreceptor types (invertebrate and vertebrate) in the same way (insufficient oxygen, and therefore ATP production, will decrease sensitivity of the photoreceptors to light), but the light level considered stressful to organisms under hypoxia may differ according to the phototransduction method (table 1). There are two primary physiological methods for phototransduction in marine organisms: rhabdomeric and ciliary. Each transduction pathway differs in the structure and kind of photoreceptor(s) (e.g. rhodopsin for rhabdomeric or rods and cones for ciliary), the proteins and biochemical cascade for signal transduction, and the direction of the response in ion channel action and membrane potential [87] (table 1).

While the oxygen consumptions of each of the three photoreceptor species identified here are essentially similar in dark conditions, the ATP demand (and therefore oxygen consumption) increases in rhabdomeric transduction pathways upon exposure to light and decreases or remains neutral in ciliary phototransduction [106–108]. For example, the oxygen demand of the retina in

Table 1. Oxygen demand and visual stress for each transduction pathway in vertebrates and invertebrates. ATP demand ($+++ > ++ > +$) indicates a relative change and does not indicate a numerical value; based on information from [106].

	invertebrate	vertebrate	
transduction pathway	rhabdomeric	ciliary (rod)	ciliary (cone)
light stimulus			
ion channels	open	close	close
membrane potential	depolarize	hyperpolarize	hyperpolarize
ATP demand			
dark	++	++	++
light	+++	+	++
stressful light level under hypoxia	high	low	neutral

mice increased by 24% under dark adaptation, indicating a higher metabolic demand at low light levels for vertebrates (which have a ciliary receptor type) [44]. This is a result of the constant influx of sodium into the photoreceptor cells to maintain a voltage of −40 mV (dark current) [109]. In rabbits, the electrical response of the retina to light was severely reduced, and that of the optic nerve eliminated without oxygen and glucose; these results were reversible with short exposure times and return to 100% oxygen [110]. Similarly, intracellular recordings of photoreceptors in the squid *Loligo pealii* (rhabdomeric receptor type) showed a depolarization of the cellular current and reduced magnitude of response to light at 140 mmHg oxygen in comparison to 740 mmHg oxygen, presumably also as a consequence of insufficient ATP production to maintain ionic gradients [111]. Both photoreceptor types appear to show a reduced response to light under low oxygen. However, a difference between these photoreceptor types is expected in the light level considered 'stressful' (i.e. when the oxygen demand is highest); this would occur in the dark for ciliary photoreceptors (primarily vertebrates) and in the light for rhabdomeric photoreceptors (primarily invertebrates).

Another effect of low oxygen concentration that could affect vision may be decreased neurological function. In many organisms, there is an increase in the production of inhibitory neurotransmitters such as γ-amino butyric acid (GABA) and/or adenosine in the brain during exposure to hypoxia [112]. GABA depresses neuronal action, which is required for the transmission of visual signals, and the increase in production of this neurotransmitter is an adaptation observed in hypoxia-/anoxia-tolerant species. As an extreme example, the crucian carp (*Carassius carassius*) is known for both its resistance to low oxygen and its unique ability to maintain its activity level during long periods of exposure to anoxia. Other species, such as freshwater turtles of the genera *Trachemys* and *Chrysemys*, are considered hypoxia- or anoxia-tolerant, but enter a semi-comatose state and have very reduced brain function under hypoxia [113]. Among other mechanisms for hypoxia tolerance, one adaptation employed by *C. carassius* is metabolic modulation, where the visual system is selectively shut off to reduce metabolic demand. A reduction in electrical response of the eye to light flashes of up to 90% was observed in the retina and optic tectum (visual portion of the brain) of the carp after only one hour of exposure to anoxia; this process is completely reversed after conditions return to normoxia [114]. The horizontal cells and amacrine cells of the retina in *C. carassius* are GABAergic [115,116], indicating that GABA may play a function in the inhibition of visual responses during anoxia [114]. Decreased neurological function in other marine organisms less tolerant to low oxygen than *C. carassius* could significantly inhibit the transmission of visual signals to and within the brain, but this has yet to be documented. Little is known about visual adaptation in other oxygen-stressed marine environments such as the deep-water fluid emergence sites of hydrothermal vents and seeps. Although there is limited or no light in these environments, the shrimp *Rimicaris exoculata* does show a very interesting modified compound

eye that is used to detect the very small amounts of light emitted from the vents themselves [117]. However, its oxygen demand is unknown.

Exposure to low oxygen additionally affects the regeneration of the visual pigments in terrestrial vertebrates. Mouse photoreceptors exposed to low and 'zero' oxygen concentrations were unable to regenerate rhodopsin [118]. This effect was also reversible after perfusion with 100% oxygen, even in exposures lasting greater than three hours. Evidence for a more metabolically efficient pigment regeneration pathway in cones has been found in *C. carassius*, suggesting further physiological adaptation to low oxygen [119]. In addition to the lack of electrical function in photoreceptors required to recognize light stimulus, a reduced or ceased regeneration would inhibit response to light signals and chronic exposure to hypoxia. For marine organisms, these responses could prevent proper visual function during exposure to hypoxia, even if the responses are reversible upon return to normoxia.

In reviewing general physiological adaptations of marine organisms to hypoxia [120], several whole-body physiological responses emerge that may affect visual tissue. These include a change in the affinity of the blood respiratory pigment to allow for a greater uptake of oxygen, such as observed in high-altitude-flying birds [121,122], altering the charge of myoglobin molecules in the blood of deep-diving mammals [123], or an increase in transcription factors such as hypoxia-inducible factor 1 (HIF-1 [120]). HIF-1 regulates a multitude of genes that enable the organism to adapt to hypoxia; it has been found in human eyes experiencing hypoxia from retinal ischaemia and glaucoma [124], and is responsible for activating the vascular endothelial growth factor (VEGF) that induces neovascularization (development of new blood vessels) in visual tissue in mice [125]. General upregulation of HIF-1 has been observed in low-oxygen conditions in mammalian cells [126], but whether HIF-1 has a similar function in the eyes of marine animals is unknown.

(d) Morphological and developmental responses of eyes to hypoxia

Morphological responses of the eye to hypoxia are also not well studied in marine organisms, and probably depend on the time frame of exposure to low oxygen. For example, in organisms developing under hypoxia, small changes in capillary structure can occur over shorter time periods (30–80 days [127]) than more permanent changes such as eye size, but both are potentially a result of chronic exposure to low oxygen. In human eyes, choroidal neovascularization, the development of new blood vessels in the choroid layer, occurs as a result of diseases like diabetes, retinopathy of prematurity (incomplete eye vascularization at birth) and macular degeneration with age causing local hypoxia [128]. While not all marine organisms have vasculature near the eye (see §2b), the expansion of sinuses, vessels or other specialized tissues that increase the oxygen concentration around the eye, such as the choroid rete mirabile found in fish [96], may indicate visual adaptation to hypoxia and would be a response similar to neovascularization in terrestrial vertebrates [128].

Local effects may also occur at the cellular level of visual cells or surrounding tissue. Mitochondria are the organelles responsible for cellular respiration and energy production (oxidative metabolism), and the oxidation capacity of the cell is directly related to the volume of its mitochondria [129]. Thus, a cell rich in mitochondria has the capacity to produce more energy, but also requires more oxygen [105]. Original studies of humans in high-altitude areas predicted an increase in the oxidative capacity of muscles in response to lower oxygen [130], but more recent work shows a decrease in mitochondria in skeletal muscle with a change in altitude, indicating that the opposite effect actually occurs [131,132]. Similarly, visual tissue normally contains densely packed mitochondria, and a reduction in oxidative capacity could be expressed as a smaller size or lower density of these organelles.

Morphological changes in the eye induced by low oxygen could also be attributed to new environmental stresses linked to behavioural or ecological responses to hypoxia. In the aquatic realm, there are changes in wavelength (= quality) and intensity (= quantity) of light with water depth, and these influence the structure and visual capabilities of each species [69]. For

example, the wavelength sensitivity (i.e. λ_{max}) of an eye in a coastal, nearshore environment will be different from the sensitivity of a deep-sea organism as a result of the difference in light quality in their respective environments [64].

If the vertical (depth) distribution of an organism is shifted or compressed as a result of oxygen stress, a subsequent change in the spectral sensitivity of the eye may occur. While this has not yet been observed in diel vertical migrators after a climate-induced change in the depth of migration (*sensu* [31]), ontogenetic changes in the spectral sensitivity (λ_{max}) or type of opsin in the eye are known to occur during development that reflect the change in the spectral characteristics of different habitats, such as river versus ocean waters. This occurs in fish that are anadromous (ocean to river migration), including the lamprey (*Petromyzon marinus* [133]) and the salmon (*Salmo salar* [134]), and catadromous (river to ocean migration), such as the eel (*Anguilla anguilla* [133,135]). Additional changes in λ_{max} or the proportion of opsin types occur seasonally in some species of fish [134]. In the rudd (*Scardinius erythrophthalmus*), a freshwater fish, the proportion of porphyropsin, a short-wavelength-sensitive opsin, to the longer-wavelength rhodopsin increases in winter, whereas in summer the proportion decreases [136]. This was reproduced in the laboratory by exposing *S. erythrophthalmus* to different light intensities; fish exposed to low-intensity light (mimicking winter conditions) showed an increase in rhodopsin, while exposure to high-intensity light (summer) resulted in an increase in porphyropsin, and the effect was reversed when light/dark conditions were switched [136]. The existing plasticity of the spectral sensitivity in marine organisms indicates that a switch in opsin type or change in opsin sensitivity (λ_{max}) could occur as an adaptation in species compressed vertically in the water column by physiological oxygen limitation, causing them to occupy a different spectral niche. These shifts may not be a direct effect of low oxygen, but could help to maintain visual function in a changing environment, and therefore be critical to fitness.

More permanent changes in visual development could occur when organisms are exposed to low oxygen during embryogenesis. Developing organisms typically have higher mass-specific metabolic requirements than adults, and as such are particularly at risk of low-oxygen stress [22]. Gas exchange is a challenge, particularly when eggs are embedded in a gelatinous mass or capsule, as is common in gastropod or cephalopod molluscs [137–139]. Embryonic visual development is vital to survival upon hatching; for example, some cephalopods develop the ability to discern contrast or learn to identify copepod prey during embryogenesis [140,141]. Hypoxia is known to cause developmental delays, mortality and/or morphological deformities in frogs [142], gastropods [138], abalone [143], brachyuran crabs [144] and squid [145,146]. Hypoxia-induced impairments to visual system development in marine organisms include a reduction in the size of the eyespot in the mussel (*Mytilus edulis* [147]) and eye deformities in hatched squid paralarvae *(Sepioteuthis australis),* potentially from lower oxygen found in capsules at the centre of egg clusters in comparison to those on the outside of the group [148]. Visual abnormalities in developing zebrafish (*Danio rerio*) occurred when different stages of development were exposed to hypoxia (approx. 6.9 $\mu mol\,l^{-1}$ O_2) [149]. Out of 1161 hatched larvae, 18% exhibited anophthalmia (absence of eyes), 14% showed microphthalmia (small size of one or both eyes) and 31% showed cyclopia (only one eye present).

A change in eye size may be one morphological adaptation that occurs in marine organisms developing under low-oxygen conditions. In general, large eyes and pupils have a greater ability to detect light [64], but have poor spatial resolution and acuity (i.e. poor image quality) in comparison to small eyes. Eye design and eye size in comparison to body size is then a trade-off between the ability to capture photons, the quality of the image and the increased metabolic demands of a larger eye [64]. In mesopelagic fishes, eye size generally increases with depth, conferring a greater ability to detect photons to accommodate the exponential decay of light intensity. This increase in eye size continues with depth, and the corresponding decrease of oxygen concentration, until the bathypelagic (greater than 1000 m), where eye size is then dictated by metabolic requirements constrained by a lower food supply [65]. Eye size may be limited by the high oxygen requirements of a large eye. Embryos developing in unusually low-oxygen

conditions may have smaller eyes than those developing in normal-oxygen conditions to reduce the metabolic demand on the body.

In addition, low oxygen may indirectly affect visual development of embryos if adults change the depth (and therefore light exposure) of benthic egg or capsule placement as a response to environmental conditions [150]. Changes in light intensity, quality and photoperiod are known to alter hatching success, development time and visual development in fish [151]. Development in low-oxygen or varied light conditions could therefore cause a change in morphological body plan and/or a reduction in success upon hatching due to an impairment of vision from either low oxygen and/or altered light intensity.

(e) Vision-mediated behavioural responses to hypoxia

If hypoxia causes the visual system to be compromised, organisms will probably demonstrate altered behaviour as a result. One major behaviour that could be significantly changed by visual hypoxia is phototaxis, defined as movement towards light (positive phototaxis) or away from light (negative phototaxis). The basic process of phototaxis is essential to a majority of marine organisms; it is used in diel vertical migration [152], larval settlement [153], mate recognition [154] and/or predator avoidance [155]. The cue responsible for this behaviour can be a simple change in the light environment (e.g. shadow of a predator), or a response that is initiated at a particular light level or age [156]. Regardless of the cue for initiation, a hypoxia-compromised visual system that has a lower sensitivity to light or lower ability to discern rapid changes in light could cause an organism to delay its response or miss the cue entirely.

A change in phototactic behaviour was observed in the walleye (*Stizostedion vitrium vitrium*) upon exposure to low oxygen concentrations [157]. Under normal dissolved oxygen (more than $6\,\mathrm{mg\,l^{-1}}$), *S. vitrium vitrium* displays negative phototaxis and moves to the bottom of the tank; this species has a well-developed tapetum lucidum (reflective layer behind the retina) and specializes in low-light vision. Under graded reductions of oxygen, beginning at 2–4 $\mathrm{mg\,l^{-1}}$ O_2, individuals increase their movement into lit areas; beyond approximately 1–2 $\mathrm{mg\,l^{-1}}$, the individuals show a reversal in phototactic response and swim upwards [157].

Feeding behaviour may also be altered by a change in light requirements or reduced visual capabilities. This could be manifested as a reduction in successful attack attempts, lack of ability to detect prey that are normally within visual range or a change in the time of day when the light is suitable for feeding. It is challenging to attribute changes in feeding behaviour directly to visual impairment. For example, reduced predation under hypoxia is commonly attributed to the organism trying to conserve energy by reducing movement [114,158] or to a lower appetite [159], but the changes could also be due to a decrease in visual system function such as acuity or sensitivity to motion. Visual acuity is the ability to discern details from a distance, while sensitivity to motion is related to the temporal resolution of the eye, usually measured by examining the flicker fusion response (ability of the eye to respond to repeated fast light stimuli [160]). Several studies in humans have shown negative effects of hypoxia on visual response time [161], visual acuity, flicker fusion and ocular muscle control [162]. While much less studied in marine organisms, this type of response to oxygen stress may explain changes in predation or feeding; a reduction in any one of these visual functions would have significant consequences for success in prey capture and swimming manoeuvrability. Although impaired vision has not been investigated as a cause, a reduction in feeding (among other processes) occurs with chronic exposure to hypoxia in many species. Among invertebrates, hypoxia reduces feeding in juvenile and adult blue crabs (*Callinectes sapidus*), juvenile lesser blue crabs (*Callinectes similus*) and the adult oyster drill (*Stramonita haemastoma*) [163,164], although predation in these species is not entirely reliant on vision [165,166]. Among vertebrates, a decrease in feeding under hypoxic conditions was seen in the European sea bass (*Dicentrarchus labrax*) [159], which is considered a highly visual predator [167]. The visual acuity in snapper (*Pagrus auratus*) was reduced beginning at oxygen concentrations of 40% air-saturated seawater, and severely compromised when the level was decreased to 25%, approaching the critical oxygen tension (P_{crit}) of this species [62].

Similarly, juveniles of the flounder (*Platichthys flesus*) showed a 64% reduction in predation success when exposed to 20–30% oxygen saturation [168], and plaice (*Pleuronectes platessa*) exposed to 30% oxygen saturation showed reduced feeding in comparison to those in 50–100% oxygen saturation [169]. These flatfish are known to be visual predators [170], and it is possible that visual impairment was causing these responses.

Other visual behaviours, such as response to visual signalling by both conspecifics and other species, ability to camouflage correctly, and/or mate selection, may be compromised, with hypoxia-impaired vision for similar reasons. However, changes in these behaviours as a result of low oxygen have not yet been directly associated with impaired vision [28,171,172]. Indirect effects of oxygen-compromised visual behaviour can subsequently lead to changes in the phenology of feeding, mating or breeding if animals are limited by the light levels (e.g. intensity and photoperiodicity) required for each action.

(f) Effects of hypoxia on visual ecology

Recently, documented changes in the ecology of marine organisms have been attributed to ocean deoxygenation [8,173]. Many pelagic marine organisms undergo a large, daily migration through the water column known as diel vertical migration (DVM), where they remain deeper during the day to avoid visual predators and then ascend to near-surface waters at night to feed [174,175], or show the reverse trend [176]. The movement of large aggregations of these organisms at particular depths, known as deep scattering layers, is often measured by mapping their acoustic signature [30,31,177]. Oxygen concentration can be a predictor of the extent and lower depth of DVM [30,178], and the current depths of vertical migration have already shoaled in comparison to previous years in areas that are experiencing ocean deoxygenation, such as the Southern California Bight (SCB) [31]. Wishner *et al.* [179] found that the upper depth of vertical migration in zooplankton corresponded to oxygen concentration; organisms needed to ascend to a shallower depth to 'repay' their oxygen debt; this repayment may also be necessary after organisms descend into low-oxygen areas in pursuit of prey [178]. As a result, habitat compression from physiological limitations attributed to low oxygen concentration has been documented or is expected to occur in many taxa, including billfish [23–25], benthic, small pelagic and mesopelagic fish [27,28,180], krill [32] and squid [178,181]. An additional concern is that the concentrated consumption of oxygen by migrating pelagic organisms in highly stratified and poorly ventilated areas of the ocean (i.e. limiting zones directly above the oxygen minimum zones) will further intensify oxygen depletion in areas that are already low in oxygen [30], potentially exacerbating these effects.

There are potential indirect effects of the responses discussed above. If prey distributions (e.g. fish and crustaceans) shoal under hypoxia, then predators may follow them into shallower waters. This is one possible explanation for the shoaling of billfish [25]. Concurrently, species with shallower distributions may become more vulnerable to predation due to increased light availability. Koslow *et al.* [28] documented major declines in the abundance of mid-water fishes of the SCB during a 9-year period of shoaling oxyclines (1999–2008) and proposed increased visual predation on these species as one explanation for their decline.

Indeed, light intensity is also a factor in determining the boundaries of vertical migration or distribution [182–184], as the organisms involved are performing the migration and distribute themselves to avoid visual predators [175]. Both metabolically driven and vision/light-driven changes in vertical distribution as a result of oxygen stress could therefore lead to increased predation risk [26], or a change in prey selection because of increased or decreased visibility from altered light availability. This has been observed in lake fish populations, where trout selectively preyed on a large species of the cladoceran *Daphnia pulex* until winter deoxygenation at the bottom of the lake created oxygen conditions below the physiological tolerance of the fish, and caused the fish to reduce their depth distribution. Because there was a greater light intensity at shallower depths, the fish were able to switch prey species and feed on a smaller copepod [185]. Thus oxygen stress has the potential to change trophic dynamics of the visual predators and their ability to feed, and also the dynamics of the prey species or lower trophic levels. Visual predation has been

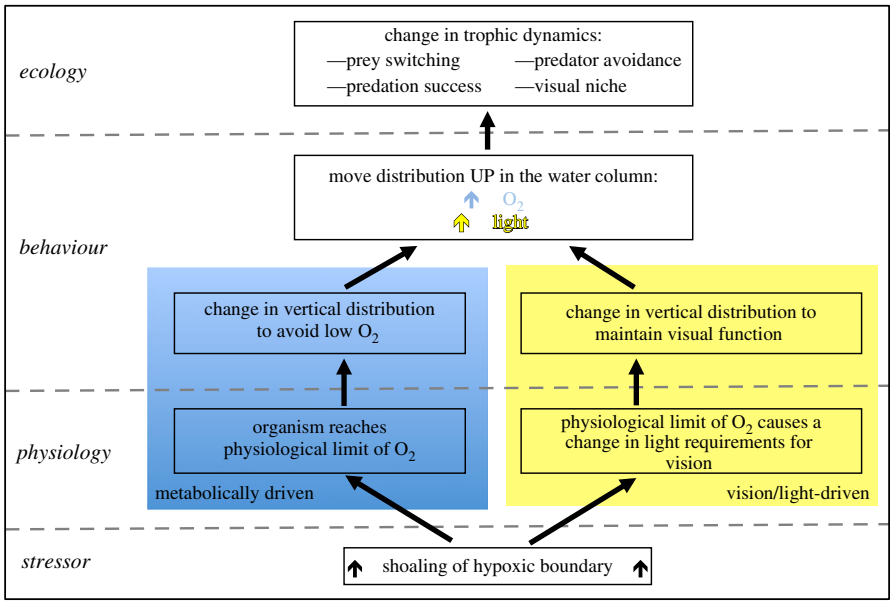

Figure 4. Dual mechanisms potentially underlying shoaling distributions as a result of hypoxia. Both metabolically driven tolerances (left, blue box) and vision/light-driven requirements (right, yellow box) may explain changes in distribution and vertical compression in the water column. (Online version in colour.)

recognized as an important driver of trophic dynamics in the marine environment [186], and implies that, even under the current hypothesis of metabolically driven movement of animals higher in the water column, direct or indirect effects of oxygen on vision play an important role (figure 4).

Current studies have not recognized limits to visual physiology as a potential cause for changes in species distribution or migration patterns in the open ocean. The effects of low oxygen on visual physiology and behaviour reviewed here offer an alternative or additional hypothesis to explain ecological responses to hypoxia (figure 4). For example, if low oxygen causes a change in the light required for vision (due to a decrease in sensitivity to light), organisms may ascend in the water column to an area where there is sufficient light for visual function. Similarly, if phototaxis behaviour is reduced, organisms may not be able to respond to visual cues and behaviours, such that the extent of DVM may be expressed differently. Both vision/light-driven scenarios yield shoaling vertical distributions in the water column, and would result in similar distributions in response to metabolically driven constraints (figure 4).

Changes in vertical distribution and compression are not only changing species interactions and trophic dynamics [187], but also exposing the organisms to light regimes that may be outside of their normal exposures (e.g. higher intensity with upward vertical motion), potentially inducing additional (light) stress on their visual systems. This may be particularly stressful for invertebrates that have a greater visual metabolic demand at higher light levels (table 1). Even a small change in depth can result in an entirely different light field with respect to intensity and spectral quality [70]. Fluctuations in the light field can occur as a result of primary production, induced by the upwelling or run-off of nutrients, or by weather patterns, and these natural light variations can be more important than abundance of prey for feeding success [188]. For example, seasonal variation in the nitracline depth, which is inversely correlated to the attenuation (dissipation) of light, consistently changes the optical properties of the water column on a yearly basis [71]. It then becomes important to examine both the oxygen and light conditions

when determining the effects of oxygen stress on the visual system, as eyes with different mechanisms of phototransduction may find different light conditions stressful under low oxygen (e.g. invertebrates versus vertebrates; table 1).

(g) A note on multiple stressors

Most observed changes in the ecology of marine organisms under deoxygenation are likely to result from a combination of environmental alterations that are tightly linked, e.g. light, nutrients, carbon dioxide (CO_2) and temperature [18,189]. We highlight here the importance of vision and light as mediators when discussing climate change impacts on distributions, behaviour and fitness of marine species. Each of the stressors mentioned above can impact vision directly or in combination with oxygen loss. Low oxygen rarely occurs without a simultaneous increase in CO_2 and decrease in pH caused by enhanced respiration linked to nutrient input from eutrophication or upwelling [17–19,190,191]. The additional stress of environmental hypercapnia can exacerbate or otherwise change the effects of low oxygen on the physiology of marine organisms [192–194], and has the potential to impact or contribute to the visual responses presented here. For example, recent work by Miller and colleagues [195] has shown that acidification exacerbates the effects of hypoxia; silversides (*Menidia menidia* and *M. beryllina*) exhibit greater mortality, increased surface respiration and reduced gill movements when exposed to both low pH and low dissolved oxygen in comparison to those exposed to only low oxygen. One cause of this may be a dampened protective physiological response to hypoxia (which allows the organism to acclimate or otherwise cope with reduced oxygen concentration) in the presence of environmental hypercapnia, which causes the effects of hypoxia to be exacerbated, as seen in the Pacific whiteleg shrimp (*Litopenaeus vannamei*) [196,197]. A similar effect (reduced adaptive response to hypoxia, and therefore exacerbation of effects) has been observed with temperature; the number of larval *Fundulus heteroclitus* showing visual defects after exposure to both hypoxia and high temperatures during development increased 8-fold in comparison to those exposed to only hypoxia [149]. Negative effects of low pH and high CO_2 on vision and other sensory systems have already been documented in marine organisms [198–200]. Organisms possessing a choroid rete, an organ that relies on using a change in pH to change the affinity of blood to oxygen (root effect), may be particularly vulnerable to the combined effects of environmental hypercapnia and hypoxia. For example, in addition to the effects of a graded reduction in oxygen, Scherer [157] showed that the phototactic reaction in the walleye (a species with a choroid rete) was also reduced under the combined effects of low oxygen and low pH. In contrast, two-spotted gobies, *Gobiusculus flavescens*, that developed under high-CO_2 conditions showed an increase in phototaxis behaviour (greater number of larvae moving towards light and faster swimming speed) after hatching in comparison to those developed in normal conditions [201]. Thus, testing effects of ocean deoxygenation with multiple stressors may be necessary to accurately resolve physiological and ecological effects on vision and visual function.

3. Conclusion and future directions

Ocean deoxygenation has the potential to impair visual function in marine organisms, and has probably done so for over a billion years. Anthropogenic influences have accelerated rates of oxygen loss in the ocean through ocean deoxygenation caused by warming and eutrophication. Oxygen stress may induce a change in the light environment from habitat compression or cause a physiological change in light requirements that could alter the behaviour and distribution of visual marine organisms, and increase their vulnerability to predators or their feeding success. Changes in the physiology, morphology, behaviour and ecology of marine animals have already been observed in response to ocean deoxygenation, but it is unclear to what extent visual limitations are driving these changes. Organisms that live full time in the oxygen minimum or oxygen-limiting zones (*sensu* [173]) may already employ adaptations to maintain visual function, whereas transient species or those that avoid areas with reduced oxygen (and are probably less

tolerant to these conditions) may be particularly at risk for a decline in visual function. This review details the importance of oxygen for visual function, and presents the case for varied and serious consequences in visual marine organisms exposed to low oxygen resulting from climate change. The effect of low oxygen on vision has been studied in humans and terrestrial animals, but is a novel theme that merits further exploration in marine organisms. Care should be taken to study visual responses in both vertebrates and invertebrates, as the effects will probably reflect the many differences in visual physiology within each group. We hypothesize that marine organisms possessing visual systems with high temporal resolution, such as fish, cephalopods and arthropods, many of which support large coastal fisheries, will be particularly at risk. Further research could help determine which specific taxa will be most susceptible to these effects, whether adaptations to lower oxygen occur on acute or chronic time scales and whether these adaptations can maintain ecosystem integrity in a future ocean subject to deoxygenation.

Data accessibility. The data for figure 3 and associated references can be found in electronic supplementary material, Supplement 1.

Authors' contributions. L.R.M. conceived the basic premise of the paper, conducted the literature review and wrote the manuscript. L.A.L. placed the work in the context of ocean deoxygenation, helped refine concepts and edited the manuscript.

Competing interests. We declare we have no competing interests.

Funding. L.R.M. was supported through an NSF Graduate Research Fellowship. L.A.L. acknowledges support from NSF-EAR 1324095.

Acknowledgements. We are grateful for the comments of two anonymous reviewers and to Dimitri Deheyn, Todd Martz, Nicholas Oesch, Frank Powell and Martin Tresguerres for their detailed discussions and insight on the concepts covered in this review. We thank the organizers of the discussion meeting for offering us the opportunity to contribute.

References

1. Keeling RE, Körtzinger A, Gruber N. 2010 Ocean deoxygenation in a warming world. *Annu. Rev. Mar. Sci.* **2**, 199–229. (doi:10.1146/annurev.marine.010908.163855)
2. Bijma J, Pörtner H-O, Yesson C, Rogers AD. 2013 Climate change and the oceans—what does the future hold? *Mar. Pollut. Bull.* **74**, 495–505. (doi:10.1016/j.marpolbul.2013.07.022)
3. Long MC, Deutsch C, Ito T. 2016 Finding forced trends in oceanic oxygen. *Global Biogeochem. Cycles* **30**, 1–17. (doi:10.1002/2015GB005310.Abstract)
4. Diaz RJ, Rosenberg R. 2008 Spreading dead zones and consequences for marine ecosystems. *Science* **321**, 926–929. (doi:10.1126/science.1156401)
5. Keeling RF, Garcia HE. 2002 The change in oceanic O_2 inventory associated with recent global warming. *Proc. Natl Acad. Sci. USA* **99**, 7848–7853. (doi:10.1073/pnas.122154899)
6. Schmidtko S, Stramma L, Visbeck M. 2017 Decline in global oceanic oxygen content during the past five decades. *Nature* **542**, 335–339. (doi:10.1038/nature21399)
7. Stramma L, Johnson GC, Sprintall J, Mohrholz V. 2008 Expanding oxygen-minimum zones in the tropical oceans. *Science* **320**, 655–659. (doi:10.1126/science.1153847)
8. Stramma L, Schmidtko S, Levin LA, Johnson GC. 2010 Ocean oxygen minima expansions and their biological impacts. *Deep Sea Res. Part I Oceanogr. Res. Pap.* **57**, 587–595. (doi:10.1016/j.dsr.2010.01.005)
9. Helm KP, Bindoff NL, Church JA. 2011 Observed decreases in oxygen content of the global ocean. *Geophys. Res. Lett.* **38**, 1–6. (doi:10.1029/2011GL049513)
10. Altieri AH, Gedan KB. 2015 Climate change and dead zones. *Global Change Biol.* **21**, 1395–1406. (doi:10.1111/gcb.12754)
11. Levin LA, Breitburg DL. 2015 Linking coasts and seas to address ocean deoxygenation. *Nat. Clim. Change* **5**, 401–403. (doi:10.1038/nclimate2595)
12. Nam S, Takeshita Y, Frieder CA, Martz T, Ballard J. 2015 Seasonal advection of Pacific Equatorial Water alters oxygen and pH in the Southern California Bight. *J. Geophys. Res. Oceans* **120**, 2331–2349. (doi:10.1002/2014JC010632)
13. Sydeman WJ, García-Reyes M, Schoeman DS, Rykaczewski RR, Thompson SA, Black BA, Bograd SJ. 2014 Climate change and wind intensification in coastal upwelling ecosystems. *Science* **345**, 77–80. (doi:10.1126/science.1251635)

14. Wang D, Gouhier TC, Menge BA, Ganguly AR. 2015 Intensification and spatial homogenization of coastal upwelling under climate change. *Nature* **518**, 390–394. (doi:10.1038/nature14235)
15. Bograd SJ, Buil MP, Lorenzo E, Castro CG, Schroeder ID, Goericke R, Anderson CR, Benitez-Nelson C, Whitney FA. 2015 Changes in source waters to the Southern California Bight. *Deep Sea Res. Part II Top. Stud. Oceanogr.* **112**, 42–52. (doi:10.1016/j.dsr2.2014.04.009)
16. Bograd SJ, Castro CG, Di Lorenzo E, Palacios DM, Bailey H, Gilly W, Chavez FP. 2008 Oxygen declines and the shoaling of the hypoxic boundary in the California Current. *Geophys. Res. Lett.* **35**, L12607. (doi:10.1029/2008GL034185)
17. Frieder CA, Nam S, Martz TR, Levin LA. 2012 High temporal and spatial variability of dissolved oxygen and pH in a nearshore California kelp forest. *Biogeosciences* **9**, 1–14. (doi:10.5194/bg-9-1-2012)
18. Breitburg DL *et al.* 2015 And on top of all that… Coping with ocean acidification in the midst of many stressors. *Oceanography* **28**, 48–61. (doi:10.5670/oceanog.2015.31)
19. Melzner F, Thomsen J, Koeve W, Oschlies A, Gutowska MA, Bange HW, Hansen HP, Körtzinger A. 2012 Future ocean acidification will be amplified by hypoxia in coastal habitats. *Mar. Biol.* **160**, 1875–1888. (doi:10.1007/s00227-012-1954-1)
20. Seibel BA. 2011 Critical oxygen levels and metabolic suppression in oceanic oxygen minimum zones. *J. Exp. Biol.* **214**, 326–336. (doi:10.1242/jeb.049171)
21. Deutsch C, Ferrel A, Seibel B, Portner H-O, Huey RB. 2015 Climate change tightens a metabolic constraint on marine habitats. *Science* **348**, 1132–1136. (doi:10.1126/science.aaa1605)
22. Somero GN, Beers JM, Chan F, Hill TM, Klinger T, Litvin SY. 2015 What changes in the carbonate system, oxygen, and temperature portend for the Northeastern Pacific Ocean: a physiological perspective. *Bioscience* **66**, 14–26. (doi:10.1093/biosci/biv162)
23. Prince ED, Goodyear CP. 2006 Hypoxia-based habitat compression of tropical pelagic fishes. *Fish. Oceanogr.* **15**, 451–464. (doi:10.1111/j.1365-2419.2005.00393.x)
24. Prince ED, Luo J, Goodyear CP, Hoolihan JP, Snodgrass D, Orbesen ES, Serafy JE, Ortiz M, Schirripa MJ. 2010 Ocean scale hypoxia-based habitat compression of Atlantic istiophorid billfishes. *Fish. Oceanogr.* **19**, 448–462. (doi:10.1111/j.1365-2419.2010.00556.x)
25. Stramma L, Prince ED, Schmidtko S, Luo J, Hoolihan JP, Visbeck M, Wallace DWR, Brandt P, Körtzinger A. 2012 Expansion of oxygen minimum zones may reduce available habitat for tropical pelagic fishes. *Nat. Clim. Change* **2**, 33–37. (doi:10.1038/nclimate1304)
26. Ekau W, Auel H, Pörtner HO, Gilbert D. 2010 Impacts of hypoxia on the structure and processes in pelagic communities (zooplankton, macro-invertebrates and fish). *Biogeosciences* **7**, 1669–1699. (doi:10.5194/bg-7-1669-2010)
27. Bertrand A, Chaigneau A, Peraltilla S, Ledesma J, Graco M, Monetti F, Chavez FP. 2011 Oxygen: a fundamental property regulating pelagic ecosystem structure in the coastal southeastern tropical Pacific. *PLoS ONE* **6**, 2–9. (doi:10.1371/journal.pone.0029558)
28. Koslow JA, Goericke R, Lara-Lopez A, Watson W. 2011 Impact of declining intermediate-water oxygen on deepwater fishes in the California Current. *Mar. Ecol. Prog. Ser.* **436**, 207–218. (doi:10.3354/meps09270)
29. Chu JWF, Tunnicliffe V. 2015 Oxygen limitations on marine animal distributions and the collapse of epibenthic community structure during shoaling hypoxia. *Global Change Biol.* **21**, 2989–3004. (doi:10.1111/gcb.12898)
30. Bianchi D, Galbraith ED, Carozza DA, Mislan KAS, Stock CA. 2013 Intensification of open-ocean oxygen depletion by vertically migrating animals. *Nat. Geosci.* **6**, 545–548. (doi:10.1038/ngeo1837)
31. Netburn AN, Koslow JA. 2015 Dissolved oxygen as a constraint on daytime deep scattering layer depth in the southern California current ecosystem. *Deep Sea Res. Part I Oceanogr. Res. Pap.* **104**, 149–158. (doi:10.1016/j.dsr.2015.06.006)
32. Seibel BA, Schneider JL, Kaartvedt S, Wishner KF, Daly KL. 2016 Hypoxia tolerance and metabolic suppression in oxygen minimum zone euphausiids: implications for ocean deoxygenation and biogeochemical cycles. *Integr. Compar. Biol.* **56**, 510–523. (doi:10.1093/icb/icw091)
33. Sato KN, Levin LA, Schiff K. 2017 Habitat compression and expansion of sea urchins in response to changing climate conditions on the California continental shelf and slope

(1994–2013). *Deep Sea Res. Part II Top. Stud. Oceanogr.* **137**, 377–389. (doi:10.1016/j.dsr2.2016.08.012)
34. Ames AI. 2000 CNS energy metabolism as related to function. *Brain Res. Rev.* **34**, 42–68. (doi:10.1016/S0165-0173(00)00038-2)
35. Stenslokken KO, Milton SL, Lutz PL, Sundin L, Renshaw GMC, Stecyk JAW, Nilsson GE. 2008 Effect of anoxia on the electroretinogram of three anoxia-tolerant vertebrates. *Compar. Biochem. Physiol. A Mol. Integr. Physiol.* **150**, 395–403. (doi:10.1016/j.cbpa.2008.03.022)
36. Wong-Riley M. 2010 Energy metabolism of the visual system. *Eye Brain* **2**, 99–116. (doi:10.2147/EB.S9078)
37. Niven JE, Laughlin SB. 2008 Energy limitation as a selective pressure on the evolution of sensory systems. *J. Exp. Biol.* **211**, 1792–1804. (doi:10.1242/jeb.017574)
38. Laughlin SB, de Ruyter van Steveninck RR, Anderson JC. 1998 The metabolic cost of neural information. *Nat. Neurosci.* **1**, 36–41. (doi:10.1038/236)
39. Winkler BS, Arnold MJ, Brassell MA, Puro DG. 2000 Energy metabolism in human retinal Müller cells. *Invest. Ophthalmol. Vis. Sci.* **41**, 3183–3190. See https://www.ncbi.nlm.nih.gov/pubmed/10967082.
40. Erecińska M, Silver IA. 2001 Tissue oxygen tension and brain sensitivity to hypoxia. *Respir. Physiol.* **128**, 263–276. (doi:10.1016/S0034-5687(01)00306-1)
41. Anderson B. 1968 Ocular effects of changes in oxygen and carbon dioxide tension. *Trans. Am. Ophthalmol. Soc.* **66**, 423–474. See https://www.ncbi.nlm.nih.gov/pubmed/5720847.
42. Yu DY, Cringle SJ. 2001 Oxygen distribution and consumption within the retina in vascularised and avascular retinas and in animal models of retinal disease. *Prog. Retin. Eye Res.* **20**, 175–208. (doi:10.1016/S1350-9462(00)00027-6)
43. Waser W, Heisler N. 2005 Oxygen delivery to the fish eye: root effect as crucial factor for elevated retinal P_{O_2}. *J. Exp. Biol.* **208**, 4035–4047. (doi:10.1242/jeb.01874)
44. Medrano CJ, Fox DA. 1995 Oxygen consumption in the rat outer and inner retina: light- and pharmacologically-induced inhibition. *Exp. Eye Res.* **61**, 273–284. (doi:10.1016/S0014-4835(05)80122-8)
45. Kaur C, Foulds WS, Ling E-A. 2008 Hypoxia–ischemia and retinal ganglion cell damage. *Clin. Ophthalmol.* **2**, 879–889. (doi:10.2147/OPTH.S3361)
46. DeVilbiss C. 1998 Altitude and night vision goggles. *United States Air Force Res. Lab*, Report AFRL-HE-BR-TP-1998-0001, 22p.
47. Balldin U, Tutt RC, Dart TS, Fischer J, Harrison RT, Anderson EL, Smith JL, Workman AJ, Pinchak AM. 2007 The effects of 12 hours of low grade hypoxia at 10,000 ft at night in special operations forces aircraft operations on cognition, night vision, goggle vision, and subjective symptoms. *Air Force Res. Lab*, Report AFRL-HE-BR-TR-2007-0047 HAS, 29p.
48. Connolly DM, Barbur JL, Hosking SL, Moorhead IR. 2008 Mild hypoxia impairs chromatic sensitivity in the mesopic range. *Invest. Ophthalmol. Vis. Sci.* **49**, 820–827. (doi:10.1167/iovs.07-1004)
49. Mora C, Tittensor DP, Adl S, Simpson AGB, Worm B. 2011 How many species are there on Earth and in the ocean? *PLoS Biol.* **9**, 1–8. (doi:10.1371/journal.pbio.1001127)
50. Peacock AJ. 1998 ABC of oxygen: oxygen at high altitude. *BMJ* **317**, 1063–1066. (doi:10.1136/bmj.317.7165.1063)
51. Keeling RF. 2016 Atmospheric oxygen data for La Jolla, California. See http://scrippso2.ucsd.edu/index.
52. Falkowski PG *et al.* 2011 Ocean deoxygenation: past, present, and future. *EOS Trans. Am. Geophys. Union* **92**, 409–420. (doi:10.1029/2011EO460001)
53. Keeling RF. 1988 Measuring correlations between atmospheric oxygen and carbon dioxide mole fractions: a preliminary study using urban air. *J. Atmos. Chem.* **7**, 153–176. (doi:10.1007/BF00048044)
54. Childress JJ. 1995 Are there physiological and biochemical adaptations of metabolism in deep-sea animals? *Trends Ecol. Evol.* **10**, 30–36. (doi:10.1016/S0169-5347(00)88957-0)
55. Seibel BA. 2007 On the depth and scale of metabolic rate variation: scaling of oxygen consumption rates and enzymatic activity in the class Cephalopoda (Mollusca). *J. Exp. Biol.* **210**, 1–11. (doi:10.1242/jeb.02588)
56. Seibel BA, Drazen JC. 2007 The rate of metabolism in marine animals: environmental constraints, ecological demands and energetic opportunities. *Phil. Trans. R. Soc. B* **362**, 2061–2078. (doi:10.1098/rstb.2007.2101)

57. Grieshaber MK, Hardewig I, Kreutzer U, Pörtner HO. 1994 Physiological and metabolic responses to hypoxia in invertebrates. *Rev. Physiol. Biochem. Pharmacol.* **125**, 43–147. (doi:10.1007/BFb0030909)
58. Portner H-O, Grieshaber MK. 1993 Characteristics of the critical P_{O_2}(s): gas exchange, metabolic rate, and the mode of energy production. In *The vertebrate gas transport cascade: adaptations to environment and mode of life* (ed. JEPW Bicudo), pp. 330–357. Boca Raton, FL: CRC Press.
59. Childress JJ, Seibel BA. 1998 Life at stable low oxygen levels: adaptations of animals to oceanic oxygen minimum layers. *J. Exp. Biol.* **201**, 1223–1232. See https://www.ncbi.nlm.nih.gov/pubmed/9510533.
60. Rogers NJ, Urbina MA, Reardon EE, McKenzie DJ, Wilson RW. 2016 A new analysis of hypoxia tolerance in fishes using a database of critical oxygen level (P_{crit}). *Conserv. Physiol.* **4**, 1–19. (doi:10.1093/conphys/cow012.)
61. Seibel BA, Childress JJ. 2013 The real limits to marine life: a further critique of the respiration index. *Biogeosciences* **10**, 2815–2819. (doi:10.5194/bg-10-2815-2013)
62. Robinson E, Jerrett A, Black S, Davison W. 2013 Hypoxia impairs visual acuity in snapper (*Pagrus auratus*). *J. Compar. Physiol. A Neuroethol. Sens. Neural. Behav. Physiol.* **199**, 611–617. (doi:10.1007/s00359-013-0809-7)
63. Land MF, Fernald RD. 1992 The evolution of eyes. *Annu. Rev. Neurosci.* **15**, 1–29. (doi:10.1146/annurev.ne.15.030192.000245)
64. Warrant E. 2000 The eyes of deep-sea fishes and the changing nature of visual scenes with depth. *Phil. Trans. R. Soc. Lond. B* **355**, 1155–1159. (doi:10.1098/rstb.2000.0658)
65. Warrant EJ, Johnsen S. 2013 Vision and the light environment. *Curr. Biol.* **23**, R990–R994. (doi:10.1016/j.cub.2013.10.019)
66. Garm A, Nilsson D-E. 2014 Visual navigation in starfish: first evidence for the use of vision and eyes in starfish. *Proc. R. Soc. B* **281**, 20133011. (doi:10.1098/rspb.2013.3011)
67. Li L, Connors MJ, Kolle M, England GT, Speiser DI, Xiao X, Aizenberg J, Ortiz C. 2015 Multifunctionality of chiton biomineralized armor with an integrated visual system. *Science* **350**, 952–956. (doi:10.1126/science.aad1246)
68. Land MF, Nilsson D-E. 2002 *Animal eyes*, 1st edn. New York, NY: Oxford University Press.
69. Lythgoe JN. 1984 Visual pigments and environmental light. *Vision Res.* **24**, 1539–1550. (doi:10.1016/S0042-6989(84)80003-6)
70. Jerlov NG. 1951 Optical studies of ocean water. In *Reports of the Swedish Deep-Sea Expedition*, vol. 3, pp. 1–59.
71. Aksnes DL, Ohman MD, Rivière P. 2007 Optical effect on the nitracline in a coastal upwelling area. *Limnol. Oceanogr.* **52**, 1179–1187. (doi:10.4319/lo.2007.52.3.1179)
72. Holland HD. 2006 The oxygenation of the atmosphere and oceans. *Phil. Trans. R. Soc. B* **361**, 903–915. (doi:10.1098/rstb.2006.1838)
73. Arendt D. 2003 Evolution of eyes and photoreceptor cell types. *Int. J. Dev. Biol.* **47**, 563–571. See https://www.ncbi.nlm.nih.gov/pubmed/14756332.
74. Lamb TD. 2013 Evolution of phototransduction, vertebrate photoreceptors and retina. *Prog. Retin. Eye Res.* **36**, 52–119. (doi:10.1016/j.preteyeres.2013.06.001)
75. Nilsson D-E. 2013 Eye evolution and its functional basis. *Vis. Neurosci.* **30**, 5–20. (doi:10.1017/S0952523813000035)
76. Porter ML, Crandall KA. 2003 Lost along the way: the significance of evolution in reverse. *Trends Ecol. Evol.* **18**, 541–547. (doi:10.1016/S0169-5347(03)00244-1)
77. Schwab IR. 2012 *Evolution's witness: how eyes evolved*, 1st edn. New York, NY: Oxford University Press.
78. Gavelis GS, Hayakawa S, White III RA, Gojobori T, Suttle CA, Keeling PJ, Leander BS. 2015 Eye-like ocelloids are built from different endosymbiotically acquired components. *Nature* **523**, 204–207. (doi:10.1038/nature14593)
79. Speiser DI, Eernisse DJ, Johnsen S. 2011 A chiton uses aragonite lenses to form images. *Curr. Biol.* **21**, 665–670. (doi:10.1016/j.cub.2011.03.033)
80. Canfield DE. 1998 A new model for Proterozoic ocean chemistry. *Nature* **396**, 450–453. (doi:10.1038/24839)
81. Planavsky NJ, Reinhard CT, Wang X, Thomson D, McGoldrick P, Rainbird RH, Johnson T, Fischer WW, Lyons TW. 2014 Low Mid-Proterozoic atmospheric oxygen

levels and the delayed rise of animals. *Science* **346**, 635–638. (doi:10.1126/science.1258410)
82. Clarkson EN, Levi-Setti R. 1975 Trilobite eyes and the optics of Des Cartes and Huygens. *Nature* **254**, 663–667. (doi:10.1038/254663a0)
83. Knoll AH, Carroll SB. 1999 Early animal evolution: emerging views from comparative biology and geology. *Science* **284**, 2129–2137. (doi:10.1126/science.284.5423.2129)
84. Sperling EA, Frieder CA, Raman AV, Girguis PR, Levin LA, Knoll AH. 2013 Oxygen, ecology, and the Cambrian radiation of animals. *Proc. Natl Acad. Sci. USA* **110**, 13 446–13 451. (doi:10.1073/pnas.1312778110)
85. Parker A. 2003 *In the blink of an eye: how vision sparked the big bang of evolution*, 1st edn. New York, NY: Perseus.
86. Hessler RR. 1983 A defense of the caridoid facies; wherein the early evolution of the Eumalacostraca is discussed. In *Crustacean issues, 1: Crustacean phylogeny* (ed. FR Schram), pp. 145–164. Rotterdam, The Netherlands: AA Balkema.
87. Fernald RD. 2006 Casting a genetic light on the evolution of eyes. *Science* **313**, 1914–1919. (doi:10.1126/science.1127889)
88. Berenbrink M. 2007 Historical reconstructions of evolving physiological complexity: O_2 secretion in the eye and swimbladder of fishes. *J. Exp. Biol.* **210**, 1641–1652. (doi:10.1242/jeb.003319)
89. Serb JM, Eernisse DJ. 2008 Charting evolution's trajectory: using molluscan eye diversity to understand parallel and convergent evolution. *Evol. Educ. Outreach* **1**, 439–447. (doi:10.1007/s12052-008-0084-1)
90. Gray JS, Wu RS, Or YY. 2002 Effects of hypoxia and organic enrichment on the coastal marine environment. *Mar. Ecol. Prog. Ser.* **238**, 249–279. (doi:10.3354/meps238249)
91. Vaquer-Sunyer R, Duarte CM. 2008 Thresholds of hypoxia for marine biodiversity. *Proc. Natl Acad. Sci. USA* **105**, 15 452–15 457. (doi:10.1073/pnas.0803833105)
92. Pechenik JA. 2005 *Biology of the invertebrates*, 5th edn. New York, NY: McGraw-Hill.
93. Wittenberg JB, Wittenberg BA. 1962 Active secretion of oxygen into the eye of fish. *Nature* **194**, 106–107. (doi:10.1038/194106a0)
94. Wittenberg JB, Wittenberg BA. 1974 The choroid rete mirabile of the fish eye I. Oxygen secretion and structure: comparison with the swim bladder rete mirabile. *Biol. Bull.* **146**, 116–136. (doi:10.2307/1540402)
95. Fairbanks MB, Hoffert JR, Fromm PO. 1969 The dependence of the oxygen-concentrating mechanism of the teleost eye (*Salmo gairdneri*) on the enzyme carbonic anhydrase. *J. Gen. Physiol.* **54**, 203–211. (doi:10.1085/jgp.54.2.203)
96. Wittenberg JB, Haedrich RL. 1974 The choroid rete mirabile of the fish eye II. Distribution and relation to the pseudobranch and to the swimbladder rete mirabile. *Biol. Bull.* **146**, 137–156. (doi:10.2307/1540403)
97. Pelster B. 2001 The generation of hyperbaric oxygen tensions in fish. *News Physiol. Sci.* **16**, 287–291. See http://physiologyonline.physiology.org/content/16/6/287.
98. Yoshida M, Tsuneki K, Furuya H. 2010 Venous branching asymmetry in the pygmy squid *Idiosepius* (Cephalopoda: Idiosepiida) with reference to its phylogenetic position and functional significance. *J. Nat. Hist.* **44**, 2031–2039. (doi:10.1080/00222933.2010.485703)
99. Kaufman R, Weiss O, Sebbagh M, Ravid R, Gibbs-Bar L, Yaniv K, Inbal A. 2015 Development and origins of zebrafish ocular vasculature. *BMC Dev. Biol.* **15**, 18. (doi:10.1186/s12861-015-0066-9)
100. Eastman JT. 1988 Ocular morphology in Antarctic notothenioid fishes. *J. Morphol.* **196**, 283–306. (doi:10.1002/jmor.1051960303)
101. Eastman JT, Lannoo MJ. 2011 Divergence of brain and retinal anatomy and histology in pelagic Antarctic notothenioid fishes of the sister taxa *Dissostichus* and *Pleuragramma*. *J. Morphol.* **272**, 419–441. (doi:10.1002/jmor.10926)
102. Wujcik JM, Wang G, Eastman JT, Sidell BD. 2007 Morphometry of retinal vasculature in Antarctic fishes is dependent upon the level of hemoglobin in circulation. *J. Exp. Biol.* **210**, 815–824. (doi:10.1242/jeb.001867)
103. Ernest JT, Krill AE. 1971 The effect of hypoxia on visual function: psychophysical studies. *Invest. Ophthalmol. Vis. Sci.* **10**, 323–328. See http://iovs.arvojournals.org/article.aspx?articleid=2122182.

104. Perkins GA, Ellisman MH, Fox DA. 2003 Three-dimensional analysis of mouse rod and cone mitochondrial cristae architecture: bioenergetic and functional implications. *Mol. Vis.* **9**, 60–73. See https://www.ncbi.nlm.nih.gov/pubmed/12632036.
105. Wagner BA, Venkataraman S, Buettner GR. 2011 The rate of oxygen utilization by cells. *Free Radic. Biol. Med.* **51**, 700–712. (doi:10.1016/j.freeradbiomed.2011.05.024)
106. Okawa H, Sampath AP, Laughlin SB, Fain GL. 2008 ATP consumption by mammalian rod photoreceptors in darkness and in light. *Curr. Biol.* **18**, 1917–1921. (doi:10.1016/j.cub.2008.10.029)
107. Niven JE, Vähäsöyrinki M, Juusola M, Vahasoyrinki M, Juusola M. 2003 Shaker K^+-channels are predicted to reduce the metabolic cost of neural information in *Drosophila* photoreceptors. *Proc. Biol. Sci.* **270**, S58–S61. (doi:10.1098/rsbl.2003.0010)
108. Nikonov SS, Kholodenko R, Lern J, Pugh ENJ. 2006 Physiological features of the S- and M-cone photoreceptors of wild-type mice from single-cell recordings. *J. Gen. Physiol.* **127**, 359–374. (doi:10.1085/jgp.200609490)
109. Hagins WA, Penn RD, Yoshikami S. 1970 Dark current and photocurrent in retinal rods. *Biophys. J.* **10**, 380–412. (doi:10.1016/S0006-3495(70)86308-1)
110. Ames III A, Gurian BS. 1963 Effects of glucose and oxygen deprivation on function of isolated mammalian retina. *J. Neurophysiol.* **26**, 617–634. See https://www.ncbi.nlm.nih.gov/pubmed/14012566.
111. Pinto LH, Brown JE. 1977 Intracellular recordings from photoreceptors of the squid (*Loligo pealii*). *J. Compar. Physiol. A* **122**, 241–250. (doi:10.1007/BF00611893)
112. Nilsson GE. 2001 Surviving anoxia with the brain turned on. *News Physiol. Sci.* **16**, 217–221. See http://physiologyonline.physiology.org/content/16/5/217.
113. Lutz PL, Nilsson GE. 1997 Contrasting strategies for anoxic brain survival—glycolysis up or down. *J. Exp. Biol.* **200**, 411–419. See http://jeb.biologists.org/content/200/2/411.
114. Johansson D, Nilsson GE, Døving KB. 1997 Anoxic depression of light-evoked potentials in retina and optic tectum of crucian carp. *Neurosci. Lett.* **237**, 73–76. See https://www.ncbi.nlm.nih.gov/pubmed/9453218.
115. Marc RE. 1982 Spatial organization of neurochemically classified interneurons of the goldfish retina I. Local patterns. *Vision Res.* **22**, 589–608. (doi:10.1016/0042-6989(82)90117-1)
116. Lasater E. 1990 Neurotransmitters and neuromodulators of the fish retina. In *The visual systems of fish* (eds RH Douglas, MBA Djamgoz), pp. 211–237. London, UK: Chapman and Hall.
117. O'Neill PJ, Jinks RN, Herzog ED, Battelle BA, Kass L, Renninger GH, Chamberlain SC. 1995 The morphology of the dorsal eye of the hydrothermal vent shrimp, *Rimicaris exoculata*. *Vis. Neurosci.* **12**, 861–875. (doi:10.1017/S0952523800009421)
118. Ostroy SE, Gaitatzes CG, Friedmann AL. 1993 Hypoxia inhibits rhodopsin regeneration in the excised mouse eye. *Invest. Ophthalmol. Vis. Sci.* **34**, 447–452. See https://www.ncbi.nlm.nih.gov/pubmed/8440599.
119. Miyazono S, Shimauchi-Matsukawa Y, Tachibanaki S, Kawamura S. 2008 Highly efficient retinal metabolism in cones. *Proc. Natl Acad. Sci. USA* **105**, 16 051–16 056. (doi:10.1073/pnas.0806593105)
120. Wu RSS. 2002 Hypoxia: from molecular responses to ecosystem responses. *Mar. Pollut. Bull.* **45**, 35–45. (doi:10.1016/S0025-326X(02)00061-9)
121. Burnett LE, Stickle WB. 2001 Physiological responses to hypoxia. *Coast. hypoxia consequences living Resour. Ecosyst*, 101–114. (doi:10.1029/CE058p0101)
122. Barve S, Dhondt AA, Mathur VB, Cheviron ZA. 2016 Life-history characteristics influence physiological strategies to cope with hypoxia in Himalayan birds. *Proc. R. Soc. B* **283**, 20162201. (doi:10.1098/rspb.2016.2201)
123. Mirceta S, Signore A V, Burns JM, Cossins AR, Campbell KL, Berenbrink M. 2013 Evolution of mammalian diving capacity traced by myoglobin net surface charge. *Science* **340**, 1234192. (doi:10.1126/science.1234192)
124. Tezel G, Wax MB. 2004 Hypoxia-inducible factor 1α in the glaucomatous retina and optic nerve head. *Arch. Ophthalmol.* **122**, 1348–1356. (doi:10.1001/archopht.122.9.1348)
125. Kelly BD *et al.* 2003 Cell type-specific regulation of angiogenic growth factor gene expression and induction of angiogenesis in nonischemic tissue by a constitutively active form of hypoxia-inducible factor 1. *Circ. Res.* **93**, 1074–1081. (doi:10.1161/01.RES.0000102937.50486.1B)

126. Fong GH. 2008 Mechanisms of adaptive angiogenesis to tissue hypoxia. *Angiogenesis* **11**, 121–140. (doi:10.1007/s10456-008-9107-3)
127. Spilsbury K, Garrett KL, Shen WY, Constable IJ, Rakoczy PE. 2000 Overexpression of vascular endothelial growth factor (VEGF) in the retinal pigment epithelium leads to the development of choroidal neovascularization. *Am. J. Pathol.* **157**, 135–144. (doi:10.1016/S0002-9440(10)64525-7)
128. Neely KA, Gardner TW. 1998 Ocular neovascularization: clarifying complex interactions. *Am. J. Pathol.* **153**, 665–670. (doi:10.1016/S0002-9440(10)65607-6)
129. Schwerzmann K, Hoppeler H, Kayar SR, Weibel ER. 1989 Oxidative capacity of muscle and mitochondria: correlation of physiological, biochemical, and morphometric characteristics. *Proc. Natl Acad. Sci. USA* **86**, 1583–1587. (doi:10.1073/pnas.86.5.1583)
130. Cerretelli P. 1976 Limiting factors to oxygen transport on Mount Everest. *J. Appl. Physiol.* **40**, 658–667. See http://jap.physiology.org/content/40/5/658.
131. Ferretti G. 2003 Limiting factors to oxygen transport on Mount Everest 30 years after: a critique of Paolo Cerretelli's contribution to the study of altitude physiology. *Eur. J. Appl. Physiol.* **90**, 344–350. (doi:10.1007/s00421-003-0923-2)
132. Howald H, Hoppeler H. 2003 Performing at extreme altitude: muscle cellular and subcellular adaptations. *Eur. J. Appl. Physiol.* **90**, 360–364. (doi:10.1007/s00421-003-0872-9)
133. Wald G. 1957 The metamorphosis of the visual systems in the sea lamprey. *J. Gen. Physiol.* **40**, 901–914. (doi:10.1085/jgp.40.6.901)
134. Beatty DD. 1984 Visual pigments and the labile scotopic visual system of fish. *Vision Res.* **24**, 1563–1573. (doi:10.1016/0042-6989(84)90314-6)
135. Carlisle DB, Denton EJ. 1959 On the metamorphosis of the visual pigments of *Anguilla anguilla* (L.). *J. Mar. Biol. Assoc. U.K.* **38**, 97–102. (doi:10.1017/S0025315400015629)
136. Dartnall HJA, Lander MR, Munz FW. 1961 Periodic changes in the visual pigment of a fish. In *Proc. 3rd Int. Congress of Photobiology, Copenhagen*, 1960, pp. 203–213.
137. Przeslawski R. 2004 A review of the effects of environmental stress on embryonic development within intertidal gastropod egg masses. *Molluscan Res.* **24**, 43–63. (doi:10.1071/MR04001)
138. Strathmann RR, Strathmann MF. 1995 Oxygen-supply and limits on aggregation of embryos. *J. Mar. Biol. Assoc. U.K.* **75**, 413–428. (doi:10.1017/S0025315400018270)
139. Gutowska MA, Melzner F. 2009 Abiotic conditions in cephalopod (*Sepia officinalis*) eggs: embryonic development at low pH and high pCO_2. *Mar. Biol.* **156**, 515–519. (doi:10.1007/s00227-008-1096-7)
140. Lee Y-H, Chang Y-C, Yan HY, Chiao C-C. 2013 Early visual experience of background contrast affects the expression of NMDA-like glutamate receptors in the optic lobe of cuttlefish, *Sepia pharaonis*. *J. Exp. Mar. Biol. Ecol.* **447**, 86–92. (doi:10.1016/j.jembe.2013.02.014)
141. Chen DS, Van Dykhuizen G, Hodge J, Gilly WF. 1996 Ontogeny of copepod predation in juvenile squid (*Loligo opalescens*). *Biol. Bull.* **190**, 69–81. (doi:10.2307/1542676)
142. Seymour RS, Roberts JD, Mitchell NJ, Blaylock AJ. 2000 Influence of environmental oxygen on development and hatching of aquatic eggs of the Australian frog, *Crinia georgiana*. *Physiol. Biochem. Zool.* **73**, 501–507. (doi:10.1086/317739)
143. Kim TW, Barry JP, Micheli F. 2013 The effects of intermittent exposure to low-pH and low-oxygen conditions on survival and growth of juvenile red abalone. *Biogeosciences* **10**, 7255–7262. (doi:10.5194/bg-10-7255-2013)
144. Fernandez M, Ruiz-Tagle N, Cifuentes S, Portner HO, Arntz W. 2003 Oxygen-dependent asynchrony of embryonic development in embryo masses of brachyuran crabs. *Mar. Biol.* **142**, 559–565. (doi:10.1007/S00227-002-0965-8)
145. Arnold JM. 1974 Embryonic development. In *A guide to laboratory use of the squid Loligo pealei* (eds JM Arnold, WC Summers, DL Gilbert, RS Manalis, NW Daw, RJ Lasek), p. 74. Woods Hole, MA: Marine Biological Laboratory.
146. Navarro MO, Kwan GT, Batalov O, Choi CY, Pierce NT, Levin LA. 2016 Development of embryonic market squid, *Doryteuthis opalescens*, under chronic exposure to low environmental pH and $[O_2]$. *PLoS ONE* **11**, e0167461. (doi:10.1371/journal.pone.0167461)
147. Wang WX, Widdows J. 1991 Physiological responses of mussel larvae *Mytilus edulis* to environmental hypoxia and anoxia. *Mar. Ecol. Prog. Ser.* **70**, 223–236. (doi:10.3354/meps070223)

148. Gowland FC, Moltschaniwskyj NA, Steer MA. 2002 Description and quantification of developmental abnormalities in a natural *Sepioteuthis australis* spawning population (Mollusca: Cephalopoda). *Mar. Ecol. Prog. Ser.* **243**, 133–141. (doi:10.3354/meps243133)
149. Ingalls TH, Philbrook FR. 1958 Monstrosities induced by hypoxia. *New Engl. J. Med.* **259**, 558–564. (doi:10.1056/NEJM199401273300403)
150. Navarro M. 2014 Consequences of environmental variability for spawning and embryo development of inshore market squid *Doryteuthis opalescens*. Doctoral thesis, University of California, San Diego, pp. 1–187.
151. Boeuf G, Le Bail P-Y. 1999 Does light have an influence on fish growth? *Aquaculture* **177**, 129–152. (doi:10.1016/S0044-8486(99)00074-5)
152. Forward RB. 1988 Diel vertical migration: zooplankton photobiology and behavior. In *Oceanography and marine biology: an annual review*, vol. 26, pp. 361–393.
153. Crisp DJ, Ritz DA. 1973 Responses of cirripede larvae to light. I. Experiments with white light. *Mar. Biol.* **23**, 327–335. (doi:10.1007/BF00389340)
154. Rivers TJ, Morin JG. 2008 Complex sexual courtship displays by luminescent male marine ostracods. *J. Exp. Biol.* **211**, 2252–2262. (doi:10.1242/jeb.011130)
155. Charpentier CL, Cohen JH. 2015 Chemical cues from fish heighten visual sensitivity in larval crabs through changes in photoreceptor structure and function. *J. Exp. Biol.* **218**, 3381–3390. (doi:10.1242/jeb.125229)
156. Cohen JH, Forward RB. 2005 Diel vertical migration of the marine copepod *Calanopia americana*. I. Twilight DVM and its relationship to the diel light cycle. *Mar. Biol.* **147**, 387–398. (doi:10.1007/s00227-005-1569-x)
157. Scherer E. 1971 Effects of oxygen depletion and of carbon dioxide buildup on the photic behavior of the walleye (*Stizostedion vitreum vitreum*). *J. Fish. Res. Board Canada* **28**, 1303–1307. (doi:10.1139/f71-197)
158. Sandberg E, Tallqvist M, Bonsdorff E. 1996 The effects of reduced oxygen content on predation and siphon cropping by the brown shrimp, *Crangon crangon*. *Mar. Ecol.* **17**, 411–423. (doi:10.1111/j.1439-0485.1996.tb00518.x)
159. Thetmeyer H, Waller U, Black KD, Inselmann S, Rosenthal H. 1999 Growth of European sea bass (*Dicentrarchus labrax* L.) under hypoxic and oscillating oxygen conditions. *Aquaculture* **174**, 355–367. (doi:10.1016/S0044-8486(99)00028-9)
160. Cohen JH, Frank TM. 2006 Visual physiology of the Antarctic amphipod *Abyssorchomene plebs*. *Biol. Bull.* **211**, 140–148. (doi:10.2307/4134588)
161. Fowler B, Banner J, Pogue J. 1993 The slowing of visual processing by hypoxia. *Ergonomics* **36**, 727–735. (doi:10.1080/00140139308967933)
162. Van Liere BJ, Stickney JC. 1963 *Hypoxia*. Chicago, IL: University of Chicago Press.
163. Das T, Stickle WB. 1993 Sensitivity of crabs *Callinectes sapidus* and *C. similis* and the gastropod *Stramonita haemastoma* to hypoxia and anoxia. *Mar. Ecol. Prog. Ser.* **98**, 263–274. (doi:10.3354/meps098263)
164. Seitz RD, Marshall LS, Hines AH, Clark KL. 2003 Effects of hypoxia on predator–prey dynamics of the blue crab *Callinectes sapidus* and the Baltic clam *Macoma balthica* in Chesapeake Bay. *Mar. Ecol. Prog. Ser.* **257**, 179–188. (doi:10.3354/meps257179)
165. Keller TA, Powell I, Weissburg MJ. 2003 Role of olfactory appendages in chemically mediated orientation of blue crabs. *Mar. Ecol. Prog. Ser.* **261**, 217–231. (doi:10.3354/meps261217)
166. Lunt J, Smee DL. 2015 Turbidity interferes with foraging success of visual but not chemosensory predators. *PeerJ* **3**, e1212. (doi:10.7717/peerj.1212)
167. Vazquez FJS, Munoz-Cueto JA (eds). 2014 *Biology of the European sea bass*. Boca Raton, FL: CRC Press.
168. Tallqvist M, Sandberg-Kilpi E, Bonsdorff E. 1999 Juvenile flounder, *Platichthys flesus* (L.), under hypoxia: effects on tolerance, ventilation rate and predation efficiency. *J. Exp. Mar. Biol. Ecol.* **242**, 75–93. (doi:10.1016/S0022-0981(99)00096-9)
169. Petersen JK, Pihl L. 1995 Responses to hypoxia of plaice, *Pleuronectes platessa*, and dab, *Limanda limanda*, in the south-east Kattegat: distribution and growth. *Environ. Biol. Fishes* **43**, 311–321. (doi:10.1007/BF00005864)
170. VanBlaricom GR. 1982 Experimental analyses of structural regulation in a marine sand community exposed to oceanic swell. *Ecol. Monogr.* **52**, 283–305. (doi:10.2307/2937332)

171. Reynolds JD, Jones JC. 1999 Female preference for preferred males is reversed under low oxygen conditions in the common goby (*Pomatoschistus microps*). *Behav. Ecol.* **10**, 149–154. (doi:10.1093/beheco/10.2.149)
172. Järvenpää M, Lindström K. 2004 Water turbidity by algal blooms causes mating system breakdown in a shallow-water fish, the sand goby *Pomatoschistus minutus*. *Proc. R. Soc. Lond. B* **271**, 2361–2365. (doi:10.1098/rspb.2004.2870)
173. Gilly WF, Beman JM, Litvin SY, Robison BH. 2013 Oceanographic and biological effects of shoaling of the oxygen minimum zone. *Annu. Rev. Mar. Sci.* **5**, 393–420. (doi:10.1146/annurev-marine-120710-100849)
174. Hutchinson GE. 1967 A treatise on limnology, Vol II: Introduction to lake biology and the limnoplankton. New York, NY: Wiley.
175. Lampert W. 1989 The adaptive significance of diel vertical migration of zooplankton. *Funct. Ecol.* **3**, 21–27. (doi:10.2307/2389671)
176. Ohman MD, Frost BW, Cohen EB. 1983 Reverse diel vertical migration: an escape from invertebrate predators. *Science* **220**, 1404–1407. (doi:10.1126/science.220.4604.1404)
177. Bertrand A, Ballón M, Chaigneau A. 2010 Acoustic observation of living organisms reveals the upper limit of the oxygen minimum zone. *PLoS ONE* **5**, e0010330. (doi:10.1371/journal.pone.0010330)
178. Alegre A, Ménard F, Tafur R, Espinoza P, Argüelles J, Maehara V, Flores O, Simier M, Bertrand A. 2014 Comprehensive model of jumbo squid *Dosidicus gigas* trophic ecology in the northern Humboldt Current system. *PLoS ONE* **9**, e85919. (doi:10.1371/journal.pone.0085919)
179. Wishner KF, Outram DM, Seibel BA, Daly KL, Williams RL. 2013 Zooplankton in the eastern tropical north Pacific: boundary effects of oxygen minimum zone expansion. *Deep Sea Res. Part I Oceanogr. Res. Pap.* **79**, 122–140. (doi:10.1016/j.dsr.2013.05.012)
180. McClatchie S, Goericke R, Cosgrove R, Auad G, Vetter R. 2010 Oxygen in the Southern California Bight: multidecadal trends and implications for demersal fisheries. *Geophys. Res. Lett.* **37**, L19602. (doi:10.1029/2010GL044497)
181. Rosa R, Seibel BA. 2008 Synergistic effects of climate-related variables suggest future physiological impairment in a top oceanic predator. *Proc. Natl Acad. Sci. USA* **105**, 20 776–20 780. (doi:10.1073/pnas.0806886105)
182. Roe, HSJ. 1983 Vertical distributions of euphausiids and fish in relation to light—intensity in the Northeastern Atlantic. *Mar. Biol.* **77**, 287–298. (doi:10.1007/BF00395818)
183. Frank TM, Widder EA. 2002 Effects of a decrease in downwelling irradiance on the daytime vertical distribution patterns of zooplankton and micronekton. *Mar. Biol.* **140**, 1181–1193. (doi:10.1007/s00227-002-0788-7)
184. Staby A, Aksnes DL. 2011 Follow the light—diurnal and seasonal variations in vertical distribution of the mesopelagic fish *Maurolicus muelleri*. *Mar. Ecol. Prog. Ser.* **422**, 265–273. (doi:10.3354/meps08938)
185. Brynildson OM, Kempinger JJ. 1973 *Production, food and harvest of trout in Nebish Lake, Wisconsin*. Tech. Bull. no. 65, Department of Natural Resources, Madison, Wisconsin, 24p.
186. De Robertis A, Ryer CH, Veloza A, Brodeur RD. 2003 Differential effects of turbidity on prey consumption of piscivorous and planktivorous fish. *Can. J. Fish. Aquat. Sci.* **60**, 1517–1526. (doi:10.1139/f03-123)
187. Zhang H, Ludsin SA, Mason DM, Adamack AT, Brandt SB, Zhang X, Kimmel DG, Roman MR, Boicourt WC. 2009 Hypoxia-driven changes in the behavior and spatial distribution of pelagic fish and mesozooplankton in the northern Gulf of Mexico. *J. Exp. Mar. Biol. Ecol.* **381**, S80–S91. (doi:10.1016/j.jembe.2009.07.014)
188. Aksnes DL, Giske J. 1993 A theoretical model of aquatic visual feeding. *Ecol. Modell.* **67**, 233–250. (doi:10.1016/0304-3800(93)90007-F)
189. Gunderson AR, Armstrong EJ, Stillman JH. 2016 Multiple stressors in a changing world: the need for an improved perspective on physiological responses to the dynamic marine environment. *Annu. Rev. Mar. Sci.* **8**, 357–378. (doi:10.1146/annurev-marine-122414-033953)
190. Gobler CJ *et al.* 2016 Hypoxia and acidification in ocean ecosystems: coupled dynamics and effects on marine life. *Biol. Lett.* **12**, 199–229. (doi:10.1098/rsbl.2015.0976)
191. Reum JCP *et al.* 2015 Interpretation and design of ocean acidification experiments in upwelling systems in the context of carbonate chemistry co-variation with temperature and oxygen. *ICES J. Mar. Sci.* **73**, 582–595. (doi:10.1093/icesjms/fsu231)

192. Burnett LE. 1997 The challenges of living in hypoxic and hypercapnic aquatic environments. *Am. Zool.* **37**, 633–640. (doi:10.1093/icb/37.6.633)
193. Stover KK, Burnett KG, McElroy EJ, Burnett LE. 2013 Locomotory fatigue and size in the Atlantic blue crab, *Callinectes sapidus*. *Biol. Bull.* **224**, 68–78. (doi:10.1086/BBLv224n2p68)
194. Lehtonen MP, Burnett LE. 2016 Effects of hypoxia and hypercapnic hypoxia on oxygen transport and acid–base status in the Atlantic blue crab, *Callinectes sapidus*, during exercise. *J. Exp. Zool. A Ecol. Genet. Physiol.* **325**, 598–609. (doi:10.1002/jez.2054)
195. Miller S, Breitburg D, Burrell R, Keppel A. 2016 Acidification increases sensitivity to hypoxia in important forage fishes. *Mar. Ecol. Prog. Ser.* **549**, 1–8. (doi:10.3354/meps11695)
196. Rathburn CK, Sharp NJ, Ryan JC, Neely MG, Cook M, Chapman RW, Burnett LE, Burnett KG. 2013 Transcriptomic responses of juvenile Pacific whiteleg shrimp, *Litopenaeus vannamei*, to hypoxia and hypercapnic hypoxia. *Physiol. Genomics* **45**, 794–807. (doi:10.1152/physiolgenomics.00043.2013)
197. Johnson JG, Paul MR, Kniffin CD, Anderson PE, Burnett LE, Burnett KG. 2015 High CO_2 alters the hypoxia response of the Pacific whiteleg shrimp (*Litopenaeus vannamei*) transcriptome including known and novel hemocyanin isoforms. *Physiol. Genomics* **47**, 548–558. (doi:10.1152/physiolgenomics.00031.2015)
198. Munday PL, Dixson DL, Donelson JM, Jones GP, Pratchett MS, Devitsina GV, Døving KB. 2009 Ocean acidification impairs olfactory discrimination and homing ability of a marine fish. *Proc. Natl Acad. Sci. USA* **106**, 1848–1852. (doi:10.1073/pnas.0809996106)
199. Dixson DL, Munday PL, Jones GP. 2010 Ocean acidification disrupts the innate ability of fish to detect predator olfactory cues. *Ecol. Lett.* **13**, 68–75. (doi:10.1111/j.1461-0248.2009.01400.x)
200. Simpson SD, Munday PL, Wittenrich ML, Manassa R, Dixson DL, Gagliano M, Yan HY. 2011 Ocean acidification erodes crucial auditory behaviour in a marine fish. *Biol. Lett.* **7**, 917–920. (doi:10.1098/rsbl.2011.0293)
201. Forsgren E, Dupont S, Jutfelt F, Amundsen T. 2013 Elevated CO_2 affects embryonic development and larval phototaxis in a temperate marine fish. *Ecol. Evol.* **3**, 3637–3646. (doi:10.1002/ece3.709)

Chapter 2, in full, is a reprint of the material as it appears in **McCormick, L. R.** and L. A. Levin. 2017. Physiological and ecological implications of ocean deoxygenation for vision in marine organisms. Philosophical Transactions of the Royal Society A 375: 20160322. http://dx.doi.org/10.1098/rsta.2016.0322. The dissertation author was the primary investigator and author of this material.

CHAPTER 3

Vision is highly sensitive to oxygen availability in marine invertebrate larvae

Synopsis

This chapter is a research article showing the effects of reduced partial pressure of oxygen on retinal function in larvae of four species of marine invertebrates. The physiological response to reduced oxygen partial pressure is tested in both the sensitivity to light and the temporal resolution.

This chapter is presented as a paper. "Vision is highly sensitive to oxygen availability in marine invertebrate larvae," was published as a research paper in *Journal of Experimental Biology* in 2019.

© 2019. Published by The Company of Biologists Ltd | Journal of Experimental Biology (2019) 222, jeb200899. doi:10.1242/jeb.200899

RESEARCH ARTICLE

Vision is highly sensitive to oxygen availability in marine invertebrate larvae

Lillian R. McCormick[1,*], Lisa A. Levin[1] and Nicholas W. Oesch[2,3]

ABSTRACT

For many animals, evolution has selected for complex visual systems despite the high energetic demands associated with maintaining eyes and their processing structures. Therefore, the metabolic demands of visual systems make them highly sensitive to fluctuations in available oxygen. In the marine environment, oxygen changes over daily, seasonal and inter-annual time scales, and there are large gradients of oxygen with depth. Vision is linked to survival in many marine animals, particularly among the crustaceans, cephalopods and fish, and early life stages of these groups rely on vision for prey capture, predator detection and their distribution in the water column. Using *in vivo* electroretinogram recordings, we show that there is a decrease in retinal sensitivity to light in marine invertebrates when exposed to reduced oxygen availability. We found a 60–100% reduction in retinal responses in the larvae of cephalopods and crustaceans: the market squid (*Doryteuthis opalescens*), the two-spot octopus (*Octopus bimaculatus*), the tuna crab (*Pleuroncodes planipes*) and the graceful rock crab (*Metacarcinus gracilis*). A decline in oxygen also decreases the temporal resolution of vision in *D. opalescens*. These results are the first demonstration that vision in marine invertebrates is highly sensitive to oxygen availability and that the thresholds for visual impairment from reduced oxygen are species-specific. Oxygen-impaired retinal function may change the visual behaviors crucial to survival in these marine larvae. These findings may impact our understanding of species' vulnerability to ocean oxygen loss and suggest that researchers conducting electrophysiology experiments should monitor oxygen levels, as even small changes in oxygen may affect the results.

KEY WORDS: Zooplankton, Phototransduction, Physiology, Electroretinogram, Hypoxia

INTRODUCTION

Phototransduction is the process by which the energy from photons of light is translated into neural signals by photoreceptor cells (Rayer et al., 1990). The neural signaling requires the constant depolarization and repolarization of photoreceptors and downstream neurons, making vision one of the most energetically expensive processes in many animal systems (Ames, 2000; Pepe, 2001). These metabolic demands increase as temporal and spatial resolution increase and the visual system becomes more complex (Niven and Laughlin, 2008; Wong-Riley, 2010). As in terrestrial vertebrates, many marine invertebrates possess complex visual systems with a range of contrast and light sensitivities as well as sufficient temporal resolution for executing vital tasks such as prey capture or predator evasion (Warrant and Johnsen, 2013). One technique used to measure visual physiology is the electroretinogram (ERG), which records the summed activity of photoreceptors and downstream neurons in the eye in response to visual stimulation (Brown, 1968). The ERG is commonly used to measure the response of retinas in both vertebrate (Brown, 1968; Chen and Stark, 1994; Chrispell et al., 2015) and invertebrate systems (Cohen et al., 2015; Cronin and Forward, 1988; Frank, 1999; Lange and Hartline, 1974). Oxygen effects on vision have been extensively studied in humans and other terrestrial vertebrates, where a decline in oxygen (hypoxia) is known to cause a decrease in both sensitivity to light (Linsenmeier et al., 1983; McFarland and Evans, 1939) and temporal resolution (Fowler et al., 1993). In these vertebrate experiments, diminished sensitivity to light is demonstrated by a decrease in amplitude of visual responses after exposure to lower levels of oxygen, whereas reduced temporal resolution is seen as an inability of the retina to respond to high-frequency flashes of light. Both light and sufficient levels of oxygen are thus required for normal visual function.

In the marine environment, large gradients of irradiance and oxygen exist with depth, and changes in the partial pressure of oxygen (P_{O_2}) with water depth in the ocean can be up to 10-fold greater than the changes in atmospheric P_{O_2} over terrestrial altitude (McCormick and Levin, 2017). For example, oxygen content with depth can decline by as much as 35% between 7 and 17 m depth off the coast of California (Frieder et al., 2012), and varies over time with diurnal/diel cycling, seasonal hypoxia and El Niño–Southern Oscillation cycles (Levin et al., 2015). Organisms that experience large changes in both irradiance and oxygen include those in regions with coastal hypoxia and diel oxygen cycling (Altieri and Gedan, 2015; Tyler et al., 2009), shallow oxygen minimum and oxygen limited zones (Gilly et al., 2013; Wishner et al., 2013; Wishner et al., 2018), and shallow embayments or fjords (Hansen et al., 2002).

Understanding how the visual systems of marine organisms respond to reduced oxygen availability will provide information on constraints on habitat preference in marine organisms. Highly visual marine organisms include cephalopods (e.g. squid, octopus), arthropods (e.g. crabs, krill) and fish (McCormick and Levin, 2017). These groups support major world fisheries (FAO, 2018), and the larval stage of marine organisms is a crucial bottleneck for survival for recruitment to the fishery and reproductive population. Early life stages of arthropods, cephalopods and fish rely on vision for behaviors essential to their survival, including prey capture and predator avoidance, and as a cue for diel vertical migration (Forward, 1988; Robin et al., 2014). Vision may also be one of the sensory modalities used in larval choice of settlement site and

[1]Integrative Oceanography Division, Center for Marine Biodiversity and Conservation, Scripps Institution of Oceanography, La Jolla, CA 92093-0218, USA. [2]Department of Psychology, University of California San Diego, La Jolla, CA 92093, USA. [3]Department of Ophthalmology, University of California San Diego, La Jolla, CA 92093, USA.

*Author for correspondence (lrmccorm@ucsd.edu)

L.R.M., 0000-0001-5299-4762; L.A.L., 0000-0002-2858-8622

Received 30 January 2019; Accepted 12 April 2019

Journal of Experimental Biology

Journal of Experimental Biology (2019) 222, jeb200899. doi:10.1242/jeb.200899

List of symbols and abbreviations

CalCOFI	California Cooperative Oceanic Fisheries Investigations
ERG	electroretinogram
IR	infrared
PFD	photon flux density (μmol photons m^{-2} s^{-1})
P_{O_2}	partial pressure of oxygen
PSD	power spectral density
V_{10}	P_{O_2} with 10% of retinal function
V_{50}	P_{O_2} with 50% of retinal function
V_{90}	P_{O_2} with 90% of retinal function

detection of conspecifics in species with an adult benthic stage (Lecchini et al., 2010; Lecchini, 2011). Hypoxia is known to affect many physiological processes in marine organisms (Grieshaber et al., 1994; Wu, 2002), but to our knowledge, the effects of hypoxia on visual physiology in marine invertebrates, and specifically their larvae, have not been studied. Here, we determined how exposure to low oxygen affects (1) visual sensitivity to light, (2) the dynamic range (range of irradiance that can be detected visually) and (3) the temporal properties of vision in larvae of the market squid (*Doryteuthis opalescens*), the two-spot octopus (*Octopus bimaculatus*), the tuna crab (*Pleuroncodes planipes*) and the graceful rock crab (*Metacarcinus gracilis*). These species are representative of highly visual invertebrates of both economic and ecological interest. We hypothesized that exposure to reduced P_{O_2} in marine invertebrate larvae would decrease the magnitude of the ERG response to light stimuli, and that reduced P_{O_2} would decrease the temporal resolution of the eye.

MATERIALS AND METHODS

To investigate how retinal function changed in response to a decline in P_{O_2}, we recorded *in vivo* ERGs in tethered, intact larvae while controlling the P_{O_2} of pH-buffered seawater flowing over the animal (Fig. 1A). To control for differences in the shape of the ERG waveform across different species, we measured the size of the ERG response by integrating over the entire response. P_{O_2} in the recording chamber was measured throughout the experiments using a fiber optic probe. Partial pressure units (kPa) are presented to best represent the oxygen available for animal tissues (Seibel, 2011), but wherever reasonable, a conversion to oxygen concentration (μmol kg^{-1} O_2) was also calculated. The term 'normoxia' is used to describe surface ocean oxygen levels, approximately 100–105% saturation for the given temperature and salinity. To compare the magnitude of visual stimulation across species, we report light stimuli as a species-specific irradiance [species photon flux density (PFD; μmol photons m^{-2} s^{-1})], which is the irradiance of light at the plane of the animal's eye weighted to the spectral sensitivities for each species (Fig. S1).

Animal collection

Larvae of *Octopus bimaculatus* Verrill 1883, *Metacarcinus gracilis* (Dana 1852) and *Pleuroncodes planipes* Stimpson 1860 were obtained by conducting plankton tows at ∼30 m depth with a 325-μm mesh net in the Southern California Bight off the coast of La Jolla, CA, USA, at a recurrent market squid egg bed site (McGowan, 1954) (CA collection permit: SCP-13633; 32°51′ 30.13″N, 117°16′25.93″W) during the natural reproductive periods of each species (August 2017–April 2018). After collection, larvae of interest were kept in 0.5-liter tanks under a strict 13 h:11 h light: dark cycle, with a consistent feeding schedule [Zeigler Larval AP100 dry food (Gardners, PA, USA; crabs) or live copepods (cephalopods)], and in near-constant water temperature (16°C) prior to testing.

To obtain larvae for *Doryteuthis opalescens* (Berry 1911), divers collected freshly laid egg capsules at the same site in La Jolla (∼30 m water depth) during the full and new moon (±2 days) in January–March 2018 during the spawning period. Capsules were placed in 4-liter tanks and water chemistry was monitored throughout development until hatching (∼3–4 weeks) using Honeywell Durafet® pH sensors (Phoenix, AZ, USA) and Aanderaa oxygen optodes (model 4531; Bergen, Norway). Squid egg capsules were maintained at constant P_{O_2} (∼22 kPa/∼260 μmol kg^{-1}), temperature (11°C) and pH (∼8.2). After hatching, paralarvae were placed in smaller tanks (0.5 liters) and maintained as described for the other species.

All recently collected/hatched larvae were held for a minimum of 24 h prior to testing, and only individuals that appeared healthy upon inspection were chosen for experimentation. Only individuals of a single larval stage were used for each species (paralarvae for *D. opalescens* and *O. bimaculatus*, Stage II for *P. planipes*, and megalopae for *M. gracilis*), as different larval stages may have distinct oxygen tolerances (Yannicelli et al., 2013) and visual capabilities and/or structures (Feller et al., 2015). Here, these stages are referred to collectively as 'larvae' when individuals of multiple species are described in the text, but only individuals of the specified life stage for each species were tested. Owing to the challenge of determining sex in larvae, differences between sexes were not quantified in this study.

Electrophysiology

All procedures were in compliance with the Institutional Animal Care and Use Committee (IACUC) of the University of California San Diego, and care was taken wherever possible to reduce the stress and discomfort of the animals (e.g. transportation at a cool temperature in darkness, etc.). All experiments were conducted within 6–10 h after sunrise each day so individuals were at the same stage of circadian rhythm. All experiments were performed on dark-adapted (30 min) individuals of each species. Infrared (IR) light (940 nm) and video microscopy were used to prepare animals for recording and view animals during recording; IR light is beyond the sensitivity of most marine organisms at low intensities (Cronin and Forward, 1988; Fernandez, 1973; McCormick and Cohen, 2012). The electrophysiology recording equipment was housed in a light-tight enclosure and, with the exception of the controlled light stimuli and IR illumination for imaging, animals were kept in complete darkness for the duration of the experiment.

The recording chamber on the microscope stage was constantly perfused (∼4 ml min^{-1}) with a solution of sterile seawater (Instant Ocean, Blacksburg, VA, USA; 27 g l^{-1} of ultrapure water, salinity 33.3) and Hepes (Fisher Scientific, Hampton, NH, USA; final concentration: 20 mmol l^{-1}). The P_{O_2} of this solution was adjusted by changing the gas concentrations and flow rate of aeration (standard aquarium pump) in a solution reservoir; seawater was cooled to ecologically relevant temperatures [range of average experimental temperatures=14.1–16.4°C (*D. opalescens*); 13.9–15.8°C (*O. bimaculatus*); 13.9–15.9°C (*M. gracilis*); 13.9–15.3°C (*P. planipes*)] in an ice bath and controlled on the stage by a heater. The average pH of the solution in all experiments was 8.04±0.04. This range is within the diel variability of nearshore Southern California Bight waters; however, under natural conditions, pH would decline with decreasing oxygen in the water column (Frieder et al., 2012). Oxygen concentration was measured in the recording chamber during all experiments using a dip optical

Journal of Experimental Biology (2019) 222, jeb200899. doi:10.1242/jeb.200899

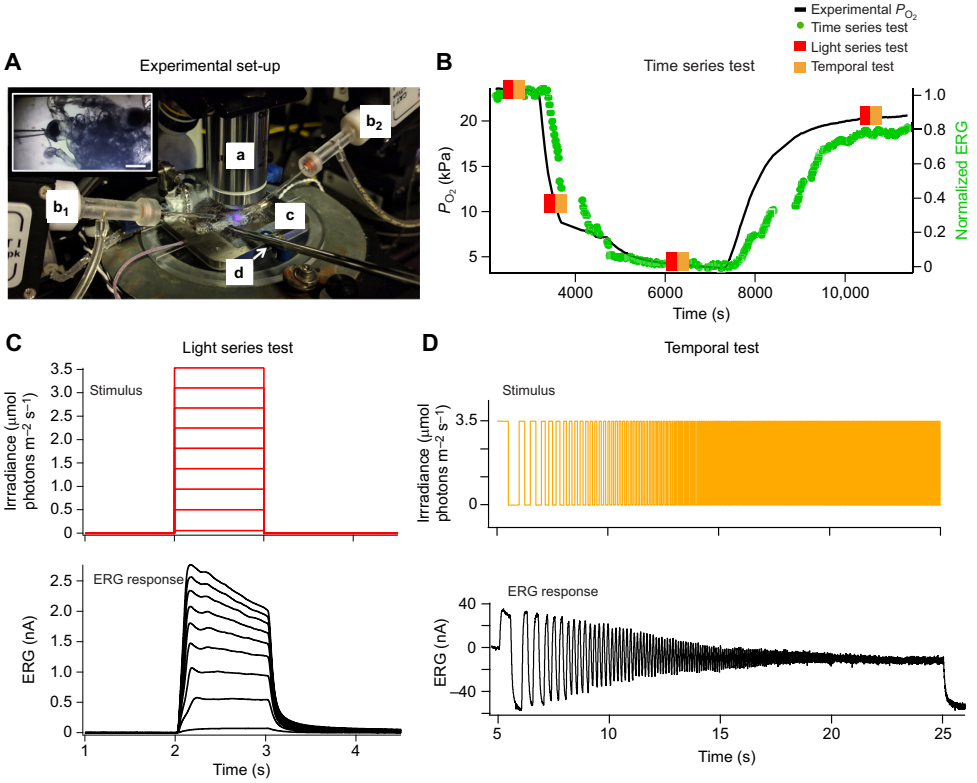

Fig. 1. Experimental design of the research project. (A) Configuration for electrophysiology experiments, showing the (a) microscope objective, (b_1/b_2) micromanipulators controlling the position of the tethered animal and the recording electrode, (c) recording stage and (d) oxygen sensor. Inset: the electrode is inserted just under the cornea of the larva (*Metacarcinus gracilis*). Scale bar: 500 µm. (B) An entire experiment consists of three visual tests. The time series test measured the electroretinogram (ERG) response (green circles) to a repeated light stimulus of a constant irradiance while the oxygen partial pressure (P_{O_2}; black line) in the recording chamber was changed gradually from normoxia to a low P_{O_2}, and then re-oxygenated to normoxia; additional experiments (described in C and D) were conducted at specific P_{O_2} values (orange and red squares). (C) The light series test consisted of nine 1-s stimuli of increasing irradiance (µmol photons m^{-2} s^{-1}; red lines) during which the change in ERG response was recorded (nA; black lines). (D) The temporal test was a chirped (1–20 Hz) square wave modulation of irradiance from darkness to a stimulus of a constant irradiance (3.5 µmol photons m^{-2} s^{-1}; orange line) used to determine the maximum frequency to which the visual system could respond (pA; black line). All example ERG responses (time series, light series and temporal test) are from a *Doryteuthis opalescens* paralarva in normoxia (P_{O_2}=21 kPa).

probe (DP-PSt7; PreSens, Regensburg, Germany; Fig. 1A). Oxygen was converted to P_{O_2} (kPa) with the 'Respirometry' package in R using the corresponding temperature and salinity from each experiment. All results are given in P_{O_2} values, with concentrations (µmol kg^{-1}) given in parentheses; all concentrations are averages of all individual trials within each species, corresponding to the temperature conditions reported above for each species.

Each larva was immobilized and its dorsal surface was attached to a borosilicate pipette using cyanoacrylate (Loctite superglue, Westlake, OH, USA) and then immediately submerged into solution on the recording chamber (using micromanipulator b_2; Fig. 1A). ERG recordings were made using a whole-cell patch clamp electrophysiology amplifier to detect and record extracellular changes in potential in the eye through a standard extracellular glass electrode. Electrodes were borosilicate pipettes pulled to a resistance of 3–6 MΩ and filled with external recording solution. Electrode tips were placed into the eye using a digital micromanipulator (micromanipulator b_1; Fig. 1A; Scientifica, Clarksburg, NJ, USA). No suction or pressure was applied to the recording electrode at any point during the experiment. The ERG signal was recorded in voltage-clamp mode using a Multiclamp 700B amplifier (Molecular Devices, San Jose, CA, USA) low-pass filtered at 4 kHz (Bessel), digitized at 20 Hz using an Instrutech ITC-18 A/D board (HEKA Elektronik, Holliston, MA, USA), and saved to a computer hard drive using the custom acquisition software writing in IgorPro (WaveMetrics, Lake Oswego, OR, USA). After obtaining an ERG recording and before beginning P_{O_2} manipulation, larvae were held in the perfusion reservoir at normoxia (equivalent to 100–105% O_2 saturation at ∼15°C and 33 salinity) to ensure there was a stable ERG response. After a stable baseline was obtained, the P_{O_2} was

decreased in the recording chamber with the addition of nitrogen gas (N_2) to the solution reservoir. After obtaining a minimum P_{O_2} value, the P_{O_2} was then increased to normoxia by adding air (21% O_2) to the reservoir (Fig. 1B).

Light stimulation

Light stimuli were generated using a collimated green super-bright T-1 3/4 package LED (525 nm; 35 nm FWHM; Thorlabs LED528EHP; Newton, NJ, USA) focused through a 2× air objective that illuminated the entire stage; stimulus irradiance was adjusted by pulse width modulation (20 kHz duty cycle) through a computer-controlled constant current driver. Irradiance (photon flux) was measured at the experimental plane with a radiometer (Thorlabs), and converted into a species-specific irradiance in units of equivalent PFD (µmol photons m^{-2} s^{-1}) for the spectral sensitivity of each species (e.g. squid PFD). Data for spectral sensitivities were obtained or modified from existing literature for the same species, or a taxonomically related species with similar life history and habitat depth: *D. opalescens* from sensitivity of *Doryteuthis pealeii* (Hubbard et al., 1959); *O. bimaculatus* from sensitivity of *O. vulgaris* (Brown and Brown, 1958); *P. planipes* (Fernandez, 1973); and *M. gracilis* from *Cancer irroratus* (Cronin and Forward, 1988). Spectral sensitivity curves were multiplied against the spectrum of the experimental light (LED) to obtain a species-specific irradiance for each species (Fig. S1). All light stimuli were presented from a dark background (no visible light), and animals were held in darkness between stimulus presentations. The term 'darkness' for this study refers to both the absence of light stimuli and the absence of environmental light within the light-tight experimental enclosure.

Three experimental irradiance manipulations were used. The time series test recorded ERG responses to a 1 s square step of light at a constant irradiance of 3.56 µmol photons m^{-2} s^{-1} repeated every 20 s, providing a nearly continuous measure of ERG response during the experimental manipulation of P_{O_2}. Two additional tests were conducted at specific oxygen conditions [normoxia (∼22 kPa/∼265 µmol kg^{-1}), intermediate reduction of P_{O_2} (∼6.5 kPa/∼95 µmol kg^{-1}) and low P_{O_2} (∼3.5 kPa/∼55 µmol kg^{-1}); Fig. 1B]. The light series test consisted of square step pulses of irradiance (1 s light stimulus every 7 s) increasing from dim light to bright light (0.056–3.53 µmol photons m^{-2} s^{-1}) at nine equally spaced irradiance increments, repeated three times with 20 s in between each series at each oxygen condition (Fig. 1C). The temporal test consisted of a chirped (1–20 Hz) square wave modulated between darkness and an irradiance of 3.26 µmol photons m^{-2} s^{-1} (Fig. 1D). Time series and light series tests were completed on larvae of all four species. The temporal test was completed on *D. opalescens* paralarvae and *P. planipes* larvae due to the lack of availability of *O. bimaculatus* paralarvae or *M. gracilis* megalopae at the time of experiments. All oxygen values were measured directly on the stage throughout visual tests. Experiments were conducted *in vivo*, with 100% survival of all larvae throughout the duration of the experiment.

Analysis of results

All electrophysiology data were analyzed using the software IgorPro (WaveMetrics). All waves were down-sampled to 2 kHz, digitally filtered with a binomial smoothing algorithm (IgorPro) with a corresponding Gaussian filter cut-off frequency of 40 Hz, and digitally notch filtered (60 Hz) before analysis. For all square waves, the amplitude of the response and the integrated area under the waveform were calculated. Within a species there was no difference in results when the measurement of the amplitude or the area was used, but because of the differences in waveform shapes between species, the integrated measurement was used for all final results.

For time series data, all measurements were normalized to the average of the ERG response in normoxia during the 5 min prior to the initiation of oxygen decline. Each normalized ERG measurement was matched to the corresponding oxygen measurement, and ERG responses were averaged over every minute to smooth the data. Oxygen metrics for retinal function, V_{90}, V_{50} and V_{10}, defined as the P_{O_2} where there was 90%, 50% and 10% retinal function, respectively, were calculated for each trial and averaged across individuals. Statistical differences between metrics (V_{90}, V_{50} and V_{10}) were determined using Kruskal–Wallis one-way ANOVAs within each species (d.f.=2 for *D. opalescens*, *O. bimaculatus* and *M. gracilis*; d.f.=1 for *P. planipes*). Pairwise differences between metrics (e.g. V_{90} versus V_{50}, etc.) were determined using Dunn's test with Bonferroni correction for multiple comparisons (d.f.=2 for *D. opalescens*, *O. bimaculatus* and *M. gracilis*; d.f.=1 for *P. planipes*).

For light series data, three repeated tests were averaged at each oxygen condition. Both the amplitude of and area under the response waveform were calculated, and the integrated area was used for final analysis as explained for the time series data. ERG responses to stimuli at each irradiance were normalized to the maximum response (during normoxia at the highest irradiance). Response–irradiance curves were fit with a Hill equation for the averages of each species, as is often used to describe visual response–irradiance functions (Shapley and Enroth-Cugell, 1984; Oesch and Diamond, 2011). Within each species, Kruskal–Wallis one-way ANOVAs were conducted to determine differences between ERG responses at each oxygen condition (normoxia, ∼22 kPa/∼265 µmol kg^{-1}; intermediate reduction of P_{O_2}, ∼6.5 kPa/∼95 µmol kg^{-1}; and low P_{O_2}, ∼3.5 kPa/∼55 µmol kg^{-1}) at each irradiance (d.f.=2; Table S1). To determine whether changes in retinal function in different oxygen conditions were consistent across irradiance (i.e. whether the shape of the response changed with oxygen condition), values were also normalized to the maximum value (ERG response at highest irradiance) within each oxygen condition. Oxygen values presented are averages from all trials within each species.

For temporal response analysis, three presentations at each oxygen concentration were averaged. In some cases, low oxygen reduced the amplitude of the response so that it became indistinguishable from the baseline noise. Therefore, only data where the light response was greater than 2 standard deviations of the baseline noise was used. Power spectral densities (PSDs) were calculated using the fast Fourier transform (window size=4000). The resulting PSD was normalized to the value at 1 Hz and converted to gain (dB). Results were analyzed for significance using a Kruskal–Wallis one-way ANOVA on the cut-off frequency (–6 dB) at each oxygen condition for each of the two species (*D. opalescens* and *P. planipes*) tested. Oxygen values (in partial pressure and concentration) presented are averages from all trials within each species.

The potential for loss of retinal function from P_{O_2} in the environment in the Southern California Bight was calculated using the physiological threshold data collected in this study and the oxygen concentration data collected via CTD (conductivity–temperature–depth) casts made during California Cooperative Oceanic Fisheries Investigations (CalCOFI) cruises. Data from springtime (March–May) cruises conducted between 2005 and 2017 were downloaded from the CalCOFI website (calcofi.org) and casts closest to the animal collection site for these experiments (line 93.3 station 26.7 and 28) between 2005 and 2017 were averaged.

Oxygen data from these casts were converted from concentration (μmol kg^{-1}) to P_{O_2} (kPa) units using the R package 'AquaEnv' and code from Hofmann et al. (2011). ERG response data from physiology experiments and the corresponding P_{O_2} were fit with the best-fit model for each species (linear for *D. opalescens* and *M. gracilis* and nonlinear for *O. bimaculatus* and *P. planipes*) to calculate the predicted retinal function at each 1-m depth bin.

Images for each species were inspired by photographs (*D. opalescens* and *O. bimaculatus*) or existing drawings of larval stages [*P. planipes* (Boyd, 1960) and *M. gracilis* (Ally, 1975)].

RESULTS

Sensitivity to light

During a continuous decline in P_{O_2} from 22 kPa (280 μmol kg^{-1} O_2=normoxia) to ∼3 kPa (∼45 μmol kg^{-1}), the amplitude of the ERG to a 1 s square step pulse of light from darkness to a constant irradiance of 3.56 μmol photons m^{-2} s^{-1} decreased by 60–100% relative to responses in normoxia in all species ('time series test'; Fig. 1B). The magnitude of retinal impairment and the P_{O_2} at which the decline began differed among species (Fig. 2). The calculated oxygen metrics for retinal function show declines across all species as P_{O_2} decreases, with significant differences between V_{90}, V_{50} and V_{10} within a species in *D. opalescens* (P=0.012) and *M. gracilis* (P=0.006), but not in *O. bimaculatus* (P=0.156) or *P. planipes* (P=0.655, Kruskal–Wallis tests; Fig. 2).

Surprisingly, retinal function (V_{90}) began declining at relatively high P_{O_2} (only 1–2 kPa/20–30 μmol kg^{-1} below oxygen saturation) in *D. opalescens* (V_{90}=22.2 kPa/258 μmol kg^{-1}) and *M. gracilis* (V_{90}=19.4 kPa/229 μmol kg^{-1}). In contrast, oxygen thresholds for vision in *O. bimaculatus* (V_{90}=11.5 kPa/133 μmol kg^{-1}) and *P. planipes* (V_{90}=5.7 kPa/68 μmol kg^{-1}) were at lower P_{O_2} values. Retinal function continued to decline with further reductions of oxygen in *D. opalescens*, *O. bimaculatus* and *M. gracilis*, and the P_{O_2} where only 50% ERG function remained (V_{50}) for each species was 13 kPa (151 μmol kg^{-1}), 7.2 kPa (85 μmol kg^{-1}) and 10.2 kPa (121 μmol kg^{-1}), respectively (Fig. 2). In all cases, the ERG response returned to at least 50% of the maximum response (relative to the initial responses in normoxia) after re-oxygenation of the solution (Fig. 3), indicating the decline in ERG response during exposure to reduced P_{O_2} was not from the death of the retinal tissue.

Dynamic range

To determine whether the oxygen effects were dependent on light level, we presented light steps over a range of irradiance from 0.056 to 3.53 μmol photons m^{-2} s^{-1} at three different oxygen conditions

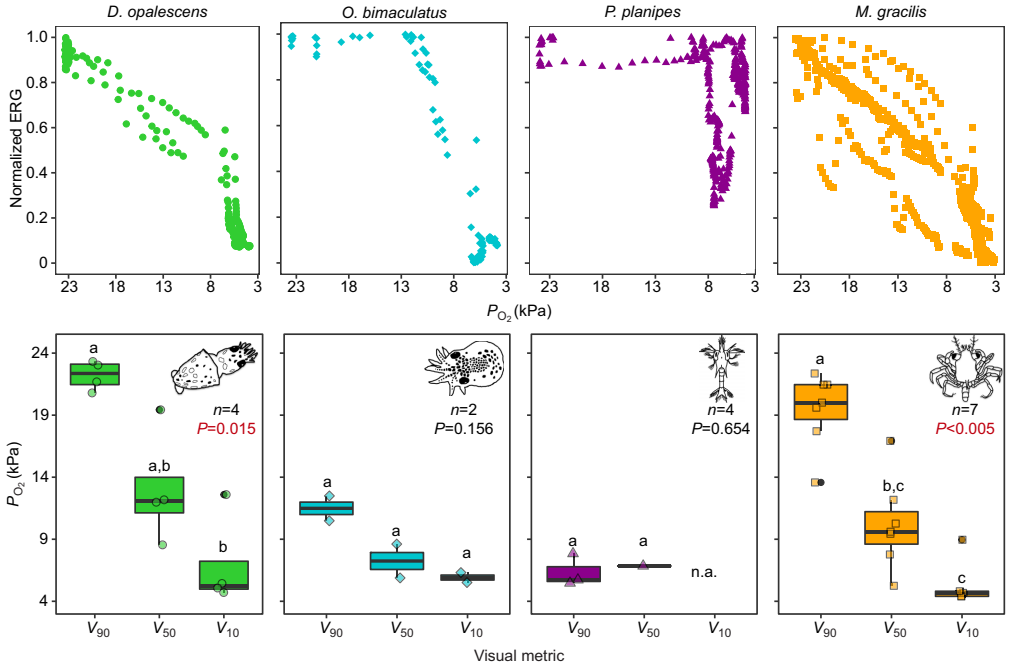

Fig. 2. Quantifying the decline in retinal function from exposure to reduced P_{O_2} in marine invertebrate larvae. Top row: change in ERG response (normalized to the average at normoxia oxygen exposure) to a 1-s light stimulus (3.56 μmol photons m^{-2} s^{-1}) every 20 s over a decline in oxygen partial pressure (kPa) for the market squid, *Doryteuthis opalescens* (green circles), the two-spot octopus, *Octopus bimaculatus* (teal diamonds), the tuna crab, *Pleuroncodes planipes* (magenta triangles), and the graceful rock crab, *Metacarcinus gracilis* (orange squares). Bottom row: visual metrics showing the partial pressure of oxygen where there is 90% (V_{90}), 50% (V_{50}) and 10% (V_{10}) of retinal function (with respect to ERG responses in normoxia) for each of the four species. The *P*-values indicate results of a Kruskal–Wallis one-way ANOVA across metrics for each species; different lowercase letters indicate significant pairwise differences (Dunn's test) between metrics (within a species). Boxes show the median (bold center line) and first and third quartiles of all individuals tested within a species; error bars show maximum/minimum values within 1.5× the inner quartile range (IQR=third quartile–first quartile), with all data points used in the analyses overlaid.

Journal of Experimental Biology (2019) 222, jeb200899. doi:10.1242/jeb.200899

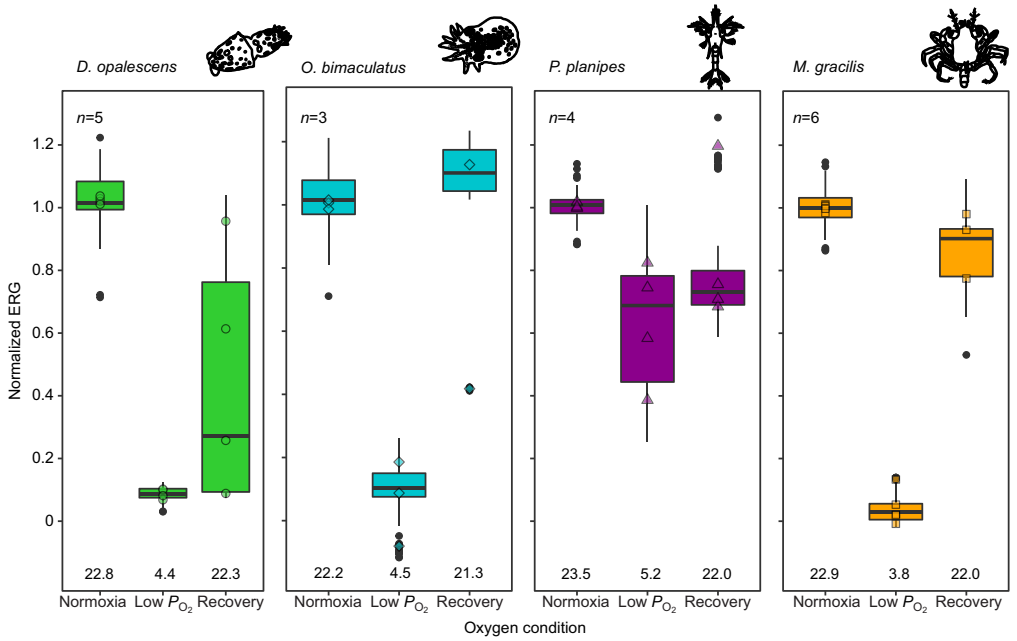

Fig. 3. Recovery of retinal function after exposure to reduced P_{O_2}. Average ERG responses (all normalized to ERG response in normoxia) during initial exposure to normoxia, low P_{O_2} and after re-oxygenation of the solution to recovery normoxia (recovery) in larvae of *D. opalescens* (green), *O. bimaculatus* (teal), *P. planipes* (magenta) and *M. gracilis* (orange). Average P_{O_2} for each condition is displayed in kPa; boxes show the median (bold line) bounded by first and third quartiles and error bars show maximum/minimum values within 1.5× the IQR, with outliers as black circles. All data used for the analyses are overlaid.

(normoxia, intermediate reduced P_{O_2} and low P_{O_2}; 'light series test'; Fig. 1C). There was a decrease in ERG amplitude across all irradiances tested in all species as P_{O_2} decreased (Fig. 4), similar to what was observed in the first experiment, indicating that declines in ERG responses observed in low P_{O_2} were not irradiance-dependent (Fig. 4A,C,E,G). At each irradiance tested, ERG responses were significantly different between the ERG response at normoxia, intermediate reduced P_{O_2} and low P_{O_2} ($P<0.05$, Kruskal–Wallis tests; Fig. 4, Table S1), with the exception of the lowest irradiance (0.056 µmol photons m^{-2} s^{-1}) in larvae of *D. opalescens*, *O. bimaculatus* and *P. planipes* ($P=0.246$, 0.301 and 0.105, respectively). To quantify the response–irradiance relationship (ERG response at each irradiance), ERG responses at each oxygen condition were fit with a Hill equation (Fig. 4A,C,E,G). To examine how the shape of the response–irradiance relationship was influenced by oxygen, we scaled the responses to the maximum ERG response within each oxygen condition (Fig. 5). Small changes in the shape of the response–irradiance relationship were seen in the cephalopods (*D. opalescens* and *O. bimaculatus*), but differences in the ERG response across oxygen conditions at each irradiance were not statistically significant in any species, indicating the response–irradiance relationships were stable at different oxygen conditions ($P>0.05$, Kruskal–Wallis tests; Table S1).

Temporal resolution

To determine how P_{O_2} affects the temporal properties of the larval ERG response, we presented square wave linear chirp stimuli (frequency modulated between 1 and 20 Hz) between darkness and a constant irradiance of 3.56 µmol photons m^{-2} s^{-1} in larvae of *D. opalescens* and *P. planipes* ('temporal test'; Fig. 1D) and measured the corresponding ERG response. With this recording of ERG response to flashes of light at multiple frequencies, we computed the PSD to determine the power of the visual signal at each frequency. As expected, there was a decline in the power of the response as frequency increased, indicative of the natural temporal resolution limit for the species (Fig. 6). We quantified the temporal resolution using a cut-off frequency (frequency at which power drops below −6 dB). During exposure to low P_{O_2}, we observed a steeper decline in the power of the response in larval *D. opalescens*, with a cut-off frequency decreasing from 4.6 Hz at normoxia (23.1 kPa) to 2.8 Hz at low P_{O_2} (3.8 kPa; $P=0.009$, Kruskal–Wallis test; Fig. 6). No significant change in temporal resolution was observed with a change of P_{O_2} in *P. planipes* (7.5 Hz at 23.4 kPa to 6.8 Hz at 3.6 kPa; $P=0.755$, Kruskal–Wallis test; Fig. 6). This indicates that the temporal resolution of vision in paralarvae of *D. opalescens* was reduced when exposed to low P_{O_2}, but that larvae of *P. planipes* were not significantly affected within the range of P_{O_2} tested here.

DISCUSSION

Based on studies in terrestrial vertebrates, we expected that large decreases in oxygen would reduce ERG responses; however, for most marine species, the magnitude of the reduction in oxygen needed to impact retinal function is unknown. It is also unknown

Journal of Experimental Biology (2019) 222, jeb200899. doi:10.1242/jeb.200899

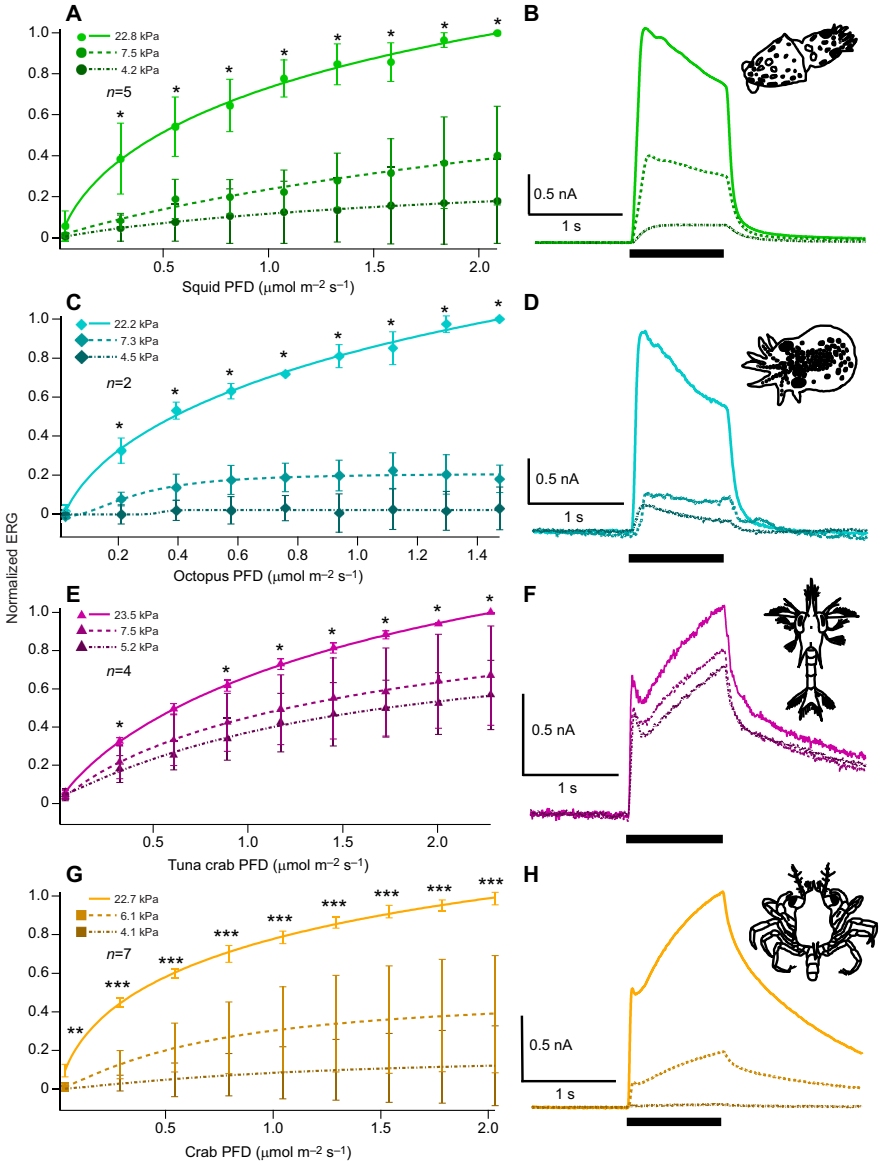

Fig. 4. Effects of reduced P_{O_2} on retinal responses at a range of irradiances. ERG response to oxygen tested at multiple irradiances in larvae of (A,B) *D. opalescens*, (C,D) *O. bimaculatus*, (E,F) *P. planipes* and (G,H) *M. gracilis*. (A,C,E,G) Response–irradiance curves show the ERG response (normalized to the maximum response in normoxia) to stimuli of nine different irradiance levels (PFD) for *D. opalescens* (green circles), *O. bimaculatus* (teal diamonds), *P. planipes* (magenta triangles) and *M. gracilis* (orange squares) during exposure to normoxia (22.3–23.5 kPa), intermediate reduced P_{O_2} (6.1–7.5 kPa) and low P_{O_2} (4.1–5.2 kPa) fit with a Hill equation (solid, dashed and dash–dotted lines, respectively). Differences between ERG responses at each oxygen condition within each of the irradiances were determined using Kruskal–Wallis one-way ANOVAs; asterisks indicate significance (*P<0.05; **P<0.01; ***P<0.001). Error bars show means±s.d. (B,D,F,H) Representative ERG responses to a 1-s stimulus at the maximum irradiance from a single larva. Horizontal scale bars (for all) indicate 1 s; vertical bars are 0.5 nA in B and H and 0.05 nA in D and F; thick black bar indicates the duration of the light stimulus. Color shades and lines follow oxygen levels in A, C, E and G.

Journal of Experimental Biology

Journal of Experimental Biology (2019) 222, jeb200899. doi:10.1242/jeb.200899

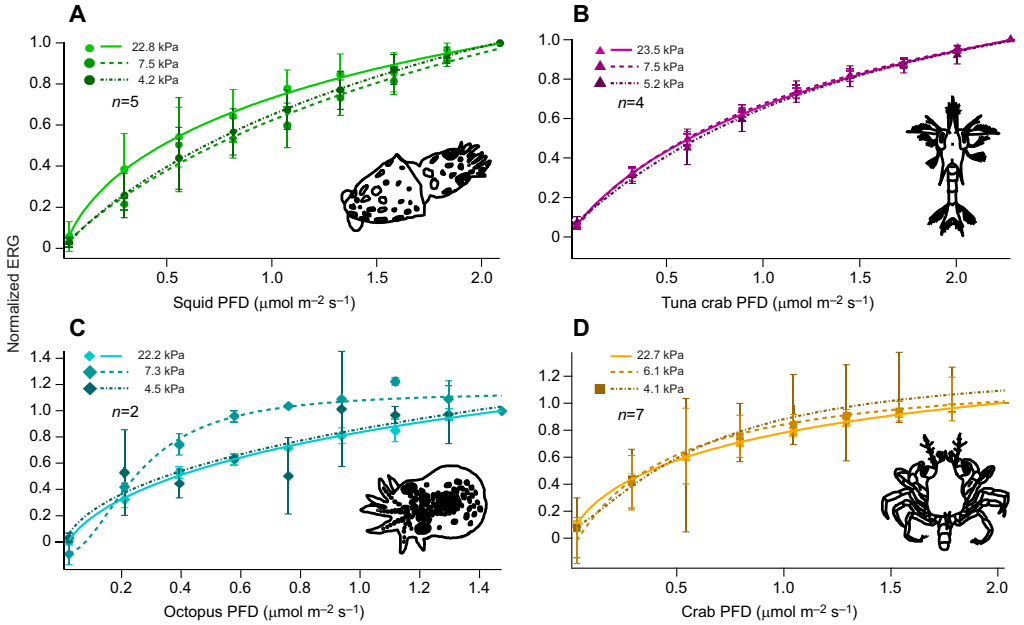

Fig. 5. Oxygen effects on response–irradiance relationships. Differences in the shape of ERG responses to increasing irradiance at each oxygen condition. Response–irradiance curves (normalized to the maximum response in each oxygen condition) show the shape of the visual response to stimuli of nine different irradiances in larvae of (A) *D. opalescens* (green circles), (B) *P. planipes* (magenta triangles), (C) *O. bimaculatus* (teal diamonds) and (D) *M. gracilis* (orange squares) during exposure to normoxia (22.3–23.5 kPa), intermediate reduced P_{O_2} (6.1–7.5 kPa) and low P_{O_2} (4.1–5.2 kPa). ERG responses during exposure to each oxygen condition are fit with a Hill equation (solid, dashed and dash–dotted lines, respectively). Error bars indicate means±s.d.

whether the decline in retinal function occurs at some threshold oxygen concentration or more continuously as oxygen is decreased below some critical threshold. To our knowledge, no direct comparisons of oxygen effects on visual physiology between different groups of marine invertebrates exist. These results demonstrated major retinal impairment in three species of marine invertebrate larvae after exposure to surprisingly minor amounts of oxygen decline (decreases of 1–2 kPa/20–30 µmol kg^{-1} from oxygen saturation). Interestingly, there were large differences in visual sensitivity to low P_{O_2} among species, with almost 100% loss of retinal function in larvae of *D. opalescens*, *O. bimaculatus* and *M. gracilis* at low P_{O_2} (~3 kPa), whereas retinal function in larvae of *P. planipes* was relatively unaffected (i.e. ERG responses never declined enough to define a V_{10} within the range of P_{O_2} tested). Additionally, during exposure to a decline in P_{O_2}, the retinal responses decreased continuously in *D. opalescens* paralarvae and *M. gracilis* megalopae, whereas *O. bimaculatus* paralarvae and *P. planipes* larvae were able to maintain ≥90% retinal responses until ~11 and ~8 kPa, respectively, before ERG responses began showing the effects of decreased oxygen availability (Fig. 2).

The two species tested for temporal resolution also had very different responses to exposure to low P_{O_2}. Paralarvae of *D. opalescens* showed a strong decrease in the power of the retinal response at higher frequencies during exposure to low P_{O_2}, whereas the larvae of *P. planipes* showed very little change in temporal resolution. These differences in retinal responses across species are likely due to different metabolic tolerances to low oxygen; however, data for critical oxygen thresholds for metabolism (as in Seibel et al., 2016) do not yet exist for larvae in these species. In addition, the decrease in retinal function after only minor declines in P_{O_2} suggest that oxygen effects on vision may be an important sublethal physiological effect of low oxygen that may not be captured completely by a metric such as the critical oxygen thresholds for metabolism.

The declines in retinal responses for these invertebrate larvae during exposure to reduced oxygen are comparable to what is reported for terrestrial mammals. For example, the ERG response in cats began decreasing almost immediately after a decline in oxygen started, at P_{O_2} values similar to what would be experienced if a human were to drive from sea level to approximately 2000 m elevation (e.g. Lake Tahoe in California) (Linsenmeier et al., 1983; Steinberg, 1987). The effects of oxygen on the visual system of the cat were noted to occur at P_{O_2} values much greater than when effects would be observed in other neural circuits (Linsenmeier et al., 1983). The P_{O_2} values that cause a reduction in marine invertebrate larval vision are well within the range of variability they experience in their natural environment. For example, the average daily range of oxygen (caused by both biological and physical forcing) in coastal areas of the Southern California Bight is ~63 µmol kg^{-1} (~4 kPa at 15°C) at 7 m depth (Frieder et al., 2012); our results suggest that this magnitude of variability (ΔP_{O_2}=4 kPa), even at high P_{O_2} (21–17 kPa), could cause a 10–20% decrease in retinal function in larvae of *D. opalescens* and *M. gracilis* (Fig. 2) if they did not move upward to better-oxygenated waters. In addition, using the

Journal of Experimental Biology (2019) 222, jeb200899. doi:10.1242/jeb.200899

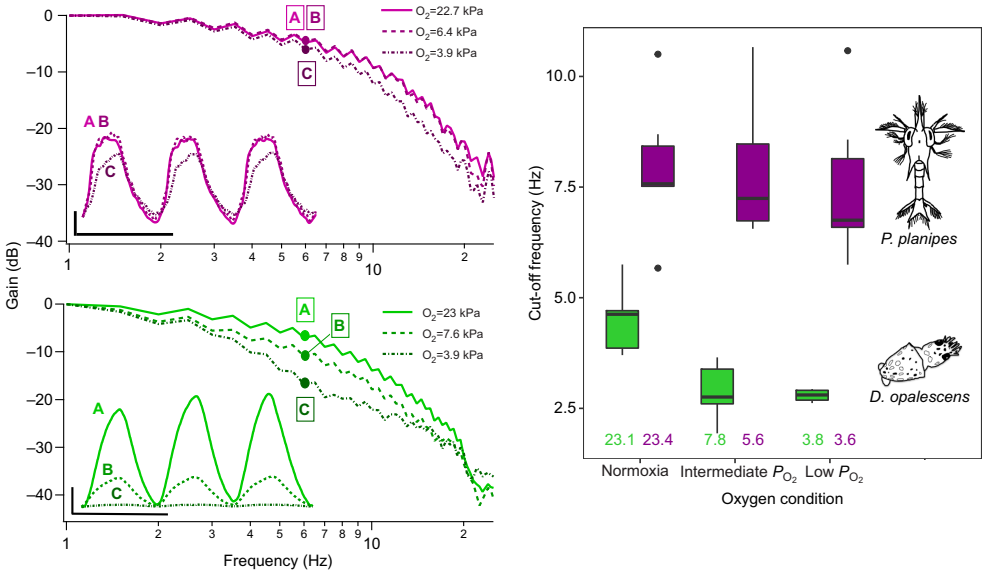

Fig. 6. Effects of reduced P_{O_2} on the temporal resolution of vision. Left: power spectral density (PSD) curves (normalized to value at 1 Hz) showing the power of the temporal response over stimulus frequencies from 1 to 20 Hz at three decreasing oxygen conditions (solid, dashed and dash–dotted lines, respectively) in an example larva of *P. planipes* (top; magenta) and an example paralarva of *D. opalescens* (bottom; green). Inset: example traces for each species showing the ERG response at the marked frequency (6 Hz) for responses in normoxia (A), intermediate reduction of P_{O_2} (B) and low P_{O_2} (C), respectively. Horizontal scale bar represents 0.25 s and the vertical scale bar represents 20 pA (top) or 100 pA (bottom). Right: calculated cut-off frequencies (–6 dB change in PSD) for each oxygen condition (values in figures on left) for all individuals of both *D. opalescens* (green; *n*=6) and *P. planipes* (magenta; *n*=6). The average P_{O_2} for each condition (kPa) is displayed for both *D. opalescens* (green) and *P. planipes* (magenta). Boxes show the median (bold center line) and first and third quartiles; whiskers show 1.5× the IQR, with outliers as black circles.

visual sensitivity of each species to P_{O_2} reported above (e.g. Fig. 2), we calculated the decrease in retinal function with depth under present-day (2005–2017) average springtime ocean oxygen conditions in the Southern California Bight. The decline in P_{O_2} alone from 0 to 30 m depth would decrease retinal function by 15–59% in larvae of *D. opalescens*, *M. gracilis*, *O. bimaculatus* and *P. planipes* in coastal Southern California (Fig. 7), even without including the effects of decreasing irradiance on the ERG response. Such changes in oxygen levels could significantly reduce larval fitness through loss of retinal function; however, the manifestation of the physiological impairment in visual behavior is unknown.

Many marine larvae remain at depth during the day to avoid visual predation, often at the depth near their threshold for light detection; they then migrate vertically to near-surface waters at night when predation pressure is reduced (diel vertical migration) (Forward, 1988; Sulkin, 1984; Zeidberg and Hamner, 2002). In all species, but especially in larvae of *D. opalescens*, *O. bimaculatus* and *M. gracilis*, retinal sensitivity to light declined during exposure to reduced oxygen (Fig. 2). Larvae of *O. bimaculatus* also experienced a decline in the range of irradiance that was physiologically detected, indicating that the sensitivity to changes in light irradiance (contrast) will be reduced during exposure to reduced P_{O_2}. For example, the shadow of a predator may become undetectable. Marine larvae require sufficiently high temporal resolution (the ability to distinguish between stimuli varying in time) to detect and appropriately respond to predators or prey (Frank, 1999). The decline in temporal resolution under reduced P_{O_2} in larvae of *D. opalescens* would reduce the ability to detect high-frequency movements, such as the burst-swimming pattern of the copepods they feed on. Decreased light sensitivity and temporal resolution induced by low oxygen may introduce a greater risk for predation, increase vulnerability to starvation (if prey detection is reduced) and/or potentially weaken detection of the light cue for vertical migration entirely if the decrease in retinal response is sufficient to change visual behaviors. All individuals recovered some level of retinal function with re-oxygenation of the solution after the acute exposure time of the experiments (~30 min at reduced oxygen; Fig. 3), indicating that the retinal response may recover during the time required for a small larva (~1.5–3 mm) to swim a few meters.

These data also have important practical implications for researchers studying these organisms in a laboratory setting. The significant changes in retinal function after even small depletions in oxygen availability for some species suggest that it is important to monitor and maintain appropriate oxygen levels during *in vitro* and *in vivo* experiments.

Knowledge of how the retinal function of marine invertebrate species changes during exposure to reduced P_{O_2} may help define species-specific vulnerabilities and resilience to future oxygen loss in the ocean. Globally, oxygen declines have resulted from warming (Schmidtko et al., 2017) and from nutrient and organic loading (Breitburg et al., 2018), and these losses can be exacerbated in areas with naturally occurring coastal hypoxia and upwelling (Altieri and Gedan, 2015; Levin and Breitburg, 2015). Given the apparent high

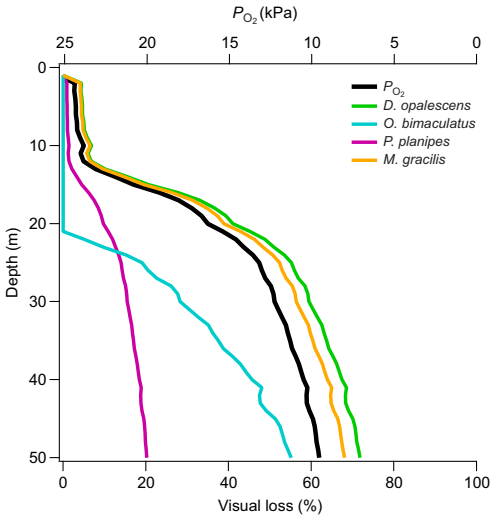

Fig. 7. Loss in retinal function in marine larvae from decreasing P_{O_2} with depth. Using physiological data from Fig. 2, the predicted change in retinal function (percent visual loss) is shown for an average springtime (March–May; data from 2005 to 2017) profile of P_{O_2} (black line) with depth in the Southern California Bight for *D. opalescens* (green line), *O. bimaculatus* (teal line), *P. planipes* (magenta line) and *M. gracilis* (orange line).

visual sensitivity and species-specificity of visual tolerance to low oxygen, documenting how larval (and adult) vulnerabilities to low oxygen are manifested in visual behaviors and ecology will be important for predicting responses to global and local declines in ocean oxygen.

Acknowledgements
We thank P. Zerofski for help with larval collections, and J. H. Cohen, D. Deheyn, T. Martz, F. Powell and M. Tresguerres for comments on data and analysis, as well as two anonymous reviewers, who helped improve the manuscript.

Competing interests
The authors declare no competing or financial interests.

Author contributions
Conceptualization: L.R.M.; Methodology: L.R.M., N.W.O.; Software: L.R.M., N.W.O.; Validation: L.R.M., N.W.O.; Formal analysis: L.R.M.; Investigation: L.R.M.; Resources: L.R.M., L.A.L., N.W.O.; Writing - original draft: L.R.M.; Writing - review & editing: L.R.M., L.A.L., N.W.O.; Visualization: L.R.M.; Supervision: L.A.L., N.W.O.; Funding acquisition: L.R.M., L.A.L., N.W.O.

Funding
This research was supported by a Charles H. Stout Foundation grant, a Frontiers of Innovation Scholars Program grant from the University of California San Diego, and the Scripps Institution of Oceanography education office for support to L.R.M., a National Science Foundation Graduate Research Fellowship grant DGE-1144086 to L.R.M., and a National Science Foundation grant OCE-1829623 to L.A.L. and N.W.O.

Supplementary information
Supplementary information available online at
http://jeb.biologists.org/lookup/doi/10.1242/jeb.200899.supplemental

References

Ally, J. R. R. (1975). A description of the laboratory-reared larvae of *Cancer gracilis* Dana, 1852 (Decapoda, Brachyura). *Crustaceana* **28**, 231-246. doi:10.1163/156854075x00496

Altieri, A. H. and Gedan, K. B. (2015). Climate change and dead zones. *Glob. Chang. Biol.* **21**, 1395-1406. doi:10.1111/gcb.12754

Ames, A. I. (2000). CNS energy metabolism as related to function. *Brain Res. Rev.* **34**, 42-68. doi:10.1016/S0165-0173(00)00038-2

Boyd, C. M. (1960). The larval stages of *Pleuroncodes planipes* Stimson (Crustacea, Decapoda, Galatheidae). *Biol. Bull.* **118**, 17-30. doi:10.2307/1539052

Breitburg, D., Levin, L. A., Oschlies, A., Grégoire, M., Chavez, F. P., Conley, D. J., Garçon, V., Gilbert, D., Gutiérrez, D., Isensee, K. et al. (2018). Declining oxygen in the global ocean and coastal waters. *Science* **359**, 7240. doi:10.1126/science.aam7240

Brown, K. T. (1968). The electroretinogram: its components and their origins. *Vision Res.* **8**, 633-677. doi:10.1016/0042-6989(68)90041-2

Brown, P. K. Brown, P. S. (1958). Visual pigments of the octopus and cuttlefish. *Nature* **182**, 1288-1290. doi:10.1038/1821288a0

Chen, D.-M. and Stark, W. S. (1994). Electroretinographic analysis of ultraviolet sensitivity in juvenile and adult goldfish retinas. *Vision Res.* **34**, 2941-2944. doi:10.1016/0042-6989(94)90265-8

Chrispell, J. D., Rebrik, T. I. and Weiss, E. R. (2015). Electroretinogram analysis of the visual response in zebrafish larvae. *J. Vis. Exp.* 97, e52662 doi:10.3791/52662

Cohen, J. H., Berge, J., Moline, M. A., Sørensen, A. J., Last, K., Falk-Petersen, S., Renaud, P. E., Leu, E. S., Grenvald, J., Cottier, F. et al. (2015). Is ambient light during the high Arctic polar night sufficient to act as a visual cue for zooplankton? *PLoS ONE* **10**, e0126247. doi:10.1371/journal.pone.0126247

Cronin, T. W. and Forward, R. B. (1988). The visual pigments of crabs: I. Spectral characteristics. *J. Comp. Physiol. A* **162**, 463-478. doi:10.1007/BF00612512

FAO (2018). *The State of World Fisheries and Agriculture 2018-Meeting the Sustainable Development Goals*. Rome: FAO.

Feller, K. D., Cohen, J. H. and Cronin, T. W. (2015). Seeing double: visual physiology of double-retina eye ontogeny in stomatopod crustaceans. *J. Comp. Physiol. A* **201**, 331-339. doi:10.1007/s00359-014-0967-2

Fernandez, H. R. (1973). Spectral sensitivity and visual pigment of the compound eye of the galatheid crab *Pleuroncodes planipes*. *Mar. Biol.* **20**, 148-153. doi:10.1007/BF00351453

Forward, R. B. (1988). Diel vertical migration: zooplankton photobiology and behavior. *Oceanogr. Mar. Biol.* **26**, 361-393.

Fowler, B., Banner, J. and Pogue, J. (1993). The slowing of visual processing by hypoxia. *Ergonomics* **36**, 727-735. doi:10.1080/00140139308967933

Frank, T. M. (1999). Comparative study of temporal resolution in the visual systems of mesopelagic crustaceans. *Biol. Bull.* **196**, 137-144. doi:10.2307/1542559

Frieder, C. A., Nam, S., Martz, T. R. and Levin, L. A. (2012). High temporal and spatial variability of dissolved oxygen and pH in a nearshore California kelp forest. *Biogeosciences* **9**, 3917-3930. doi:10.5194/bg-9-3917-2012

Gilly, W. F., Beman, J. M., Litvin, S. Y. and Robison, B. H. (2013). Oceanographic and biological effects of shoaling of the oxygen minimum zone. *Ann. Rev. Mar. Sci.* **5**, 393-420. doi:10.1146/annurev-marine-120710-100849

Grieshaber, M. K., Hardewig, I., Kreutzer, U. and Pörtner, H. O. (1994). Physiological and metabolic responses to hypoxia in invertebrates. *Rev. Physiol. Biochem. Pharmacol.* **125**, 43-147.

Hansen, B. W., Ea, S., Petersen, J. K. and Ellegaard, C. (2002). Invertebrate re-colonisation in Mariager Fjord (Denmark) after severe hypoxia. I. Zooplankton and settlement. *Ophelia* **56**, 197-213. doi:10.1080/00785236.2002.10409499

Hofmann, A. F., Peltzer, E. T., Walz, P. M. and Brewer, P. G. (2011). Hypoxia by degrees: establishing definitions for a changing ocean. *Deep Sea Res. Part 1* **58**, 1212-1226. doi:10.1016/j.dsr.2011.09.004

Hubbard, R., Brown, P. K. and Kropf, A. (1959). Action of light on visual pigments. *Nature* **183**, 442-446. doi:10.1038/183442a0

Lange, G. D. and Hartline, P. H. (1974). Retinal responses in squid and octopus. *J. Comp. Physiol. A* **93**, 19-36. doi:10.1007/BF00608757

Lecchini, D. (2011). Visual and chemical cues in habitat selection of sepioid larvae. *C. R. Biol.* **334**, 911-915. doi:10.1016/j.crvi.2011.08.003

Lecchini, D., Mills, S. C., Brié, C., Maurin, R. and Banaigs, B. (2010). Ecological determinants and sensory mechanisms in habitat selection of crustacean postlarvae. *Behav. Ecol.* **21**, 559-607. doi:10.1093/beheco/arq029

Levin, L. A. and Breitburg, D. L. (2015). Linking coasts and seas to address ocean deoxygenation. *Nat. Clim. Chang.* **5**, 401-403. doi:10.1038/nclimate2595

Levin, L. A., Liu, K. K., Emeis, K. C., Breitburg, D. L., Cloern, J., Deutsch, C., Giani, M., Goffart, A., Hofmann, E. E., Lachkar, Z. et al. (2015). Comparative biogeochemistry-ecosystem-human interactions on dynamic continental margins. *J. Mar. Syst.* **141**, 3-17. doi:10.1016/j.jmarsys.2014.04.016

Linsenmeier, R. A., Mines, A. H. and Steinberg, R. H. (1983). Effects of hypoxia and hypercapnia on the light peak and electroretinogram of the cat. *Invest. Ophthalmol. Vis. Sci.* **24**, 37-46.

McCormick, L. R. and Cohen, J. H. (2012). Pupil light reflex in the Atlantic brief squid, *Lolliguncula brevis*. *J. Exp. Biol.* **215**, 2677-2683. doi:10.1242/jeb.068510

McCormick, L. R. and Levin, L. A. (2017). Physiological and ecological implications of ocean deoxygenation for vision in marine organisms. *Philos. Trans. R. Soc. A* **375**, 20160322. doi:10.1098/rsta.2016.0322

McFarland, R. A. and Evans, J. N. (1939). Alterations in dark adaptation under reduced oxygen tensions. *Am. J. Physiol. Leg. Content* **127**, 37-50. doi:10.1152/ajplegacy.1939.127.1.37
McGowan, J. (1954). Observations on the sexual behavior and spawning of the squid, *Loligo opalescens*, at La Jolla, California. *Calif. Dep. Fish Game Fish. Bull.* **40**, 47-54.
Niven, J. E. and Laughlin, S. B. (2008). Energy limitation as a selective pressure on the evolution of sensory systems. *J. Exp. Biol.* **211**, 1792-1804. doi:10.1242/jeb.017574
Oesch, N. W. and Diamond, J. S. (2011). Ribbon synapses compute temporal contrast and encode luminance in retinal rod bipolar cells. *Nat. Neurosci.* **14**, 1555-1561. doi:10.1038/nn.2945
Pepe, I. M. (2001). Recent advances in our understanding of rhodopsin and phototransduction. *Prog. Retin. Eye Res.* **20**, 733-759. doi:10.1016/S1350-9462(01)00013-1
Rayer, B., Naynert, M. and Stieve, H. (1990). Phototransduction: different mechanisms in vertebrates and invertebrates. *J. Photochem. Photobiol. B* **7**, 107-148. doi:10.1016/1011-1344(90)85151-L
Robin, J.-P., Roberts, M., Zeidberg, L., Bloor, I., Rodriguez, A., Briceño, F., Downey, N., Mascaró, M., Navarro, M., Guerra, A. et al. (2014). Transitions during cephalopod life history: the role of habitat, environment, functional morphology, and behaviour. *Adv. Mar. Biol.* **67**, 361-437. doi:10.1016/B978-0-12-800287-2.00004-4
Schmidtko, S., Stramma, L. and Visbeck, M. (2017). Decline in global oceanic oxygen content during the past five decades. *Nature* **542**, 335-339. doi:10.1038/nature21399
Seibel, B. A. (2011). Critical oxygen levels and metabolic suppression in oceanic oxygen minimum zones. *J. Exp. Biol.* **214**, 326-336. doi:10.1242/jeb.049171
Seibel, B. A., Schneider, J. L., Kaartvedt, S., Wishner, K. F. and Daly, K. L. (2016). Hypoxia tolerance and metabolic suppression in oxygen minimum zone euphausiids: implications for ocean deoxygenation and biogeochemical cycles. *Integr. Comp. Biol.* **56**, 510-523. doi:10.1093/icb/icw091
Shapley, R. and Enroth-Cugell, C. (1984). Visual adaptation and retinal gain controls. *Prog. Retin. Res.* **3**, 263-346. doi:10.1016/0278-4327(84)90011-7
Steinberg, R. H. (1987). Monitoring communications between photoreceptors and pigment epithelial cells: effects of 'mild' systemic hypoxia (Friedenwald Lecture). *Investig. Ophthalmol. Vis. Sci.* **12**, 1888-1904.
Sulkin, S. (1984). Behavioral basis of depth regulation in the larvae of brachyuran crabs. *Mar. Ecol. Prog. Ser.* **15**, 181-205. doi:10.3354/meps015181
Tyler, R. M., Brady, D. C. and Targett, T. E. (2009). Temporal and spatial dynamics of diel-cycling hypoxia in estuarine tributaries. *Estuaries Coasts* **32**, 123-145. doi:10.1007/s12237-008-9108-x
Warrant, E. J. and Johnsen, S. (2013). Vision and the light environment. *Curr. Biol.* **23**, R990-R994. doi:10.1016/j.cub.2013.10.019
Wishner, K. F., Outram, D. M., Seibel, B. A., Daly, K. L. and Williams, R. L. (2013). Zooplankton in the eastern tropical north Pacific: boundary effects of oxygen minimum zone expansion. *Deep Sea Res. Part I Oceanogr. Res. Pap.* **79**, 122-140. doi:10.1016/j.dsr.2013.05.012
Wishner, K. F., Seibel, B. A., Roman, C., Deutsch, C., Outram, D., Shaw, C. T., Birk, M. A., Mislan, K. A. S., Adams, T. J., Moore, D. et al. (2018). Ocean deoxygenation and zooplankton: very small oxygen differences matter. *Sci. Adv.* **4**, eaau5180. doi:10.1126/sciadv.aau5180
Wong-Riley, M. (2010). Energy metabolism of the visual system. *Eye Brain* **2**, 99-116. doi:10.2147/EB.S9078
Wu, R. S. S. (2002). Hypoxia: from molecular responses to ecosystem responses. *Mar. Pollut. Bull.* **45**, 35-45. doi:10.1016/S0025-326X(02)00061-9
Yannicelli, B., Paschke, K., González, R. R. and Castro, L. R. (2013). Metabolic responses of the squat lobster (*Pleuroncodes monodon*) larvae to low oxygen concentration. *Mar. Biol.* **160**, 961-976. doi:10.1007/s00227-012-2147-7
Zeidberg, L. D. and Hamner, W. M. (2002). Distribution of squid paralarvae, *Loligo opalescens* (Cephalopoda: Myopsida), in the Southern California Bight in the three years following the 1997-1998 El Niño. *Mar. Biol.* **141**, 111-112. doi:10.1007/s00227-002-0813-x

Chapter 3 Appendix

Journal of Experimental Biology: doi:10.1242/jeb.200899: Supplementary information

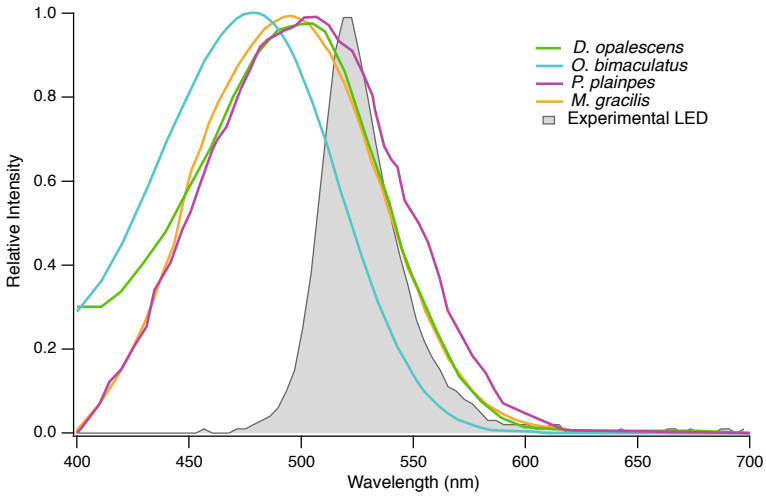

Fig S1. Comparison of experimental light and spectral sensitivities of each species. Estimated spectral sensitivities of the market squid, *Doryteuthis opalescens* (green line); the octopus, *Octopus bimaculatus* (teal line); the tuna crab, *Pleuroncodes planipes* (magenta line); and the graceful rock crab, *M. gracilis* (orange line), in comparison to the spectrum of the green LED (gray line and shading) used in all experiments (525 nm, 35 nm FWHM; Thorlabs). Data for spectral sensitivities were obtained or modified from existing literature for the same species, or a taxonomically related species with similar life history and habitat depth: *D. opalescens* from sensitivity of *Doryteuthis pealeii* (Hubbard et al., 1959); *O. bimaculatus* from sensitivity of *O. vulgaris* (Brown and Brown, 1958); *P. planipes* (Fernandez, 1973); and *M. gracilis* from *Cancer irroratus* (Cronin and Forward, 1988). These spectra were used to determine the species-specific photon flux density.

Table S1. Statistical results of response-irradiance relationships.

Statistical comparisons of light series tests (Figs. 4, 5) conducted on the larvae of the market squid, *D. opalescens* (green); the octopus, *O. bimaculatus* (teal); the tuna crab, *P. planipes* (magenta); and the graceful rock crab, *M. gracilis* (orange). Differences between visual responses at three oxygen conditions (normoxia, ~22 kPa/~265 μmol kg^{-1}; intermediate reduction of pO_2, ~6.5 kPa/~95 μmol kg^{-1}; and low pO_2, ~3.5 kPa/~55 μmol kg^{-1}) at each experimental irradiance [in species-specific photon flux density (μmol photons m^{-2} s^{-1})] were determined using Kruskal-Wallis tests in each species. Results are presented for the light series visual responses normalized to both the maximum value of normoxia ("Normalized to normoxia"; Fig. 4) and the maximum value within each oxygen condition ("Normalized within each condition"; Fig 5). Significant values ($p < 0.05$) are presented in bold. Abbreviations: df = degrees of freedom; NA = not applicable; PFD = photon flux density.

df = 2		Squid PFD	0.033	0.296	0.557	0.815	1.073	1.327	1.581	1.834	2.087
D. opalescens	Normalized to normoxia	Chi squared	2.808	8.000	8.769	8.000	8.000	8.346	8.346	8.346	8.649
		p-value	0.246	**0.018**	**0.012**	**0.018**	**0.018**	**0.015**	**0.015**	**0.015**	**0.013**
	Normalized within each condition	Chi squared	1.423	4.154	3.846	1.654	4.962	2.808	0.269	3.039	NA
		p-value	0.491	0.125	0.146	0.437	0.084	0.246	0.874	0.219	NA
df = 2		Octopus PFD	0.024	0.209	0.393	0.576	0.758	0.938	1.117	1.296	1.474
O. bimaculatus	Normalized to normoxia	Chi squared	2.400	6.489	7.200	6.489	6.489	6.489	6.489	6.489	6.713
		p-value	0.301	**0.039**	**0.027**	**0.039**	**0.039**	**0.039**	**0.039**	**0.039**	**0.035**
	Normalized within each condition	Chi squared	5.067	2.222	5.067	5.600	4.267	2.756	5.689	1.689	NA
		p-value	0.079	0.329	0.079	0.061	0.118	0.252	0.058	0.430	NA
df = 2		Tuna Crab PFD	0.036	0.323	0.608	0.891	1.173	1.450	1.727	2.004	2.280
P. planipes	Normalized to normoxia	Chi squared	4.500	6.731	5.654	6.269	6.000	6.731	6.000	7.731	8.290
		p-value	0.105	**0.035**	0.059	**0.044**	**0.050**	**0.035**	**0.050**	**0.021**	**0.016**
	Normalized within each condition	Chi squared	1.500	0.269	1.192	3.136	0.615	0.115	0.154	1.631	NA
		p-value	0.472	0.874	0.551	0.209	0.735	0.944	0.926	0.443	NA
df = 2		Crab PFD	0.032	0.288	0.542	0.794	1.045	1.292	1.539	1.786	2.031
M. gracilis	Normalized to normoxia	Chi squared	12.737	15.431	14.794	14.500	14.500	14.222	14.222	14.500	14.005
		p-value	**0.002**	**0.000**	**0.001**	**0.001**	**0.001**	**0.001**	**0.001**	**0.001**	**0.001**
	Normalized within each condition	Chi squared	4.774	1.433	2.151	0.693	2.821	0.693	3.468	2.331	NA
		p-value	0.092	0.488	0.341	0.707	0.244	0.707	0.177	0.312	NA

Chapter 3, in full, is a reprint of the material as it appears in **McCormick, L.R.,** Levin, L. A. and N.W. Oesch. 2019. Vision is highly sensitive to oxygen availability in marine invertebrate larvae. Journal of Experimental Biology 222:10. DOI: 10.1242/jeb.200899. The dissertation author was the primary investigator and author of this material.

CHAPTER 4

Comparing critical oxygen limits for metabolism and vision in cephalopod paralarvae

Lillian R. McCormick, Lisa A. Levin, and Nicholas C. Wegner

Abstract

The ocean contains strong decreasing gradients of oxygen with depth, and many marine organisms regulate their internal oxygen partial pressure (pO_2) independent of the environmental pO_2. Some animals maintain a constant metabolic rate over higher oxygen conditions, and after a critical pO_2 (P_{crit}), they become unable to regulate their internal pO_2 and conform to the external pO_2. Cephalopods have especially high oxygen demands due to their inefficient locomotion mechanism and developed sensory systems that support their active, predatory life style. Recently hatched cephalopods, called paralarvae, are highly visual and their visual function is severely inhibited during exposure to reduced pO_2, beginning at approximately 22 and 11.5 kPa for paralarvae of *D. opalescens* and *O. bimaculatus*, respectively. It is unclear whether the visual impairment is a result of general metabolic decline or is occurring at a different rate. Here we conducted respirometry experiments to determine the P_{crit} and routine metabolic rate in paralarvae of the market squid, *Doryteuthis opalescens* and the octopus, *Octopus bimaculatus*, and compare critical oxygen limits for metabolism (P_{crit}) with oxygen metrics for retinal function. The P_{crit} of both *D. opalescens* and *O. bimaculatus* was lower than the predicted pO_2 where all retinal function would cease, indicating the visual impairment is occurring at higher pO_2 than changes in metabolic rate. Hence, if paralarvae have any physiological mechanisms to increase pO_2 locally at the eyes, these are not sufficient to maintain visual function at pO_2 levels sufficient to maintain whole body oxygen consumption.

The greater metabolic rate and P_{crit} at higher pO_2 in *D. opalescens* paralarvae indicated a greater sensitivity to reduced pO_2 compared to paralarvae of *O. bimaculatus* and suggests general species-specific trends in vulnerabilities to oxygen loss.

Introduction

Oxygen is introduced into the ocean as a product of photosynthesis and from mixing at the surface, and removed from the water column by the respiration of plants, animals, and microbes. As a result, strong gradients of oxygen exist with depth in the ocean and marine organisms can be exposed to fluctuating oxygen conditions over a variety of time scales (Levin et al. 2015). Some marine organisms have the challenge of regulating their internal oxygen partial pressure (pO_2) independent of external pO_2, which can be much lower than air oxygen content. Obtaining sufficient oxygen supply can be particularly taxing for marine organisms with high metabolic oxygen demands, and in the marine environment, this includes active arthropods, cephalopods, and fish (Seibel and Drazen 2007). Cephalopods in particular have extremely high oxygen requirements, in part due to their jet-propulsion locomotion (O'Dor and Webber 1991, Rosa and Seibel 2008). To facilitate their fast-paced, highly mobile and predatory lifestyle, cephalopods have also evolved sophisticated sensory systems that enable prey capture, predator detection, and vertical migration at all life stages, which increase the metabolic demand (Seibel and Drazen 2007, McCormick and Levin 2017). In addition, many coastal cephalopod species lay benthic clusters of eggs/capsules. Despite the protection these capsules offer, they also limit the diffusion of oxygen to the embryos (Gutowska and Melzner 2009, Long et al. 2016), which can be exacerbated when spawning occurs in areas with naturally occurring low oxygen (Navarro et al. 2018). Hatched cephalopod larvae that undergo a planktonic phase, called paralarvae, also experience large gradients of oxygen in their habitat. For example, in the nearshore environment in La Jolla, California, the daily range of oxygen at 7 m depth can be up to 220 μmol kg^{-1} and the change in oxygen over a 10 m depth range (7- 17 m) is greater than the change in oxygen over a 5 km

horizontal stretch of shelf (Frieder et al. 2012). Similar to adults, cephalopod paralarvae have high oxygen requirements (Pimentel et al. 2012) and typically have well-developed sensory systems essential to survival (Robin et al. 2014, McCormick and Levin 2017).

Sensory reception, particularly vision, is essential and metabolically demanding for both vertebrates and invertebrates (Niven and Laughlin 2008). Oxygen is necessary for photoreceptors (the light-sensitive cells in the eye) to function. The retina, containing the photoreceptor cells, is the tissue with one of the highest metabolic demands in the vertebrate body (Anderson 1968, Waser and Heisler 2005, Wong-Riley 2010). In humans, a decrease in atmospheric oxygen (to 10% air saturation) decreases the sensitivity of the eye to light, and also changes color perception (Ernest and Krill 1971). Effects of low oxygen on vision have also been observed in larvae of highly visual marine organisms. A decrease in retinal function and sensitivity to light, in addition to changes in the temporal response of vision occurred during exposure to reduced pO_2 (21-3 kPa) in larvae of two species of cephalopod and two species of crustaceans (McCormick et al. 2019). In that study, three oxygen metrics for retinal function were developed to quantify the decline in retinal response under a reduction in pO_2. Retinal sensitivity to low oxygen showed species-specific differences, even within taxonomic groups; paralarvae of the California market squid, *Doryteuthis opalescens* showed declines in retinal responses at a higher pO_2 than paralarvae of the two-spot octopus, *Octopus bimaculatus*.

Some organisms physiologically regulate oxygen supply to their tissues based on their oxygen demands, and highly visual organisms may have mechanisms to keep visual tissues sufficiently oxygenated until they experience system-wide metabolic failure, such as the choroid rete in fish (Waser and Heisler 2005). A traditional metric used to describe oxygen

tolerance for metabolism is the P_{crit} value, defined as the partial pressure of oxygen below which the organism cannot maintain its general rate of oxygen consumption and is no longer able to regulate its internal pO_2 independent of the environment (Pörtner & Grieshaber 1993; Grieshaber et al. 1994; Childress & Seibel 1998). At pO_2 greater than the P_{crit}, organisms maintain a specific metabolic rate, independent of the external pO_2 (oxy-regulating). This can be a standard metabolic rate (SMR) if animals are either anesthetized or not moving, but is very often presented as a routine metabolic rate (RMR), where the animal is free swimming and maintains a normal activity level. At pO_2 lower than the P_{crit}, the animal can no longer maintain its metabolic rate, and oxy-conforms to its external pO_2 (Peck and Moyano 2016).

The use of P_{crit} for determining oxygen tolerances in marine organisms has recently been debated (Wood 2018) and alternative metrics for metabolic sensitivity to oxygen have been suggested (Seibel and Deutsch, pers. comm.). However, when the P_{crit} value is used as the lowest pO_2 where the animal can maintain a stable rate of oxygen consumption, it serves an excellent gauge for examining the metabolic capacity of an animal to tolerate low pO_2 (Regan et al. 2019). Metabolic rates and oxygen limits for metabolism (P_{crit}) have been collected in a wide variety of adult cephalopods (e.g., Birk et al. 2019; Burford et al. 2019; Seibel 2007; Seibel and Childress 2000; Zielinski et al. 2000), and metabolic rates have been determined in paralarvae of several cephalopod species including the squid *Loligo (=Doryteuthis) opalescens* (Hurley 1975), *Loligo vulgaris* (Pimentel et al. 2012), and *L. vulgaris reynaudii* (Vidal et al. 2019), and the octopuses *Octopus mimus* (Zúñiga et al. 2013) and *O. huttoni* (Higgins et al. 2012). To our knowledge, oxygen critical limits (P_{crit}) have not been determined in cephalopod paralarvae. These critical limits are most useful when they consider the specific physiological demands and ecological functions for a species (Seibel and

Childress 2013), and it is currently unclear whether the effects of reduced pO_2 on visual physiology in marine larvae are a result of a general metabolic decline or whether visual effects are occurring at a differential rate than metabolic losses.

For paralarvae of both *D. opalescens* and *O. bimaculatus*, the decline of retinal function occurred at pO_2 already occurring within the habitat of these species (McCormick et al. 2019), and at higher oxygen levels than the suggested oxygen limits for marine benthic organisms (Vaquer-Sunyer and Duarte 2008). Vaquer-Sunyer and Duarte (2008) found that many sublethal effects of reduced oxygen, such as reduced feeding or changes in ventilation rate or activity level, occur at approximately 2.61 mg L^{-1} O_2 (~6.73 kPa at 15 °C) in many species of highly mobile organisms. However, the study was on primarily benthic organisms, and data from only one cephalopod species was included in the study. In contrast to the sublethal oxygen limits found by Vaquer-Sunyer and Duarte (2008), changes in retinal function began at approximately 22 and 11.5 kPa for paralarvae of *D. opalescens* and *O. bimaculatus*, respectively. There are very few studies examining sublethal effects of reduced pO_2 on marine larvae, especially in either of these species. As a result, it is unknown whether the reported changes in retinal function are occurring as a symptom of general metabolic loss/decline, or whether the effects of reduced pO_2 on vision are differentiated from the changes in metabolic rates (e.g. P_{crit}).

Here, we 1) determine the P_{crit} values for paralarvae of two species of cephalopods, *D. opalescens* and *O. bimaculatus*, and 2) compare the oxygen metrics for metabolism (P_{crit}) to the oxygen metrics for retinal function based on data from McCormick et al. (2019) to test the hypothesis that visual oxygen thresholds occur at higher pO_2 than metabolic thresholds. Additionally, we compare the effects of reduced pO_2 on oxygen consumption rates relative to

rates of decline in retinal responses to test the hypothesis that visual sensitivity to low oxygen is distinct from metabolic sensitivity to low oxygen in each species. Finally, we establish relative vulnerabilities to oxygen loss for each species by examining trends of oxygen sensitivity across both visual physiology and metabolism.

Methods

Animal Collection

Paralarvae of *D. opalescens* were hatched from 16 egg capsules laid by a single female squid in captivity in Monterey Bay, California. Egg capsules were transported to San Diego in a dark cooler on March 30, 2019. After transport, the capsules were kept in light-controlled experimental room and housed in a 4-L tank with flowing, aerated seawater at a constant temperature of 14° C under a 13h light and 11h dark cycle and ~21 kPa oxygen (equivalent to surface ocean oxygen levels). All paralarvae hatched between April 12-20, 2019 and were kept in separate 1-L containers with their hatching cohort under the same light cycle with daily feeding of *Artemia* brine shrimp larvae and/or wild-collected copepods.

Paralarvae of *O. bimaculatus* were hatched from a cluster of eggs opportunistically collected from a marine sensor off Newport Beach, California on March 7, 2019. The eggs were kept in a 2-L tank with flowing seawater (~16° C) under a natural light cycle (13 h light: 11 h dark) and ~21 kPa oxygen (equivalent to surface ocean oxygen levels). They were identified as *O. bimaculatus* because of their small size (in comparison to *O. bimaculoides* eggs) and planktonic phase, in addition to larval identification upon hatching. Paralarvae used in these experiments hatched on April 25 and April 29, 2019. After hatching, the paralarvae were moved into a light-controlled experimental room (13 h light: 11 h dark cycle), placed

into 1-L tanks at 15° C with their hatching cohort, and free-fed *Artemia* brine shrimp larvae and/or wild-collected copepods daily.

Paralarvae of both species underwent an initial stabilization period of, at minimum, 24h prior to testing. Experiments were conducted on all paralarvae of both species within 2-4 days of hatching, which is a similar developmental stage to paralarvae in McCormick et al. (2019).

Respiration Experiments

Individual, closed-chamber respiration experiments were conducted to determine critical oxygen limits for metabolism and the metabolic rate for each species. Paralarvae were each placed in a 2-mL vial with an oxygen sensor spot (PreSens, De.) and oxygen partial pressure (pO_2) was continuously measured at 1-min intervals using a Loligo Systems SDR729 Microplate Reader. All vials were placed in a continuously circulating water bath placed on top of the microplate reader with stable temperature conditions throughout each experiment (average temperature ± standard error was 14.84 ±0.02 °C for *D. opalescens* and 14.68 ±0.63 °C for *O. bimaculatus*). Due to the sensitivity of oxygen tolerance to temperature (Pörtner 2010), respiration experiments were conducted at a similar temperature to the electrophysiology experiments measuring retinal function (McCormick et al. 2019). Seawater for all experiments and calibration was filtered using an Oceans Design filtration system (filtered with sand, charcoal, ozone, and ultraviolet radiation) and additionally filtered through a 45-μm GFF filter. Before experiments began, larvae were kept in air-saturated (21 kPa) seawater at the same temperature as the experiments. A two-point calibration was performed on each individual sensor spot prior to every experiment with air-saturated seawater (21 kPa)

and sodium-sulfite saturated seawater (0 kPa) at the experimental temperature. For each experiment, the vials containing either larvae or blanks were randomized to prevent biasing results due to either differences between different placement locations within the bath or the vials themselves.

Each individual was placed in a vial filled with seawater; the vial was sealed underwater to prevent air bubbles, and then placed in the water bath. Oxygen logging began ~15 minutes after all vials were closed in order to make sure the temperature and flow rate in the water bath were stable. Logging continued until the animals had exhausted all oxygen from the chamber (10.5-13.2 h for *D. opalescens* and 42-46 h for *O. bimaculatus*). Due to the size of the vials and the mobility of the larvae, vials were assumed to be well-mixed. At the end of experiments, vials were manually mixed and the oxygen measured again to confirm a change in mobility throughout the experiments did not prevent all oxygen from being consumed. After experiments were concluded, individuals were placed into 0.5-mL plastic vials, excess water removed with a Kimwipe, and the vial frozen at -80° C. After ~3 days, individuals were moved to pre-weighed aluminum boats and dried in an oven at 60° C. Wet weights were obtained from the aluminum boats prior to drying, and dry weights were taken after 20h and 44h of drying in the oven. In a few cases where the weight of the individual was not reliable (e.g. tissue lost during transfer), the average weight within the species was used to calculate mass-specific oxygen consumption rate (MO_2; μmol O_2 g^{-1} h^{-1}).

Calculation of metabolic rates and P_{crit}

Respiration trials were analyzed using the 'respirometry' package (v1.0.0) in R version 3.3.3 (Birk 2019). Data from the first 60 min of logging were removed to prevent any

stress response from the animals, and data were terminated after 30 min of recording ~0 kPa. The oxygen consumption rate was calculated using the remaining data for each individual by binning data points so there would be high precision at high pO_2 and high resolution at lower pO_2. The calculated metabolic rate was plotted against pO_2 and analyzed for the pO_2 below which the individual could no longer sustain its routine metabolic rate (P_{crit}). The 'respirometry' package calculates P_{crit} using three different methods; the "breakpoint" method was used in this analysis because it provided the best fits to the data (Birk 2019). This method determines P_{crit} as the intersection of two linear regressions (Fig. 1, yellow stars) calculated from the range of pO_2 where the animal regulates its oxygen, and the range of pO_2 where the animal oxy-conforms (Fig. 1, black solid lines). In the few cases where the "breakpoint" method seemed to overestimate the P_{crit} (2 out of 35 *D. opalescens* individuals), the "sub-prediction interval" (Sub-PI) calculated values were used. The Sub-PI method estimates the lowest reasonable P_{crit} value using a similar breakpoint analysis, but fits the regression lines with 95% confidence intervals (Fig. 1, red dashed lines and red circle); P_{crit} is calculated as the pO_2 at the intersection of the oxy-conforming regression with the lower 95% confidence interval of the regulating regression (Birk et al. 2019). The non-linear regression method (as in Marshall et al. 2013) was calculated, but not used in this analysis.

The oxygen consumption rate (MO_2) was calculated where the oxygen was > 10 kPa during the experiment, using only regressions with an $R^2 > 0.7$. Oxygen consumption was also calculated for each blank in the same method as for animals. Blanks from each trial were averaged and subtracted from the animal MO_2 to correct for any microbial respiration that might have occurred. A corrected MO_2 was calculated for each individual larva and then averaged across species. Metabolic rate traditionally scales with size according to a power

function ($MO_2 = b_0 * M^b$), where 'M' is the mass of the individual, 'b_0' is the normalization constant, and 'b' is the metabolic scaling coefficient (Birk et al. 2019). It was unclear whether the small differences in larval mass would change the metabolic rate, so a mass-scaling coefficient (b) was calculated for each species to test whether rates needed to be corrected to a single mass for all individuals.

Results from all individuals tested were used for *O. bimaculatus* paralarvae. Out of 50 total individual *D. opalescens* paralarvae tested, 15 trials were removed and the results from 35 individuals are presented here. Three individuals out of the 15 removed appeared to be either oxy-conforming, or the experiment was terminated too early to determine a proper P_{crit}. The remaining 12 individuals either showed results with unreasonable P_{crit} values (negative, or > 15 kPa), or the calculated fit did not visually match the data. We believe the results not included in this dataset were due to experimental issues and not individual variability, as the results presented here still show considerable variability across individuals. Anomalous results could be due to the condition of the animal, from too much background respiration, or the calculation method of the P_{crit}.

Determining differences between trials

A total of 4 experiments were conducted on *D. opalescens* paralarvae ranging from 2-4 days post-hatching, with a total of 35 individuals used in this analysis. Previous studies have observed no difference in metabolic rate within the first 4 days of hatching in *Octopus mimus* (Zúñiga et al. 2013) or *Octopus huttoni* (Higgins et al. 2012) paralarvae, however, to ensure no effects of age or other metabolic differences existed between trials in this experiment, Kruskal-Wallis one-way analysis of variance (ANOVA) tests were conducted for each species

(df = 3 for all *D. opalescens* trial Kruskal-Wallis tests). Results showed no significant differences in individual masses ($p = 0.1646$), calculated mass-corrected MO_2 ($p = 0.1310$), or calculated P_{crit} values ($p = 0.1863$) between experiments, so individuals in all trials of *D. opalescens* paralarvae were combined (Fig. 2).

Two experiments were conducted on *O. bimaculatus* paralarvae, with a total of 11 individuals used in this analysis. As in *D. opalescens*, Kruskal-Wallis ANOVA test were completed to determine differences between trials (df = 1 for all *O. bimaculatus* trial Kruskal-Wallis tests). No significant differences were detected between the two trials for *O. bimaculatus* individuals in mass ($p = 0.8548$) or P_{crit} ($p = 0.4652$) using Kruskal-Wallis ANOVA tests (Fig S1). Mass-corrected MO_2 were different between trials ($p= 0.0441$), so MO_2 results are presented individually for each experiment, but both trials were combined for P_{crit} analysis (Fig. 2).

Visual critical limits

Critical oxygen limits for vision in marine invertebrate larvae were calculated in previous experiments using electroretinogram (ERG) recordings of retinal responses during exposure to decreasing pO_2. All visual experiments were conducted in 2018 using different sets of animals, and the full results and methods are in McCormick et al. (2019). Briefly, individual larvae were tethered under a microscope in a small volume of pH-buffered and temperature-controlled seawater (recording chamber), and retinal responses to a 1-s light stimulus of constant irradiance were simultaneously measured using electrophysiology. After a brief period in normoxia (surface-ocean oxygen levels, ~21 kPa), the pO_2 was decreased in the recording chamber while the *in vivo* ERGs were recorded. The resulting series of retinal

responses as a function of pO_2 were used to calculate three oxygen metrics for retinal function; V_{90}, V_{50}, and V_{10} are the pO_2 values where there is 90%, 50%, and 10%, respectively, of retinal function remaining in comparison to retinal responses in normoxia. These metrics allow for a quantitative analysis of the decrease in retinal function observed with exposure to reduced pO_2, and were designed to be compared with other metrics for oxygen sensitivity (e.g., P_{crit}). Paralarvae of both *D. opalescens* and *O. bimaculatus* were tested in this way to determine visual sensitivity to reduced pO_2.

Analysis of Results

All statistics were computed in R (version 3.3.3). Kruskal-Wallis one-way analysis of variance (ANOVA) tests were used to determine whether any differences existed between individuals or results of any experiments for both species, and also to determine differences between oxygen metrics. Dunn's tests were additionally conducted for significant results ($p< 0.05$) to determine which pairwise comparisons were significant.

Results

Relationship between mass and metabolic rate

Species differences were evident for both routine metabolic rates (RMR) and individual masses (wet weights, g). *Octopus bimaculatus* paralarvae were smaller than *D. opalescens* paralarvae (average wet weights of 0.002 ± 0.0001 g and 0.004± 6.4e-5 g, respectively) (Fig. 3). The average mass-corrected MO_2 (± standard error; s.e.) for *O. bimaculatus* paralarvae for both experiments 1 and 2 (2.33 ±0.25 and 1.84 ±0.24 μmol O_2 g^{-1} h^{-1}, respectively) were lower than that of *D. opalescens* paralarvae (19.43 ±0.93 μmol O_2 g^{-1}

h^{-1}) (Fig. 2) by almost an order of magnitude. Metabolic rate showed very small, non-significant trends with mass in paralarvae of both *O. bimaculatus* (b= -0.92) and *D. opalescens* (b= 0.03) (Fig. 3). Therefore, RMR is presented for each individual, without mass-correcting MO_2 values across all individuals.

P_{crit} and relative sensitivity to oxygen

The average P_{crit} (± s.e.) calculated using the "breakpoint" method for *D. opalescens* paralarvae was 2.47 ±0.26 kPa (29.38 μmol kg^{-1}). The average P_{crit} for *O. bimaculatus* paralarvae was much lower, at 0.48 kPa ±0.09 kPa (5.72 μmol kg^{-1}) (Fig. 4).

Comparisons of oxygen limits for metabolism and vision

To determine whether there were differences among oxygen limits for metabolism and oxygen limits for visual function, all oxygen metrics (V_{90}, V_{50}, V_{10}, and P_{crit}) were compared for paralarvae of *D. opalescens* and *O. bimaculatus* (Fig 5). Significant differences were observed between oxygen metrics for *D. opalescens* (Kruskal-Wallis, p= 7.8e-06). The average P_{crit} (2.47 kPa) was lower than $V_{90,}$ V_{50}, and V_{10} (22.2, 13.0, and 6.9 kPa, respectively). Pairwise comparisons between P_{crit} and each visual metric (e.g. P_{crit} vs. V_{10}, P_{crit} vs. V_{50}, etc.) were also significant (Dunns' test, $p< 0.05$) for all oxygen metrics for vision. An exponential fit to percent retinal function and pO_2 ($y=5.7462e^{0.0143x}$; $R^2= 0.80$) was calculated using the visual metrics (V_{90}, V_{50}, and V_{10}). Using this fit, the pO_2 that would cause 0% retinal function in paralarvae of *D. opalescens* is 5.75 kPa (closed green circle, Fig. 5).

Differences across oxygen metrics in paralarvae of *O. bimaculatus* were also significant (Kruskal-Wallis, p = 0.0092) (Fig. 5). Similar to the trends observed in *D.*

opalescens, the average P_{crit} for *O. bimaculatus* (0.48 kPa) was lower than $V_{90,}$ V_{50}, and V_{10} (11.5, 7.2, and 5.9 kPa, respectively). Statistical comparisons between the P_{crit} and visual metrics in *O. bimaculatus* paralarvae showed significant differences between the P_{crit} and V_{90} and V_{50} (Dunn's test, $p< 0.05$), but not between P_{crit} and V_{10} (Dunn's test, $p> 0.05$). An exponential fit to percent retinal function and pO_2 for paralarvae of *O. bimaculatus* ($y=4.5855e^{0.0125x}$; $R^2= 0.79$) predicted that paralarvae would lose all visual function at 4.59 kPa.

These results follow a trend of general oxygen sensitivity observed in the retinal responses to low oxygen for both species. Paralarvae of *D. opalescens* showed changes to retinal responses at a higher pO_2 than *O. bimaculatus* paralarvae, and a similar trend is observed with the metabolic sensitivity.

Discussion

In paralarvae of both *D. opalescens* and *O. bimaculatus*, critical limits for metabolism (P_{crit}) occurred at a lower pO_2 than all oxygen metrics for retinal function. The pO_2 for V_{90}, V_{50}, and V_{10} were all significantly higher than the P_{crit} in paralarvae of *D. opalescens*, indicating these paralarvae would lose all retinal function before reaching true metabolic decline and oxy-conforming to the environmental pO_2. In paralarvae of *O. bimaculatus*, V_{90} and V_{50} were significantly higher than P_{crit}, and while the P_{crit} occurred at a lower pO_2 than V_{10}, the difference was not significant. In addition, the pO_2 predicted to cause 0% visual function in paralarvae of *D. opalescens* and *O. bimaculatus* (5.75 and 4.59 kPa, respectively) were at a higher pO_2 than the P_{crit} (2.47 and 0.48 kPa, respectively), indicating both species would have no retinal function before reaching their P_{crit}. These results suggest that retinal

responses are affected at higher pO_2 than what causes the animal to deviate from its normal routine metabolic rate (RMR), suggesting the physiological effects of low oxygen on retinal function are slightly decoupled from metabolic decline and the critical oxygen limit for metabolism. These results also indicate that if the paralarvae tested here have any internal structures that locally regulate pO_2 at the level of the eye, as seen in fish (e.g., choroid rete), they may not be sufficient to maintain visual function at pO_2 where paralarvae can still regulate their oxygen consumption rate. Importantly, the effects of reduced oxygen for both retinal function and metabolism may depend on the magnitude and duration of exposure to reduced pO_2; the pattern and extent of exposure can determine the effects of low pO_2 on ventilation physiology in mammalian respiration (Powell et al. 1998) and oxygen consumption rate can change if animals are exposed to reduced oxygen prior to the start of experiments (Seibel et al. 2018). The effects of oxygen on retinal function still involves circulation and metabolic function, and so it is important to determine smaller-scale physiological changes that are occurring at the level of the visual system.

Trends for oxygen sensitivity, as indicated by metabolic and retinal function, were maintained between species, even within the close taxonomic grouping of cephalopods. In both oxygen metrics for retinal function (V_{90}, V_{50}, and V_{10}) and the P_{crit}, the pO_2 at which these oxygen metrics occurred was higher for paralarvae of *D. opalescens* compared to paralarvae of *O. bimaculatus* (Fig. 5). This indicates a higher sensitivity to low oxygen in *D. opalescens* and shows a potentially higher vulnerability to changing oxygen conditions. This trend of general oxygen sensitivity was, not surprisingly, also observed in the metabolic rate of each species. The RMR of *D. opalescens* paralarvae (19.43 ±0.93 μmol O_2 g^{-1} h^{-1}) was almost an order of magnitude higher than that of *O. bimaculatus* (1.84 and 2.33 ±0.25 μmol

O_2 g^{-1} h^{-1}) (Fig. 2). However, squid and octopus have very different activity levels as adults, and these changes may be reflected in their paralarvae. For example, the oxygen consumption rates of paralarvae of the squid, *Loligo vulgaris*, were 28 and 59.1 μmol O_2 g^{-1} h^{-1} at 13 °C and 19°C, respectively, in comparison to oxygen consumption rates of 3.84 and 11.1 μmol O_2 g^{-1} h^{-1} at 13 °C and 19°C, respectively, in larvae of the cuttlefish, *Sepia officinalis* (Pimentel et al. 2012). Pimentel et al. (2012) attributed the difference between metabolic rates across species to locomotion; *L. vulgaris* paralarvae have constant jet propulsion locomotion, in contrast to the nektobenthic lifestyle of *S. officinalis* larvae with reduced jet propulsion, supporting the argument that highly mobile visual predators typically have higher metabolic demands (Seibel and Drazen 2007). Given these trends, it is reasonable that the metabolic rate for *D. opalescens* paralarvae was higher than that of O. *bimaculatus*, which has a slower jet propulsion and more globular body design than *D. opalescens* (Villanueva and Norman 2008).

Following general trends for metabolism in marine organisms showing an inverse relationship with size and oxygen consumption rates in cephalopods (Seibel and Childress 2000, Birk et al. 2019), the RMRs calculated here for paralarval *D. opalescens* (19.43 ±0.93 μmol O_2 g^{-1} h^{-1}) and *O. bimaculatus* (1.84 and 2.33 ±0.25 μmol O_2 g^{-1} h^{-1}) were higher than the RMR reported for adults. The reported RMR of individually tested adult *D. opalescens* is 13.4 μmol O_2 g^{-1} h^{-1} (converted from 0.43 mg O_2 g^{-1} h^{-1} at 15 °C) (Burford et al. 2019). To our knowledge, the RMR or P_{crit} of adult *O. bimaculatus* has not been determined, but the RMR in adult *O. bimaculoides* (a similar species in habitat/ecology) was 0.73 μmol O_2 g^{-1} h^{-1} at 10 °C (Seibel and Childress 2000). Despite the higher metabolic rates in paralarvae, the calculated P_{crit} was lower than that of the adults in both species. In *D. opalescens*, the average

P_{crit} for an individually tested adult was 4.96 kPa (±1.03) (Burford et al. 2019), whereas the P_{crit} for paralarvae was 2.47 kPa. In adult *O. bimaculoides*, the P_{crit} was reported as between 2.13-3.73 kPa (16-28 mmHg at 10 °C) (Seibel and Childress 2000), which was at a higher pO_2 than the P_{crit} in *O. bimaculatus* paralarvae (0.48 kPa). To our knowledge, no studies have determined the critical oxygen pressure in cephalopod paralarvae, but in most aquatic organisms, such as zebrafish, the P_{crit} would normally decrease with age (Barrionuevo and Burggren 1999). One explanation for increased tolerance in paralarvae in comparison to adults may be the exposure to severe hypoxia and low pH during embryogenesis (Gutowska and Melzner 2009, Long et al. 2016). These metabolic experiments were all completed within 4 days post hatching, and it would be interesting to test later stage paralarvae and juveniles to determine when the change P_{crit} occurs in each species.

These results demonstrate that trends of oxygen sensitivity span a range of physiological parameters, and indicate that P_{crit} is still a valid way of estimating the oxygen tolerance of marine organisms. However, if some effects of reduced pO_2 (e.g., visual impairment) are occurring at pO_2 prior to the P_{crit}, it will be crucial to incorporate the results of additional metrics for oxygen sensitivity to the traditional methods.

Conclusions

Given the importance of vision for survival in cephalopod paralarvae, these results show that retinal impairment from low pO_2 may be a very important, sub-lethal and sub-P_{crit} effect of exposure to low oxygen. Both *D. opalescens* and *O. bimaculatus* paralarvae are found in coastal areas off the coast of California, USA. Oxygen loss in the Southern California Bight (SCB) over the past 25 years has been fairly severe, with losses of up to 2.1

μmol kg^{-1} $year^{-1}$ at 50 m depth (Bograd et al. 2008, 2015). Oxygen loss is also present in the northern span of the range of both species, with large interannual fluctuations and declining surface oxygen (~100 m depth) in the last sixteen years off the coast of Monterey Bay (Ren et al. 2018). Paralarvae of *D. opalescens* and *O. bimaculatus* vertically migrate between the surface and approximately 80 m depth in the SCB (Ambrose 1981, Zeidberg and Hamner 2002), and can be exposed to reduced pO_2 within their habitat, especially during the seasonal upwelling of low oxygen water (McCormick et al. 2019). While paralarvae in both species seemed to be metabolically robust to reduced pO_2 in comparison to adults, the visual effects of reduced pO_2 happen at relatively high oxygen levels. As a result, it is crucial to determine the vulnerability of each species to oxygen stress. Additionally, we found that species-specific trends of oxygen sensitivity are maintained in both retinal physiology and metabolic physiology, and show a higher sensitivity to reduced pO_2 in *D. opalescens* paralarvae compared to *O. bimaculatus* paralarvae. Trends in oxygen tolerance can be used to inform the vulnerabilities of marine larvae to decreasing oxygen in the marine environment local to these cephalopod species.

Acknowledgements

We thank W. Gilly and P. Teal at Stanford University for providing us with *D. opalescens* egg capsules, and P. Lertvilai and P. Zerofski for obtaining the *O. bimaculatus* eggs. All experiments were conducted at the National Marine Fisheries Southwest Fisheries Science Center (SWFSC), and we thank the Fisheries Resource Division staff for their assistance in setting up the experimental room. This research was supported by a Charles H. Stout Foundation grant to L.R.M., a National Science Foundation grant OCE-1829623 to

L.A.L. and N.W.O., and the National Oceanic and Atmospheric Administration Office of Agriculture for support to the SWFSC Fisheries Resources Division. Any opinion, findings, and conclusions or recommendations expressed in this material are those of the authors and do not necessarily reflect the views of the National Science Foundation.

Chapter 4, in part, is in preparation for submission for publication. The dissertation author was the primary investigator and author of this material. **McCormick, L. R.**, Levin, L. A., and N. C. Wegner. Comparing critical oxygen limits for metabolism and vision in cephalopod paralarvae.

Literature Cited

Ambrose, R. F. 1981. Observations on the embryonic development and early post-embryonic behavior of *Octopus bimaculatus* (Mollusca: Cephalopoda). The Veliger 24:139–146.

Anderson, B. 1968. Ocular effects of changes in oxygen and carbon dioxide tension. Transactions of the American Ophthalmological Society 66:423–74.

Barrionuevo, W. R., and W. W. Burggren. 1999. O_2 consumption and heart rate in developing zebrafish (*Danio rerio*): influence of temperature and ambient O_2. American Journal of Physiology 276:505–513.

Birk, M. A. 2019. Respirometry: Tools for conducting and analyzing respirometry experiments. R Package Version 1.0.0.

Birk, M. A., K. A. S. Mislan, K. F. Wishner, and B. A. Seibel. 2019. Metabolic adaptations of the pelagic octopod *Japetella diaphana* to oxygen minimum zones. Deep-Sea Research Part I 148:123–131.

Bograd, S. J., M. P. Buil, E. Di Lorenzo, C. G. Castro, I. D. Schroeder, R. Goericke, C. R. Anderson, C. Benitez-Nelson, and F. A. Whitney. 2015. Changes in source waters to the Southern California Bight. Deep Sea Research Part II: Topical Studies in Oceanography 112:42–52.

Bograd, S. J., C. G. Castro, E. Di Lorenzo, D. M. Palacios, H. Bailey, W. Gilly, and F. P. Chavez. 2008. Oxygen declines and the shoaling of the hypoxic boundary in the California Current. Geophysical Research Letters 35:L12607.

Burford, B. P., N. Carey, W. F. Gilly, and J. A. Goldbogen. 2019. Grouping reduces the metabolic demand of a social squid 612:141–150.

Childress, J. J., and B. a Seibel. 1998. Life at stable low oxygen levels : Adaptations of animals to oceanic oxygen minimum layers. The Journal of Experimental Biology 201:1223–1232.

Ernest, J. T., and A. E. Krill. 1971. The effect of hypoxia on visual function: psychophysical studies. Investigative Ophthalmology and Visual Science 10:323–328.

Frieder, C. A., S. Nam, T. R. Martz, and L. A. Levin. 2012. High temporal and spatial variability of dissolved oxygen and pH in a nearshore California kelp forest. Biogeosciences 9:1–14.

Grieshaber, M. K., I. Hardewig, U. Kreutzer, and H. O. Pörtner. 1994. Physiological and metabolic responses to hypoxia in invertebrates. Reviews of physiology, biochemistry and pharmacology 125:43–147.

Gutowska, M. A., and F. Melzner. 2009. Abiotic conditions in cephalopod (*Sepia officinalis*) eggs: Embryonic development at low pH and high pCO_2. Marine Biology 156:515–519.

Higgins, F. A., A. E. Bates, and M. D. Lamare. 2012. Heat tolerance, behavioural temperature selection and temperature-dependent respiration in larval *Octopus huttoni*. Journal of Thermal Biology 37:83–88.

Hurley, A. C. 1975. Feeding behavior, food consumption, growth, and respiration of the squid, *Loligo opalescens* raised in the laboratory. Fishery Bulletin 74:176–182.

Long, M. H., T. A. Mooney, and C. Zakroff. 2016. Extreme low oxygen and decreased pH conditions naturally occur within developing squid egg capsules 550:111–119.

Marshall, D. J., M. Bode, and C. R. White. 2013. Estimating physiological tolerances – a comparison of traditional approaches to nonlinear regression techniques. Journal of Experimental Biology 216:2176–2182.

McCormick, L. R., and L. A. Levin. 2017. Physiological and ecological implications of ocean deoxygenation for vision in marine organisms. Philosophical Transactions of the Royal Society A 375.

McCormick, L. R., L. A. Levin, and N. W. Oesch. 2019. Vision is highly sensitive to oxygen availability in marine invertebrate larvae. Journal of Experimental Biology 222:1–11.

Navarro, A. M. O., P. E. Parnell, and L. A. Levin. 2018. Essential market squid (*Doryteuthis opalescens*) embryo habitat : A baseline for anticipated ocean climate change. Journal of Shellfish Research 37:601–614.

Niven, J. E., and S. B. Laughlin. 2008. Energy limitation as a selective pressure on the evolution of sensory systems. The Journal of experimental biology 211:1792–804.

O'Dor, R. K., and D. M. Webber. 1991. Invertebrate athletes: trade-offs between transport efficiency and power density in cephalopod evolution. Journal of Experimental Biology 160:93–112.

Peck, M. A., and M. Moyano. 2016. Measuring respiration rates in marine fish larvae: challenges and advances. Journal of Fish Biology 88:173–205.

Pimentel, M. S., K. Trubenbach, F. Faleiro, J. Boavida-Portugal, T. Repolho, and R. Rosa. 2012. Impact of ocean warming on the early ontogeny of cephalopods: a metabolic approach. Marine Biology 159:2051–2059.

Powell, F. L., W. K. Milsom, and G. S. Mitchell. 1998. Time domains of hypoxic ventilatory response. Respiration Physiology 112:123-134.

Pörtner, H. -O., and M. K. Grieshaber. 1993. Characteristics of the critical PO_2(s): gas exchange, metabolic rate, and the mode of energy production. Pages 330–357 *in* J. E. P. W. Bicudo, editor. The Vertebrate Gas Transport Cascade: Adaptations to Environment and Mode of Life. CRC Press, Boca Raton, FL.

Pörtner, H. -O. 2010. Oxygen- and capacity-limitation of thermal tolerance: a matrix for integrating climate-related stressor effects in marine ecosystems. Journal of Experimental Biology 213:881–893.

Regan, M. D., M. Mandic, R. S. Dhillon, G. Y. Lau, A. P. Farrell, P. M. Schulte, B. A. Seibel, B. Speers-roesch, G. R. Ultsch, and J. G. Richards. 2019. Don't throw the fish out with the respirometry water. Journal of Experimental Biology 222:9–10.

Ren, A. S., F. Chai, H. Xue, D. M. Anderson, and F. P. Chavez. 2018. A sixteen-year decline in dissolved oxygen in the Central California Current. Scientific Reports 8:1–9.

Robin, J., M. Roberts, L. Zeidberg, I. Bloor, A. Rodriguez, F. Briceño, N. Downey, M. Mascaró, M. Navarro, A. Guerra, J. Hofmeister, D. D. Barcellos, S. A. P. Lourenço, C. F. E. Roper, N. A. Moltschaniwskyj, C. P. Green, and J. Mather. 2014. Transitions during cephalopod life history: The role of habitat, environment, functional morphology, and behaviour. Advances in Marine Biology 67:361–437.

Rosa, R., and B. A. Seibel. 2008. Synergistic effects of climate-related variables suggest future physiological impairment in a top oceanic predator. Proceedings of the National Academy of Sciences 105:20776–20780.

Seibel, B. A. 2007. On the depth and scale of metabolic rate variation: scaling of oxygen consumption rates and enzymatic activity in the Class Cephalopoda (Mollusca). Journal of Experimental Biology 210:1–11.

Seibel, B. A., and J. J. Childress. 2000. Metabolism of benthic octopods (Cephalopoda) as a function of habitat depth and oxygen concentration. Deep-Sea Research Part I: Oceanographic Research Papers 47:1247–1260.

Seibel, B. A., and J. J. Childress. 2013. The real limits to marine life: A further critique of the Respiration Index. Biogeosciences 10:2815–2819.

Seibel, B. A., and J. C. Drazen. 2007. The rate of metabolism in marine animals: environmental constraints, ecological demands and energetic opportunities. Philosophical transactions of the Royal Society of London. Series B, Biological sciences 362:2061–78.

Seibel, B. A., B. E. Luu, S. N. Tessier, T. Towanda, and K. B. Storey. 2018. Metabolic suppression in the pelagic crab, *Pleuroncodes planipes*, in oxygen minimum zones. Comparative Biochemistry and Physiology, Part B 224:88-97.

Vaquer-Sunyer, R., and C. M. Duarte. 2008. Thresholds of hypoxia for marine biodiversity. Proceedings of the National Academy of Sciences of the United States of America 105:15452–15457.

Vidal, E. A. G., M. J. Roberts, and R. S. Martins. 2019. Yolk utilization, metabolism and growth in reared *Loligo vulgaris reynaudii* paralarvae 393:385–393.

Villanueva, R., and M. D. Norman. 2008. Biology of the planktonic stages of benthic octopuses. Oceanography and Marine Biology: an Annual Review 46:105–202.

Waser, W., and N. Heisler. 2005. Oxygen delivery to the fish eye: root effect as crucial factor for elevated retinal PO_2. The Journal of experimental biology 208:4035–47.

Wong-Riley, M. 2010. Energy metabolism of the visual system. Eye and Brain 2:99–116.

Wood, C. M. 2018. The fallacy of the P_{crit} – are there more useful alternatives? Journal of Experimental Biology 221.

Zeidberg, L. D., and W. M. Hamner. 2002. Distribution of squid paralarvae, *Loligo opalescens* (Cephalopoda: Myopsida), in the Southern California Bight in the three years following the 1997-1998 El Niño. Marine Biology 141:111–122.

Zielinski, S., P. G. Lee, and H. O. Pörtner. 2000. Metabolic performance of the squid *Lolliguncula brevis* (Cephalopoda) during hypoxia: an analysis of the critical PO_2. Journal of Experimental Marine Biology and Ecology CN - 808 243:241–259.

Zuniga, O., A. Olivares, M. Rojo, M. E. Chimal, F. Diaz, I. Uriarte, and C. Rosas. 2013. Thermoregulatory behavior and oxygen consumption of *Octopus mimus* paralarvae: The effect of age. Journal of Thermal Biology 38:86–91.

Figures

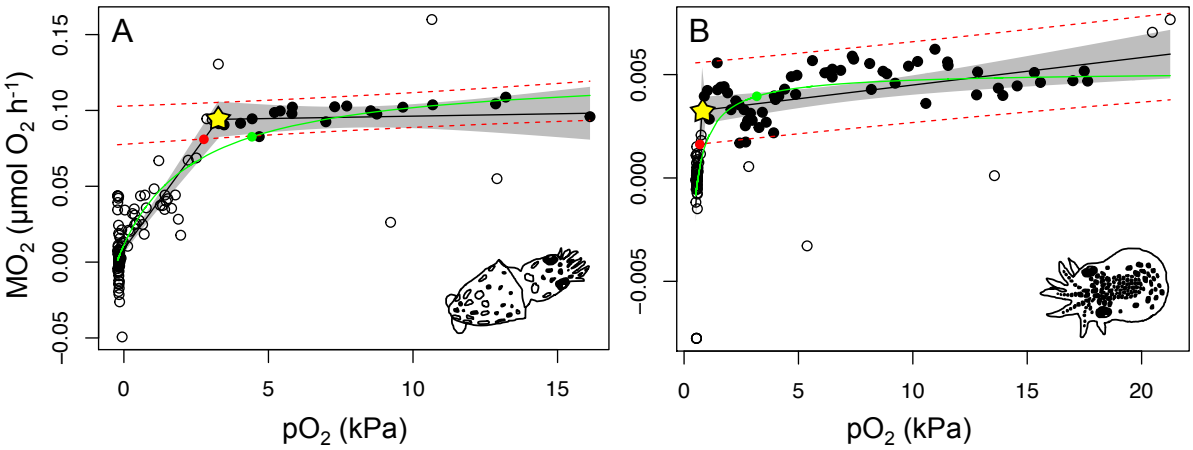

Figure 4.1. Calculation of P_{crit} using the 'respirometry' package in R (version 3.3.3). An example calculation of P_{crit} using regressions of oxygen consumption rates (MO_2, µmol O_2 h^{-1}, solid and open circles) against the partial pressure of oxygen (pO_2, kPa) in a (A) *Doryteuthis opalescens* paralarva and (B) *Octopus bimaculatus* paralarva. Solid black lines show regressions of both the oxy-regulating range of pO_2 where the animal maintains a relatively constant metabolic rate and the oxy-conforming range. The pO_2 at which the regressions (solid black lines) intersect is the "breakpoint" method of calculating P_{crit} (yellow stars). An alternative method, the sub-prediction interval, calculates the P_{crit} as the intersection of the lower limit of the 95% confidence intervals (red dashed lines) of the oxy-regulating regression with the oxy-conforming regression (red circle). The non-linear regression model method (green line and circle) was not used in this analysis.

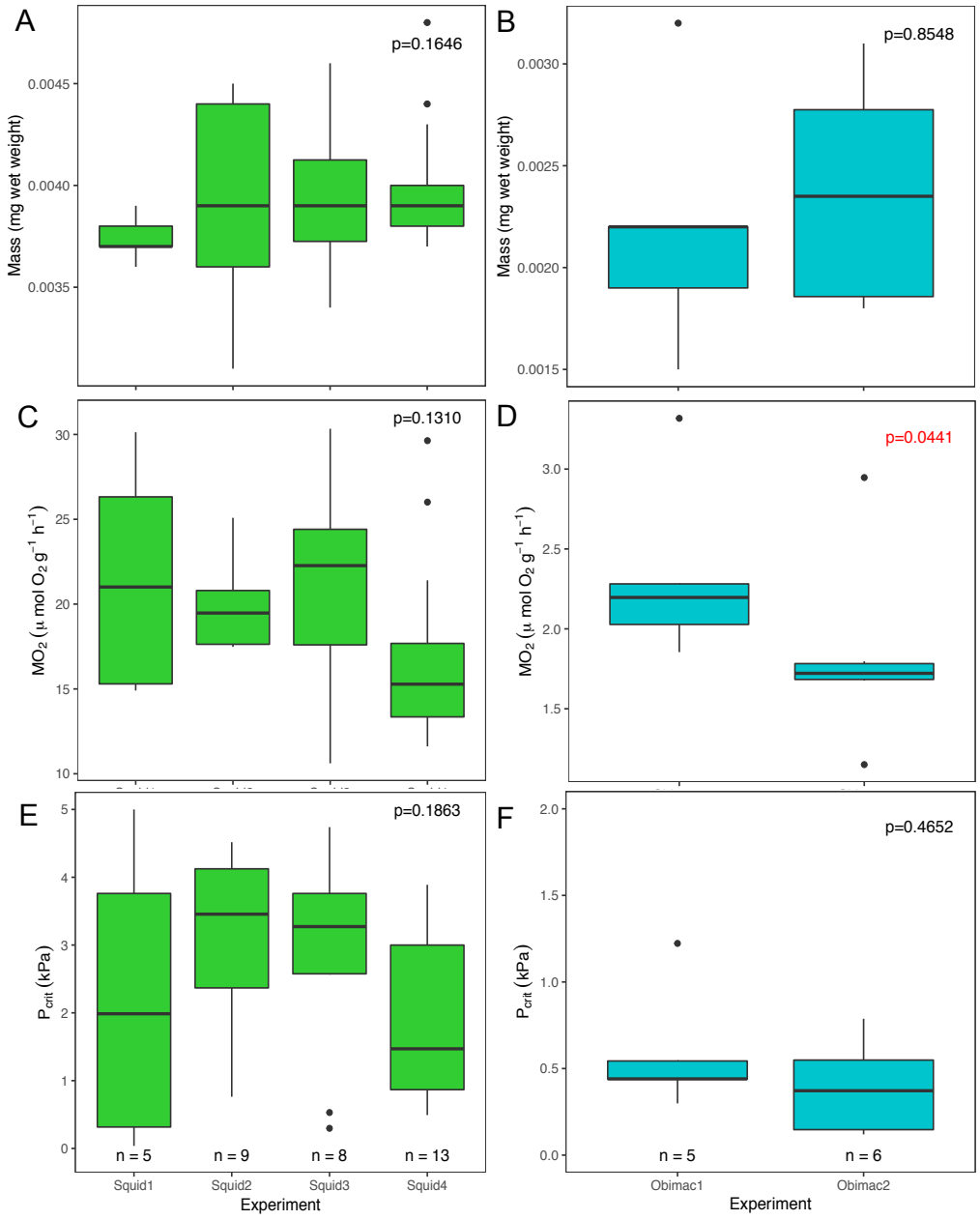

Figure 4.2. Variation across respiration trials. Differences among individual mass (A, B; mg wet weight), calculated MO_2 (C, D; µmol O_2 h^{-1}), and calculated P_{crit} (E, F; kPa) for 4 trials of *D. opalescens* paralarvae (A, C, E; green boxes) and 2 trials of *O. bimaculatus* paralarvae (B, D, F; teal boxes). Boxes show the median (bold center line) and first and third quartiles of all individuals tested within a species; error bars show maximum/minimum values within 1.5x the inner quartile range (IQR=third quartile–first quartile) and outlier points are shown as black circles. Differences were tested using Kruskal-Wallis one- way ANOVAs, p-values are presented for each variable and species; $p > 0.05$ for all tests. Sample sizes for each of the trials are presented in the bottom figures (E, F) for each species.

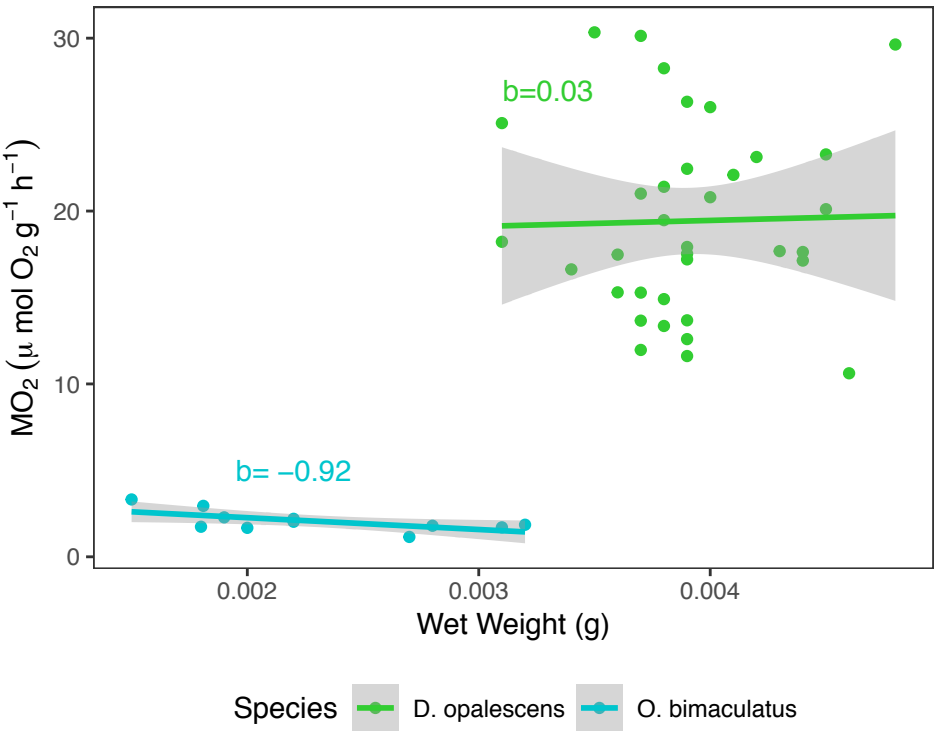

Figure 4.3. Metabolic rate and mass scaling relationship. Individual oxygen consumption rates (MO_2, μmol O_2 g^{-1} h^{-1}) were calculated for paralarvae of *D. opalescens* (green circles) and *O. bimaculatus* (teal circles). A scaling coefficient (b) was determined for each species using a linear model (green line and teal line for *D. opalescens* and *O. bimaculatus*, respectively).

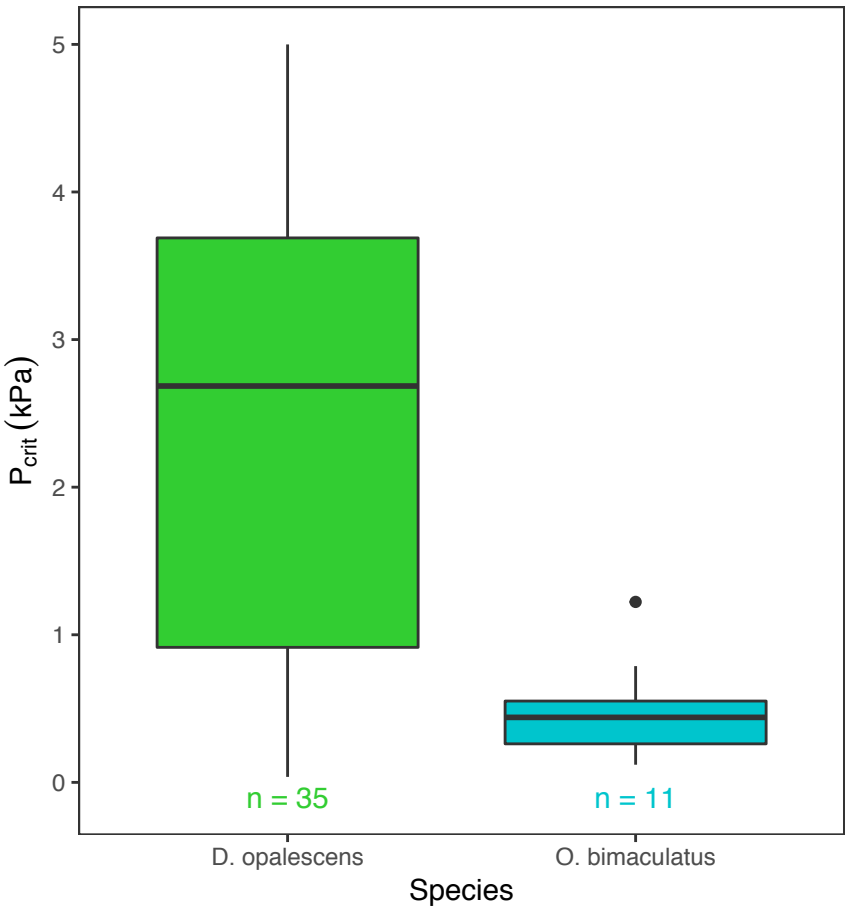

Figure 4.4. Calculated P_{crit} values for cephalopod paralarvae. "Breakpoint" P_{crit} values (kPa) determined for individual paralarvae of *D. opalescens* (green box) and *O. bimaculatus* (teal box). Boxes show the median (bold center line) and first and third quartiles of all individuals tested within a species; error bars show maximum/minimum values within 1.5x the inner quartile range (IQR=third quartile–first quartile) and outlier points are shown as black circles. The number of individuals tested for each species is below each box.

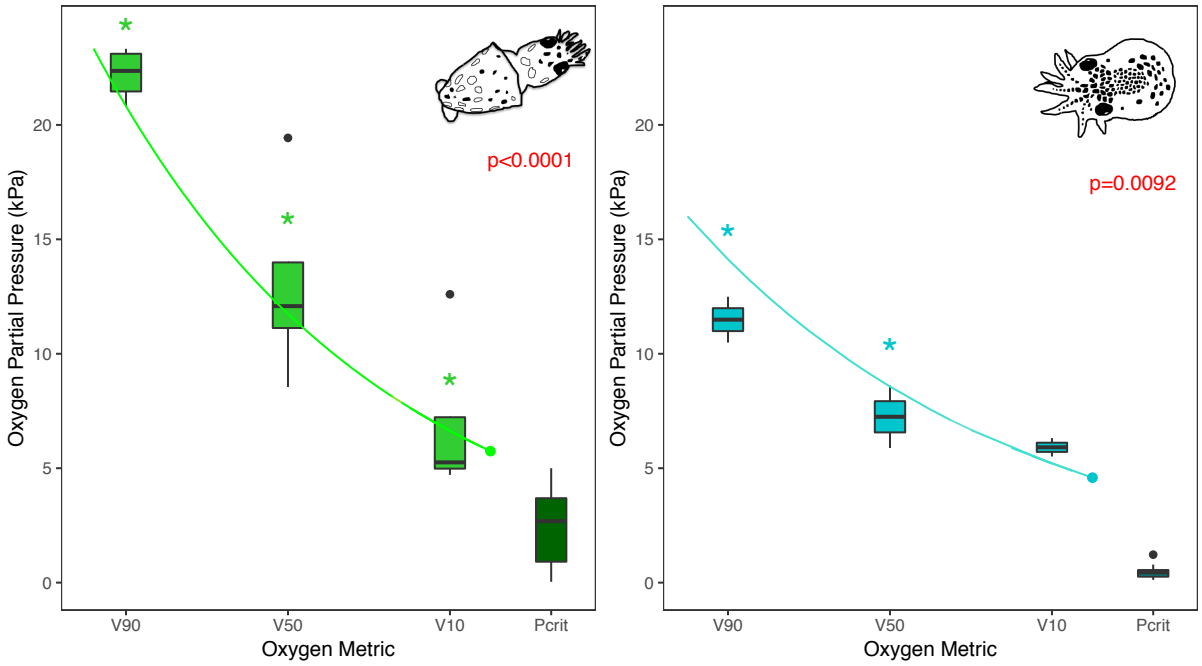

Figure 4.5. Comparison of oxygen metrics for retinal function and metabolism. Oxygen metrics for vision, V_{90}, V_{50}, and V_{10}, defined as the pO_2 (kPa) where 90%, 50%, and 10%, of retinal function remains, respectively, in comparison to retinal responses in normoxia are compared to a traditional metric for metabolic sensitivity to oxygen (P_{crit}, kPa) in paralarvae of *D. opalescens* (green boxes) and *O. bimaculatus* (teal boxes). Lines indicate a non-linear fit to the retinal decline as a function of pO_2 ending with 0% retinal function (closed circles) for *D. opalescens* (green line and circle) and *O. bimaculatus* (teal line and circle). Boxes show the median (bold center line) and first and third quartiles of all individuals tested within a species; error bars show maximum/minimum values within 1.5x the inner quartile range (IQR=third quartile–first quartile) and outlier points are shown as black circles. Differences across all oxygen metrics were tested using Kruskal-Wallis one- way ANOVAs, p-values are presented for each species; significant values are in red text. Comparisons between individual metrics were tested with Dunn's test, and significant differences between the P_{crit} and each visual metric are marked with an asterisk ($p < 0.05$).

CHAPTER 5

Oxygen sensitivity of phototaxis behavior in highly visual cephalopod paralarvae

Lillian R. McCormick, Lisa A. Levin, and Nicholas W. Oesch

Abstract

Coastal upwelling areas around the world have higher rates of deoxygenation as a result of changes to circulation patterns, stratification, and temperature. Organisms that reside in these areas, including the Southern California Bight (SCB), experience naturally high variability in oxygen over time and steep oxygen gradients with depth. Cephalopod paralarvae rely on vision for feeding, evading predators, and directing their movement in the water column. As with most marine larvae, cephalopod paralarvae undergo diel vertical migration and ascend to the surface to feed at night after avoiding predation at deeper depths during the day. The cue for vertical migration is often a specific irradiance that initiates a phototaxis behavior where larvae move towards or away from light. This behavior is crucial to their survival, and despite the physiological findings of high oxygen requirements for retinal function in paralarvae, the effects of reduced oxygen on phototaxis behavior in paralarvae has not been determined. Phototaxis experiments on paralarvae of the squid *Doryteuthis opalescens* and the octopus *Octopus bimaculatus*, cephalopods commonly found in the SCB, were conducted in a chamber that allowed larvae to move vertically in response to light stimuli of 9 irradiances, with trials completed at 4 different oxygen partial pressures (pO_2). Results showed clear irradiance thresholds for phototaxis behavior in both species; exposure to reduced oxygen increased the irradiance required for phototaxis. In addition to a loss of sensitivity to light, low oxygen decreased in the mean distance moved and mean velocity, and caused paralarvae to be distributed farthest from the light stimulus in the chamber. Phototaxis behavior was significantly impaired during exposure to < 12.9 and < 7.4 kPa pO_2 (< 151.6 and < 86.9 μmol kg^{-1} at 15.3 °C, respectively) for *D. opalescens* and *O. bimaculatus* paralarvae, respectively, and the magnitude of the change in phototaxis from reduced pO_2 was

even at all irradiances tested. Vision in *D. opalescens* paralarvae showed a greater sensitivity to reduced oxygen than *O. bimaculatus* vision, indicating species-specific effects of reduced oxygen on phototaxis behavior. These findings suggest that ongoing deoxygenation in the SCB will increase irradiance requirements for phototaxis and likely affect the migration behavior and survival of these species.

Introduction

Larvae of highly visual marine species rely on vision for a variety of behaviors, including feeding, evading predators, detecting prey, and distributing themselves vertically in the water column (Forward 1988, Robin et al. 2014, Charpentier and Cohen 2015). Diel vertical migration (DVM) is the daily migration of marine organisms from deeper in the water column during the day to the surface of the ocean at night, and from the surface to depth again at dawn. A primary explanation for DVM in marine larvae is to allow feeding on aggregations of small zooplankton at the surface at night when the pressure of visual predation on the larvae is lower. During the day, larvae can hide under lower light conditions (irradiance) in deeper water. Alternative mechanisms of migration include sinking to deeper depths in the middle of the night after an ascent to the surface at twilight, and reverse migration, where the zooplankton are in shallower water during the day and deeper water at night (Ohman et al. 1983, Forward 1988, Ohman 1990). DVM has been documented in larvae of both pelagic and benthic marine invertebrates (Forward, 1988; Randel and Jékley, 2015), including cephalopods (Ambrose 1981, Zeidberg and Hamner 2002, Puneeta et al. 2018).

Larvae that are vertically migrating through the water column also have to be adapted to very different environmental conditions at each end of their distribution. Both light and oxygen concentration exhibit strong gradients with depth in the ocean, particularly on highly productive margins with eastern boundary currents where the upwelling of low-oxygen water creates steep gradients at shallow depths, such as in the Southern California Bight (SCB). On upwelling margins, the partial pressure of oxygen (pO_2) drops quickly from surface waters over the first 300 m of the water column, and low oxygen effects on marine organisms may occur well above the depth of the mid-water low oxygen zones (Gilly et al. 2013). Similar to oxygen, steep gradients in total irradiance and spectral composition of light also exist with depth in the water column (Jerlov 1951). Both factors are known to limit or influence the distribution of marine organisms (e.g., Netburn and Koslow, 2015), but how these two constraints interact and impact vision is poorly understood.

For most marine larvae, the *zeitgeber*, a rhythmically occurring natural cue, for migration is primarily light, either a specific irradiance or the detection of a change in light irradiance at a specific rate that initiates behavior (Forward 1988, Cohen and Forward 2005, 2009). The visual behavior associated with light is phototaxis, which is defined as movement towards light (positive phototaxis) or away from light (negative phototaxis) (Diehn et al. 1977). For negatively buoyant larvae in the ocean, positive phototaxis is associated with a swimming ascent in the water column, and negative phototaxis is usually a passive sinking descent (Rudjakov 1970). Additional factors that can enhance or change the swimming patterns of larvae are geotaxis, which would produce an upward swimming movement (negative geotaxis) or an active swimming descent (positive geotaxis).

Vision is essential to the survival of the early life stages of cephalopods. The eyes are considered fully developed at the time of hatching in the larvae (called "paralarvae" during their planktonic larval stage; Robin et al. 2014). Some cephalopods develop the ability to discern contrast or learn to identify copepod prey during embryogenesis and a successful attack strike for feeding after hatching is a visually learned behavior (Chen et al. 1996, Lee et al. 2013). Feeding must begin immediately because hatching embryos retain only a small volume of yolk reserve sufficient to get them to the first feeding time (Vidal et al. 2002). Hatching of cephalopod paralarvae primarily occurs at night, and positive phototactic behavior enables them to swim up to the food-rich surface waters before there is enough light for predators to see them at the spawning grounds (Fields 1965). Positive phototaxis, and presumably the use of light as the cue for diel vertical migration, has been shown in a variety of squid paralarvae including that of *Todarodes pacificus* (Puneeta et al. 2018), *Doryteuthis* (= *Loligo*) *opalescens* (Fields 1965, Arnold et al. 1974, Zeidberg and Hamner 2002), and *Loligo forbesii* (Martins 1997). Positive phototaxis and diel vertical migration has also been observed in several species of octopus with a paralarval stage (Villanueva and Norman 2008), including paralarvae of *Octopus bimaculatus* (Ambrose 1981). Cephalopod paralarvae also have strong negative geotaxis after hatching, but this behavior lessens with time after hatching, and is almost diminished after 12 h post hatching in *Loligo pealei* (Sidie and Holloway 1999) and after 2 days in *L. forbesii* (Martins 1997).

Vision has high oxygen demands because of the need to maintain energetically expensive ion gradients to prime visual cells (photoreceptors) and neurons for signaling (Niven and Laughlin 2008, Wong-Riley 2010). The retina, containing the photoreceptor cells, is the tissue with one of the highest metabolic demands in the vertebrate body (Anderson

1968, Waser and Heisler 2005, Wong-Riley 2010). The oxygen demand will be especially high in visual structures with high temporal resolution, or 'fast vision', where light response reactions are happening at a high rate (Niven and Laughlin 2008); in the marine environment this occurs in active arthropods, cephalopods, and fish (McCormick and Levin 2017). The effects of reduced oxygen on vision has been well documented in terrestrial vertebrates and in some fish (McFarland and Evans 1939, Linsenmeier et al. 1983, Johansson et al. 1997), but little work has been done to examine the oxygen demands in vision of marine invertebrates, especially larvae. Recently, it was found that exposure to reduced pO_2 decreased the retinal responses and sensitivity to light in larvae of two species of crustaceans and two species of cephalopods (McCormick et al. 2019). Retinal sensitivity to reduced pO_2 was quantified using oxygen metrics for visual function that show the amount of retinal function for a given pO_2. Reduced oxygen impaired the physiological response of the eyes to light in cephalopod paralarvae, and determining the manifestation of retinal impairment in visual behaviors is crucial for evaluating the effects of declining oxygen on the ecology of SCB species.

Phototaxis requires the visual detection of light and a swimming behavior. In addition to the oxygen requirements for vision, most cephalopod paralarvae are active swimmers, and locomotion after hatching is achieved by jet propulsion, as in adults (Villaneuva and Norman 2008, Bartol et al. 2009, Staaf et al. 2014). Jet propulsion is extremely energy inefficient, however, and although the efficiency is higher in paralarvae compared to adults (Bartol et al. 2008, Staaf et al. 2014), cephalopods have high oxygen requirements to support the metabolic demands of locomotion (O'Dor and Webber 1991, Seibel 2007). Cephalopod paralarvae also have very high metabolic requirements as a result of jet propulsion locomotion, high activity

levels, and complex visual systems (Chapter 4; Hurley 1975, Higgins et al. 2012, Pimentel et al. 2012, Zuñiga et al. 2013, Vidal et al. 2019).

The effects of oxygen on phototaxis behavior have only been examined in a few marine or aquatic organisms. Scherer (1971) found that the negative phototaxis behavior in the walleye fish, *Stizostedion vitreum vitreum*, under normoxic conditions was reversed after oxygen was decreased below 1.5 mg O_2 L^{-1} (4.3 kPa at 22 °C). Similarly, normal phototaxis behavior was reversed in the anemone, *Anthopleura elegantissima*, and the aquatic mayfly larvae, *Cloeon dipterum*, after exposure to 4.5 mL O_2 L^{-1} (15.4 kPa at 13 °C) and anoxia, respectively (Fredericks 1976, Nagell 1977).

We conducted phototaxis experiments in paralarvae of the market squid, *Doryteuthis opalescens*, and the two-spot octopus, *Octopus bimaculatus* as representatives of two cephalopod species common to the SCB. The objectives were to 1) establish whether there are oxygen and light thresholds for phototaxis behavior in cephalopod paralarvae, 2) examine whether there is oxygen sensitivity of visual behavior and whether it changes across irradiance gradients, and 3) determine whether oxygen sensitivity in visual behavior is species-specific by comparing responses between the two species. Additionally, an objective was to compare the oxygen sensitivity for phototaxis behavior to the oxygen limits for retinal function (McCormick et al. 2019) and determine whether physiological and behavioral limits for vision were at the same oxygen levels. Phototaxis experiments were conducted using light stimuli of a range of irradiances during exposure to four different oxygen conditions for paralarvae of each species. Based on the visual impairment observed in physiological retinal function in these species (Chapter 3; McCormick et al. 2019), we hypothesized that there

would be certain oxygen conditions below which visual behaviors cease, or where phototaxis patterns reverse.

Methods

Animal Collection:

Paralarvae of *D. opalescens* were hatched from 16 egg capsules laid by a single female squid in captivity in Monterey Bay, California. Egg capsules were transported to San Diego in a dark cooler on March 30, 2019. After transport, the capsules were kept in a light-controlled experimental room and housed in a 4-L tank with flowing, aerated seawater at a constant temperature of 14° C under a 13h light and 11h dark cycle. All paralarvae hatched between April 12-20, 2019 and were kept in separate 1-L containers with their hatching cohort under the same light cycle with daily feeding of *Artemia* brine shrimp larvae and/or wild-collected copepods.

Paralarvae of *O. bimaculatus* were hatched from a cluster of eggs opportunistically collected from a marine sensor off Newport Beach, California on March 7, 2019. The eggs were kept in a 5-L tank with flowing seawater (~16° C) under a natural light cycle (13 h light: 11 h dark). They were identified as *O. bimaculatus* because of their small size (in comparison to *O. bimaculoides* eggs) and planktonic phase, in addition to larval identification upon hatching (Ambrose 1981). Paralarvae used in these experiments hatched on April 25 and April 29, 2019. After hatching, the paralarvae were moved into a light-controlled experimental room (13 h light: 11 h dark cycle), placed into 1-L tanks at 15° C with their hatching cohort, and free-fed *Artemia* brine shrimp larvae and/or wild-collected copepods daily.

Paralarvae of both species underwent an initial stabilization period of at least 24h prior to testing. Experiments were conducted within 1-6 days of hatching for *D. opalescens* paralarvae and 1-4 days post hatching for *O. bimaculatus* paralarvae.

Phototaxis Experiments:

All procedures were in compliance with the Institutional Animal Care and Use Committee (IACUC) of the University of California San Diego, and care was taken wherever possible to reduce the stress and discomfort of the animals (e.g. transportation at a cool temperature in darkness, minimal handling of animals, etc.). To prevent changes in swimming behavior due to endogenous circadian rhythms found in other invertebrate larvae (Forward and Cronin 1980), experiments were only conducted between 09:00 and 17:00 (~3-11 h after sunrise).

All phototaxis experiments were conducted in a vertically oriented, 5-sided plexiglass container (dimensions 20cm H x 5 cm L x 4 cm W) placed in a light-tight enclosure (Fig. 1). Light stimuli were generated by a green super-bright T-1 3/4 package LED (525 nm; 35 nm FWHM; Thorlabs LED528EHP; Newton, NJ, USA) suspended above the chamber; this wavelength was chosen to match the spectral sensitivity of the larvae (McCormick et al. 2019). Light irradiance was controlled using an Arduino Uno microcontroller board and variable LED driver (Adafruit). The absolute irradiance of the LED was measured using a fiber spectrometer (FLAME-S-VIS-NIR-ES; Ocean Optics) with a cosine corrector (CC-3-UV-S; Ocean Optics) calibrated using a NIR-calibrated lamp (HL-3P-CAL; Ocean Optics). Light stimuli irradiances were chosen to mimic the stimuli used to test oxygen effects on retinal responses in marine larvae (Chapter 3; McCormick et al. 2019). The overhead light

passed through a white diffuser filter before reaching the chamber to mimic a natural angular light distribution and prevent abnormal phototaxis responses that can occur from direct, artificial lighting (Forward 1986). For each experiment, the chamber was filled to 1 cm from the top with filtered seawater, and 20 individuals (*D. opalescens*) or 5 individuals (*O. bimaculatus*) were added individually into the chamber and tested together. The temperature and pO_2 in the chamber was recorded using a micro-oxygen sensor and temperature probe (PreSens; Microx 4, Pst-7, and St26) and a clear plexiglass cover was added before the chamber was put into the enclosure. The animals were allowed to acclimate to the chamber in the dark enclosure for 15 minutes, illuminated only with infrared light (IR; >940 nm) for video recording; these wavelengths are outside the sensitivity range of cephalopods (McCormick and Cohen 2012). Hereafter, illumination with only IR and no visible light is referred to as "dark" or "in darkness". The experiment began after this acclimation period, and consisted of 3 minutes in the dark for a representation of normal 'dark' behavior, followed by a series of 9, 10-second light stimuli, each followed by a 3-minute dark adaptation (control) period, with another 2-minute dark control after the series. The light stimuli decreased in intensity, from 2.45 to 0.063 μmol photons m^{-2} s^{-1}, and the total trial duration was 33 minutes. After each trial, the temperature and pO_2 in the chamber were recorded and the paralarvae were removed. Each trial was completed 2-3 times with different individuals for each of the four different oxygen conditions. Most individuals were only tested once; in the case where they were tested twice it was at least 24 h after the first test and only if the first test was at the highest oxygen condition.

Oxygen Treatment:

Phototaxis behavior experiments were completed at four different oxygen conditions for each species, chosen based on the results of oxygen sensitivity in retinal physiology (Chapter 3; McCormick et al. 2019). Critical limits for metabolic oxygen sensitivity (Chapter 4) were not available at the time of these experiments. For all experiments, "normoxia" refers to 100-105% oxygen saturation, and is representative of pO_2 at the ocean surface. The methods and results of all visual metrics for oxygen sensitivity are published in McCormick et al. (2019), but briefly, V_{90}, V_{50}, and V_{10} are the pO_2 at which 90%, 50%, and 10% retinal function existed, respectively, in comparison to retinal responses in normoxia. These oxygen metrics were determined by measuring the decline in retinal response (electroretinogram; ERG) during a decrease in the ambient pO_2 the larvae were exposed to. Results of the oxygen metrics for visual function (Table 1) were used in order to compare the oxygen sensitivity of phototaxis behavior to sensitivity in retinal physiology.

For *D. opalescens* paralarvae, the target oxygen conditions tested were normoxia (21 kPa), V_{50} (13 kPa), V_{10} (6.9 kPa), and a "Low" pO_2 (4 kPa), which was a lower pO_2 than V_{10}. Trials for *O. bimaculatus* paralarvae were conducted at normoxia (21 kPa), V_{90} (11.5 kPa), V_{50} (7.2 kPa), and V_{10} (5.9 kPa) (Table 2). The average pO_2 for normoxia, V_{50}, V_{10}, and Low pO_2 were 21.1 ±0.2 kPa, 12.9 ±0.2 kPa, 6.6 ±0.3 kPa, and 4.2 ±0.4, respectively, for *D. opalescens* paralarvae. The average pO_2 conditions during the trials for *O. bimaculatus* paralarvae in normoxia, V_{90}, V_{50}, and V_{10} were 21.3 ±0.3 kPa, 10.7 ±0.1 kPa, 7.4 ±0.5 kPa, and 5.8 ±0.03, respectively (Table 2).

A custom oxygen and pH control system was used to create all oxygen conditions for trials. This system was a modified version of the Multiple Stressor Experimental Aquarium at Scripps (MSEAS) originally designed in 2013 (Bockmon et al. 2013). This system

independently controls the oxygen, temperature, and carbonate chemistry from separate oxygen, carbon dioxide, and nitrogen cylinders using mass flow controllers operated by a laptop with custom LabVIEW software (National Instruments). The system used here (modified in 2017 by E. Bockmon and L. McCormick) differs in the use of Venturi injectors for gas mixing instead of the Liqui-Cel contactors (Membrana). Ideal water chemistry conditions were programmed approximately 2-3 hours before experiments began, and allowed for a decrease in pO_2 with little change in the carbonate chemistry. For all trials, pH was maintained at 8.16 ± 0.12 for *D. opalescens* paralarvae and 8.12 ± 0.10 for *O. bimaculatus* paralarvae, which is slightly higher than usual surface pH for this area (~8.07 at 7 m depth), but within normal diurnal variability (0.10-0.36) (Frieder et al. 2012). Normally, pH would also decrease with a decrease in pO_2, but it was important to isolate the effects of oxygen here. For trials with reduced oxygen, the pO_2 and temperature were measured just before the start of the trial and immediately after its conclusion. Averages of the start and end pO_2 were used for the analysis of each trial. With the cap on the chamber, there was relatively little change in oxygen or temperature for the duration of the experiment (Table 2).

Experiment Analysis:

All trials were recorded under IR illumination using a 2 MP 5-50 mm varifocal lens USB camera (ELP) and saved as a video using the open-source software Bonsai as an interface. Bonsai also enabled the capture of exact times for each video frame (30 frames s^{-1}) and the serial read output of each change in irradiance from the Arduino and LED driver, which was used in video analysis later. All experimental videos were analyzed using EthoVision XT motion tracking software (Noldus Information Technology). Using this

software, the chamber was split into 5 “zones” for analysis of the location of paralarvae within the chamber to determine the directionality of the phototaxis response. These zones were split evenly in 5 sections (‘S1’, ‘S2’, ‘S3’, ‘S4’, and ‘S5’), with ‘S1’ at the top of the chamber closest to the light stimulus, and ‘S5’ at the lower part of the chamber (Fig. 1). In addition, the number of paralarvae at the bottom of the chamber (< 0.5cm from the bottom or on the bottom) was quantified (‘Bottom’ zone). Data were additionally collected on the distance moved, the velocity, acceleration, and the heading of the paralarvae for examination of differences in swim behavior in the larvae under each stimulus and oxygen condition. Results were quantified for each video frame (~ 60,000 frames for each trials) and then binned into averages for every 20 seconds in each dark period and every 2 seconds for each light stimulus for each of the parameters (chamber location, mean distance moved, mean velocity, etc.) and species.

For each experiment, the camera was focused on the front of the chamber. Due to the threshold limitations of the software detection, animals that were unfocused in the rear of the chamber were not detected, and the results presented here are the 2D analysis of vertical motion of the larvae in response to light stimuli. Despite the viscous effects of the walls and the moderate Reynolds number the larvae experience, wall effects would likely not alter the speed or distribution of the larvae because of their size and swimming speed (Vogel 1981, Zakroff et al. 2018).

A total of 18 trials were conducted on *D. opalescens* paralarvae, with approximately 19-21 individuals per trial, testing a total of 322 individuals. Only 0.85% of individuals were tested two times. The software did not allow for tracking of all individuals, so 14 individuals were tracked in each trial for *D. opalescens*. Nine trials of 5 paralarvae each were conducted

on *O. bimaculatus* paralarvae, with 52 individuals tested, and 9.6% tested in two trials. For this study, only 12 *D. opalescens* trials were analyzed to maintain consistent oxygen and temperature conditions within the experiment (Table 2). All individuals and trials were analyzed for *O. bimaculatus* paralarvae.

In order to determine whether thresholds for phototaxis behavior existed in *D. opalescens* and *O. bimaculatus* paralarvae, we compared swim behavior during each stimulus irradiance to behavior during the 3-minute dark period immediately after the stimulus with Kruskal-Wallis one-way analysis of variance tests. Irradiance thresholds for phototaxis were considered the lowest irradiance where swim behavior was significantly different between the light stimulus and the respective dark period. Phototaxis behavior was characterized by examining results of the location of the paralarvae within the chamber, the distance moved, and the swimming velocity of paralarvae. To determine differences across the irradiance and oxygen conditions among trials, non-parametric Kruskal-Wallis one-way analysis of variance tests (K-W) were carried out, and Dunn tests (with the Holm method of adjustment for multiple comparisons) were conducted on significant results to determine pairwise differences. Unless otherwise stated, all values are given as mean ± 1 standard deviation around the mean (s.d.), and 'df' denotes degrees of freedom for the given statistical test.

Results

Irradiance thresholds for phototaxis behavior

In *D. opalescens* paralarvae in normoxia (21.1 ±0.2 kPa) subject to 9 light stimuli of decreasing irradiance, significant differences between swimming behavior during the light stimulus and during the subsequent dark period were observed in the mean distance moved

beginning at 0.853 μmol photons m^{-2} s^{-1} and at all stimuli equal to and greater than 1.48 μmol photons m^{-2} s^{-1} (Fig. 2). In V_{50} trials (12.9 ±0.2 kPa), the threshold was at 0.0626 μmol photons m^{-2} s^{-1}, with significant differences in the mean distance moved at every stimulus (except 0.853 and 1.15 μmol photons m^{-2} s^{-1}). In V_{10} trials (6.6 ±0.3 kPa), differences between the mean distance moved in the light stimulus and dark period were significantly different beginning at 0.853 μmol photons m^{-2} s^{-1} and at all stimuli equal to and greater than 1.48 μmol photons m^{-2} s^{-1}. At the Low pO_2 (4.2 ±0.4 kPa), there was an increase in the irradiance threshold, and differences in the mean distance moved were only significant at high irradiances (2.15 and 2.45 μmol photons m^{-2} s^{-1}).

Similar patterns of irradiance thresholds for phototaxis behavior were observed in *O. bimaculatus* paralarvae. The irradiance threshold for the mean distance moved in normoxia (21.3 ±0.3 kPa) was 0.853 μmol photons m^{-2} s^{-1} (Fig. 2). Significant differences between the mean distance moved during the light stimulus and in the subsequent dark period were observed at all irradiances greater than the threshold with the exception of 1.15 and 1.48 μmol photons m^{-2} s^{-1} in normoxia. In V_{90} trials (10.7 ±0.1 kPa), significant differences were observed at 0.062 and 1.15 μmol photons m^{-2} s^{-1}, but not at any other stimulus irradiance. For V_{50} trials (7.4 ±0.4 kPa), the irradiance threshold for the mean distance moved was at 0.853 μmol photons m^{-2} s^{-1}, with all stimuli of greater irradiance also showing significant differences except 1.78 μmol photons m^{-2} s^{-1}. No significant differences were observed in the mean distance moved between light stimuli and the subsequent dark period in *O. bimaculatus* V_{10} trials (5.8 ±0.03 kPa) at any irradiance, indicating a cessation of phototaxis behavior at low pO_2.

Another aspect of swimming behavior quantified during the trials was the vertical swimming velocity of the paralarvae, and thresholds for mean velocity were considered the lowest irradiance at which there was a difference in mean velocity during the light stimulus in comparison to the dark period immediately after the stimulus. For *D. opalescens* paralarvae in normoxia (21.1 ±0.2 kPa), the irradiance threshold for the mean velocity was 0.853 μmol photons m^{-2} s^{-1} and differences were observed at all stimuli equal to and greater than 1.48 μmol photons m^{-2} s^{-1} (Fig. 3). In V_{50} trials (12.9 ±0.2 kPa), the mean velocity was significantly different between the light stimulus and the subsequent dark period beginning at 0.062 μmol photons m^{-2} s^{-1} and for every irradiance except 0.853 and 1.15 μmol photons m^{-2} s^{-1}. In V_{10} behavior trials (6.6 ±0.3 kPa), the irradiance threshold was at a much higher irradiance, with the mean velocity only showing significant differences between the light stimulus and dark at 2.45 μmol photons m^{-2} s^{-1}. Similarly, in the Low pO_2 trials (4.2 ±0.4 kPa), the threshold was at 2.15 μmol photons m^{-2} s^{-1}, with differences in mean velocity also observed at 2.45 μmol photons m^{-2} s^{-1}.

In normoxia trials for *O. bimaculatus* paralarvae (21.3 ±0.3 kPa), the irradiance threshold for differences in the (swimming) velocity during the light stimulus and the subsequent dark period was 0.853 μmol photons m^{-2} s^{-1} (Fig. 3). Differences were also significant for all stimuli of a greater irradiance with the exception of 1.15 and 1.48 μmol photons m^{-2} s^{-1}. Paralarvae in the V_{90} trials (10.7 ±0.1 kPa), showed a threshold in the mean velocity at 0.062 μmol photons m^{-2} s^{-1} and significant differences at 1.15 μmol photons m^{-2} s^{-1}, but not at any other irradiance. During the V_{50} trials (7.4 ±0.4 kPa), the threshold was observed at 0.853 μmol photons m^{-2} s^{-1} and there were differences in mean velocity at all

higher irradiance stimuli except at 1.78 μmol photons m^{-2} s^{-1}. No significant differences were observed in the mean velocity in V_{10} trials (5.8 ±0.03 kPa) at any irradiance.

All significance values for comparisons of swimming behavior (mean distance moved and mean velocity) during the light stimuli compared to the subsequent dark for each oxygen condition using a Kruskal-Wallis test for both species are presented in Table 3.

The location of the larvae within the chamber is important to determine directed swimming behavior for phototaxis in the paralarvae. The percentages of larvae in each zone (S1, S2, S3, S4, S5, and Bottom; Fig. 1) for each stimulus and for the respective dark period immediately afterwards were used to show directionality of swimming. For *D. opalescens* paralarvae in normoxia and V_{50} trials, there were more larvae swimming in S1 and S2 (closest to the light stimulus) at higher irradiance stimuli compared to at lower irradiances, showing positive phototaxis. Concurrently, at lower irradiances and in the dark (absence of a stimulus) more individuals were swimming in lower zones (S4, and S5), or were in the Bottom zone. In the trials with lower pO_2 (V_{10} and Low pO_2), approximately 50% of *D. opalescens* paralarvae were at the bottom of the chamber. For individuals that were not on the bottom, the majority of paralarvae were in S1 or S2, but the percentages in each zone changed very little across the different stimulus irradiances (Fig. 4).

Results were similar for *O. bimaculatus* paralarvae. Paralarvae in normoxia, V_{90}, and V_{50} trials were primarily swimming in zones S1 and S2 during light stimuli, and the percentage in the zones at the top of the chamber increased during stimuli of increasing irradiance. This trend disappeared in trials of the lowest pO_2, V_{10}, where the number of paralarvae on the bottom increased to ~30% and the swimming paralarvae did not show differential responses to light stimuli (Fig. 4).

Oxygen thresholds for visual behavior

In order to examine whether the oxygen sensitivity of visual behavior changes across irradiance, tests were conducted to determine differences in the mean distance moved, mean velocity, and location of the paralarvae between oxygen conditions for each light stimulus. In *D. opalescens* paralarvae, differences were observed in the mean distance moved and the mean velocity at all stimulus irradiances with the exception of 0.287, 0.567, and 1.15 μmol photons m^{-2} s^{-1} (K-W; $p < 0.05$) (Fig. 5A,B). Using a Dunn test for pairwise comparisons, differences were primarily between normoxia and V_{10} and normoxia and Low pO_2 (Table 4). The mean distance moved or mean velocity was not significantly different between normoxia and V_{50} at any irradiance. At higher irradiance stimuli (≥ 1.48 μmol photons m^{-2} s^{-1}), there were differences between V_{50} and Low pO_2 and V_{50} and V_{10} in both the mean distance moved and the mean velocity.

In *O. bimaculatus* paralarvae, differences among oxygen conditions were only observed at 1.48 and 2.45 μmol photons m^{-2} s^{-1} for both the mean distance moved and the mean swimming velocity (Fig 5B, C). Dunn test pairwise comparisons showed differences between normoxia and V_{50} and V_{10} and V_{50} at 1.48 μmol photons m^{-2} s^{-1} for both the mean distance moved and the mean velocity. During the 2.45 μmol photons m^{-2} s^{-1} stimulus, the mean distance moved and the mean velocity were different between V_{90} and V_{50} and V_{50} and V_{10} (Table 5). No differences were observed between normoxia and V_{90} at any irradiance in *O. bimaculatus* paralarvae.

To simplify the discussion of whether the percentages of paralarvae in each zone and light stimulus were different across oxygen conditions, the zones closest to the stimulus (S1 and S2) were combined into the 'Upper' chamber, and the zones furthest away from the

stimulus (S4 and S5) were combined into the 'Lower' chamber. Zone S3 was kept as the 'Mid' chamber, and the bottom of the chamber (on the bottom or < 5 mm off the bottom) was the 'Bottom' zone. Differences between trials in normoxia, V_{50}, V_{10}, and Low pO_2 within each of the chamber zones were very similar across all stimulus irradiances in *D. opalescens* paralarvae. The percentages of *D. opalescens* paralarvae in the upper chamber and at the bottom of the chamber were significantly different across oxygen conditions at all of the light stimuli (Fig. 6). Significant differences were observed at all stimulus irradiances except 2.45 μmol photons m^{-2} s^{-1} in the mid chamber, and all stimuli except 1.78 μmol photons m^{-2} s^{-1} in the lower chamber. Overall, percentages in every zone were very similar between normoxia and V_{50} and V_{10} and Low pO_2, but there was a difference in percent paralarvae between the two groups. Differences between normoxia and V_{10} and normoxia and Low pO_2 were significant at all irradiances in the upper chamber and at the bottom (with the exception of normoxia vs. Low pO_2 at 0.567 μmol photons m^{-2} s^{-1} in the upper chamber) (Table 4).

Differences between oxygen conditions at each stimulus irradiance and zone were more variable in *O. bimaculatus* paralarvae compared to *D. opalescens* paralarvae. Differences were observed between trials in normoxia, V_{90}, V_{50}, and V_{10} at every irradiance except 0.287 and 2.15 μmol photons m^{-2} s^{-1} in the upper section of the chamber for *O. bimaculatus* paralarvae, and every irradiance except 1.15, 1.48, and 2.15 μmol photons m^{-2} s^{-1} in the middle of the chamber (Fig. 7). In the lower part of the chamber, differences were observed between oxygen conditions for all light stimuli except 0.287 μmol photons m^{-2} s^{-1}. At the bottom of the chamber, differences were observed at all irradiances except 0.853 μmol photons m^{-2} s^{-1}. Overall, the percentages of *O. bimaculatus* paralarvae in each zone under V_{10} oxygen conditions were highly variable, especially in the upper part of the chamber. Pairwise

differences showed greater similarities in percentages of paralarvae between normoxia, V_{90}, and V_{50} than at V_{10} pO_2, but the large variance around the mean caused few other patterns of significance to emerge (Table 5).

Irradiance thresholds for cephalopod paralarvae increased to higher irradiances during exposure to reduced pO_2 (Fig. 8). The irradiance threshold for phototaxis behavior in *D. opalescens* paralarvae was at 0.837 µmol photons m^{-2} s^{-1} in normoxia (22.1 ±0.2 kPa). In the lower oxygen exposures of V_{10} (6.6 ±0.3 kPa) and Low pO_2 (4.2 ±0.4 kPa), the irradiance threshold increased in intensity, with behavior and location becoming significantly different between the light stimulus and the subsequent dark period at 2.15-2.45 µmol photons m^{-2} s^{-1}. The threshold of the mean distance moved at V_{10} was the same as in normoxia, but there is a clear reduction in movement over all stimulus irradiances, indicating effects of oxygen on light sensitivity may already be occurring (Fig. 2). Similarly, the location of *D. opalescens* paralarvae in the chamber more closely aligns with the irradiance threshold in the mean velocity, with a high percentage of larvae at the bottom of the chamber and relatively little change of percentage of paralarvae in the top two zones (S1 and S2) at different irradiances (Figs. 4, 9). This indicates that exposure to low oxygen reduces the mean distance traveled and the mean velocity during the light stimulus. At the highest irradiance stimulus, 2.45 µmol photons m^{-2} s^{-1}, the mean distance moved changed from ~1 mm at normoxia and V_{50} to ~0.5 mm at V_{10} and the low pO_2, and the mean velocity changed from 25-30 mm s^{-1} at normoxia and V_{50} to < 20 mm s^{-1} at V_{10} and the low pO_2 (Figs. 2, 3).

Exposure to reduced pO_2 affected the phototaxis behavior of *O. bimaculatus* paralarvae in a threshold manner (Fig. 8). Under normoxia (22.3 ±0.3 kPa) and V_{50} (7.4 ±0.4 kPa), paralarvae showed phototaxis behavior at 0.853 µmol photons m^{-2} s^{-1} for both the mean

distance moved and the mean velocity, whereas at V_{90} (10.7 ±0.1 kPa), the threshold was 0.062 μmol photons m^{-2} s^{-1}. At the lowest oxygen condition, V_{10} (5.8 ±0.03 kPa), there was no significant phototaxis behavior observed at any irradiance (Fig. 8). There was a clear reduction in the mean distance moved during exposure to reduced pO_2; in normoxia and V_{50}, the mean distance moved during the 2.45 μmol photons m^{-2} s^{-1} was ~0.5 mm, which decreased to ~0.25 mm at V_{10} (Fig. 2). Similarly, the mean velocity during the highest irradiance stimulus was ~12 mm s^{-1} in normoxia and V_{50} and ~6 mm s^{-1} in V_{10}. Results for both the mean distance moved and the mean velocity were abnormal at V_{90}, with the behavior in the dark period greater than the respective behavior during the light stimulus. This was even across all irradiances, and could potentially indicate differences between the two trials of this oxygen exposure. As in *D. opalescens* paralarvae, the location of the *O. bimaculatus* paralarvae reflected the change in activity level (mean distance moved and mean velocity). In normoxia, V_{90}, and V_{50}, there were higher percentages of paralarvae in the upper two zones of the chamber (S1 and S2), and this percent increased with increasing irradiance (Fig. 4). During exposure to the V_{10} pO_2, this trend disappeared and there was a higher percentage of paralarvae at the bottom of the chamber and almost no variation in the percentages of paralarvae in zones S1 and S2 at different irradiances (Fig. 9).

Overall, paralarvae of both species still showed evidence of negative geotaxis behavior, as many paralarvae were concentrated in the upper chamber even during dark periods after light stimuli, although the percentage was greater during light stimuli (Fig. 4). Individual ages in this study ranged from 1-6 days post hatching (DPH) for *D. opalescens* paralarvae and 1-4 DPH for *O. bimaculatus* paralarvae, which is older than the reported age where geotaxis overwhelmed the phototactic response (12h; Sidie and Holloway, 1999).

Paralarvae of *Loligo forbesii* were shown to have geotaxis until 2 DPH (Martins 1997). Negative geotaxis was observed in this study for the maximum age tested here; paralarvae 6 DPH in *D. opalescens* and 4 DPH for *O. bimaculatus*.

Discussion

There was strong evidence for positive phototaxis behavior in both *D. opalescens* and *O. bimaculatus* paralarvae during light stimuli, shown by an increase in the mean distance traveled (Fig. 2), the mean velocity (Fig. 3), and a concentration of paralarvae in the upper chamber during light stimuli; this behavior increased at higher irradiances (Fig. 4). This trend was removed at lower oxygen conditions, with an increase in the irradiance required to elicit phototaxis behavior and a cessation of phototaxis behavior at low pO_2 in *O. bimaculatus*. While experiments for *D. opalescens* and *O. bimaculatus* were conducted at different oxygen conditions and based on their respective oxygen metrics for retinal function, both species showed changes in phototaxis behavior at pO_2 lower than their respective V_{50} metrics, and demonstrated species-specific trends of sensitivity consistent with the oxygen sensitivity and metabolic sensitivity.

Positive phototaxis and diel vertical migration have been observed in paralarvae of the squid, *Todarodes pacificus* in a much larger (6 m tall) tank (Puneeta et al. 2018). Immediately after hatching, paralarvae swam upwards and showed negative geotaxis. Additionally, they showed a consistent vertical migration pattern; at night, paralarvae swam towards the surface and were located in the upper tank (~0.1 m depth) and then remained at > 1 m depth during the day (Puneeta et al. 2018). During intermediate exposures to a light stimulus during the night (~ 10 min), paralarvae swam to the immediate surface of the tank during the stimulus

and then sank after the stimulus was turned off before swimming back to the subsurface region (Puneeta et al. 2018). Paralarvae of *D. opalescens* and *O. bimaculatus* showed very similar behavior here, where the paralarvae were closest to the surface during a light stimulus, and there was a strong sinking behavior of paralarvae in the 20- 30 s after the light stimulus was completed. Paralarvae of *T. pacificus* also showed migration to the tank surface when a 60-minute dark stimulus was given during the day. Paralarvae swam from their deep daytime distribution in the tank to the surface during the dark stimulus, and then started sinking to the lower tank immediately after the stimulus was removed and the lights were turned on (Puneeta et al. 2018).

When examining the effects of reduced pO_2 on retinal function in paralarvae of *D. opalescens* and *O. bimaculatus*, oxygen effects on retinal function were similar at all irradiances tested (Chapter 3; McCormick et al. 2019). The same trend appears in phototaxis behavior in *D. opalescens* paralarvae, with significant differences among oxygen trials within each stimulus at almost all stimulus irradiances in the mean distance moved and the mean velocity (Fig. 5A, B). In contrast, trials with *O. bimaculatus* paralarvae showed significance between oxygen conditions in the mean distance moved and the mean velocity only at 1.48 and 2.45 μmol photons m^{-2} s^{-1} (Fig. 5 C, D). This could reflect a threshold response in oxygen sensitivity, with behavior only differing between oxygen conditions at V_{10}, or it could be a result of the small sample size (5 individuals per trial) and low values (mean distance moved and mean velocity) compared to trials with *D. opalescens* paralarvae. Pairwise comparisons do not support the former explanation, because comparisons between oxygen conditions were significant for V_{10} compared with V_{50} and normoxia compared with V_{50}, indicating variation was not only from V_{10} trials (Table 5).

Oxygen effects on the location of paralarvae within the chamber were also even across most stimulus irradiances, indicating the magnitude of oxygen sensitivity was the same at all irradiances tested here for both *D. opalescens* and *O. bimaculatus* (Fig. 6). In the upper chamber, the percentage of *D. opalescens* paralarvae was very similar in normoxia and V_{50} trials except at the two highest irradiance stimuli. However the percentage of paralarvae at the bottom of the chamber showed differences between normoxia and V_{50} beginning at a much lower irradiance (~0.853 μmol photons m^{-2} s^{-1}), indicating the number of paralarvae actively swimming was reduced during exposure to V_{50} pO_2. As with *D. opalescens* paralarvae, the number of *O. bimaculatus* paralarvae at the bottom of the chamber was greatest during exposure to V_{10} and at higher irradiance stimuli (Fig. 7).

Paralarvae of *D. opalescens* and *O. bimaculatus* showed different irradiance and oxygen thresholds for phototaxis behavior. The species-specificity of the response was very similar to the oxygen sensitivity of retinal function for paralarvae of these two species; *D. opalescens* paralarvae were more sensitive to oxygen loss than *O. bimaculatus* (Chapter 3; McCormick et al. 2019). Paralarvae of *D. opalescens* showed decreases in retinal function that began almost as soon as the pO_2 was reduced. By ~13 kPa, paralarvae had only ~50% of retinal function compared to responses in normoxia, and responses continued to decline with a decrease in pO_2 (Chapter 3; McCormick et al. 2019). Phototaxis behavior in *D. opalescens* was slightly more resilient to reduced pO_2, with the mean distance moved, mean velocity, and location within the chamber changing only during exposure to 6.6 kPa (V_{10}) and 4.2 kPa (low pO_2) (Fig. 2, 3, 4). Retinal responses in paralarvae of *O. bimaculatus* were much less sensitive to decreasing pO_2, with paralarvae still showing 90% of retinal function at 11.5 kPa, 50% at 7.2 kPa, and 10% at 5.9 kPa (Chapter 3; McCormick et al. 2019). Similarly, phototaxis

behavior in *O. bimaculatus* paralarvae showed changes in the irradiance thresholds for the mean distance moved, mean velocity, and the location of the paralarvae within the chamber at 5.8 kPa (± 0.03 kPa; V_{10}).

It is reasonable that phototactic behavior can persist with some level of retinal impairment, as long as the detection of the change in irradiance is transmitted to the brain. Given the oxygen effects on the thresholds of phototaxis behavior in *D. opalescens* paralarvae, it appears that phototaxis begins changing when paralarvae are exposed to pO_2 less than 12.9 kPa (V_{50}). For *O. bimaculatus* paralarvae, phototaxis behavior appears to change at pO_2 lower than 7.4 kPa (V_{50}). These are conservative estimates, as phototaxis experiments were not tested across a smooth gradient of pO_2, and where the exact threshold for phototaxis behavior falls between the pO_2 of 12.9 – 6.6 kPa for *D. opalescens* and 7.4 – 5.8 kPa for *O. bimaculatus* (V_{50} and V_{10}) is unknown. In addition, phototaxis is a complicated behavior that employs other sensory modalities in addition to vision (e.g. extra-ocular photoreception) (Ramirez et al. 2011), and so this trend may not hold true for larvae of other marine species. The visual sensitivity of each species to reduced pO_2 was overall very similar between changes to retinal function and changes in phototaxis behavior. The irradiance thresholds for the distance moved, the mean velocity, and the location of the paralarvae within the chamber slowly decreased with a decrease in pO_2 for *D. opalescens* (continuous response), whereas in *O. bimaculatus* paralarvae, the irradiance thresholds stayed very similar in normoxia, V_{90}, and V_{50} and then no significant phototaxis behavior was observed at V_{10} (threshold response). A similar effect was observed in the retinal responses, where responses in *D. opalescens* paralarvae decreased with changing pO_2 and responses in *O. bimaculatus* paralarvae stayed the same until a certain oxygen threshold was reached (Chapter 3;

McCormick et al. 2019). The oxygen threshold for phototaxis behavior was higher than the critical oxygen limit for metabolism (P_{crit}) for both *D. opalescens* (P_{crit} = 2.47 ±0.26 kPa) and *O. bimaculatus* (P_{crit} = 0.48 ±0.09 kPa) (Chapter 4), consistent with results of retinal sensitivity to reduced oxygen in each species in comparison to metabolic sensitivity to reduced pO_2.

In addition, the mean distance moved and mean velocity during phototaxis were both lower in *O. bimaculatus* paralarvae than *D. opalescens* paralarvae. In *D. opalescens* paralarvae, the mean velocity was ~15 mm s^{-1} during low irradiance stimuli and in the dark and up to 25-30 mm s^{-1} at higher irradiances, in comparison to *O. bimaculatus* paralarvae, which moved ~10 mm s^{-1} in the dark and at low irradiances and ~15 mm s^{-1} at high irradiances (Fig. 3). The mean velocity decreased under the lowest oxygen condition for both *D. opalescens* (~ 17 mm s^{-1}) and *O. bimaculatus* (~8 mm s^{-1}). Even at the highest irradiance stimulus, the mean distance moved and mean velocity in *O. bimaculatus* paralarvae in normoxia (~0.5 mm and ~12 mm s^{-1}) were the same or lower in value as the mean distance moved and mean velocity in *D. opalescens* at low pO_2 (~0.5 mm and ~17 mm s^{-1}). The differences in the mean distance moved and the mean velocity between *D. opalescens* and *O. bimaculatus* paralarvae observed here may explain the variation observed in the metabolic rates between paralarvae of each species (Chapter 4). The active swimming of *D. opalescens* paralarvae could explain the high metabolic rate observed (19.43 μmol O_2 g^{-1} h^{-1}), compared to the lower metabolic rate in *O. bimaculatus* paralarvae (1.84- 2.33 μmol O_2 g^{-1} h^{-1}), which move slower and in shorter distances, as oxygen uptake rate changes when paralarvae hatch and begin swimming (Villaneuva and Norman 2008).

The reduction in swimming velocity and phototaxis, observed with a decrease in pO_2 in *D. opalescens* and *O. bimaculatus* paralarvae may be exacerbated by other environmental stressors. Changes in swimming behavior have been observed under reduced pH in *Doryteuthis pealeii*, with a decrease in the distance traveled, negative and positive vertical velocity, and mean velocity of day-old paralarvae during exposure to partial pressures of carbon dioxide (pCO_2) between 400 and 1000 ppm (Zakroff et al. 2018). Additionally, during trials recorded in 2D (similar to the setup in this study), most paralarvae were swimming near the surface of the chamber, and the number of paralarvae at the surface decreased during higher pCO_2 (1900 and 2200 ppm) treatments (Zakroff et al. 2018). Reduced velocity and a change in the location of the *D. pealeii* paralarvae during exposure to increased pCO_2 (low pH) could additionally decrease the phototactic abilities of paralarvae if they experience multiple stressors. In the SCB, pH correlates with oxygen (Frieder et al. 2012, Navarro et al. 2018), and high variability in both stressors can be observed in the egg development grounds and paralarval habitat for *D. opalescens* and *O. bimaculatus* (Ambrose 1981, Zeidberg and Hamner 2002, Zeidberg et al. 2012, Navarro et al. 2018).

Directed swimming movement is crucial to the survival of cephalopod paralarvae after hatching, and changing oxygen patterns may have direct implications for larval success and recruitment to the adult population. In addition to moving the paralarvae away from potential predators at the egg site and towards their prey (Fields 1965, Villaneuva and Norman 2008), moving upwards in the water column could also enable cephalopod paralarvae to be transported away from the hatching site by tides and currents (Villaneuva and Norman 2008, Robin et al. 2014). This has an added benefit of removing paralarvae from potentially stressful (low oxygen, low pH) conditions at the egg bed site (Robin et al. 2014, Navarro et al.

2018). Paralarvae of the ommastrephid squid, *Sthenoteuthis oualaniensis* and *Dosidicus gigas* live in areas with a very shallow oxygen minimum zone in the eastern tropical Pacific (Staaf et al. 2013). Paralarvae of these species are often found in areas with higher oxygen between the thermocline and the surface (Sánchez-Velasco et al. 2016), and can be especially concentrated in convergent zones (e.g., fronts) of mesoscale circulation patterns and (Ruvalcaba-Aroche et al. 2018). Spatial variability in conditions is also observed in the SCB, and the abundance and dispersal of *D. opalescens* paralarvae has also been correlated to tidal currents and fronts, in addition to longer-term temporal variability in *D. opalescens* populations during El Niño-Southern Oscillation (ENSO) cycles (Zeidberg and Hamner 2002). An oxygen-impaired decrease or cessation of phototaxis may inhibit the ability of paralarvae to move to areas with sufficient prey items, fewer predators, and with the preferred environmental conditions.

Conclusions

The impairment of phototaxis behavior during exposure to reduced oxygen in paralarvae of *D. opalescens* and *O. bimaculatus* indicate that visual behavior will be significantly inhibited by exposure to a reduction in pO_2. Paralarvae of both species showed a change in the irradiance threshold that initiated positive phototaxis behavior under reduced pO_2 shown in the mean distance moved, the mean velocity, and the location within the chamber in relation to the light stimulus. Decreasing pO_2 increased the irradiance thresholds for phototaxis behavior, and critical oxygen limits for phototaxis behavior were below 12.9 kPa for *D. opalescens* and below 7.4 kPa for *O. bimaculatus*. Phototaxis experiments conducted at more gradual changes in pO_2 will pinpoint the exact oxygen thresholds for

phototaxis behavior in each species. The differences in phototaxis behavior here also show that general oxygen sensitivity in each species of paralarvae is maintained in the retinal physiology, metabolism, and phototaxis behavior, with a greater sensitivity to oxygen loss in *D. opalescens* than *O. bimaculatus*. Given the inhibition of phototaxis and swimming behavior at moderate oxygen conditions, paralarvae may show changes to diel vertical migration behaviors if oxygen impairment causes the paralarvae to miss the light *zeitgeber* for migration during exposure to reduced pO_2 in their habitat. Paralarval survival may also be impaired if reduced phototaxis behavior during exposure to reduced oxygen decreased the ability of paralarvae to move to habitats with sufficient prey, fewer predators, and optimal environmental conditions. Careful considerations should be made for the visual oxygen vulnerabilities of cephalopod paralarvae during seasonal and long-term changes to oxygen content in the Southern California Bight.

Acknowledgements

We thank W. Gilly and P. Teal at the Hopkins Marine Laboratory, Stanford University, for providing us with *D. opalescens* egg capsules, and P. Lertvilai and P. Zerofski for obtaining the *O. bimaculatus* eggs and zooplankton for feeding the hatched larvae. E. Bockmon was essential to refurbishing the MSEAS system for these experiments, and J. Gonzalez assisted with the set-up and design of tanks. We thank E. Peichel for her tireless efforts on the video processing for each trial. We thank J.H. Cohen for initial discussions on conducting phototaxis experiments and for providing equipment to get preliminary experiments started. This research was supported by a P.E.O. Scholar Award to L.R.M. and a National Science Foundation grant OCE-1829623 to L.A.L. and N.W.O.

Chapter 5, in part, is in preparation for submission for publication. The dissertation author was the primary investigator and author of this material. **McCormick, L. R.**, Levin, L. A., and N. W. Oesch. Oxygen sensitivity of phototaxis behavior in highly visual cephalopod paralarvae.

Literature Cited

Ambrose, R. F. 1981. Observations on the embryonic development and early post-embryonic behavior of *Octopus bimaculatus* (Mollusca: Cephalopoda). The Veliger 24:139–146.

Anderson, B. 1968. Ocular effects of changes in oxygen and carbon dioxide tension. Transactions of the American Ophthalmological Society 66:423–74.

Arnold, J. M., W. C. Summers, D. L. Gilbert, R. S. Manalis, N. W. Daw, and R. J. Lasek. 1974. Embryonic development. Page 74 A guide to laboratory use of the squid *Loligo pealei*. Marine Biological Laboratory, Woods Hole, MA.

Bartol, I. K., P. S. Krueger, W. J. Stewart, and J. T. Thompson. 2009. Pulsed jet dynamics of squid hatchlings at intermediate Reynolds numbers. Journal of Experimental Biology 212:1506–1518.

Bartol, I. K., P. S. Krueger, J. T. Thompson, and W. J. Stewart. 2008. Swimming dynamics and propulsive efficiency of squids throughout ontogeny. Integrative and Comparative Biology 48:720–733.

Bockmon, E. E., C. A. Frieder, M. O. Navarro, L. A. White-Kershek, and A. G. Dickson. 2013. Technical Note: Controlled experimental aquarium system for multi-stressor investigation of carbonate chemistry, oxygen saturation, and temperature. Biogeosciences 10:5967–5975.

Charpentier, C. L., and J. H. Cohen. 2015. Chemical cues from fish heighten visual sensitivity in larval crabs through changes in photoreceptor structure and function. The Journal of experimental biology 218:3381–3390.

Chen, D. S., G. Van Dykhuizen, J. Hodge, and W. F. Gilly. 1996. Ontogeny of copepod predation in juvenile squid (*Loligo opalescens*). Biological Bulletin 190:69–81.

Cohen, J. H., and R. B. Forward. 2005. Diel vertical migration of the marine copepod *Calanopia americana*. I. Twilight DVM and its relationship to the diel light cycle. Marine Biology 147:387–398.

Cohen, J. H., and R. B. J. Forward. 2009. Zooplankton diel vertical migration — A review of proximate control. Oceanography and Marine Biology: an Annual Review 47:77–110.

Diehn, B., M. Feinleib, W. Haupt, E. Hildebrand, F. Lenci, and W. Nultsch. 1977. Terminology of behavioral responses of motile microorganisms. Photochemistry and Photobiology 26:559–560.

Fields, W. G. 1965. The structure, development, food relations, reproduction, and life history of the squid *Loligo opalescens* Berry. State of California, Department of Fish and Game Fish Bulletin 131.

Forward, R. B. 1988. Diel vertical migration- Zooplankton photobiology and behavior. Oceanography and Marine Biology 26:361–393.

Forward, R. B. J. 1986. A reconsideration of the shadow response of a larval crustacean. Marine and Freshwater Behaviour and Physiology 12:99–113.

Forward, R. B. J., and T. W. Cronin. 1980. Tidal rhythms of activity and phototaxis of an estuarine crab larva. Biological Bulletin 158:295–303.

Fredericks, C. A. 1976. Oxygen as a limiting factor in phototaxis and in intraclonal spacing of the sea anemone *Anthopleura elegantissima*. Marine Biology 38:25–28.

Frieder, C. A., S. Nam, T. R. Martz, and L. A. Levin. 2012. High temporal and spatial variability of dissolved oxygen and pH in a nearshore California kelp forest. Biogeosciences 9:1–14.

Gilly, W. F., J. M. Beman, S. Y. Litvin, and B. H. Robison. 2013. Oceanographic and biological effects of shoaling of the oxygen minimum zone. Annual Review of Marine Science 5:393–420.

Higgins, F. A., A. E. Bates, and M. D. Lamare. 2012. Heat tolerance, behavioural temperature selection and temperature-dependent respiration in larval *Octopus huttoni*. Journal of Thermal Biology 37:83–88.

Hurley, A. C. 1975. Feeding behavior, food consumption, growth, and respiration of the squid, *Loligo opalescens* raised in the laboratory. Fishery Bulletin 74:176–182.

Jerlov, N. G. 1951. Optical studies of ocean water. Reports of the Deep-Sea Swedish Expedition 3:1–59.

Johansson, D., G. E. Nilsson, and K. B. Døving. 1997. Anoxic depression of light-evoked potentials in retina and optic tectum of crucian carp. Neuroscience letters 237:73–6.

Lee, Y.-H., Y.-C. Chang, H. Y. Yan, and C.-C. Chiao. 2013. Early visual experience of background contrast affects the expression of NMDA-like glutamate receptors in the optic lobe of cuttlefish, *Sepia pharaonis*. Journal of Experimental Marine Biology and Ecology 447:86–92.

Linsenmeier, R. A., A. H. Mines, and R. H. Steinberg. 1983. Effects of hypoxia and hypercapnia on the light peak and electroretinogram of the cat. Investigative ophthalmology & visual science 24:37–46.

Martins, M. C. P. R. 1997. Biology of pre- and post-hatching stages of *Loligo vulgaris* Lamarck, 1798 and *Loligo forbesi* Steenstrup 1856 (Mollusca, Cephalopoda). University of Aberdeen.

McCormick, L. R., and J. H. Cohen. 2012. Pupil light reflex in the Atlantic brief squid, *Lolliguncula brevis*. The Journal of Experimental Biology 215:2677–2683.

McCormick, L. R., and L. A. Levin. 2017. Physiological and ecological implications of ocean deoxygenation for vision in marine organisms. Philosophical Transactions of the Royal Society A 375.

McCormick, L. R., L. A. Levin, and N. W. Oesch. 2019. Vision is highly sensitive to oxygen availability in marine invertebrate larvae. Journal of Experimental Biology 222:1–11.

McFarland, R. A., and J. N. Evans. 1939. Alterations in dark adaptation under reduced oxygen tensions. American Journal of Physiology- Legacy Content 127:37–50.

Nagell, B. 1977. Phototactic and thermotactic responses facilitating survival of *Cloeon dipterum* (Ephemeroptera) larvae under winter anoxia. Oikos 29:342–347.

Navarro, A. M. O., P. E. Parnell, and L. A. Levin. 2018. Essential market squid (*Doryteuthis opalescens*) embryo habitat : A baseline for anticipated ocean climate change. Journal of Shellfish Research 37:601–614.

Netburn, A. N., and J. A. Koslow. 2015. Dissolved oxygen as a constraint on daytime deep scattering layer depth in the southern California current ecosystem. Deep Sea Research Part I: Oceanographic Research Papers 104:149–158.

Niven, J. E., and S. B. Laughlin. 2008. Energy limitation as a selective pressure on the evolution of sensory systems. The Journal of experimental biology 211:1792–804.

O'Dor, R. K., and D. M. Webber. 1991. Invertebrate athletes: trade-offs between transport efficiency and power density in cephalopod evolution. Journal of Experimental Biology 160:93–112.

Ohman, M. D. 1990. The demographic benefits of diel vertical migration by zooplankton. Ecological Monographs 60:257–281.

Ohman, M. D., B. W. Frost, and E. B. Cohen. 1983. Reverse diel vertical migration: An escape from invertebrate predators. Science 220:1404–1407.

Pimentel, M. S., K. Trubenbach, F. Faleiro, J. Boavida-Portugal, T. Repolho, and R. Rosa. 2012. Impact of ocean warming on the early ontogeny of cephalopods: a metabolic approach. Marine Biology 159:2051–2059.

Puneeta, P., D. Vijai, J. Yamamoto, and Y. Sakurai. 2018. Orientation patterns of Japanese flying squid *Todarodes pacificus* embryos within egg masses and responses of paralarvae to light. Zoological Science 35:293–298.

Ramirez, M. D., D. I. Speiser, M. S. Pankey, and T. H. Oakley. 2011. Understanding the dermal light sense in the context of integrative photoreceptor cell biology. Visual Neuroscience 28:265-279.

Randel, N., and G. Jékely. 2015. Phototaxis and the origin of visual eyes. Philosophical Transactions of the Royal Society B 371:20150042.

Robin, J., M. Roberts, L. Zeidberg, I. Bloor, A. Rodriguez, F. Briceño, N. Downey, M. Mascaró, M. Navarro, A. Guerra, J. Hofmeister, D. D. Barcellos, S. A. P. Lourenço, C. F. E. Roper, N. A. Moltschaniwskyj, C. P. Green, and J. Mather. 2014. Transitions during cephalopod life history: The role of habitat, environment, functional morphology, and behaviour. Advances in Marine Biology 67:361–437.

Rudjakov, J. A. 1970. The possible causes of diel vertical migrations of planktonic animals. Marine Biology 6:98–105.

Ruvalcaba-Aroche, E. D., L. Sánchez-Velasco, E. Beier, V. M. Godínez, E. D. Barton, and M. R. Pachecho. 2018. Effects of mesoscale structures on the distribution of cephalopod paralarvae in the Gulf of California and adjacent Pacific. Deep Sea Research Part I 131:62–74.

Sánchez-Velasco, L., E. D. Ruvalcaba-Aroche, E. Beier, V. M. Godínez, E. D. Barton, N. Díaz-Viloria, and M. R. Pachecho. 2016. Paralarvae of the *complex Sthenoteuthis oualaniensis-Dosidicus gigas* (Cephalopoda: Ommastrephidae) in the northern limit of the shallow oxygen minimum zone of the Eastern Tropical Pacific Ocean (April 2012). Journal of Geophysical Research: Oceans 121:1998–2015.

Scherer, E. 1971. Effects of oxygen depletion and of carbon dioxide buildup on the photic behavior of the walleye (*Stizostedion vitreum vitreum*). Journal of the Fisheries Research Board of Canada 28:1303–1307.

Seibel, B. A. 2007. On the depth and scale of metabolic rate variation: scaling of oxygen consumption rates and enzymatic activity in the Class Cephalopoda (Mollusca). Journal of Experimental Biology 210:1–11.

Sidie, J., and B. Holloway. 1999. Geotaxis in the squid hatchling *Loligo pealei*. American Zoology 39.

Staaf, D. J., W. F. Gilly, and M. W. Denny. 2014. Aperture effects in squid jet propulsion. Journal of Experimental Biology 217:1588–1600.

Staaf, D. J., J. V. Redfern, W. F. Gilly, W. Watson, and L. T. Ballance. 2013. Distribution of ommastrephid paralarvae in the eastern Tropical Pacific. Fishery Bulletin 111:78–89.

Vidal, E. A. G., M. J. Roberts, and R. S. Martins. 2019. Yolk utilization, metabolism and growth in reared *Loligo vulgaris reynaudii* paralarvae 393:385–393.

Vidal, E. a G., F. P. DiMarco, J. H. Wormuth, and P. G. Lee. 2002. Optimizing rearing conditions of hatchling loliginid squid. Marine Biology 140:117–127.

Villanueva, R., and M. D. Norman. 2008. Biology of the planktonic stages of benthic octopuses. Oceanography and Marine Biology: an Annual Review 46:105–202.

Vogel, S. 1981. The physical biology of flow. Princeton University Press, Princeton, New Jersey.

Waser, W., and N. Heisler. 2005. Oxygen delivery to the fish eye: root effect as crucial factor for elevated retinal PO_2. The Journal of experimental biology 208:4035–47.

Wong-Riley, M. 2010. Energy metabolism of the visual system. Eye and Brain 2:99–116.

Zakroff, C., T. A. Mooney, and C. Wirth. 2018. Ocean acidification responses in paralarval squid swimming behavior using a novel 3D tracking system. Hydrobiologia 808:83–106.

Zeidberg, L. D., J. L. Butler, D. Ramon, A. Cossio, K. L. Stierhoff, and A. Henry. 2012. Estimation of spawning habitats of market squid (*Doryteuthis opalescens*) from field surveys of eggs off Central and Southern California. Marine Ecology 33:326–336.

Zeidberg, L. D., and W. M. Hamner. 2002. Distribution of squid paralarvae, *Loligo opalescens* (Cephalopoda: Myopsida), in the Southern California Bight in the three years following the 1997-1998 El Niño. Marine Biology 141:111–122.

Zuñiga, O., A. Olivares, M. Rojo, M. E. Chimal, F. Díaz, I. Uriarte, and C. Rosas. 2013. Thermoregulatory behavior and oxygen consumption of *Octopus mimus* paralarvae : The effect of age. Journal of Thermal Biology 38:86–91.

Tables

Table 5.1. Oxygen metrics for visual function in *D. opalescens* and *O. bimaculatus* paralarvae determined as the oxygen at which there is 90%, 50%, and 10% retinal function, respectively, in comparison to retinal responses in normoxia (21 kPa/ 248.2 µmol O_2 kg^{-1}) (McCormick et al. 2019). Results are presented in both partial pressure (pO_2; kPa) and oxygen concentration (O_2; µmol kg^{-1}).

Oxygen metric for retinal function	***D. opalescens***		***O. bimaculatus***	
	pO_2 (kPa)	O_2 (µmol kg^{-1})	pO_2 (kPa)	O_2 (µmol kg^{-1})
V_{90}	22.2	262.4	11.5	135.9
V_{50}	13.0	153.6	7.2	85.1
V_{10}	6.9	81.6	5.9	69.7

Table 5.2. Description of behavior experiments conducted on *D. opalescens* and *O. bimaculatus* paralarvae. Trials were conducted at a variety of ages (days post hatching; DPH) and at four different oxygen (O_2) conditions for each species. V_{90}, V_{50}, and V_{10} are oxygen metrics for retinal function derived from McCormick et al. (2019). The pH, and average and standard deviation (s.d.) oxygen partial pressure (pO_2; kPa) and temperature (°C) are given for each trial.

Species	Trial	Larval Age	O_2 Condition	Average pO_2	pO_2 st. dev.	Average Temp.	Temp. st.dev.	pH
Doryteuthis opalescens	Squid7	3 DPH	Control	21.20	0.280	16.1	1.27	8.04
	Squid8	3 DPH	Control	21.22	0.254	16.1	0.848	8.04
	Squid10	3 DPH	Control	21.20	0.00	16.15	0.919	8.04
	Squid18	6 DPH	Control	20.82	0.169	14.8	0.990	8.05
	Squid23	1 DPH	V50	13.07	0.396	14.35	1.06	8.06
	Squid24	1 DPH	V50	12.74	0.403	14.75	1.20	8.04
	Squid11	4 DPH	V10	6.30	0.707	14.3	1.69	8.28
	Squid16	5 DPH	V10	6.86	0.601	14.85	1.77	8.27
	Squid17	5 DPH	V10	6.57	0.544	15.15	1.63	8.27
	Squid20	6 DPH	Low	3.99	0.601	16.2	1.27	8.29
	Squid21	6 DPH	Low	3.95	0.693	16.15	1.20	8.30
	Squid22	6 DPH	Low	4.70	0.552	14.6	2.12	8.30
Octopus bimaculatus	Obimac1	2 DPH	Control	21.66	0.163	16.35	0.495	8.04
	Obimac5	4 DPH	Control	21.43	0.156	16.45	0.919	8.19
	Obimac6	1 DPH	Control	21.08	0.417	14.8	1.70	8.04
	Obimac8	2 DPH	V90	10.78	0.608	15.05	1.63	8.28
	Obimac9	2 DPH	V90	10.65	0.651	15.6	1.41	8.28
	Obimac4	3 DPH	V50	7.68	0.601	14.5	1.84	8.07
	Obimac7	1 DPH	V50	7.02	0.799	14.1	1.70	8.09
	Obimac2	2 DPH	V10	5.85	0.692	15.45	1.20	8.08
	Obimac3	2 DPH	V10	5.80	0.467	16	1.13	8.02

Table 5.3. Statistical results for Kruskal-Wallis one-way analysis of variance tests comparing swimming behavior (mean distance moved and mean velocity) under each of 9 different light stimuli (irradiance; µmol photons m^{-2} s^{-1}) and the respective 3-minute dark period after each stimulus. Results are shown for 4 different oxygen conditions (pO_2; kPa) in paralarvae of *D. opalescens* and *O. bimaculatus*. P-values <0.05 indicate significant differences between the given behavior during the light stimulus and the subsequent dark period, shown in red text.

Doryteuthis opalescens				***Octopus bimaculatus***			
Oxygen Condition	Irradiance (µmol photons m^{-2} s^{-1})	Mean distance moved (mm) p-value	Mean velocity (mm s^{-1}) p-value	Oxygen Condition	Irradiance (µmol photons m^{-2} s^{-1})	Mean distance moved (mm) p-value	Mean velocity (mm s^{-1}) p-value
Normoxia (21.1 kPa) df= 1	0.062	0.3568	0.3615	**Normoxia (21.3 kPa)** df= 1	0.062	0.4296	0.4296
	0.287	0.2341	0.2341		0.287	0.05584	0.05584
	0.567	0.9287	0.9358		0.567	0.09725	0.09725
	0.853	1.90E-05	2.02E-05		0.853	0.03818	0.03818
	1.15	0.3662	0.3662		1.15	0.8211	0.8211
	1.48	2.33E-07	2.33E-07		1.48	0.1051	0.1051
	1.78	1.90E-05	1.62E-05		1.78	0.01945	0.01945
	2.15	9.25E-05	9.25E-05		2.15	0.005287	0.005287
	2.45	4.74E-07	4.12E-07		2.45	0.001357	0.001357
V_{50} (12.9 kPa) df= 1	0.062	0.001849	0.0153	**V_{90} (10.7 kPa)** df= 1	0.062	0.04994	0.04994
	0.287	0.0153	0.0153		0.287	0.1124	0.1124
	0.567	0.02374	0.02374		0.567	0.3258	0.3258
	0.853	0.1588	0.1588		0.853	0.1097	0.1097
	1.15	0.455	0.455		1.15	0.05004	0.05004
	1.48	0.04776	0.04776		1.48	0.4057	0.4057
	1.78	1.76E-05	1.76E-05		1.78	0.3643	0.3643
	2.15	0.003182	0.003182		2.15	0.8206	0.8206
	2.45	2.38E-05	2.38E-05		2.45	0.6501	0.6501
V_{10} (6.6 kPa) df= 1	0.062	0.3734	0.3734	**V_{50} (7.4 kPa)** df= 1	0.062	0.1213	0.1213
	0.287	0.1048	0.1048		0.287	0.8327	0.8327
	0.567	0.6177	0.6177		0.567	0.9215	0.9215
	0.853	0.4409	0.4409		0.853	0.03464	0.03464
	1.15	0.8684	0.8684		1.15	0.05726	0.05726
	1.48	0.2244	0.2244		1.48	0.0386	0.0386
	1.78	0.5602	0.5602		1.78	0.341	0.341
	2.15	0.3392	0.3392		2.15	0.0386	0.0386
	2.45	0.001132	0.001132		2.45	0.01975	0.01975
Low (4.2 kPa) df= 1	0.062	0.7726	0.7726	**V_{10} (5.8 kPa)** df= 1	0.062	0.6256	0.6256
	0.287	0.9168	0.9168		0.287	0.1124	0.1124
	0.567	0.06358	0.06358		0.567	0.435	0.435
	0.853	0.3694	0.3694		0.853	0.8453	0.8453
	1.15	0.4094	0.4094		1.15	0.2207	0.2207
	1.48	0.3606	0.3606		1.48	0.9349	0.9349
	1.78	0.1291	0.1291		1.78	0.1651	0.1651
	2.15	0.0001494	0.0001494		2.15	0.1651	0.1651
	2.45	0.03013	0.03013		2.45	0.7898	0.7898

Table 5.4. Statistical comparisons of swim behavior (mean distance moved and mean velocity) and paralarvae distribution (chamber zones) for *D. opalescens* paralarvae across oxygen conditions within each stimulus irradiance. Kruskal-Wallis one-way analysis of variance test were conducted to determine differences among the mean distance moved, mean velocity, and the percentage of paralarvae in each zone (Upper, Middle, Lower, and Bottom chamber) between oxygen conditions. Red values indicate significance.

Doryteuthis opalescens		**Irradiance (µmol photons m^{-2} s^{-1})**								
	Statistic	**0.062**	**0.287**	**0.567**	**0.853**	**1.15**	**1.48**	**1.78**	**2.15**	**2.45**
Mean distance moved (mm) df =3	Kruskal-Wallis test	0.02402	0.4771	0.09241	7.49E-05	0.1839	2.59E-05	1.12E-07	0.0001726	9.70E-05
	Normoxia vs. Low	0.1052	NA	NA	0.0001	NA	0.0013	0.0001	0.5249	0.017
	Normoxia vs. V_{10}	0.1139	NA	NA	0.0007	NA	0.0001	0.0066	0.0001	0.02
	Normoxia vs. V_{50}	0.4257	NA	NA	0.0902	NA	0.4385	0.1207	0.3881	0.1217
	Low vs. V_{10}	0.4659	NA	NA	0.2663	NA	0.2197	0.1044	0.0049	0.4804
	Low vs. V_{50}	0.0424	NA	NA	0.0738	NA	0.0277	0	0.4865	0.0004
	V_{10} vs. V_{50}	0.0404	NA	NA	0.1557	NA	0.0044	0.0001	0.005	0.0004
Mean velocity (mm s^{-1}) df = 3	Kruskal-Wallis test	0.02377	0.4771	0.09241	7.39E-05	0.1839	2.54E-05	1.09E-07	0.0001717	9.58E-05
	Normoxia vs. Low	0.1037	NA	NA	0.0001	NA	0.0013	0.0001	0.523	0.0169
	Normoxia vs. V_{10}	0.1132	NA	NA	0.0007	NA	0.0001	0.0066	0.0001	0.0197
	Normoxia vs. V_{50}	0.4272	NA	NA	0.0888	NA	0.4371	0.1212	0.3848	0.1222
	Low vs. V_{10}	0.4672	NA	NA	0.2663	NA	0.2206	0.1039	0.0049	0.4815
	Low vs. V_{50}	0.0421	NA	NA	0.0745	NA	0.0275	0	0.4879	0.0004
	V_{10} vs. V_{50}	0.0404	NA	NA	0.1568	NA	0.0044	0.0001	0.0051	0.0004
Chamber Zones		**0.062**	**0.287**	**0.567**	**0.853**	**1.15**	**1.48**	**1.78**	**2.15**	**2.45**
Upper chamber df =3	Kruskal-Wallis test	1.25E-05	3.75E-05	0.005283	2.23E-07	7.54E-05	0.0008922	0.0001733	0.001074	1.41E-05
	Normoxia vs. Low	0.0023	0	0.1623	0.0082	0.0012	0.0041	0.0018	0.0011	0
	Normoxia vs. V_{10}	0.0029	0.0016	0.0142	0	0.0002	0.0006	0.0019	0.0048	0.0007
	Normoxia vs. V_{50}	0.2856	0.3117	0.2892	0.0143	0.4491	0.205	0.8464	0.0075	0.122
	Low vs. V_{10}	0.4289	0.181	0.2466	0.0083	0.3222	0.2805	0.4864	0.9727	0.1395
	Low vs. V_{50}	0.0002	0.0084	0.084	0.4282	0.0265	0.1851	0.007	0.7792	0.0265
	V_{10} vs. V_{50}	0.0003	0.0611	0.0058	0.0091	0.0107	0.1301	0.0085	0.4493	0.1314
Middle Chamber df = 3	Kruskal-Wallis test	1.29E-09	0.0001461	5.46E-06	3.19E-06	5.61E-06	0.0005242	0.0009435	0.02404	0.1549
	Normoxia vs. Low	0	0.0269	0	0	0.0072	0.0012	0.0002	0.0366	NA
	Normoxia vs. V_{10}	0	0	0	0.0001	0.0973	0.0967	0.0806	0.4496	NA
	Normoxia vs. V_{50}	0.0938	0.1552	0.00004	0.1643	0.0298	0.0009	0.0457	0.1752	NA
	Low vs. V_{10}	0.3397	0.0744	0.4537	0.2489	0.1054	0.1288	0.0791	0.0307	NA
	Low vs. V_{50}	0.0007	0.2149	0.8049	0.0089	0	0.3126	0.2277	0.5382	NA
	V_{10} vs. V_{50}	0.0054	0.0273	1	0.038	0.0003	0.0972	0.2628	0.1853	NA
Lower chamber df = 3	Kruskal-Wallis test	2.10E-08	4.84E-09	0.03215	0.0001442	0.000638	0.0001072	0.2812	1.03E-06	0.01007
	Normoxia vs. Low	0	0	0.0874	0.0001	0.0005	0.0019	NA	0	0.1972
	Normoxia vs. V_{10}	0.0001	0.0003	0.434	0.2866	0.2848	0.1835	NA	0.0747	0.2928
	Normoxia vs. V_{50}	0.0012	0.1456	0.5744	0.4693	0.1021	0.1493	NA	0.001	0.0044
	Low vs. V_{10}	0.0565	0.029	0.0726	0.0118	0.0033	0.0001	NA	0.0022	0.3355
	Low vs. V_{50}	0.0443	0	0.0191	0.00009	0.1522	0.1738	NA	0.1308	0.134
	V_{10} vs. V_{50}	0.3496	0.0277	0.4718	0.2747	0.2239	0.049	NA	0.0721	0.0147
Bottom chamber df = 3	Kruskal-Wallis test	9.81E-09	5.02E-08	1.26E-07	3.87E-08	2.05E-05	1.11E-06	1.06E-05	8.76E-06	8.51E-06
	Normoxia vs. Low	0	0	0	0	0	0	0	0	0
	Normoxia vs. V_{10}	0	0	0	0	0.0029	0.0018	0.0002	0.0021	0.0035
	Normoxia vs. V_{50}	0.0712	0.138	0.5598	0.0716	0.201	0.084	0.0946	0.0018	0.013
	Low vs. V_{10}	0.2399	0.158	0.4955	0.4977	0.14	0.071	0.2417	0.1529	0.0948
	Low vs. V_{50}	0.0024	0.0013	0.0004	0.0079	0.0128	0.0043	0.0282	0.3141	0.072
	V_{10} vs. V_{50}	0.0138	0.0182	0.0005	0.0104	0.0798	0.0977	0.1015	0.3241	0.4453

Table 5.5. Statistical comparisons of swim behavior (mean distance moved and mean velocity) and paralarvae distribution (chamber zones) for *O. bimaculatus* paralarvae across oxygen conditions within each stimulus irradiance. Kruskal-Wallis one-way analysis of variance test were conducted to determine differences among the mean distance moved, mean velocity, and the percentage of paralarvae in each zone (Upper, Middle, Lower, and Bottom chamber) between oxygen conditions. Red values indicate significance.

Octopus bimaculatus		**Irradiance (µmol photons m^{-2} s^{-1})**								
	Statistic	**0.062**	**0.287**	**0.567**	**0.853**	**1.15**	**1.48**	**1.78**	**2.15**	**2.45**
Mean distance moved (mm) df =3	Kruskal-Wallis test	0.2439	0.2769	0.5506	0.08699	0.08073	0.005658	0.3735	0.1187	0.01052
	Normoxia vs. V_{10}	NA	NA	NA	NA	NA	0.458	NA	NA	0.1465
	Normoxia vs. V_{50}	NA	NA	NA	NA	NA	0.0046	NA	NA	0.152
	Normoxia vs. V_{90}	NA	NA	NA	NA	NA	0.2422	NA	NA	0.1182
	V_{10} vs. V_{50}	NA	NA	NA	NA	NA	0.0107	NA	NA	0.0121
	V_{10} vs. V_{90}	NA	NA	NA	NA	NA	0.2182	NA	NA	0.3695
	V_{50} vs. V_{90}	NA	NA	NA	NA	NA	0.1593	NA	NA	0.0174
Mean velocity (mm s^{-1}) df = 3	Kruskal-Wallis test	0.2439	0.2769	0.5506	0.08699	0.08073	0.005658	0.3735	0.1187	0.01052
	Normoxia vs. V_{10}	NA	NA	NA	NA	NA	0.458	NA	NA	0.1465
	Normoxia vs. V_{50}	NA	NA	NA	NA	NA	0.0046	NA	NA	0.152
	Normoxia vs. V_{90}	NA	NA	NA	NA	NA	0.2422	NA	NA	0.1882
	V_{10} vs. V_{50}	NA	NA	NA	NA	NA	0.0107	NA	NA	0.0121
	V_{10} vs. V_{90}	NA	NA	NA	NA	NA	0.2182	NA	NA	0.3695
	V_{50} vs. V_{90}	NA	NA	NA	NA	NA	0.1593	NA	NA	0.0174
Chamber Zones		**0.062**	**0.287**	**0.567**	**0.853**	**1.15**	**1.48**	**1.78**	**2.15**	**2.45**
Upper chamber df =3	Kruskal-Wallis test	1.90E-05	0.0762	6.63E-06	0.002394	7.14E-06	4.69E-05	0.0003481	0.1805	0.01314
	Normoxia vs. V_{10}	0.4417	NA	0.2886	0.4554	0.4578	0.1036	0.2738	NA	0.4697
	Normoxia vs. V_{50}	0.0363	NA	0.0026	0.6828	0	0.0066	0.0012	NA	0.0147
	Normoxia vs. V_{90}	0.2271	NA	0.0011	0.0013	0.0027	0	0.0014	NA	0.1742
	V_{10} vs. V_{50}	0.2804	NA	0.0003	0.5623	0.0003	0.1663	0.0432	NA	0.0209
	V_{10} vs. V_{90}	0.2361	NA	0.0001	0.0048	0.007	0.0069	0.0564	NA	0.1542
	V_{50} vs. V_{90}	0.5465	NA	0.386	0.0233	0.3143	0.184	0.4966	NA	0.3142
Middle Chamber df = 3	Kruskal-Wallis test	0.001057	0.007855	0.0008974	0.001785	0.1101	0.07288	0.0001307	0.226	0.01303
	Normoxia vs. V_{10}	0.1108	0.1309	0.2164	0.0015	NA	NA	0.0026	NA	0.0955
	Normoxia vs. V_{50}	0.1852	0.1869	0.0066	0.2377	NA	NA	0.0238	NA	0.0939
	Normoxia vs. V_{90}	0.0115	0.1804	0.0547	0.0121	NA	NA	0	NA	0.0058
	V_{10} vs. V_{50}	0.0221	0.009	0.0016	0.0714	NA	NA	0.4783	NA	0.4689
	V_{10} vs. V_{90}	0.0006	0.5	0.0173	0.2724	NA	NA	0.1329	NA	0.3483
	V_{50} vs. V_{90}	0.2115	0.0087	0.4035	0.2025	NA	NA	0.0993	NA	0.4644
Lower chamber df = 3	Kruskal-Wallis test	0.03916	0.153	1.59E-07	0.002106	7.33E-05	1.84E-05	0.001599	0.01318	0.003707
	Normoxia vs. V_{10}	0.0481	NA	0.2958	0.4931	0.3151	0.0793	0.1194	0.9042	0.0042
	Normoxia vs. V_{50}	0.041	NA	0.0001	0.4933	0.0002	0.0001	0.0009	0.0159	0.0117
	Normoxia vs. V_{90}	0.3012	NA	0	0.0113	0.0957	0.0001	0.0126	1	0.2512
	V_{10} vs. V_{50}	0.4789	NA	0.0019	0.3953	0.0001	0.0626	0.1707	0.0158	0.3697
	V_{10} vs. V_{90}	0.3492	NA	0.0001	0.0041	0.0749	0.0469	0.3997	0.4787	0.1239
	V_{50} vs. V_{90}	0.4051	NA	0.4573	0.0019	0.0657	0.5	0.2299	0.0169	0.1875
Bottom chamber df = 3	Kruskal-Wallis test	4.02E-05	0.0002404	0.0004016	0.0754	0.0001803	1.63E-05	0.04799	1.52E-05	2.67E-06
	Normoxia vs. V_{10}	0.2029	0.3089	0.0047	NA	0.1969	0.0198	0.0661	0.0178	0.0007
	Normoxia vs. V_{50}	0.0006	0.0009	0.4083	NA	0.0001	0.0528	0.4801	0.0377	0.2831
	Normoxia vs. V_{90}	0.0294	0.0457	0.3975	NA	0.0102	0.0352	0.2513	0.0544	0.1029
	V_{10} vs. V_{50}	0.0001	0.0006	0.001	NA	0.0081	0.0001	0.3343	0	0.0001
	V_{10} vs. V_{90}	0.0077	0.03	0.0004	NA	0.1131	0	0.025	0.0001	0
	V_{50} vs. V_{90}	0.244	0.1708	0.3964	NA	0.243	0.5	0.3133	0.3865	0.2474

Figures

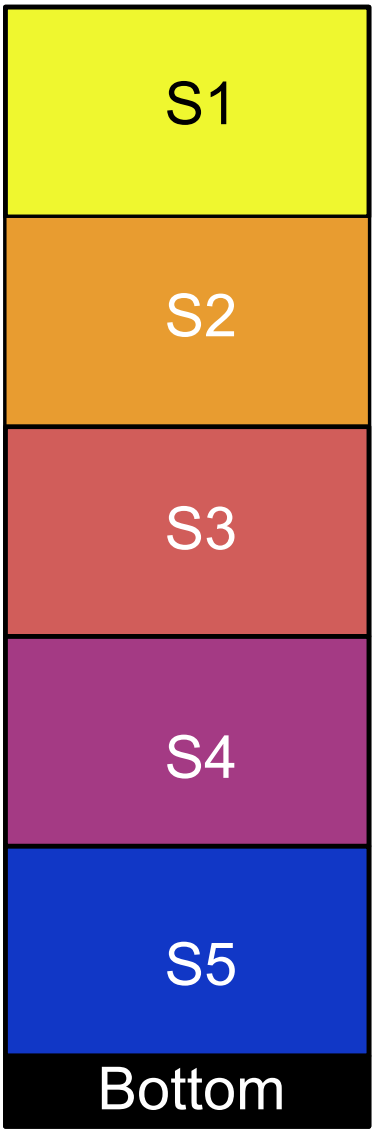

Figure 5.1. Separation of phototaxis arena into zones for quantifying paralarvae distribution. A schematic of the phototaxis chamber (20cm H x 4 cm W x 5 cm L) separated into 5 evenly-spaced zones, with S1 in the upper chamber closest to the light stimulus and S5 as the lower segment. A 'Bottom' segment was created to count cephalopod paralarvae that were not actively swimming.

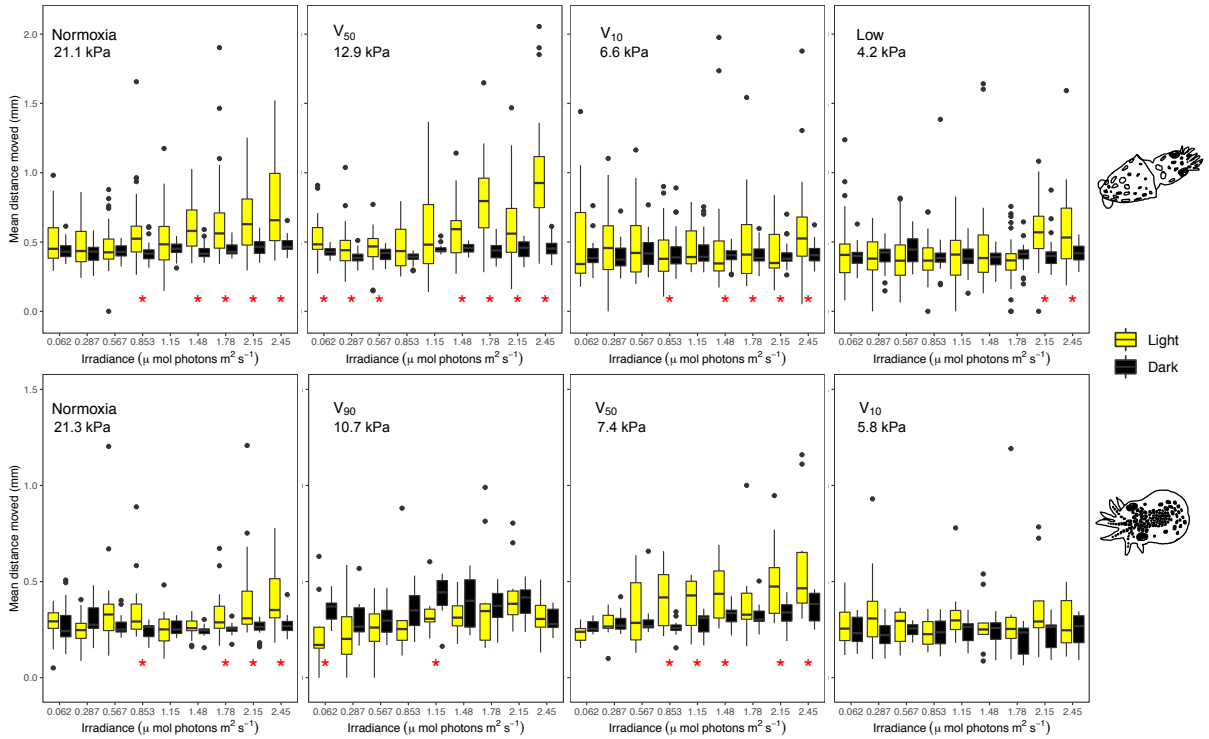

Figure 5.2. Differences in the mean distance moved of cephalopod paralarvae during a light stimulus (10 s) compared to the mean distance moved in darkness immediately after the stimulus (3 min). The mean distance moved (mm) was calculated for each stimulus irradiance (increasing from 0.062 – 2.45 μmol photons m^{-2} s^{-1}) for paralarvae of *D. opalescens* (top) and *O. bimaculatus* (bottom) under 4 different oxygen conditions, with the average pO_2 (kPa) displayed on each figure. Significance between the mean distance moved during the light stimulus (yellow boxes) compared with the dark period (black boxes) was determined using Kruskal-Wallis one-way analysis of variance tests at each stimulus (red asterisk). Boxes show the median (bold center line) and first and third quartiles of all individuals tested within a species; error bars show maximum/minimum values within 1.5x the inner quartile range (IQR=third quartile–first quartile).

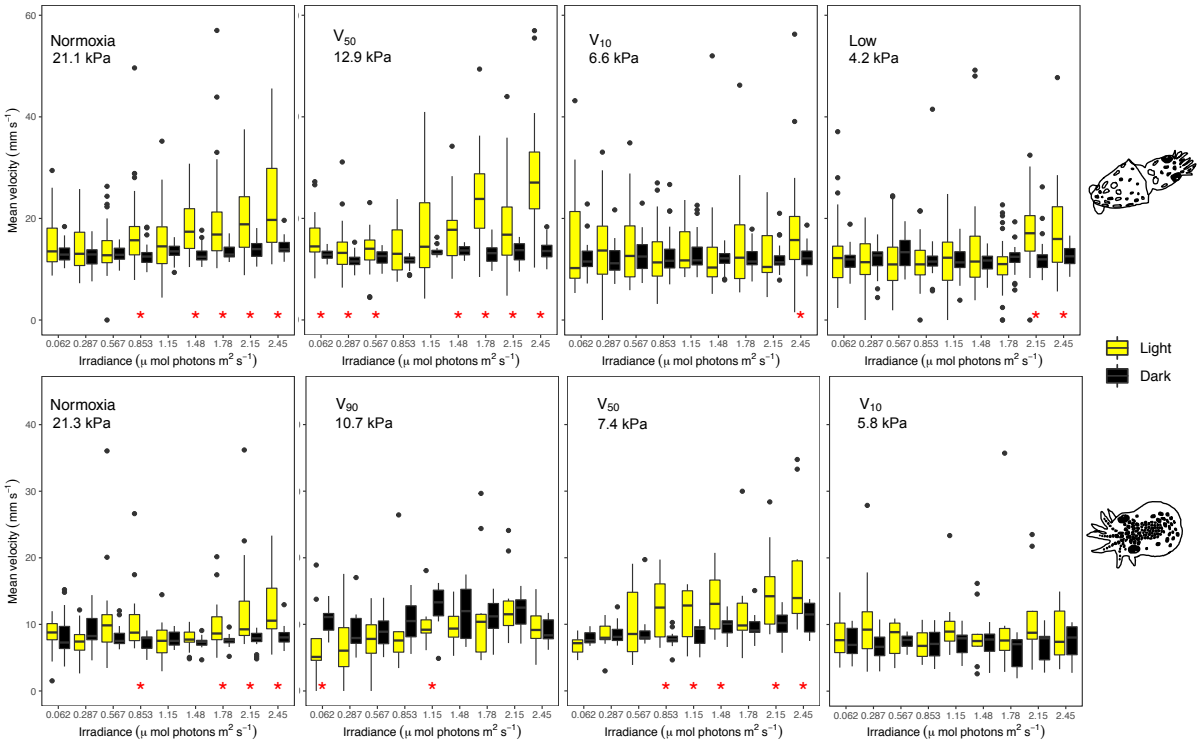

Figure 5.3. Location of cephalopod paralarvae in the chamber during phototaxis experiments during a light stimulus (10 s) compared to the location in darkness ('Dark', first bar). The percentage of paralarvae swimming in each zone was calculated for each stimulus irradiance (increasing from 0.062 – 2.45 µmol photons m^{-2} s^{-1}) for *D. opalescens* (top) and *O. bimaculatus* (bottom) under 4 different oxygen conditions, with the average pO_2 (kPa) displayed on each figure. The chamber was split into 5 equal zones, with 'S1' closest to the overhead light stimulus and 'S5' farthest away, with an additional 'Bottom' zone to quantify individuals on the bottom of the chamber. All dark periods after each light stimuli were averaged ('Dark') for comparison across light stimuli.

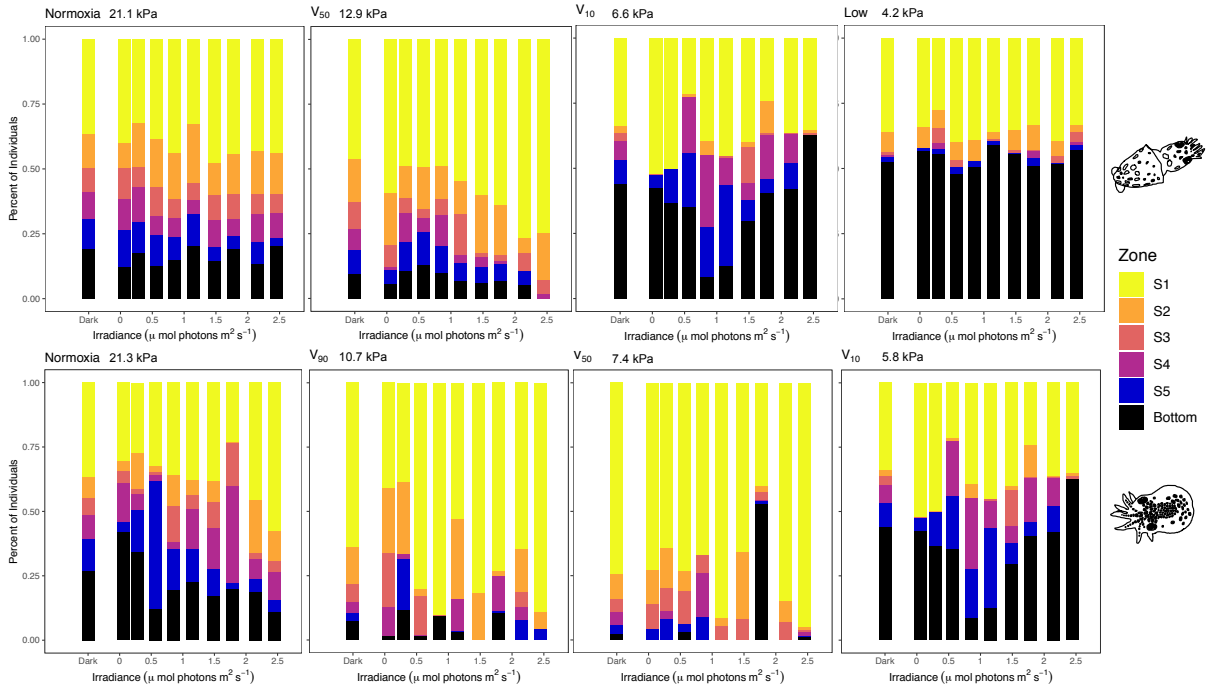

Figure 5.4. Location of cephalopod paralarvae in the chamber during phototaxis experiments during a light stimulus (10 s) compared to the location in darkness ('Dark', first bar). The percentage of paralarvae swimming in each zone was calculated for each stimulus irradiance (increasing from 0.062 – 2.45 µmol photons m^{-2} s^{-1}) for *D. opalescens* (top) and *O. bimaculatus* (bottom) under 4 different oxygen conditions, with the average pO_2 (kPa) displayed on each figure. The chamber was split into 5 equal zones, with 'S1' closest to the overhead light stimulus and 'S5' farthest away, with an additional 'Bottom' zone to quantify individuals on the bottom of the chamber. All dark periods after each light stimuli were averaged ('Dark') for comparison across light stimuli.

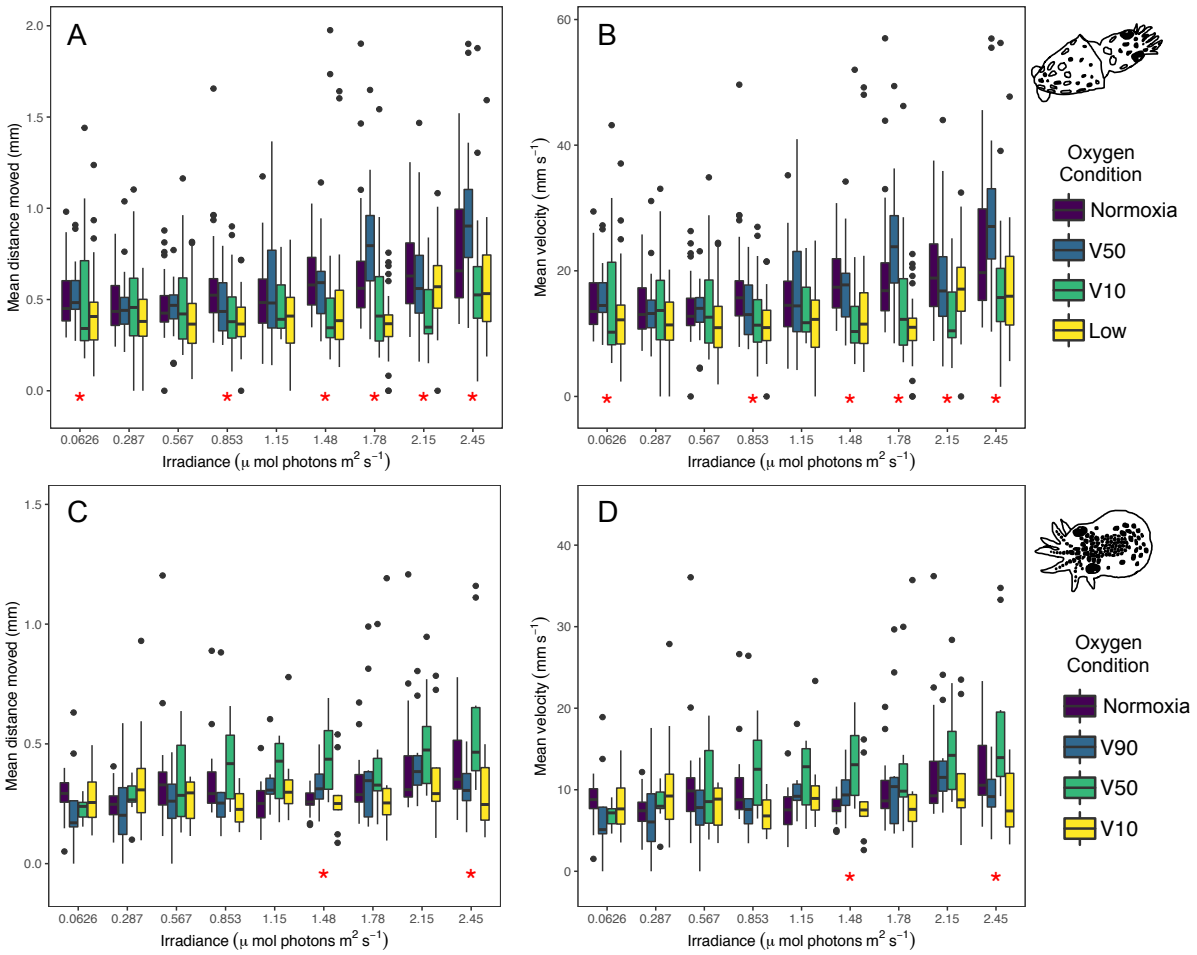

Figure 5.5. Differences in phototaxis swim behavior in cephalopod paralarvae across oxygen conditions for all light stimuli. Differences in the (A) mean distance moved and (B) mean velocity in *D. opalescens* paralarvae during 10-second light stimuli of increasing irradiance (0.0626 – 2.45 μmol photons m^{-2} s^{-1}) were determined between trials in normoxia (purple boxes; 21.1 ±0.2 kPa), V_{50} (blue boxes; 12.9 ±0.2 kPa), V_{10} (green boxes; 6.6 ±0.3 kPa), and Low pO_2 (yellow boxes; 4.2 ±0.4 kPa). For *O. bimaculatus* paralarvae, differences in the (C) mean distance moved and (D) mean velocity were determined across the same light stimuli, between trials in normoxia (purple boxes; 21.3 ±0.3 kPa), V_{90} (blue boxes; 10.7 ±0.1 kPa), V_{50} (green boxes; 7.4 ±0.4 kPa), and V_{10} (yellow boxes; 5.8 ±0.03 kPa). Significance within each light stimulus tested with a Kruskal-Wallis one-way analysis of variance is noted with red asterisks. Boxes show the median (bold center line) and first and third quartiles of all individuals tested within a species; error bars show maximum/minimum values within 1.5x the inner quartile range (IQR=third quartile–first quartile).

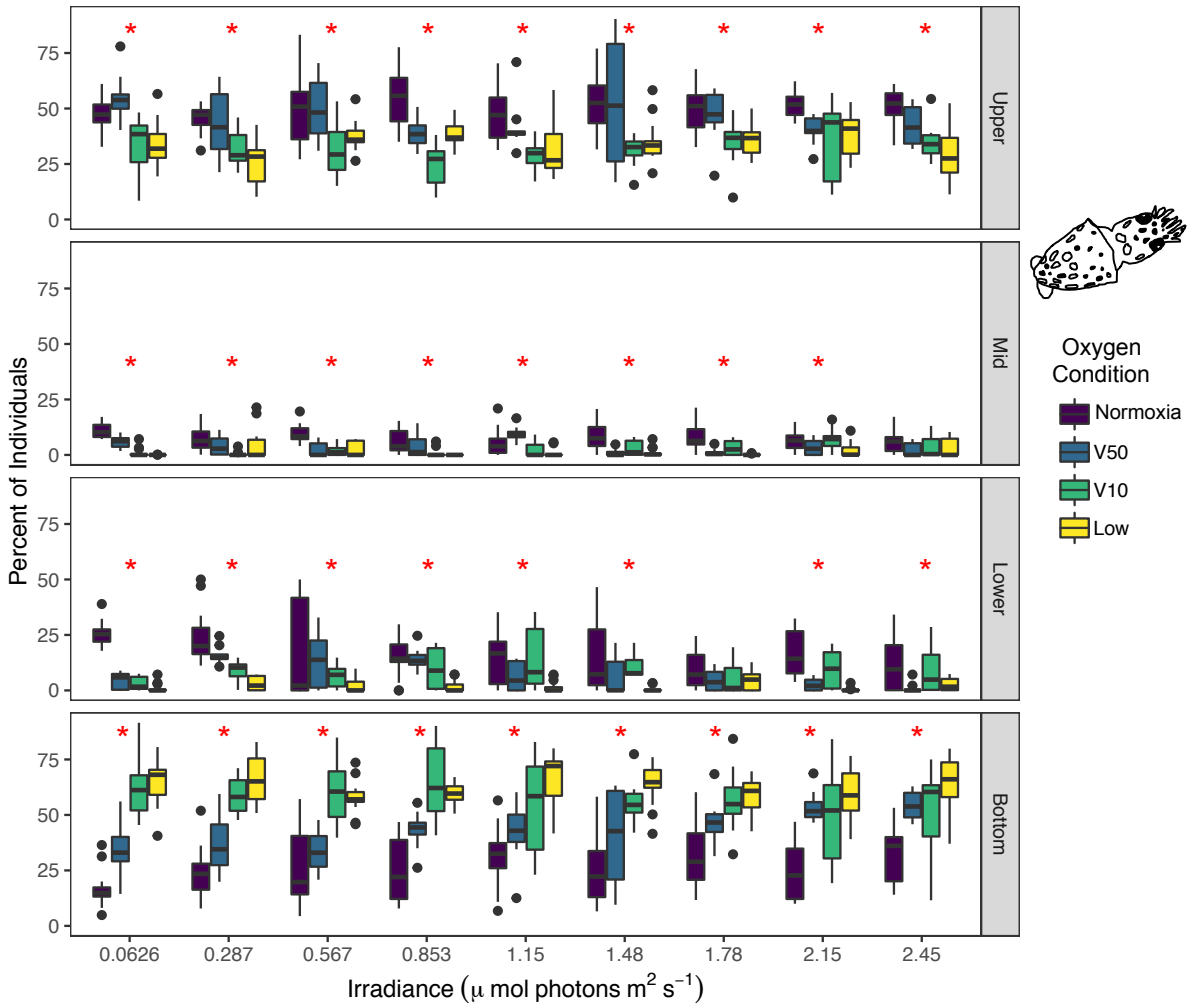

Figure 5.6. The location of *D. opalescens* paralarvae in the phototaxis chamber under different oxygen conditions. The percentages of paralarvae in the upper, middle ('Mid'), lower chamber during 9 light stimuli of increasing irradiance (0.0626 – 2.45 µmol photons m^{-2} s^{-1}) during phototaxis trials in normoxia (purple boxes; 21.1 ±0.2 kPa), V_{50} (blue boxes; 12.9 ±0.2 kPa), V_{10} (green boxes; 6.6 ±0.3 kPa), and Low pO_2 (yellow boxes; 4.2 ±0.4 kPa). Differences within each stimulus irradiance among oxygen conditions were determined with Kruskal-Wallis one-way analysis of variance tests, with significant values ($p > 0.05$) noted as red asterisks. Boxes show the median (bold center line) and first and third quartiles of all individuals tested within a species; error bars show maximum/minimum values within 1.5x the inner quartile range (IQR=third quartile–first quartile).

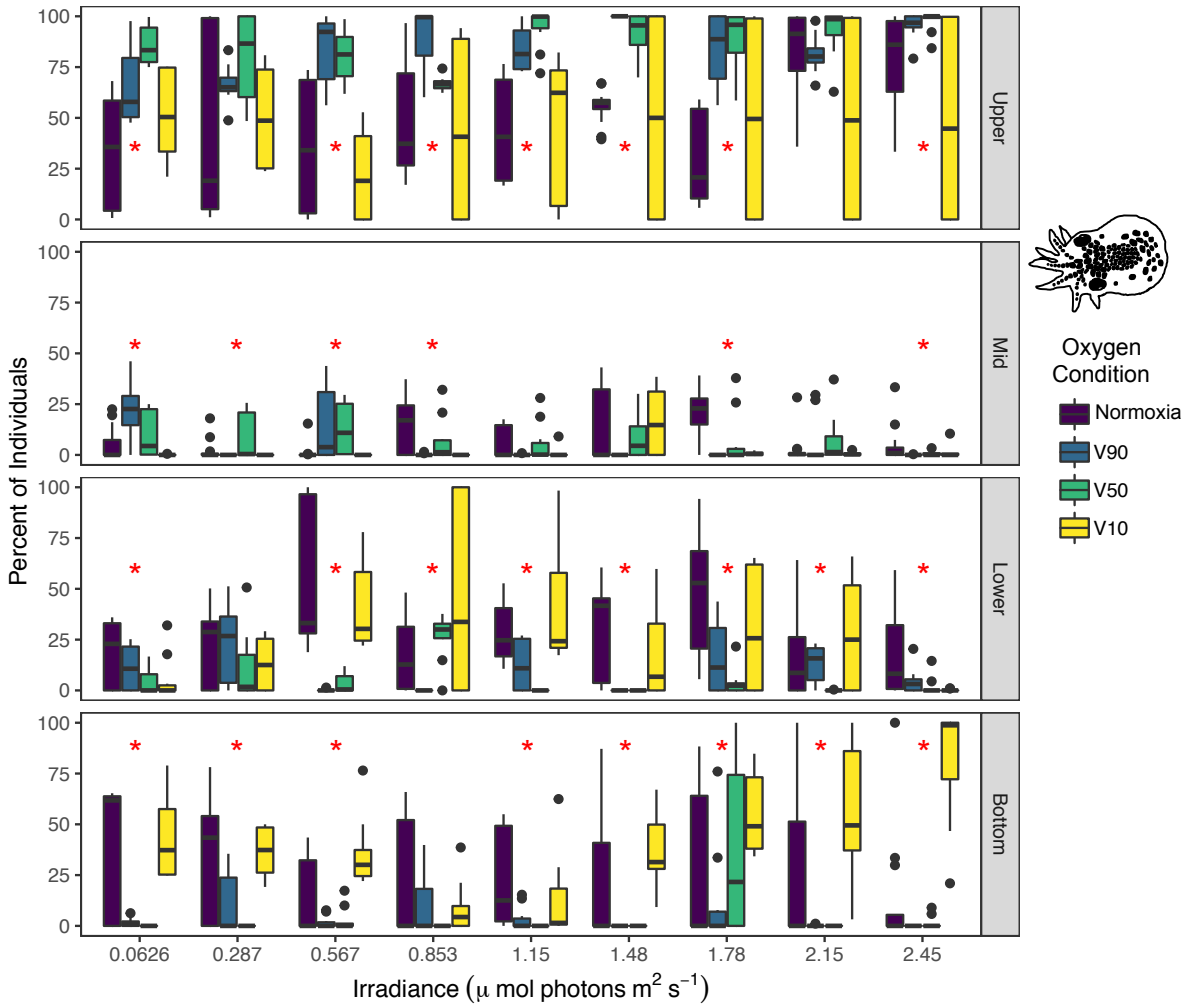

Figure 5.7. The location of *O. bimaculatus* paralarvae in the phototaxis chamber during light stimuli under different oxygen conditions. The percentages of paralarvae in the upper, middle ('Mid'), lower chamber during 9 light stimuli of increasing irradiance (0.0626 – 2.45 µmol photons m^{-2} s^{-1}) during phototaxis trials in normoxia (purple boxes; 21.3 ±0.3 kPa), V_{90} (blue boxes; 10.7 ±0.1 kPa), V_{50} (green boxes; 7.4 ±0.4 kPa), and V_{10} (yellow boxes; 5.8 ±0.03 kPa). Differences within each stimulus irradiance among oxygen conditions were determined with Kruskal-Wallis one-way analysis of variance tests, with significant values ($p > 0.05$) noted as red asterisks. Boxes show the median (bold center line) and first and third quartiles of all individuals tested within a species; error bars show maximum/minimum values within 1.5x the inner quartile range (IQR=third quartile–first quartile).

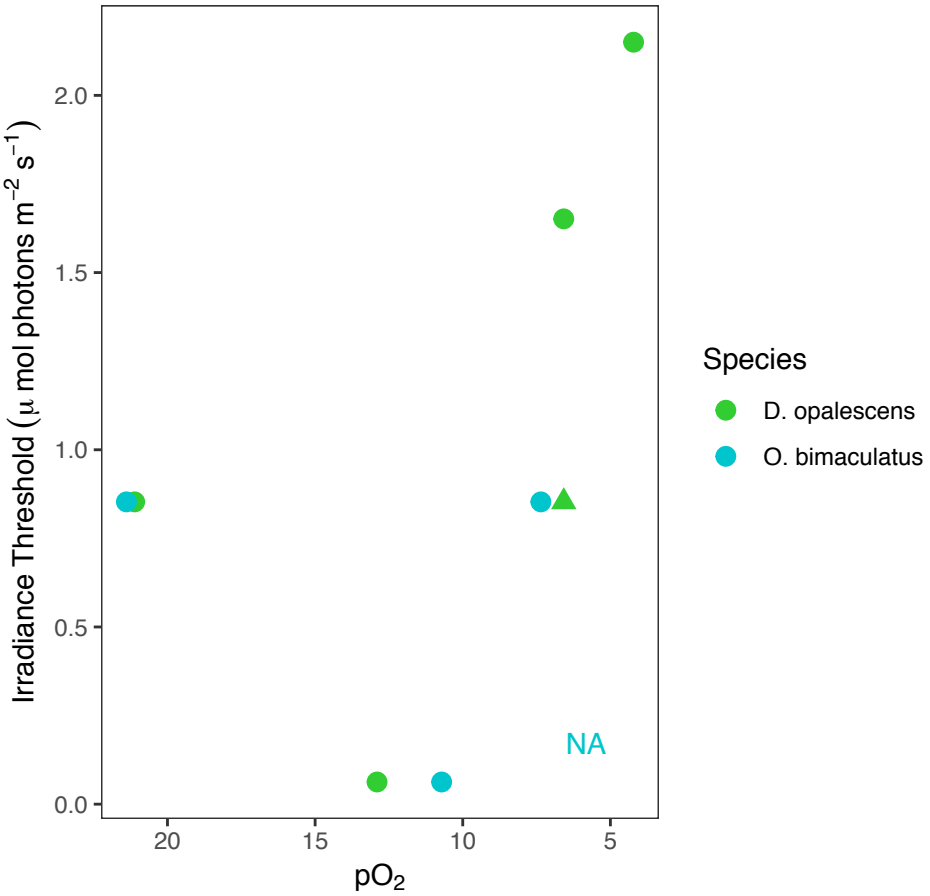

Figure 5.8. Changes in the irradiance threshold for phototaxis at different oxygen conditions in cephalopod paralarvae. The irradiance threshold was calculated as the lowest irradiance at which swimming behavior (mean distance moved and mean velocity) during a light stimulus was significantly different from behavior in the dark. The thresholds for the mean distance moved and the mean velocity were the same for *O. bimaculatus* (teal circles), and *D. opalescens* (green circles) only showed a threshold difference between the mean distance moved and mean velocity at 6.6 kPa (green triangle and green circle, respectively).

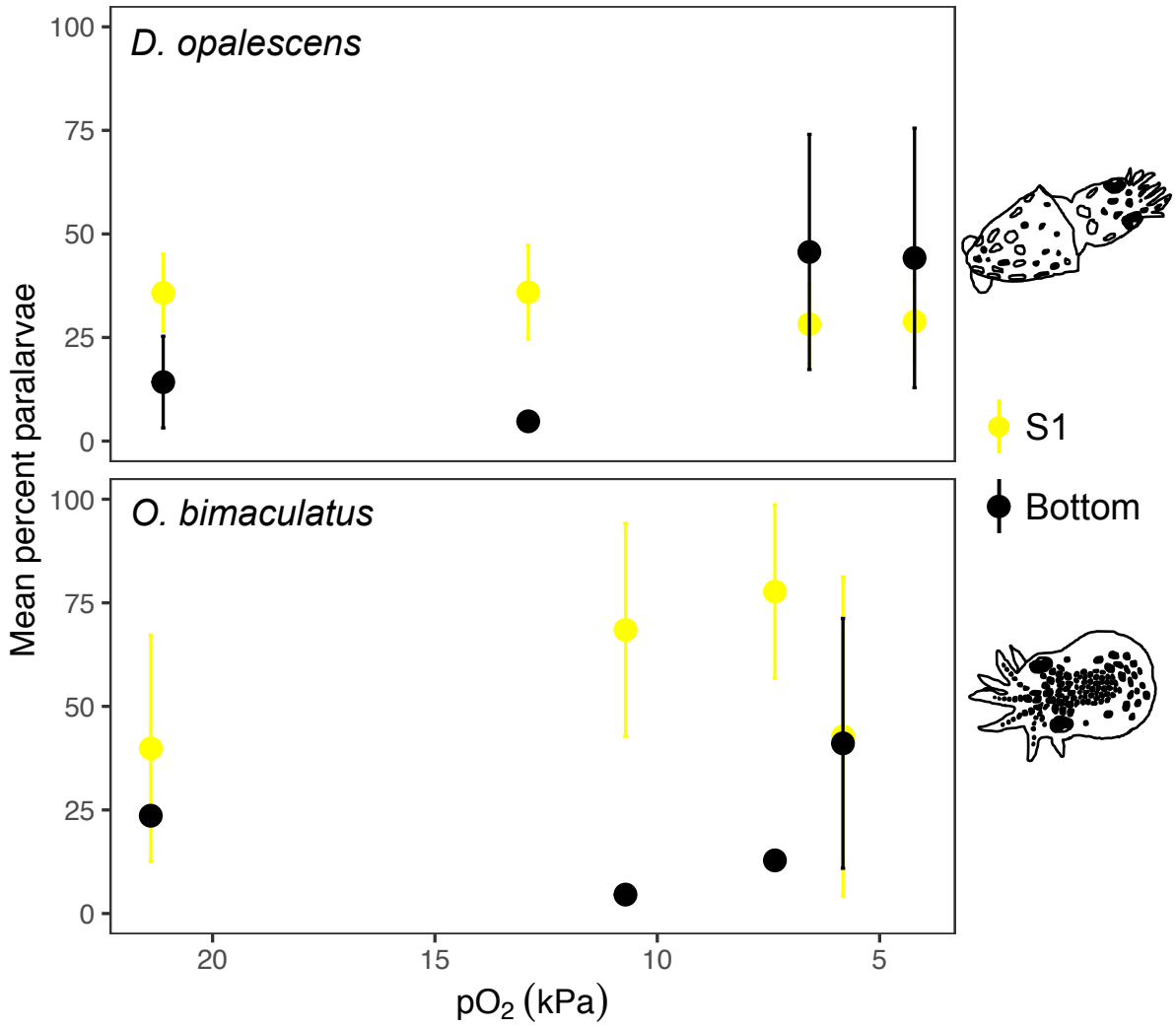

Figure 5.9. Differences in the location of paralarvae within the phototaxis chamber at different oxygen partial pressures (pO_2; kPa). The mean percentages of paralarvae in the top zone, closest to the light stimulus (S1; yellow circles) and at the bottom of the chamber (Bottom; black circles) are shown for paralarvae of *D. opalescens* and *O. bimaculatus* for multiple partial pressures of oxygen (pO_2; kPa). Error bars show s.d.

CHAPTER 6

Defining a suitable "luminoxyscape" to evaluate changing light requirements under oxygen-limitation in visual marine organisms

Lillian R. McCormick, Shailja Gangrade, Jessica C. Garwood, Taylor Wirth, Todd R. Martz, and Lisa A. Levin

Abstract

Marine organisms have distributions guided by the strong gradients of abiotic and biotic stressors in the ocean, including (but not limited to), oxygen, irradiance, temperature, pH, and salinity. This is true for both vertically migrating pelagic organisms and stationary organisms, such as benthic animals or deposited egg capsules, which experience changes in stressors over a broad range of spatial and temporal scales. Vision requires both suitable oxygen and light to function, and we propose the concept of a 'luminoxyscape' to describe the light and oxygen conditions highly visual species experience in their habitat. The suitable visual habitat is reduced to a 'critical luminoxyscape' bounded by oxygen and irradiance limits for vision. We characterized the luminoxyscape for larvae of four species common to the Southern California Bight using a custom-designed sensor package, the SeapHOx deLUX that measured oxygen and irradiance over temporal scales of hours to months, and by analyzing spatial differences in hydrographic profile data from the long-term monitoring program, the California Cooperative Oceanic Fisheries Investigations (CalCOFI). The critical luminoxyscapes for larvae of the market squid *D. opalescens*, the two-spot octopus *O. bimaculatus*, the graceful rock crab *Metacarcinus gracilis*, and the tuna crab *Pleuroncodes planipes* were determined by combining oxygen and irradiance measurements and constraining the visual habitat with previously determined oxygen limits for visual function and metabolism. At a known *D. opalescens* egg bed site at 30-m depth in La Jolla, organisms could have experienced conditions that may cause visual impairment 50-75% of the time when the sensor was deployed (2015-2017), primarily during the Spring upwelling season and between sunset and sunrise daily. Nearshore CalCOFI data (1999-2017) also showed seasonality of potential visual impairment, with the maximum depth of the critical

luminoxyscape for all levels of visual impairment shoaling during the Spring. A strong shoaling of the maximum depth of the critical luminoxyscape for 50% visual function was observed close to the coast, with a deepening of the oxycline with increasing distance from shore. Over all analyses, larvae of *D. opalescens* and *M. gracilis* exhibited the greatest vulnerability to the loss of visual habitat from reduced oxygen. We present evidence that larvae of these species are likely already experiencing oxygen- and light-limitation for vision within their habitat, but not metabolic limitation, and propose the critical luminoxyscape as an important method for understanding how species distributions might respond to low oxygen exposure.

Introduction

Organisms have evolved under selective pressure from their environment, and have developed a variety of physiological and behavioral mechanisms to cope with the stressors they experience within their habitat. In the marine environment, and especially in coastal upwelling regions like the Southern California Bight (SCB), both benthic and pelagic organisms experience highly variable oxygen, light intensity (irradiance), temperature, pH, and salinity, among other conditions. Conditions vary on multiple scales, including temporal changes (from tidal and diel to inter-annual time scales) and spatially (with latitudinal and longitudinal gradients and with depth in the water column (Booth et al. 2012, Frieder et al. 2012, Levin et al. 2015). Organisms that undergo diel vertical migration and swim up to the surface to feed on aggregations of zooplankton around sunset and then return to deeper in the water column at dawn, where they stay throughout the day avoiding visual predation (Forward 1988, Ohman 1990, Bianchi and Mislan 2016), experience large changes of ocean

conditions at either end of their migration. The pelagic environment, in contrast to shallow coastal areas, does not contain any structure that inhibits movement through the water column, such as a shallow seafloor with rocks, macroalgae, etc. Instead, the constantly changing variables and gradients with depth and over time combined with the physiological and behavioral thresholds of animals to various conditions provide an invisible and very fluid "structure" that can define suitable habitat and stressful habitat for each species. For example, organisms have been known to alter the daytime maximum depth of vertical migration based on temperature and density (Cade and Benoit-bird 2015), oxygen (Bertrand et al. 2011, Bianchi et al. 2013), and irradiance (Røstad et al. 2016).

A threshold is considered a physiological or behavioral limit to any given condition or stressor (e.g., temperature, oxygen, irradiance) where there is a change in the ability of the animal to function (Somero et al. 2015). For example, oxygen limits for organisms describe the range of oxygen where an animal can realistically function; outside of this range there would be a change in physiology or behavior that would inhibit survival by decreasing the ability for normal mobility, reproduction, sensory functions, and activity level, among other functions. Importantly, thresholds for one condition can change when the animal is also approaching or past the limits of another environmental condition (Somero et al. 2015, Baumann 2016, Gunderson et al. 2016). For example, an increase in temperature can cause an animal to be less tolerant of reduced oxygen and show impairment to swimming behavior, feeding, or reproductive function (Burnett and Stickle 2001, Hochachka and Somero 2002, Pörtner 2010). Reactions to multiple stressors have also been observed in combinations of increased temperature and reduced pH impairing survival and ventilation rate in bamboo shark, *Chiloscyllium punctatum* (Rosa et al. 2014) and survival in bivalve larvae (Talmage

and Gobler 2011). Combinations of reduced oxygen and pH, which are commonly observed in nearshore coastal areas in the United States (Baumann and Smith 2018), can also cause negative effects; there was no effect of low pH on growth in scallop larvae until larvae were exposed to both low pH and low oxygen and growth rates were reduced (Gobler et al. 2014) and larval silversides, *Menidia menidia*, performed aquatic surface respiration and died at higher oxygen levels during exposure to reduced oxygen and pH compared to reduced oxygen alone (Miller et al. 2016). Light is primarily examined as a stressor in photosynthetic organisms such as corals or algae (e.g., Porter et al. 1999, York et al. 2013), and most studies on heterotrophic organisms use UV light and do not examine multiple stressors (Bai et al. 2016, Gunderson et al. 2016). Only a few examples are presented here, and more in-depth reviews about multiple stressors can be found elsewhere (Pörtner 2010, Breitburg et al. 2015, Gobler and Baumann 2016, Gunderson et al. 2016).

It is important to note that thresholds for one condition, or combinations of conditions can be completely different at the various life history stages of marine organisms, which can involve very different habitats and morphology compared to adults (Byrne and Przeslawski 2013, Schiffer et al. 2014). Larvae may be more sensitive to the effects of multiple stressors, with effects carrying over from previous stages (Rosa et al. 2012, Przeslawski et al. 2015, Long et al. 2016b). Stressful oxygen conditions can be particularly challenging for developing or early life stages because they generally have higher mass-specific metabolic requirements than adults and gas exchange during development is a challenge (Somero et al. 2015). The larvae of highly visual marine organisms (arthropods, cephalopods, and fish) may be particularly at risk to low oxygen given the higher oxygen demands of complex visual structures and function (McCormick and Levin 2017). The larvae of the highly visual taxa

(arthropods, cephalopods, and fish) rely on vision for survival (Blaxter 1986, Cronin and Jinks 2001, Villaneuva and Norman 2008), and thus are excellent models for the study of low-oxygen influence on visual ecology.

For highly visual marine organisms, sufficient oxygen and light are required to maintain optimal visual function. Eyes have high oxygen metabolic demands, and this is especially true for active arthropods, cephalopods, and fish in the marine environment due to their complex eyes that are capable of sensing a variety of irradiance levels and movements (temporal resolution) (Niven and Laughlin 2008, Wong-Riley 2010, McCormick and Levin 2017). Both invertebrates and vertebrates show visual impairment in insufficient oxygen, often manifested as a decrease in the physiological response of the retina (the tissue layer containing the visual cells) to light and the ability to resolve fast motion during exposure to low oxygen (McFarland and Evans 1939, Linsenmeier et al. 1983, Fowler et al. 1993). Varying sensitivities of visual responses to low oxygen have been observed in adults of a few aquatic species, including the crucian carp, *Carassius carassius* (Johansson et al. 1997) and the squid, *Loligo pealii* (Pinto and Brown 1977). In addition, retinal responses declined by 60-100% during exposure to reduced partial pressure of oxygen (pO_2; ~3 kPa) in the larvae of the market squid, *Doryteuthis opalescens*, the two-spot octopus, *Octopus bimaculatus*, the tuna crab, *Pleuroncodes planipes*, and the graceful rock crab, *Metacarcinus gracilis* (McCormick et al. 2019). Retinal declines were most severe in larvae of *D. opalescens* and *M. gracilis*, but occurred to some extent in all species, and retinal sensitivity to oxygen occurred at all irradiances tested within each species (McCormick et al. 2019).

Oxygen thresholds for marine organisms are critical to behavior and survival (Seibel 2011), and determining the manifestation of declines in retinal physiology in visual behavior

and ecology are equally important to accurately determine how reduced oxygen will affect vision in marine organisms. Phototaxis, defined as directed movement towards or away from light (Diehn et al. 1977) is a behavior essential to many marine organisms, and light serves as the cue for the diel vertical migration in many species (Forward 1988, Cohen and Forward 2009). The effects of oxygen on phototaxis behavior has been observed in the walleye fish, *Stizostedion vitreum vitreum*, with the animal reversing its normal negative phototactic behavior and moving towards light below an oxygen threshold of 1.5 mL L^{-1} (Scherer 1971). Additionally, two species of cephalopod paralarvae showed a decrease in phototaxis behavior at a wide range of irradiances when exposed to low pO_2 (Chapter 5). The irradiance threshold for phototaxis, defined as the lowest irradiance where the paralarvae showed active phototaxis behavior, increased at lower pO_2, indicating that more light was required to elicit visual behavior under reduced oxygen (Chapter 5). Additional studies have shown the effects of oxygen on behavior in marine organisms; a decrease in feeding under low O_2 (40% air saturation) was seen in the European sea bass, *Dicentrarchus labrax* (Thetmeyer et al. 1999), which is a highly visual predator (Vázquez & Muñoz-Cueto 2014). Similarly, fathead minnows, *Pimephales promelas*, showed a reduced response to predators, *Perca flavescens*, under low oxygen (2.74 mg L^{-1} O_2) in comparison to normoxia (8.22 mg L^{-1} O_2; (Robb and Abrahams 2002). While these results were not directly attributed to a loss in visual function, a decline in visual function from low oxygen (e.g. slower temporal response or change in light sensitivity) may impact feeding success and/or predator avoidance.

Light can also be considered a stressor if animals are exposed to insufficient or overly intense irradiance, and light stress is thought to be involved with the development of visual systems (Swafford and Oakley 2019). In addition to steep gradient of oxygen with depth in

the marine environment, the total irradiance and spectral composition of light change with depth in the water column (Jerlov 1951). Marine organisms are thought to maintain depths of either a constant irradiance (isolume) (Cohen and Forward 2009), or a depth distribution within their light comfort zone, where they avoid areas of too high and too low irradiance (Dupont et al. 2009, Røstad et al. 2016, Aksnes et al. 2017). In areas with very low ambient light or at night, light pollution (e.g., from a research vessel) is sufficient to elicit an escape response down to ~100 m and change distributions in zooplankton (Ludvigsen et al. 2018). Both light and oxygen are known to limit or influence the distribution of adult marine organisms (Netburn and Koslow 2015), thus a thorough study of larval distributions in these species relative to both light intensity and oxygen is crucial to understanding vision-mediated changes in fitness in larvae.

Given the above evidence for both oxygen and light influencing the distributions of marine organisms, there is a need to identify combinations of light and oxygen in the habitat of highly visual species that determine areas where visual function is at optimal levels (in both space and time), and where vision might be inhibited. We propose that this creates a visual 'luminoxyscape' (from the Latin root for light, "lumin"), which can be defined as the levels of oxygen and irradiance which animals experience within their habitat. When oxygen and/or irradiance becomes limiting and impairs visual function, the habitat range may be reduced into the 'critical luminoxyscape'.

A challenge to determining the luminoxyscape for marine species is the lack of systems capable of measuring irradiance and oxygen simultaneously. Oceanographic data in coastal waters are often collected by either deploying sensors in Eularian mode, to measure changing conditions at one location over time, or by conducting hydrographic profiles using a

CTD rosette to conduct vertical profiles throughout the water column. Over larger spatial and temporal scales (open ocean), Lagrangian, free-drifting profiling floats (such as in the Argo network) can be deployed and transmit information via satellite. The collection of environmental data can be expanded by changing the location of the deployment or having multiple sensors deployed, and by conducting long-term monitoring cruises which sample vertical profiles in similar locations over a long time period. The California Cooperative Oceanic Fisheries Investigations (CalCOFI) is one such program that has been making sustained hydrographic and biological observations in the California Current System along the west coast of the United States for the past 70 years (McClatchie 2014). Data from these cruises are freely available on the CalCOFI website. For this long-term sampling program, the CTD rosette contains one or two oxygen sensors, and has included a PAR sensor in the CTD sampling protocol since 1993. There are very few commercial sensor packages, however, that can be deployed in the marine environment and are capable of measuring both oxygen and light in nearshore coastal areas. Some of the biogeochemical Argo floats (BGC-Argo) have recently been equipped with both oxygen sensors and sensors measuring downwelling irradiance at several wavelengths and PAR, but these are expensive and used primarily in open ocean areas (Organelli et al. 2017). In addition to the challenges of successfully capturing the physics of light in an underwater environment, light sensors are very prone to bio-fouling that would render data useless during long-term deployments. Most commercially available irradiance sensors measure photosynthetically active radiation (PAR). While this may not be as ideal as measuring irradiance at one or several specific wavelengths, a system with custom wavelengths (e.g., SATLANTIC OCR-504) is very costly, and a first step would be to create a sensor package that combines the commercially available technology to

measure PAR and oxygen simultaneously in the marine environment. This is especially important for characterizing the luminoxyscape of benthic visual species and stationary developing eggs. For example, many cephalopod species deposit or brood eggs on the seafloor, and cannot move to a more suitable area if environmental conditions become suboptimal (Robin et al. 2014).

Below, we describe the development of an instrument, the SeapHOx deLUX, capable of measuring oxygen and PAR (among other variables) on the seafloor in the nearshore marine environment. This sensor package allowed us to assess combined oxygen and irradiance regimes at a market squid (*D. opalescens*) egg bed site in La Jolla in the SCB. We develop the concept of a luminoxyscape in order to describe the combinations of light and oxygen experienced by four species of marine invertebrate larvae within the SCB, and identify the depths or times of light- and/or oxygen-limitation ('critical luminoxyscape'). Different aspects of the luminoxyscape were calculated for larvae of the market squid *D. opalescens*, the two-spot octopus *O. bimaculatus*, the tuna crab *P. planipes*, and the graceful rock crab *M. gracilis*; these represent early life stages of highly visual marine species in the SCB. The primary objectives were to characterize the changes in the luminoxyscape by 1) developing and deploying a marine sensor capable of measuring temporal changes in irradiance and oxygen at one location on the seafloor, 2) examining existing hydrographic profiles (from CalCOFI) showing spatial and temporal changes in oxygen and irradiance and 3) combining spatial and temporal changes in the luminoxyscape with previously calculated oxygen thresholds for visual function and metabolic function to determine whether there are specific depths, locations, or time periods when oxygen or light could limit vision in marine invertebrate larvae.

Methods

Given the need for continuous monitoring of oxygen and irradiance simultaneously in the marine environment to identify temporal variation over tidal, diel, and lunar cycles, a robust, deployable sensor was created to measure changes in ocean conditions for 2-3 months at a time at one depth on the seafloor (SeapHOx deLUX). Data from this instrument and data from a long-term ecological monitoring program, the California Cooperative Oceanic Fisheries Investigation (CalCOFI) were used to characterize the 'luminoxyscape' (available irradiance and oxygen) within the known habitat of marine larvae. In this way, the changes in the habitat suitable for vision were determined using a Eularian approach; the SeapHOx measured conditions at a single depth over time, and hydrographic profiles from CalCOFI conducted at various depths, locations, and time points. Oxygen and irradiance limits for visual function and metabolism determined previously (McCormick et al. 2019; Chapter 4; Chapter 5) were used to constrain suitable visual habitat for each of the marine larvae.

Temporal variation in the luminoxyscape- SeapHOx deLUX

A sensor measuring irradiance (photosynthetically active radiation; PAR) was added into an existing sensor package, the SeapHOx (Bresnahan et al. 2014). The SeapHOx consists of an oxygen optode (Aanderaa; model 3835), an ion-sensitive field effect transistor pH sensor (Honeywell Durafet III), and a MicroCAT CTD (SBE-37) measuring pressure, temperature, and conductivity (Martz et al. 2010, Bresnahan et al. 2014). The 'SeapHOx deLUX' was created by integrating an Apogee SQ-100 PAR sensor directly into the arm board of the instrument enabling simultaneous measurements and logging of irradiance,

oxygen, pH, temperature, salinity, and depth (Fig. 1A). The cosine-corrected PAR sensor measured downwelling irradiance from 410-655 nm with a sensitivity of 0.2 mV per μmol photons m^{-2} s^{-1}. The sensor was connected to the SeapHOx body through an additional cable port, and cables were joined using a custom waterproof connection. Voltage measurements (mV) were later converted to photon flux measurements (μmol photons m^{-2} s^{-1}) and an additional underwater weighting factor was added to correct for the selective attenuation of longer visible light wavelengths with depth in the ocean according to the specifications for the sensor (Apogee). Prior to deployment, the SeapHOx deLUX was tested first in a saltwater tank at Scripps Institution of Oceanography and then at 14 m depth in La Jolla, CA to ensure the PAR sensor and cable connection could work in seawater and under pressure.

The SeapHOx deLUX was deployed periodically at a recurrent market squid (*D. opalescens*) egg bed site in north La Jolla, CA (McGowan 1954) (32°51′30.13″N, 117°16′25.93″W) at 30 m depth at the edge of the La Jolla Canyon (Fig. 1B). Deployments occurred periodically between 2015 and 2018 (Table 2). The instrument was located ~0.5 m above the seafloor mounted at a 45° angle on one leg of a fiberglass tripod (sea spider; Teledyne) as has been described previously for a SeapHOx (Navarro et al. 2018). The light sensor was secured on a level stainless steel post, 30.5 cm above the top of the sea spider to prevent shading from the sensor body (Fig. 1A). To maintain a stable measurement quality, divers cleaned the PAR sensor approximately every 2 weeks during deployment, with almost no bio-fouling observed between cleanings. Data for all parameters were measured at 30-minute intervals, offering sufficient resolution to observe diel and seasonal changes in both oxygen and irradiance, but allowing for deployments of up to 2-3 months at a time. After each deployment, the sensor was returned to the laboratory to download the data, switch the

battery, and clean thoroughly prior to the next deployment. To achieve congruency for time of day analyses, times were not changed for daylight savings and the time zone was always calculated in PST.

Spatial and temporal variation in the luminoxyscape- Hydrographic data

Spatial and temporal changes in the luminoxyscape were determined using environmental data (conductivity, temperature, oxygen, irradiance, and other variables) from hydrographic profiles obtained during quarterly cruises by the California Cooperative Oceanic Fisheries Investigations (CalCOFI) program (McClatchie 2014). Vertical profile data from CTD casts were obtained from cruises between 1999 and 2017. To standardize for diurnal changes in light, the search was restricted to daytime casts (between 09:00-15:00) containing data for both oxygen concentration and PAR. All oxygen concentrations were converted to partial pressure units (pO_2) using the simultaneously measured temperature, pressure, and salinity data as a better representation of the oxygen available to organisms (Seibel 2011). Photosynthetically active radiation (PAR) values from the light sensor were used to estimate downwelling irradiance at wavelengths of ecological relevance by weighting the intensity to the spectral sensitivity of each species as in McCormick et al. (2019). Two analyses were completed with CalCOFI data. First, a spatial and temporal analysis of nearshore, southern stations from lines 93.3, 90, and 86.7, and stations along these lines within 28 km from shore (< station 30) was conducted to compare temporal data with results from the SeapHOx deLUX and examine nearshore spatial differences within 200 m depth; all stations were combined in this analysis. Second, a spatial analysis of CalCOFI data was conducted where we examined data from lines between 32.17 and 34.45 °N (lines 93.3 to 80) and stations

within 190 km from shore to determine the potential changes in the critical luminoxyscape with distance from shore.

Oxygen and irradiance limits for vision and metabolism

Oxygen and irradiance limits for vision and metabolism were determined in three different sets of experiments completed prior to this analysis. Methods and results will be briefly described here (Table 1), and the full details for the physiology, metabolism, and behavior experiments can be found in McCormick et al. (2019) (physiological limits), Chapter 4 (metabolic limits), and Chapter 5 (behavioral limits).

Physiological limits to vision. Critical oxygen limits for visual physiology in marine invertebrate larvae were calculated using electroretinogram (ERG) recordings of retinal responses during exposure to decreasing pO_2. All electrophysiology experiments were conducted in 2018, and the full results and methods are in McCormick et al. (2019). Briefly, individual larvae were tethered under a microscope in a small volume of pH-buffered and temperature-controlled seawater (recording chamber), and retinal responses to a 1-s light stimulus of constant irradiance were simultaneously measured during a decrease in pO_2 in the recording chamber. The resulting series of retinal responses from surface-ocean oxygen levels (normoxia) to ~3 kPa were used to calculate three oxygen metrics for retinal function; V_{90}, V_{50}, and V_{10} are the pO_2 values where there is 90%, 50%, and 10%, respectively, of retinal function remaining in comparison to retinal responses in normoxia (Table 1). This analysis was conducted for paralarvae of *D. opalescens*, paralarvae of *O. bimaculatus*, zoea of *P. planipes*, and megalopae of *M. gracilis* (McCormick et al. 2019).

Metabolic limits. The critical oxygen limit for metabolism (P_{crit}) was determined for paralarvae of *D. opalescens* and *O. bimaculatus* (Chapter 4). Respirometry experiments were conducted on individual larvae at a stable temperature in 2-mL closed, oxygen-tight vials where the animal was allowed to use oxygen until all was consumed. In both species, paralarvae maintained a stable oxygen consumption rate until reaching a threshold pO_2 (P_{crit}), after which the metabolic rate conformed to the decreasing pO_2. Results of all experiments were averaged to determine the routine metabolic rate and P_{crit} for each species (Table 1).

Behavioral limits. Oxygen and irradiance limits for phototaxis behavior were calculated for paralarvae of *D. opalescens* and *O. bimaculatus* (Chapter 5). Paralarvae were placed in a vertically oriented clear plexiglass chamber (20 cm L x 4 cm W x 5 cm) and exposed to 10-second light stimuli followed by a 3-minute dark period for 9 irradiance levels. The mean velocity, mean distance traveled, and location in the chamber of the paralarvae were quantified to determine differences between the light stimulus and dark period immediately after, and across irradiance stimuli. These trials were completed at four oxygen conditions per species, and the irradiance threshold for phototaxis was calculated for each oxygen condition and species (Table 1).

Data analysis for the characterization of the luminoxyscape

All data were analyzed in R Studio (Version 1.1.463; R version 3.3.3 Mavericks build). For this analysis, the previously identified oxygen thresholds for vision were used to predict retinal responses for any given pO_2 and irradiance in the environment. SeapHOx data

were analyzed from all deployments between 2015 and 2017, using only time periods where both the PAR sensor and the oxygen optode were collecting data, as some issues with one or more sensors occurred in several deployments (Table 2). Analyses were completed to determine the maximum depth where the animal could potentially experience the given threshold (V_{90}, V_{50}, V_{10}, or phototaxis) across seasons and time of day and to determine the percentage of time when the animal could experience each limitation. Sunrise and sunset times were obtained using the R package 'suncalc' (version 0.5.0) for all dates of deployment (Thieurmel and Elmarhraoui 2019).

Hydrographic data were analyzed in a similar fashion, and differences in oxygen and light conditions in relation to oxygen limits for visual function were identified as a luminoxyscape. Each cast date was converted into Julian day so results could be combined across years. Changes in the depth of the critical luminoxyscape for the southern, nearshore stations were determined across seasons. When the maximum depth of the luminoxyscape was calculated for each cast, values where the maximum depth of the luminoxyscape was the same as the maximum depth of the cast were removed (to prevent bias from shallow stations). For both SeapHOx and hydrographic data, seasons followed the CalCOFI sampling timeline and were defined as 'Winter' (December, January, February), 'Spring' (March, April, May), 'Summer' (June, July, August), and 'Fall' (September, October, November). Data did not show normal distributions, and so Kruskal-Wallis one-way analysis of variance tests (K-W) were used to determine differences in the maximum depth of each visual metric across seasons and the differences in the maximum depth of the luminoxyscape with distance from shore.

Results

Temporal variation in the luminoxyscape- SeapHOx deLUX

The SeapHOx deLUX successfully measured temporal changes in oxygen and irradiance during 11 deployments between 2015-2017 (Table 2) at 30 m water depth (Fig. 2), in addition to pH, temperature, and salinity (data not shown). Both irradiance and oxygen partial pressure (pO_2) were highest in 2015, likely due to the additive effects of the warm water anomaly in the NE Pacific and minor El Niño that occurred between 2014-2015 (Bond et al. 2015). Increased temperatures and higher oxygen is usually an indication of weakened upwelling of cold, high nutrient, and low oxygen water which would decrease the productivity at the surface and reduce the attenuation of light.

In order to visualize the distribution of different oxygen conditions with respect to the visual function that would occur, the times when pO_2 was below or between each of the visual metrics (V_{90}, V_{50}, and V_{10}) were determined for each of the four species (Fig. 3). With all results, it is important to note that these are estimates of potential exposure times within the total deployment period at 30 m depth, if the larvae were in the location of the sensor. Larvae may have considerable horizontal movement within the habitat that is not accounted for here. The species-specific trends in oxygen sensitivity are clearly observed in the data, with species more sensitive to oxygen loss for visual function, such as *D. opalescens* and *M. gracilis*, showing a greater time of exposure to potentially reduced retinal function (50-90% or 10-50% retinal function) at 30 m depth. The same analysis was completed for the oxygen limits for phototaxis in paralarvae of *D. opalescens* and *O. bimaculatus*, where *D. opalescens* shows a greater time period in oxygen conditions that could potentially inhibit phototaxis behavior (Fig. 4).

To further quantify the likelihood of retinal impairment for each species, we calculated the percent of the observation period that the pO_2 was below the levels that could have potentially reduced retinal function (V_{90}, V_{50}, or V_{10}) for all species and impaired phototaxis for paralarvae of *D. opalescens* and *O. bimaculatus*. Paralarvae of *D. opalescens* could have experienced retinal impairment from pO_2 between 22.2- 13 kPa (V_{90} -V_{50}), 12-6.9 kPa (V_{50} - V_{10}), and less than 6.9 kPa (V_{10}) for 41.9%, 52.2%, and 5.9% of the total sampling time, respectively. For *D. opalescens*, phototaxis could have been oxygen-inhibited 57.2% of the time (i.e., when pO_2 was below 12.9 kPa; Fig. 5). In *O. bimaculatus* paralarvae, retinal impairment could have occurred at pO_2 between 11.5-7.2 kPa (V_{90} -V_{50}), 7.1-5.9 kPa (V_{10} – V_{50}), and less than 5.9 kPa (V_{10}) for 33.5%, 7.1%, and 0.8% of the time, respectively. Paralarvae of *O. bimaculatus* could have had pO_2 greater than 11.5 kPa (V_{90}) for 58.5% of the total deployment, indicating the majority of the time of this deployment would have been potentially suitable for >90% visual function. Phototaxis behavior could be impaired below 7.4 kPa in *O. bimaculatus* paralarvae, which was 9.5% of the time the sensor was deployed (Fig. 5). Larvae of *M. gracilis* could have experienced 50-90% visual function (19.4-10.2 kPa; V_{50}-V_{90}) 70% of the time, and could have been exposed to 10.1-5.4 kPa (V_{50} –V_{10}) 29.1% of the time during 2015-2017. Larvae of *P. planipes* seem to be very tolerant of low oxygen, and could have experienced pO_2 greater than 5.7 kPa more than 99% of the time (Fig. 5).

Paralarvae of *D. opalescens* and *O. bimaculatus* would have never experienced pO_2 below their P_{crit} (2.47 and 0.48 kPa, respectively) during these SeapHOx deployments at 30 m depth in La Jolla, CA. Critical oxygen limits for *M. gracilis* and *P. planipes* larvae have not been measured.

To determine whether specific seasons or times of day would be more stressful for vision in each species, we calculated the proportion of time each oxygen limit for vision would potentially occur, within the percentages presented in Figure 5. There was large seasonal variation in when pO_2 would be potential stress vision (Fig. 6). For all larvae, the pO_2 conditions most likely to cause visual impairment occurred in the Spring and Summer. There was a clear trend in which the oxygen thresholds for visual function at low pO_2 in *D. opalescens* (13-6.9 kPa, V_{10}-V_{50}) and *O. bimaculatus* (7.2 kPa, V_{50}) were more common in the Spring, when the seasonal upwelling begins. Intermediate pO_2 limits for *D. opalescens* (13 kPa, V_{50}) and *O. bimaculatus* (11.5 kPa, V_{90}) were more common in the Summer, when upwelling is still present, but weakening (Fig. 6).

There was little change in the time of day when >90% and 50-90% retinal function could potentially occur in *D. opalescens, O. bimaculatus*, *M. gracilis*, and *P. planipes* (Fig. 6). A clear diel cycle was observed in the lower oxygen metrics for visual function; the percent of time when visual impairment could potentially occur for *D. opalescens* (<6.9 kPa, V_{10}), *O. bimaculatus* (<5.9 kPa, V_{10}), and *M. gracilis* (<5.4 kPa, V_{10}) was about twice as likely to occur between 00:00 and 05:00, and decreased between 07:00 and 15:00 (Fig. 6). The same trend was observed for times when *P. planipes* larvae could potentially experience <50% retinal function. This diel pattern is consistent with changes in coastal respiration, with an increase in oxygen production from photosynthesis during daylight hours and net decline in oxygen from respiration at night (Baumann and Smith 2018). Therefore, at 30 m depth, larvae have the most potential to be visually impaired during the Spring and Summer upwelling periods. Larvae are equally likely to experience moderate visual impairment (pO_2 causing 50-90% retinal function and impaired phototaxis) throughout the entire day and are more likely

to experience severe visual impairment (pO_2 causing <10% retinal function) between sunrise and sunset, which could potentially alter phototaxis behavior for vertical migration.

To determine what seasons or times of day phototaxis could potentially be impaired for paralarvae of *D. opalescens* and *O. bimaculatus*, the previously calculated irradiance and oxygen thresholds for phototactic behavior were compared with environmental data from the SeapHOx deLUX. Combinations of irradiance and oxygen that could facilitate unimpaired phototaxis primarily occurred during the day, when both irradiance and oxygen were sufficient for optimal visual behavior. The times of potentially impaired phototaxis were split into "light inhibited", where there was sufficient pO_2 but the irradiance was below the threshold for phototaxis (0.853 μmol m^{-2} s^{-1}) in both species, or "pO_2 inhibited" where pO_2 was less than 12.9 kPa in *D. opalescens* and less than 7.4 kPa in *O. bimaculatus*. Phototaxis was also light inhibited in *D. opalescens* when irradiance fell below 2.15 μmol m^{-2} s^{-1} if oxygen was less than 12.9 kPa (Chapter 5). In the environment, light and oxygen effects on phototaxis would occur together, but for the purposes of this analysis the potential limitation for each was considered separately. For both species, the potential for limited phototaxis was seasonal, and beginning ~1 hour before sunset and through the night until ~1-2 hours after sunrise (Figure 7). Due to the higher tolerance of low pO_2 in *O. bimaculatus*, phototaxis was potentially more often light inhibited (18.3%) than oxygen inhibited (4.1%) compared to phototaxis in *D. opalescens*, which was likely to be more strongly oxygen inhibited (34.0%) than light inhibited (5.8%). However, for the majority of the time the sensor was deployed, conditions would not likely inhibit phototaxis for *O. bimaculatus* paralarvae (65.3%). In *D. opalescens* paralarvae, phototaxis would not be inhibited for less than half of the time the

sensor was deployed (47.8%), indicating oxygen limits to phototaxis might occur more often with oxygen stress in this species (Figure 8).

As with the luminoxyscape for retinal function, we calculated the proportion of time within each hour of the day and within each season where potential phototaxis limitation could occur. Phototaxis was more likely to be oxygen inhibited during the spring and light inhibited in the Winter and Summer for both *D. opalescens* and *O. bimaculatus*. Light is not usually limiting during Summer months, but this could be an effect of phytoplankton blooms at the surface attenuating the downwelling irradiance. As seen in with oxygen-inhibited retinal function (Fig. 7), a clear diurnal trend is observed in the critical luminoxyscape, where phototaxis is not likely inhibited during the middle of the day when there is both sufficient irradiance and oxygen. However, phototaxis was likely to be inhibited between sunset and sunrise daily (Figs. 7,8). Usually light is considered the limiting factor for phototaxis behavior, but for *D. opalescens*, the paralarvae are oxygen-limited at times after the lines for normal phototaxis and light-inhibited phototaxis intersect, suggesting *D. opalescens* may be oxygen inhibited during sunrise and sunset when vertical migration occurs (Fig. 8).

Spatial and temporal variation in the luminoxyscape- Hydrographic data

Spatial and temporal changes in oxygen and irradiance across seasons were found in the nearshore (< 30 km from shore), southern range (32.8- 33.8 °N) of the CalCOFI hydrographic sampling data. Using the oxygen limits for visual function, we first examined potential changes in the luminoxyscape with water depth down to 200 m. Out of the four invertebrate larvae species examined, those very sensitive to low oxygen (*D. opalescens* and

M. gracilis) could show visual impairment at shallower depths than species more visually tolerant of low oxygen (*O. bimaculatus* and *P. planipes*) (Fig. 9).

The maximum depth of the critical luminoxyscape was calculated for each species and their respective visual metrics (V_{90}, V_{50}, V_{10}, and phototaxis, where available) to determine the potential changes across seasons. The maximum depth of the potential critical luminoxyscape within each oxygen metric was shallowest in the Spring (with the exception of the Winter maximum depth for V_{90} in *D. opalescens*) (Fig. 10). Differences in the maximum depth across seasons were only statistically significant in the maximum depth of V_{90} in both *D. opalescens* (K-W; p=0.0091, df= 3) and *M. gracilis* (K-W; p=0.0254, df= 3), but were not significant across seasons for any other limit or species (K-W; p>0.05, df=3). As expected, the maximum depths for each type of critical luminoxyscape (V_{90}, V_{50}, V_{10}, and phototaxis) were deeper for the lower oxygen limits.

For *D. opalescens* and *O. bimaculatus* paralarvae, the maximum depths for uninhibited phototaxis and the maximum depth of pO_2 above the P_{crit} were also calculated (Fig. 11). The maximum depths for optimal phototaxis were overall very similar to the maximum depths for V_{50} due to a similar oxygen limit (12.9 kPa and 13 kPa) and were most likely to be between 29 m depth in Spring and 41 m depth in Fall (Fig. 11). Paralarvae of *O. bimaculatus* could have experienced smaller variability in the maximum depths, between 38 m depth in Winter and 43.5 m depth in Summer. Paralarvae of *O. bimaculatus* would not have experienced pO_2 below their P_{crit} during any time or at any depth within the spatial and temporal constraints of this analysis (< 500 m depth). Paralarvae of *D. opalescens* would potentially experience pO_2 less than their P_{crit} below ~240 m depth in the Spring and Summer, and 291 m depth in the Winter and Fall (Fig. 11). Differences between the maximum depth of

the critical luminoxyscape across season were not significant (K-W, $p>0.05$, df=3) for phototaxis or the maximum depth of pO_2 greater than the P_{crit} for either species.

In order to determine the potential changes in the luminoxyscape between nearshore and offshore habitats in the SCB, data from additional CalCOFI stations were used; lines between 32.17 and 34.45 °N and stations within 190 km from shore were analyzed to determine changes in the critical luminoxyscape with distance from shore. For the two species where oxygen and irradiance limits for phototaxis have been determined (*D. opalescens* and *O. bimaculatus*), the pO_2 at which phototaxis behavior changes is very similar to the pO_2 at which there was 50% retinal function (V_{50}). As a result, the pO_2 for V_{50} in each species was used to determine how the maximum depth of the critical luminoxyscape could potentially change with the distance to shore (Fig. 12). The maximum depth of the critical luminoxyscape was significantly different with distance from shore in all 4 species (K-W; $p <0.0001$; df= 30). The maximum depth of light limitation for all species was also significantly different with distance from shore (K-W; $p<0.0001$; df= 30). The shallowest lower limit of the critical luminoxyscape was at 18m within 2 km, and this value decreased to 65 m, 142 m, 92 m, and 148 m depth by 12 km from shore for larvae of *D. opalescens*, *O. bimaculatus*, *M. gracilis*, and *P. planipes*, respectively (Fig. 12). Farther offshore, the maximum lower limits of the luminoxyscape determined in this analysis were 94.5 m, 191.4 m, 129 m, and 198.6 m depth for larvae of *D. opalescens, O. bimaculatus*, *M. gracilis*, and *P. planipes*, respectively (Fig. 12). Larvae of species more sensitive to low oxygen (*D. opalescens* and *M. gracilis*) would potentially experience oxygen limitation for retinal function with increasing distance from shore, while more tolerant species (*O. bimaculatus* and *P. planipes*) could become light limited before vision would be impaired by oxygen (Fig. 12).

Discussion

There was variability in the potential critical luminoxyscapes measured over time and space for larvae of *D. opalescens*, *O. bimaculatus*, *M. gracilis*, and *P. planipes* using data from both a stationary, deployed sensor at 30 m depth, and hydrographic data over a broad spatial range. Overall, we calculated the critical luminoxyscapes for retinal function (all species) and for phototaxis behavior (*D. opalescens* and *O. bimaculatus*), with retinal impairment and phototaxis impairment potentially occurring up to 50-75% of the entire deployment period for highly sensitive species (Fig. 5).

In the nearshore area, at 30-m depth, there was a seasonal trend of when visual impairment would occur, with the majority of the potential for visual impairment (at any level) occurring during the Spring season (Figs. 6, 9). Reduced oxygen in Spring may have strong consequences for stationary organisms that are unable to swim or move to areas with higher oxygen, such as non-migratory benthic species, or developing embryos. Adult *D. opalescens* spawn in shallow, nearshore habitats and deposit egg capsules on the seafloor, where they develop and then hatch ~3-4 weeks later (Fields 1965, Zeidberg et al. 2011). During development, cephalopod eggs are often severely gas limited at the end of their development; oxygen and pH both decline as the larvae approach hatching (Gutowska and Melzner 2009, Long et al. 2016a). Squid have been shown to lay egg capsules selectively where and when oxygen conditions are above 160 μmol O_2 kg^{-1} (13.52 kPa at 15 °C) in La Jolla (Navarro et al. 2018) and above 4 mL O_2 L^{-2} (13.94 kPa at 15 °C) near the Channel Islands farther offshore (Zeidberg et al. 2012). These oxygen limits for spawning are very similar to the pO_2 at which paralarvae would experience 50% retinal function (13 kPa;

McCormick et al. 2019) and below which phototaxis behavior would be impaired (< 12.9 kPa; Chapter 5) determined here. We found that the maximum depth of 50% retinal function shoaled to up to 18 m depth within 2 km to the coast. The Channel Islands are ~100 km from the coast of California (within the location of this analysis), and these islands are key spawning grounds for the southern California population of *D. opalescens*, with high numbers of paralarvae found near the islands (Zeidberg and Hamner 2002, Zeidberg et al. 2012). This indicates that paralarvae of *D. opalescens* may potentially experience oxygen- and light-impaired vision after hatching, which may decrease their chances of survival to first feeding (Robin et al. 2014).

Larvae (megalopae) of *M. gracilis* are thought to reside between 30-60-m depth during the day, and 0-30-m depth at night near Point Reyes, CA (Wing et al. 1998). If their depth range is similar in southern California, larvae would be have the potential to experience moderately impaired retinal function (50-90%) 70% of the time at 30 m depth, and < 50% retinal function 29.1% of the time (Fig. 5). If larvae moved or were transported farther offshore, the maximum depth of their luminoxyscape would only drop below 60 m at 12 km from the shore (Fig. 12). Paralarvae of *O. bimaculatus* are likely at risk as well, despite their greater tolerance for low oxygen compared to *D. opalescens* and *M. gracilis* (McCormick et al. 2019; Chapter 4; Chapter 5). Very little is known about the extent of vertical migration in cephalopod paralarvae, but Zeidburg and Hamner (2002) found that *D. opalescens* paralarvae vertically migrate between 30 m during the day and 15 m at night. In all previous sampling, *O. bimaculatus* paralarvae have been found in the same depth range as *D. opalescens*, and eggs have been collected on sensors deployed between 10-30 m depth in the SCB (Zerofski, pers. comm.). Adults are known to prefer coastal areas with enough complexity to hide, and

are often captured as shallow as 4-10 m depth off La Jolla (Ambrose 1988). Phototaxis for paralarvae of both species was potentially inhibited at 30 m depth both seasonally and over a diel cycle (Figs. 7,8). Importantly, oxygen (*D. opalescens*) and light (*O. bimaculatus*) could potentially limit normal phototaxis up to two hours before sunset or after sunrise, which is when animals might be relying on a light cue for either the ascent to the surface (sunset) or sinking to deeper water (sunrise). Retinal function could also have been impaired at 30 m depth (Fig. 5), and paralarvae might have a higher risk for predation or starvation if retinal impairment inhibits their ability to detect predators or find and catch prey. Larvae of *P. planipes* may be the only study species that would not regularly be visually inhibited by low oxygen very often; the larvae could have potentially experienced >90% retinal function for greater than 99% of the total SeapHOx deLUX deployment at 30 m depth (Figs. 3, 5), and the maximum depth of the critical luminoxyscape was much deeper than in other species; larvae of *P. planipes* are regularly found offshore (McClatchie et al. 2016). While the vertical distributions of larvae have not been described in detail off the coast of California, early stage larvae of a similar species, *Pleuroncodes monodon*, are found within the top 40 m of the water column off south-central Chile (Yannicelli et al. 2012); larvae of this species are also very tolerant of low oxygen (Yannicelli et al. 2013).

The timing of exposure to oxygen conditions that could potentially impair vision is important to consider relative to the breeding periods for each species. Gravid females of *P. planipes* are usually found between December and March, with the greatest abundance of larvae in February or March (Longhurst 1968), coinciding with the greatest potential for oxygen-impaired vision in the spring. Spawning for *D. opalescens* occurs at the same time of year, with paralarvae found primarily between January and April. In contrast, paralarvae of *O.*

bimaculatus usually hatch between June and September (Ambrose 1981) and the larval stage of *M. gracilis* occurs in the late Summer and Fall (Ally 1975, Wing et al. 1998), and so the early life stages of these species might miss the time periods with the greatest likelihood for oxygen-impaired vision.

If the oxygen thresholds for vision determined in the laboratory are similar to what is expressed in the environment for these species, visual impairment from low oxygen is potentially already occurring within the natural habitat of the four study species. For the two species the P_{crit} was determined for (*D. opalescens* and *O. bimaculatus*), paralarvae were not likely to be exposed to pO_2 below their P_{crit} at any time during the 30 m deployments in La Jolla, CA used for this analysis. This was also reflected in the spatial analysis of the CalCOFI hydrographic data, where *O. bimaculatus* were never exposed to pO_2 less than their P_{crit} above 1,000-m depth, and *D. opalescens* would have only experienced pO_2 at their P_{crit} at ~290 m depth (Fig. 11), which is well below the maximum depths of the visual critical luminoxyscapes determined here (Fig. 10).

Exposure to stressors as a result of environmental changes has the potential to alter both the vertical (depth) habitat and spatial range of species in the marine environment. There was a clear shoaling of the oxycline closer to the shore in the SCB (Fig. 12) and seasonal differences in the maximum depth of the critical luminoxyscape (Fig. 11). Mobile pelagic organisms that have larger horizontal and depth ranges will likely be affected more by spatial changes to their luminoxyscape, where visual limits may constrain the depth of vertical migration. Spatial ranges of mobile, pelagic organisms are likely already "structured" from environmental constraints, and it is important to determine whether a changing luminoxyscape may provide additional habitat compression. Over the last 50 years, the ocean

oxygen content has been declining as a result of global deoxygenation, coastal hypoxia, and the expansion of oxygen minimum zones (Stramma et al. 2010, Schmidtko et al. 2017, Breitburg et al. 2018). Oxygen loss has been especially intense off California (Bograd et al. 2015, Ren et al. 2018), where the study species occur. Changes in the distribution of marine organisms (e.g. habitat compression) in response to reduced oxygen have largely been attributed to physiological constraints imposed by metabolic oxygen tolerances (Stramma et al. 2012, Netburn and Koslow 2015), as well as increased vulnerability to predators in better-lighted waters (Koslow et al. 2011). Oxygen-limited light requirements present an additional, "visual" hypothesis for the shoaling of pelagic species reported as the SCB experiences expanding deoxygenation, especially for highly visual marine organisms with "fast" vision (Koslow et al. 2011, Netburn and Koslow 2015, McCormick and Levin 2017). Avoidance of low oxygen areas and physiological adaptations to low oxygen in adult decapod crustaceans (Seibel et al. 2016), cephalopods (Alegre et al. 2014, Seibel et al. 2014), and fish (Stramma et al. 2012, Netburn and Koslow 2015), have been observed, and it is crucial to predict whether changes in the luminoxyscape of marine larvae have the potential to also constrain their suitable habitat and survival.

Conclusions

The concept of a luminoxyscape can be used to determine the range of oxygen and irradiance conditions marine organisms are exposed to in their habitat. When combined with oxygen limits for retinal function and phototaxis, the oxygen- and light- inhibited area can be characterized as a critical luminoxyscape where visual function would be potentially be reduced. Using data from a custom sensor package, the SeapHOx deLUX, changes in oxygen

and irradiance were determined over various temporal scales. Larvae of several marine species could potentially experience retinal impairment (*D. opalescens*, *O. bimaculatus*, *M. gracilis*, and *P. planipes*) and changes to phototaxis behavior (*D. opalescens*, *O. bimaculatus*) at 30 m depth in La Jolla. The potential for visual impairment primarily occurred during the Spring upwelling season, and oxygen could limit visual function from sunset to sunrise, presumably as a result of diel respiration and no counterbalancing oxygen production in the nearshore environment during those hours. This is especially a concern when oxygen limitation occurs around sunset and sunrise, as it may impair the ability of larvae to vertically migrate if the light cue is not detected.

Analysis of hydrographic data from a long-term monitoring program, CalCOFI, showed the seasons and spatial scales over which visual impairment could occur. While the maximum depth of the critical luminoxyscape was not significantly different across seasons for all visual metrics, the maximum depth of the critical luminoxyscape where retinal function and phototaxis could potentially be inhibited shoaled during the Spring, consistent with results from the SeapHOx deLUX at 30 m depth. The depth of the critical luminoxyscape was shallower immediately near the coast, indicating that upwelling, or a greater oxygen demand inshore, is driving any visual impairment that may occur. The critical luminoxyscape of oxygen-sensitive species (*D. opalescens* and *M. gracilis*) was more likely to be limited by oxygen, whereas the maximum depth of the critical luminoxyscape was potentially light limited in larvae of *O. bimaculatus* and *P. planipes*. Therefore, larvae may be able to move offshore for a greater depth range where vision may not be oxygen-inhibited.

Predicting the critical luminoxyscape by comparing oxygen limits for vision determined in the laboratory and comparing environmental data over various spatial and

temporal scales is a first step in understanding how vision, light, and oxygen may determine distributions and survival for marine organisms. These results show periods of potential oxygen vulnerability for vision in marine invertebrate larvae that will set the scene for future field studies determining the actual distributions of larvae in response to sub-optimal conditions. Determining the temperature effects on visual physiology and behavior should allow for a more accurate prediction of luminoxyscapes, as the critical thresholds for retinal physiology, metabolism, and phototaxis could change with temperature. These results suggest that oxygen-mediated visual impairment offers an additional explanation for vertical habitat compression from reduced oxygen, and show that vision may be an important driver for the distribution and survival of marine organisms, given the declines in oxygen observed in the SCB.

Acknowledgements

We thank the California Cooperative Fisheries Investigations for collecting all CTD hydrographic data that was used in this analysis. We thank E. Briggs for rewriting the arm-board coding for the SeapHOx deLUX. Extreme gratitude is extended to R. Walsh for assisting with the deployment logistics, setup, and diving of the SeapHOx deLUX, and I. Arzeno for being the best dive buddy. Additional divers: I. Arzeno, R. Walsh, T. Pierce, A. Canon, M.T. Costa, M. Harvey, M. Sedarat, B. French. Additional thanks to M.T. Costa for helping come up with a 'punny' name for the instrument. We thank D. Deheyn, N. Oesch, F. Powell, and M. Tresguerres for comments and discussion on this research. The SURF REU program provided support for one excellent summer student.

Chapter 6, in part, is in preparation for submission for publication. The dissertation author was the primary investigator and author of this material. **McCormick, L. R.**, Gangrade, S., Garwood, J. C., Wirth, T., Martz, T. R. and L. A. Levin. Defining a suitable "luminoxyscape" to evaluate changing light requirements under oxygen-limitation in visual marine organisms.

Literature Cited

Aksnes, D. L., A. Røstad, S. Kaartvedt, U. Martinez, C. M. Duarte, and X. Irigoien. 2017. Light penetration structures the deep acoustic scattering layers in the global ocean. Science Advances 3:1–6.

Alegre, A., F. Ménard, R. Tafur, P. Espinoza, J. Argüelles, V. Maehara, O. Flores, M. Simier, and A. Bertrand. 2014. Comprehensive model of jumbo squid *Dosidicus gigas* trophic ecology in the northern humboldt current system. PLoS ONE 9:e85919.

Ally, J. R. R. 1975. A description of the laboratory-reared larvae of *Cancer gracilis* Dana, 1852 (Decapoda, Brachyura). Crustaceana 28:231–246.

Ambrose, R. F. 1981. Observations on the embryonic development and early post-embryonic behavior of *Octopus bimaculatus* (Mollusca: Cephalopoda). The Veliger 24:139–146.

Ambrose, R. F. 1988. Population dynamics of *Octopus bimaculatus*: influence of life history patterns, synchroneous reproduction and recruitment. Malacologia 29:23–39.

Bai, Y., H. Liu, B. Huang, M. Wagle, and S. Guo. 2016. Identification of environmental stressors and validation of light preference as a measure of anxiety in larval zebrafish. BMC Neuroscience 17:1–12.

Baumann, H. 2016. Combined effects of ocean acidification, warming, and hypoxia on marine organisms. Limnology and Oceanography e-Lectures 6.

Baumann, H., and E. M. Smith. 2018. Quantifying metabolically driven pH and oxygen fluctuations in US nearshore habitats at diel to interannual time scales. Estuaries and Coasts 41:1102–1117.

Bertrand, A., A. Chaigneau, S. Peraltilla, J. Ledesma, M. Graco, F. Monetti, and F. P. Chavez. 2011. Oxygen: A fundamental property regulating pelagic ecosystem structure in the coastal southeastern tropical pacific. PLoS ONE 6:2–9.

Bianchi, D., E. D. Galbraith, D. A. Carozza, K. A. S. Mislan, and C. A. Stock. 2013. Intensification of open-ocean oxygen depletion by vertically migrating animals. Nature Geoscience 6:545–548.

Bianchi, D., and K. A. S. Mislan. 2016. Global patterns of diel vertical migration times and velocities from acoustic data. Limnology and Oceanography 61:353–364.

Blaxter, J. H. S. 1986. Development of sense organs and behavior of teleost larvae with special reference to feeding and predator avoidance. Pages 98–114 *in* C. Hubbs, editor. Ninth Larval Fish Conference, Transactions of the American Fisheries Society.

Bograd, S. J., M. P. Buil, E. Di Lorenzo, C. G. Castro, I. D. Schroeder, R. Goericke, C. R. Anderson, C. Benitez-Nelson, and F. A. Whitney. 2015. Changes in source waters to the Southern California Bight. Deep Sea Research Part II: Topical Studies in Oceanography 112:42–52.

Bograd, S. J., C. G. Castro, E. Di Lorenzo, D. M. Palacios, H. Bailey, W. Gilly, and F. P. Chavez. 2008. Oxygen declines and the shoaling of the hypoxic boundary in the California Current. Geophysical Research Letters 35:L12607.

Bond, N. A., M. F. Cronin, H. Freeland, and N. Mantua. 2015. Causes and impacts of the 2014 warm anomaly in the NE Pacific. Geophysical Research Letters 42:1–7.

Booth, J. A. T., E. E. McPhee-Shaw, P. Chua, E. Kingsley, M. Denny, R. Phillips, S. J. Bograd, L. D. Zeidberg, and W. F. Gilly. 2012. Natural intrusions of hypoxic, low pH water into nearshore marine environments on the California coast. Continental Shelf Research 45:108–115.

Breitburg, D. L., J. Salisbury, J. M. Bernhard, W.-J. Cai, S. Dupont, S. Doney, K. J. Kroeker, L. A. Levin, W. C. Long, L. M. Milke, S. Miller, B. Phelan, U. Passow, B. A. Seibel, A. E. Todgham, and A. M. Tarrant. 2015. And on top of all that... Coping with ocean acidification in the midst of many stressors. Oceanography 28:48–61.

Breitburg, D., L. A. Levin, A. Oschlies, M. Grégoire, F. P. Chavez, D. J. Conley, V. Garçon, D. Gilbert, D. Gutiérrez, K. Isensee, G. S. Jacinto, K. E. Limburg, I. Montes, S. W. A. Naqvi, G. C. Pitcher, N. N. Rabalais, M. R. Roman, K. A. Rose, B. A. Seibel, M. Telszewski, M. Yasuhara, and J. Zhang. 2018. Declining oxygen in the global ocean and coastal waters. Science 7240.

Bresnahan, P. J., T. R. Martz, Y. Takeshita, K. S. Johnson, and M. Lashomb. 2014. Best practices for autonomous measurement of seawater pH with the Honeywell Durafet. Methods in Oceanography 9:44–60.

Burnett, L. E., and W. B. Stickle. 2001. Physiological responses to hypoxia. Coastal hypoxia: consequences for living resources and ecosystems:101–114.

Byrne, M., and R. Przeslawski. 2013. Multistressor impacts of warming and acidification of the ocean on marine invertebrates' life histories. Integrative and Comparative Biology 53:582–596.

Cade, D. E., and K. J. Benoit-bird. 2015. Depths, migration rates and environmental associations of acoustic scattering layers in the Gulf of California. Deep-Sea Research Part I 102:78–89.

Cohen, J. H., and R. B. J. Forward. 2009. Zooplankton diel vertical migration — A review of proximate control. Oceanography and Marine Biology: an Annual Review 47:77–110.

Cronin, T. W., and R. N. Jinks. 2001. Ontogeny of vision in marine crustaceans. American Zoology 41:1098–1107.

Diehn, B., M. Feinleib, W. Haupt, E. Hildebrand, F. Lenci, and W. Nultsch. 1977. Terminology of behavioral responses of motile microorganisms. Photochemistry and Photobiology 26:559–560.

Dupont, N., T. A. Klevjer, S. Kaartvedt, and D. L. Aksnes. 2009. Diel vertical migration of the deep-water jellyfish *Periphylla periphylla* simulated as individual responses to absolute light intensity. Limnology and Oceanography 54:1765–1775.

Fields, W. G. 1965. The structure, development, food relations, reproduction, and life history of the squid *Loligo opalescens* Berry. State of California, Department of Fish and Game Fish Bulletin 131.

Forward, R. B. 1988. Diel vertical migration- Zooplankton photobiology and behavior. Oceanography and Marine Biology 26:361–393.

Fowler, B., J. Banner, and J. Pogue. 1993. The slowing of visual processing by hypoxia. Ergonomics 36:727–735.

Frieder, C. A., S. Nam, T. R. Martz, and L. A. Levin. 2012. High temporal and spatial variability of dissolved oxygen and pH in a nearshore California kelp forest. Biogeosciences 9:1–14.

Gobler, C. J., and H. Baumann. 2016. Hypoxia and acidification in ocean ecosystems: coupled dynamics and effects on marine life. Biology letters 12:199–229.

Gobler, C. J., E. L. Depasquale, A. W. Griffith, and H. Baumann. 2014. Hypoxia and acidification have additive and synergistic negative effects on the growth, survival, and metamorphosis of early life stage bivalves. PLoS ONE 9.

Gunderson, A. R., E. J. Armstrong, and J. H. Stillman. 2016. Multiple stressors in a changing world: The need for an improved perspective on physiological responses to the dynamic marine environment. Annual Review of Marine Science 8:357–378.

Gutowska, M. A., and F. Melzner. 2009. Abiotic conditions in cephalopod (*Sepia officinalis)* eggs: Embryonic development at low pH and high pCO_2. Marine Biology 156:515–519.

Hochachka, P. W., and G. N. Somero. 2002. Biochemical adaptation: Mechanism and process in physiological evolution. Oxford University Press, Inc., New York.

Jerlov, N. G. 1951. Optical studies of ocean water. Reports of the Deep-Sea Swedish Expedition 3:1–59.

Johansson, D., G. E. Nilsson, and K. B. Døving. 1997. Anoxic depression of light-evoked potentials in retina and optic tectum of crucian carp. Neuroscience letters 237:73–6.

Koslow, J. A., R. Goericke, A. Lara-Lopez, and W. Watson. 2011. Impact of declining intermediate-water oxygen on deepwater fishes in the California Current. Marine Ecology Progress Series 436:207–218.

Levin, L. A., K. K. Liu, K. C. Emeis, D. L. Breitburg, J. Cloern, C. Deutsch, M. Giani, A. Goffart, E. E. Hofmann, Z. Lachkar, K. Limburg, S. M. Liu, E. Montes, W. Naqvi, O. Ragueneau, C. Rabouille, S. K. Sarkar, D. P. Swaney, P. Wassman, and K. F. Wishner. 2015. Comparative biogeochemistry-ecosystem-human interactions on dynamic continental margins. Journal of Marine Systems 141:3–17.

Linsenmeier, R. A., A. H. Mines, and R. H. Steinberg. 1983. Effects of hypoxia and hypercapnia on the light peak and electroretinogram of the cat. Investigative ophthalmology & visual science 24:37–46.

Long, M. H., T. A. Mooney, and C. Zakroff. 2016a. Extreme low oxygen and decreased pH conditions naturally occur within developing squid egg capsules. Marine Ecology Progress Series 550:111–119.

Long, W. C., K. M. Swiney, and R. J. Foy. 2016b. Effects of high pCO_2 on Tanner crab reproduction and early life history, Part II: Carryover effects on larvae from oogenesis and embryogenesis are stronger than direct effects. ICES Journal of Marine Science 73:836–848.

Longhurst, A. R. 1968. Distribution of the larvae of *Pleuroncodes planipes* in the California Current. Limnology and Oceanography 13:143–155.

Ludvigsen, M., J. Berge, M. Geoffroy, J. H. Cohen, P. R. D. La Torre, S. M. Nornes, H. Singh, and A. J. Sørensen. 2018. Use of an Autonomous Surface Vehicle reveals small-scale diel vertical migrations of zooplankton and susceptibility to light pollution under low solar irradiance. Science Advances 4.

Martz, T. R., J. G. Connery, K. S. Johnson, E. W. Road, and M. Glen. 2010. Testing the Honeywell Durafet ® for seawater pH applications. Limnology and Oceanography: Methods 8:172–184.

McClatchie, S. 2014. Oceanography of the Southern California Current system relevant to fisheries. Page Regional Fisheries Oceanography of the California Current System. Springer, Dordrecht.

McClatchie, S., R. Goericke, A. Leising, T. D. Auth, E. Bjorkstedt, R. R. Robertson, R. D. Brodeur, X. Du, C. A. Morgan, F. P. Chavez, A. J. Debich, J. Hildebrand, J. Field, K. Sakuma, M. G. Jacox, M. Kahru, R. Kudela, C. Anderson, B. E. Lavaniegos, J. Gomez-Valdes, S. P. A. Jimenez-Rosenburg, R. Mccabe, S. R. Melin, L. M. Sala, M. D. Ohman, B. Peterson, J. Fisher, I. D. Schroeder, S. J. Bograd, E. L. Hazen, S. R. Schneider, R. T. Golightly, R. M. Suryan, A. J. Gladics, S. Loredo, J. M. Porquez, A. R. Thompson, E. D. Weber, W. Watson, V. Trainer, P. Warzybok, R. Bradley, and J. Jahncke. 2016. State of the California Current 2015-2016: Comparisons with the 1997-98 El Nino. California Cooperative Oceanic Fisheries Investigations Reports 57:1–57.

McCormick, L. R., and L. A. Levin. 2017. Physiological and ecological implications of ocean deoxygenation for vision in marine organisms. Philosophical Transactions of the Royal Society A 375.

McCormick, L. R., L. A. Levin, and N. W. Oesch. 2019. Vision is highly sensitive to oxygen availability in marine invertebrate larvae. Journal of Experimental Biology 222:1–11.

McFarland, R. A., and J. N. Evans. 1939. Alterations in dark adaptation under reduced oxygen tensions. American Journal of Physiology- Legacy Content 127:37–50.

McGowan, J. 1954. Observations on the sexual behavior and spawning of the squid, *Loligo opalescens*, at La Jolla, California. California Department of Fish and Game, Fishery Bulletin 40:47–54.

Miller, S., D. Breitburg, R. Burrell, and A. Keppel. 2016. Acidification increases sensitivity to hypoxia in important forage fishes. Marine Ecology Progress Series 549:1–8.

Navarro, A. M. O., P. E. Parnell, and L. A. Levin. 2018. Essential market squid (*Doryteuthis opalescens*) embryo habitat : A baseline for anticipated ocean climate change. Journal of Shellfish Research 37:601–614.

Netburn, A. N., and J. A. Koslow. 2015. Dissolved oxygen as a constraint on daytime deep scattering layer depth in the southern California current ecosystem. Deep Sea Research Part I: Oceanographic Research Papers 104:149–158.

Niven, J. E., and S. B. Laughlin. 2008. Energy limitation as a selective pressure on the evolution of sensory systems. The Journal of experimental biology 211:1792–804.

Ohman, M. D. 1990. The demographic benefits of diel vertical migration by zooplankton. Ecological Monographs 60:257–281.

Organelli, E., H. Claustre, A. Bricaud, M. Barbiuex, J. Uitz, F. D'Ortenzio, and G. Dall'Olmo. 2017. Bio-optical anomalies in the world's oceans: An investigation on the diffuse attenuate coefficients for downward irradiance derived from Biogeochemical Argo float measurements. Journal of Geophysical Research: Oceans 122:3543–3564.

Pinto, L. H., and J. E. Brown. 1977. Intracellular recordings from photoreceptors of the squid (*Loligo pealii*). Journal of Comparative Physiology A 122:241–250.

Porter, J. W., S. K. Lewis, and K. G. Porter. 1999. The effect of multiple stressors on the Florida Keys coral reef ecosystem: A landscape hypothesis and a physiological test. Limnology and Oceanography 44:941–949.

Pörtner, H. 2010. Oxygen- and capacity-limitation of thermal tolerance: a matrix for integrating climate-related stressor effects in marine ecosystems. Journal of Experimental Biology 213:881–893.

Przeslawski, R., M. Byrne, and C. Mellin. 2015. A review and meta-analysis of the effects of multiple abiotic stressors on marine embryos and larvae. Global Change Biology 21:2122–2140.

Ren, A. S., F. Chai, H. Xue, D. M. Anderson, and F. P. Chavez. 2018. A sixteen-year decline in dissolved oxygen in the Central California Current. Scientific Reports 8:1–9.

Robb, T., and M. V Abrahams. 2002. The influence of hypoxia on risk of predation and habitat choice by the fathead minnow, *Pimephales promelas*. Behavioral Ecology and Sociobiology 52:25–30.

Robin, J., M. Roberts, L. Zeidberg, I. Bloor, A. Rodriguez, F. Briceño, N. Downey, M. Mascaró, M. Navarro, A. Guerra, J. Hofmeister, D. D. Barcellos, S. A. P. Lourenço, C. F. E. Roper, N. A. Moltschaniwskyj, C. P. Green, and J. Mather. 2014. Transitions during cephalopod life history: The role of habitat, environment, functional morphology, and behaviour. Advances in Marine Biology 67:361–437.

Rosa, R., M. Baptista, V. M. Lopes, M. R. Pegado, R. Paula, K. Tru, M. C. Leal, R. Calado, T. Repolho, R. P. J, and R. Rosa. 2014. Early-life exposure to climate change impairs tropical shark survival. Proceedings of the Royal Society B 281:0–6.

Rosa, R., M. S. Pimentel, J. Boavida-Portugal, T. Teixeira, K. Trübenbach, and M. Diniz. 2012. Ocean warming enhances malformations, premature hatching, metabolic suppression and oxidative stress in the early life stages of a keystone squid. PLoS ONE 7:e38282.

Røstad, A., S. Kaartvedt, and D. L. Aksnes. 2016. Light comfort zones of mesopelagic acoustic scattering layers in two contrasting optical environments. Deep-Sea Research Part I 113:1–6.

Scherer, E. 1971. Effects of oxygen depletion and of carbon dioxide buildup on the photic behavior of the walleye (*Stizostedion vitreum vitreum*). Journal of the Fisheries Research Board of Canada 28:1303–1307.

Schiffer, M., L. Harms, M. Lucassen, F. C. Mark, H. Pörtner, and D. Storch. 2014. Temperature tolerance of different larval stages of the spider crab *Hyas araneus* exposed to elevated seawater pCO2. Frontiers in Zoology 11:1–22.

Schmidtko, S., L. Stramma, and M. Visbeck. 2017. Decline in global oceanic oxygen content during the past five decades. Nature 542:335–339.

Seibel, B. A. 2011. Critical oxygen levels and metabolic suppression in oceanic oxygen minimum zones. The Journal of experimental biology 214:326–336.

Seibel, B. A., N. S. Hafker, K. Trubenbach, J. Zhang, S. N. Tessier, H.-O. Pörtner, R. Rosa, and K. B. Storey. 2014. Metabolic suppression during protracted exposure to hypoxia in the jumbo squid, *Dosidicus gigas*, living in an oxygen minimum zone. Journal of Experimental Biology 217:2555–2568.

Seibel, B. A., J. L. Schneider, S. Kaartvedt, K. F. Wishner, and K. L. Daly. 2016. Hypoxia tolerance and metabolic suppression in oxygen minimum zone Euphausiids: Implications for ocean deoxygenation and biogeochemical cycles. Integrative and Comparative Biology:1–14.

Somero, G. N., J. M. Beers, F. Chan, T. M. Hill, T. Klinger, and S. Y. Litvin. 2015. What changes in the carbonate system, oxygen, and temperature portend for the Northeastern Pacific Ocean: A physiological perspective. BioScience 66:14–26.

Stramma, L., E. D. Prince, S. Schmidtko, J. Luo, J. P. Hoolihan, M. Visbeck, D. W. R. Wallace, P. Brandt, and A. Körtzinger. 2012. Expansion of oxygen minimum zones may reduce available habitat for tropical pelagic fishes. Nature Climate Change 2:33–37.

Stramma, L., S. Schmidtko, L. A. Levin, and G. C. Johnson. 2010. Ocean oxygen minima expansions and their biological impacts. Deep Sea Research Part I: Oceanographic Research Papers 57:587–595.

Swafford, A. J. ., and T. H. Oakley. 2019. Light-induced stress as a primary evolutionary driver of eye origins. Page 22 International Conference on Invertebrate Vision.

Talmage, S. C., and C. J. Gobler. 2011. Effects of elevated temperature and carbon dioxide on the growth and survival of larvae and juveniles of three species of Northwest Atlantic bivalves. PLoS ONE 6.

Thetmeyer, H., U. Waller, K. D. Black, S. Inselmann, and H. Rosenthal. 1999. Growth of European sea bass (*Dicentrarchus labrax* L.) under hypoxic and oscillating oxygen conditions. Aquaculture 174:355–367.

Thieurmel, B., and A. Elmarhraoui. 2019. Package "suncalc." R Package Version 0.5.0.

Vazquez, F. J. S., and J. A. Munoz-Cueto, editors. 2014. Biology of the European sea bass. CRC Press.

Villaneuva, R., and M. D. Norman. 2008. Biology of the planktonic stages of benthic octopuses. Oceanography and Marine Biology: an Annual Review 46:105–202.

Wing, S. R., L. W. Botsford, S. V Ralston, and J. L. Largier. 1998. Meroplanktonic distribution and circulation in a coastal retention zone of the northern California upwelling system. Limnology and Oceanography 43:1710–1721.

Wong-Riley, M. 2010. Energy metabolism of the visual system. Eye and Brain 2:99–116.

Yannicelli, B., L. Castro, C. Parada, W. Schneider, F. Colas, and D. Donoso. 2012. Distribution of *Pleuroncodes monodon* larvae over the continental shelf of south-central Chile: Field and modeling evidence for partial local retention and transport. Progress in Oceanography 92–95:206–227.

Yannicelli, B., K. Paschke, R. R. González, and L. R. Castro. 2013. Metabolic responses of the squat lobster (*Pleuroncodes monodon*) larvae to low oxygen concentration. Marine Biology 160:961–976.

York, P. H., R. K. Gruber, R. Hill, P. J. Ralph, D. J. Booth, and P. I. Macreadie. 2013. Physiological and morphological responses of the temperate seagrass *Zostera muelleri* to multiple stressors: Investigating the interactive effects of light and temperature. PLoS ONE 8:1–12.

Zeidberg, L. D., J. L. Butler, D. Ramon, A. Cossio, K. L. Stierhoff, and A. Henry. 2012. Estimation of spawning habitats of market squid (*Doryteuthis opalescens*) from field surveys of eggs off Central and Southern California. Marine Ecology 33:326–336.

Zeidberg, L. D., and W. M. Hamner. 2002. Distribution of squid paralarvae, *Loligo opalescens* (Cephalopoda: Myopsida), in the Southern California Bight in the three years following the 1997-1998 El Niño. Marine Biology 141:111–122.

Zeidberg, L. D., G. Isaac, C. L. Widmer, H. Neumeister, and W. F. Gilly. 2011. Egg capsule hatch rate and incubation duration of the California market squid, *Doryteuthis* (=*Loligo*) *opalescens*: Insights from laboratory manipulations. Marine Ecology 32:468–479.

Tables

Table 6.1. Oxygen metrics for vision in marine invertebrate larvae. Physiological oxygen metrics for retinal function are the partial pressure of oxygen (pO_2) where there was 90%, 50%, and 10% retinal function remaining during a decline in oxygen (McCormick et al. 2019). Oxygen limits for phototaxis are the oxygen condition below which phototaxis behavior is reduced (Chapter 5). The P_{crit} is the critical oxygen limit for metabolism, which is the pO_2 at which an animal's oxygen consumption rate changes (Chapter 4). For each metric, oxygen values are presented in both pO_2 and concentration units (O_2; μmol kg^{-1}) at 15 °C and 33.5 salinity; NA* denotes that experiments were conducted, but a value could not be calculated, NA indicates that tests were not run.

Species	V_{90}		V_{50}		V_{10}		Phototaxis		P_{crit}	
	pO_2 (kPa)	O_2 (μmol kg^{-1})	pO_2 (kPa)	O_2 (μmol kg^{-1})	pO_2 (kPa)	O_2 (μmol kg^{-1})	pO_2 (kPa)	O_2 (μmol kg^{-1})	pO_2 (kPa)	O_2 (μmol kg^{-1})
D. opalescens	22.2	262.38	13	153.64	6.9	81.55	< 12.9	152.46	2.47	29.19
O. bimaculatus	11.5	135.9	7.2	85.09	5.9	69.73	< 7.4	87.46	0.48	5.67
M. gracilis	19.4	229.2	10.2	120.55	5.4	63.82	NA	NA	NA	NA
P. planipes	5.7	67.37	6.8	80.37	NA*	NA*	NA	NA	NA	NA

Table 6.2. SeapHOx deLUX deployment information. The SeapHOx deLUX was deployed 11 times between 2015-2018 at 30 m depth in La Jolla, CA at a known *D. opalescens* spawning site. The sensor package measures oxygen (O_2), irradiance (PAR; photosynthetically active radiation), pH, temperature (T), conductivity (S), and pressure (P). Sensors that recorded for part of the deployment are denoted with an asterisk.

Date of deployment	Sensors working	Used in this analysis
6/9/15-8/6/15	O_2, PAR, pH, T, S, P	yes
8/6/15-10/9/15	O_2, PAR*, pH, T, S, P	yes
4/21/16-6/13/16	O_2, PAR, pH*, T, S, P	yes
6/13/16-7/28/16	O_2, PAR, T, S, P	yes
8/1/16-9/28/16	O_2, PAR, T, S, P	yes
10/12/16-10/21/16	PAR	yes
11/3/16-12/19/16	O_2, PAR, pH, T, S, P	yes
12/21/16-4/13/17	PAR*	yes
5/5/17-6/15/17	O_2, pH, T, S, P	no
8/3/17-9/7/17	O_2, pH, T, S, P	no
11/17/17-2/26/18	O_2, pH, T, S, P	no

Figures

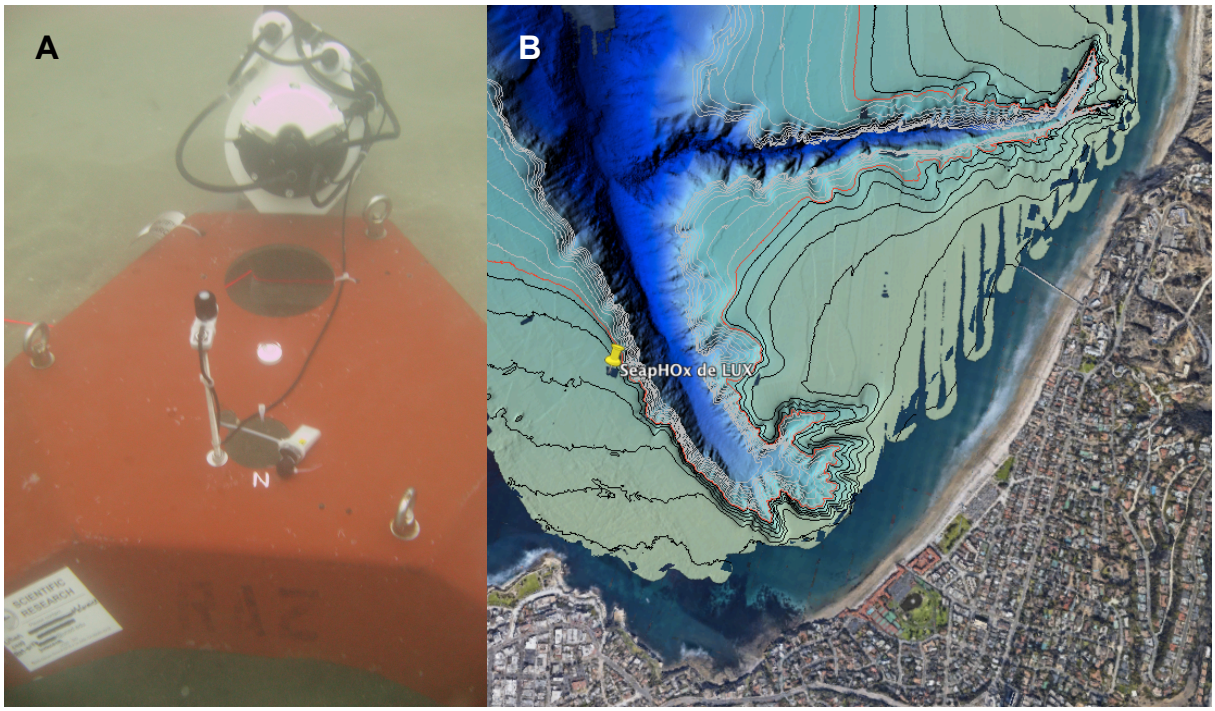

Figure 6.1. The SeapHOx deLUX as a custom sensor package deployed in La Jolla, CA, USA. A) A sensor package capable of recording oxygen, temperature, pH, and salinity was modified to include an irradiance sensor (photosynthetically active radiation; PAR), which was placed away from the sensor body to prevent shading. B) The location of deployment of the SeapHOx deLUX (yellow pin) was at ~30 m depth at the edge of the La Jolla Canyon, with 20 ft depth contours (black lines) and the location of the 130 ft contour in red. Map from Google Earth.

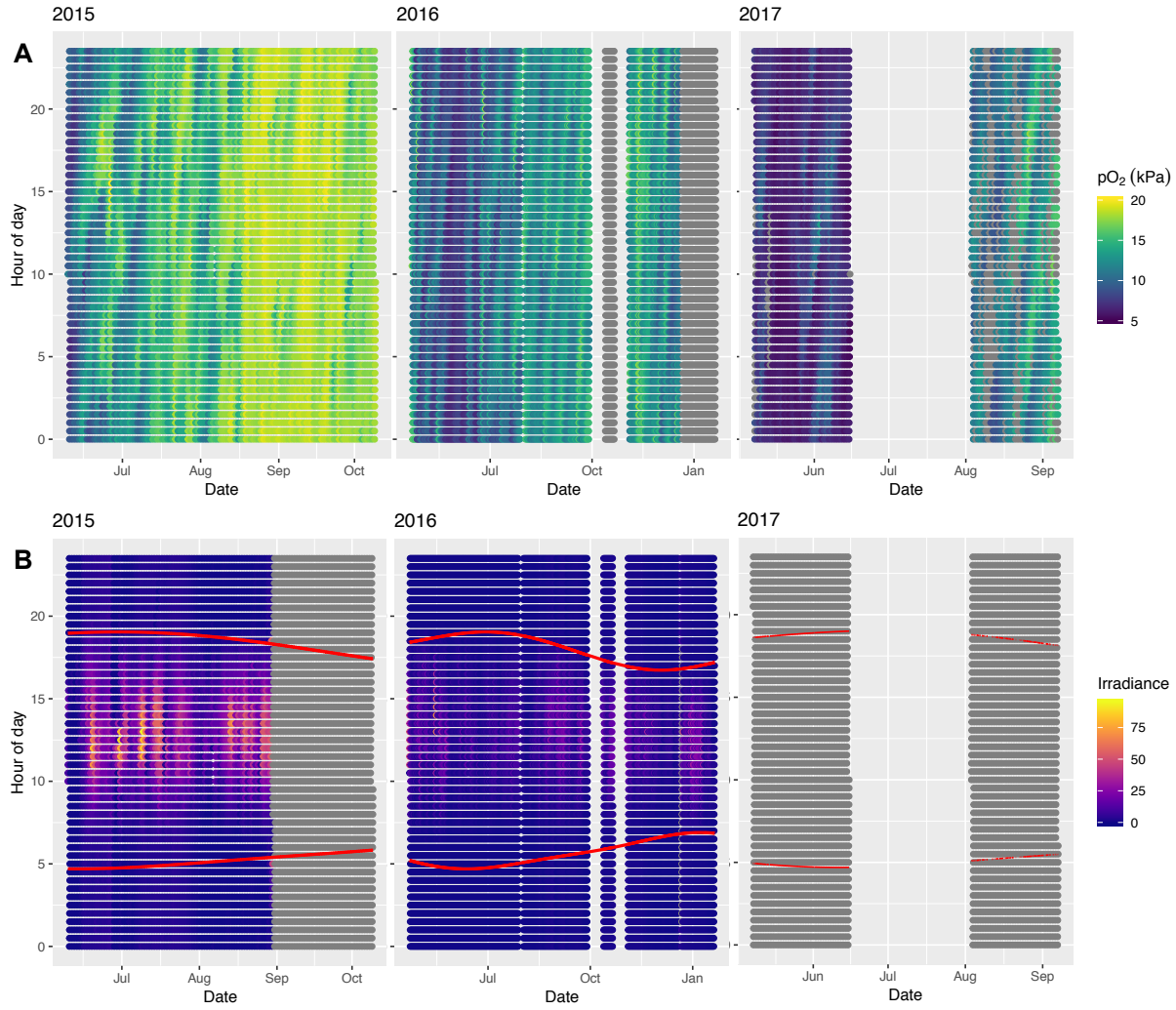

Figure 6.2. Temporal changes in oxygen and irradiance measured with the SeapHOx deLUX from 2015-2017 at 30 m depth in La Jolla. The SeapHOx deLUX was deployed periodically between 2015-2017 (Table 6.2) to measure A) oxygen partial pressure (pO_2) and B) irradiance (µmol photons m^{-2} s^{-1}). The times of sunset and sunrise are shown as red lines, and periods when the instrument was deployed, but the sensor was not working are shown in grey.

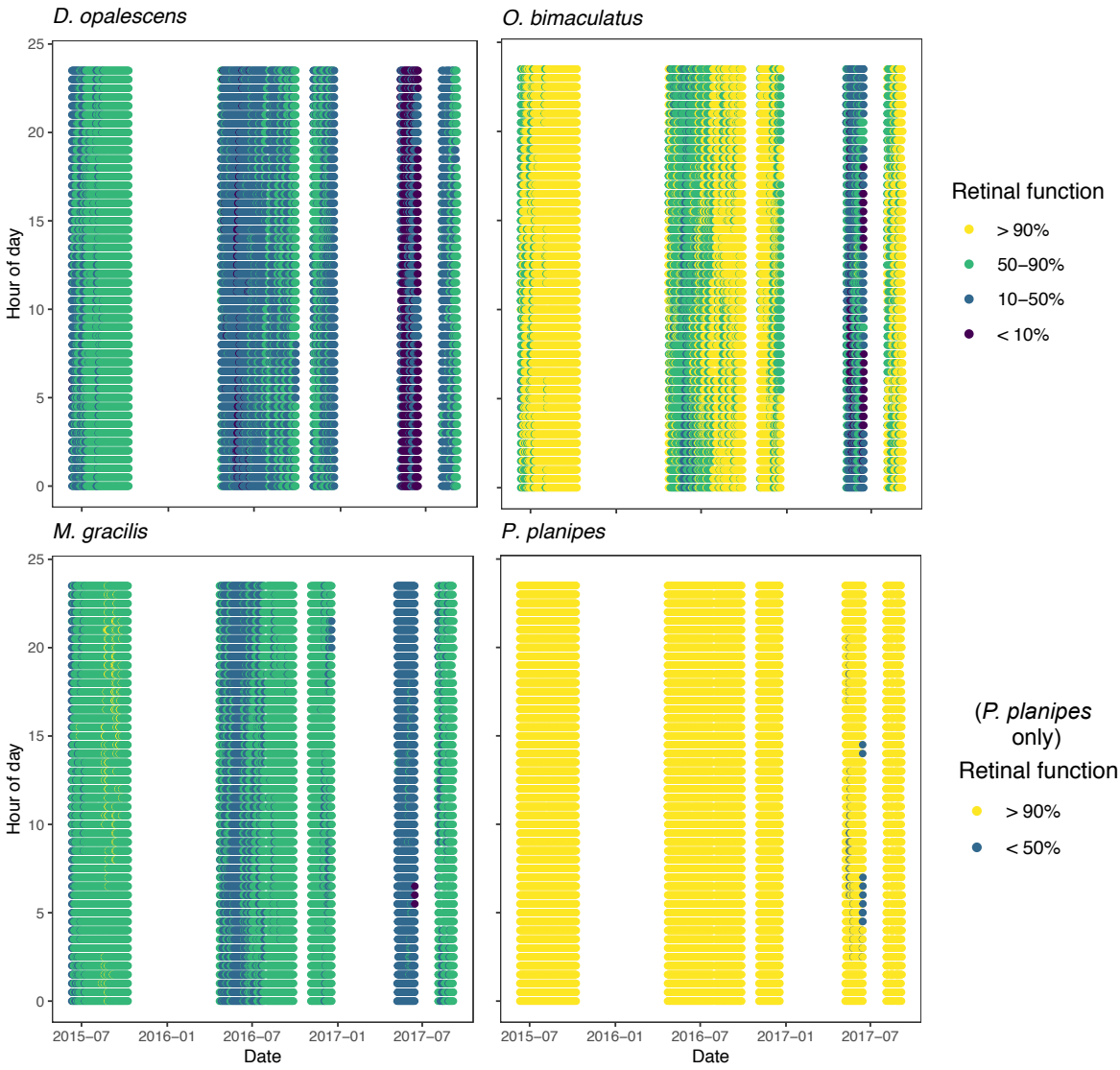

Figure 6.3. Potential changes in the critical luminoxyscape for retinal function over temporal scales. Time periods where oxygen partial pressure (pO_2) was suitable for retinal function >90% (yellow), 50-90% (green), 10-50% (blue), and <10% (purple) in comparison to retinal responses in normoxia at 30 m depth in La Jolla between 2015-2017. Data are shown for paralarvae of *Doryteuthis opalescens, Octopus bimaculatus*, *Metacarcinus gracilis*, and *Pleuroncodes planipes*. See Table 6.1 for oxygen metric details.

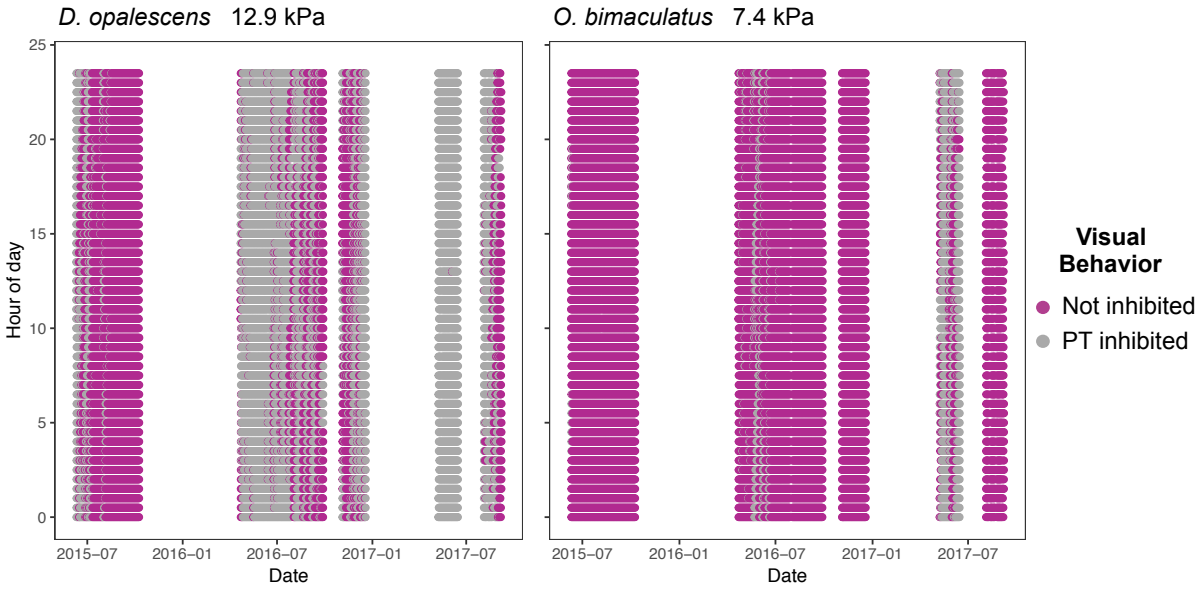

Figure 6.4. Critical luminoxyscape for phototaxis at 30 m depth in La Jolla. Paralarvae of *D. opalescens* (left) and *O. bimaculatus* (right) have different times when the oxygen is potentially sufficient for normal phototaxis (magenta circles) and when phototaxis would potentially be oxygen-limited (gray circles). Oxygen limits for phototaxis from Table 6.1.

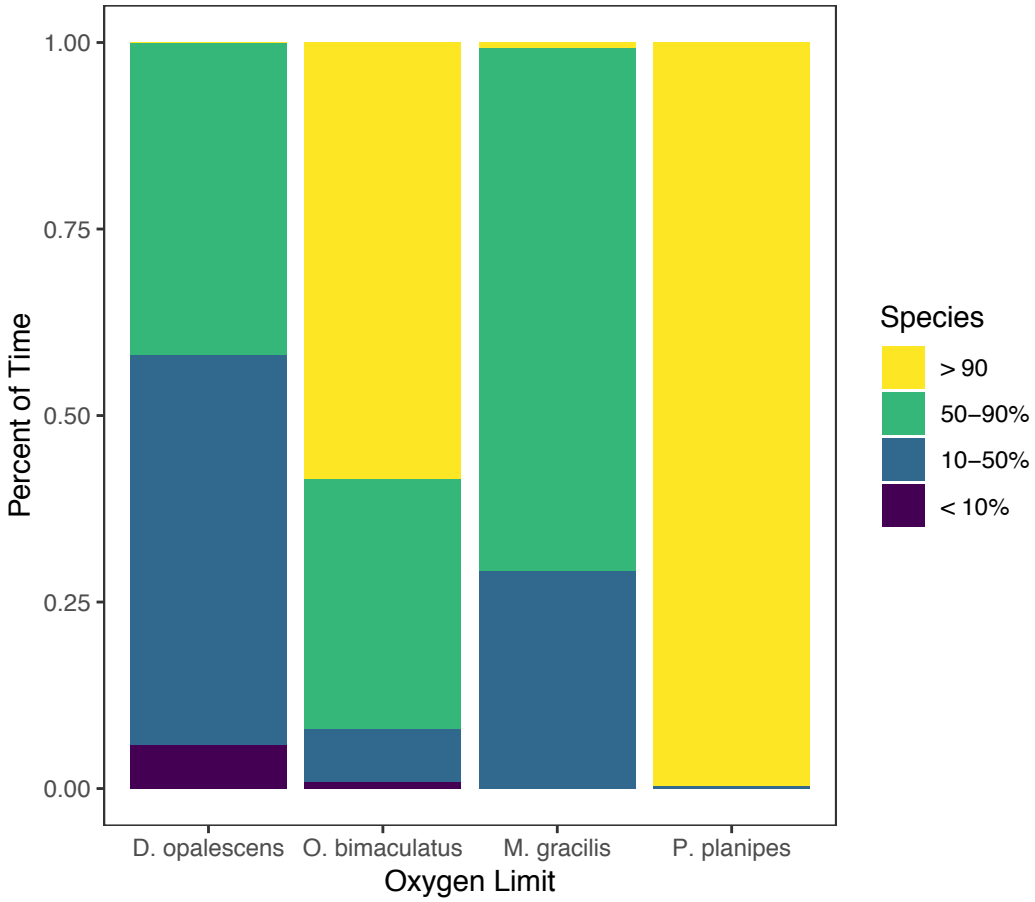

Figure 6.5. Percentage of time oxygen-impaired visual function of different magnitudes could potentially occur at 30 m depth in La Jolla for *D. opalescens*, *O. bimaculatus*, *M. gracilis*, and *P. planipes*. For the duration of the 2015-2017 deployments of the SeapHOx deLUX at 30 m depth in La Jolla, the percentage of time pO_2 was at the oxygen threshold for >90% (V_{90}; yellow), 50-90% (V_{50}-V_{90}; green), 10-50% (V_{10}-V_{50}; blue), and less than 10% retinal function (V_{10}; purple) were calculated (see Table 6.1 for pO_2 limits).

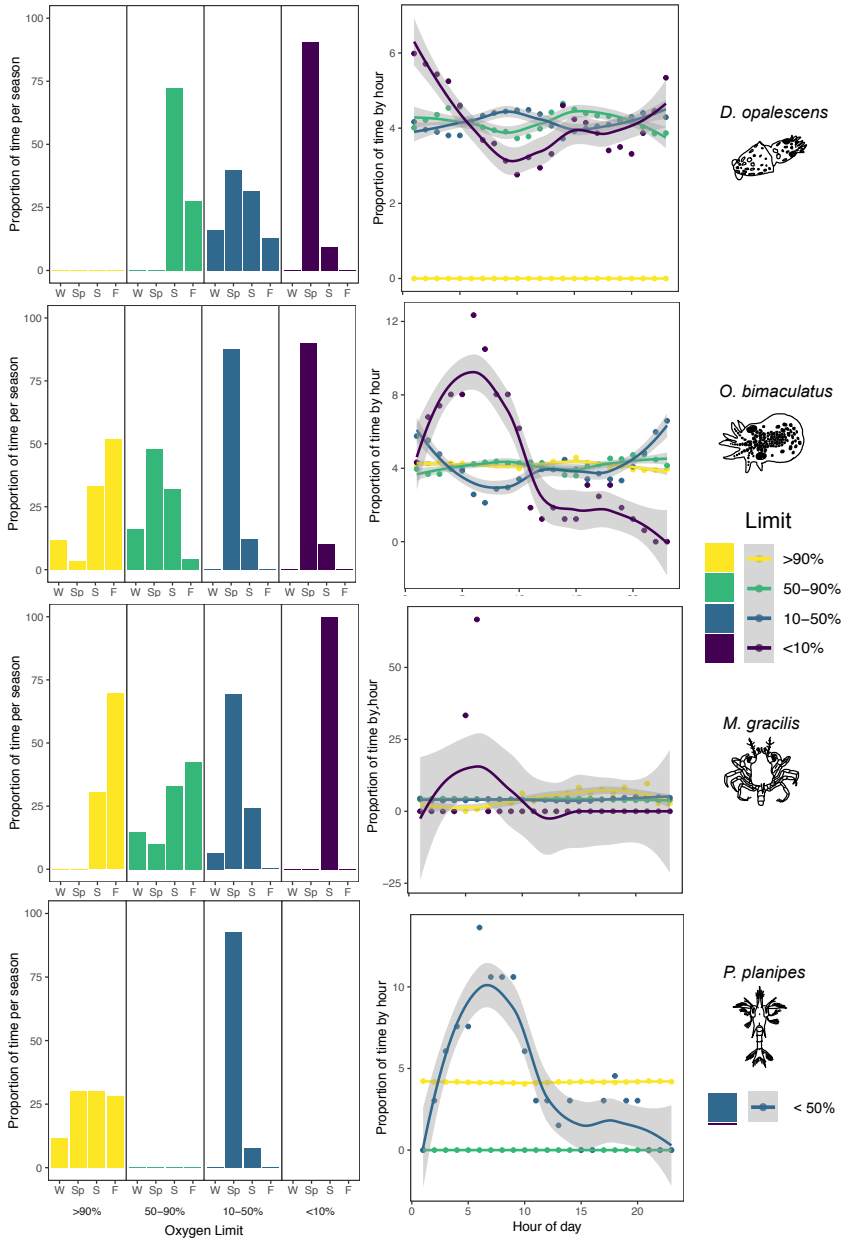

Figure 6.6. The distribution of oxygen conditions with the potential to cause visual impairment to marine invertebrate larvae by season and by hour. The percentage of time when pO_2 could facilitate >90% retinal function (V_{90}; yellow bars, circles, and lines) and that is sufficiently low to cause 50-90% retinal function (V_{50}-V_{90}; green bars, circles, and lines), 10-50% retinal function (V_{10}-V_{50}; blue bars, circles, and lines), and <10% retinal function (V_{10}; purple bars, circles, and lines) are shown within seasons (Winter, Spring, Summer, and Fall; left column) and within the time of day (right column) for larvae of *D. opalescens*, *O. bimaculatus*, *M. gracilis*, and *P. planipes*. Lines are a smoothing function for visibility of the data and gray shading in the time of day plots show the 95% confidence intervals. Blue bars, circles, and lines indicate pO_2 that could cause <50% retinal function in larvae of *P. planipes* (no V_{10} was calculated). All oxygen thresholds are in Table 6.1.

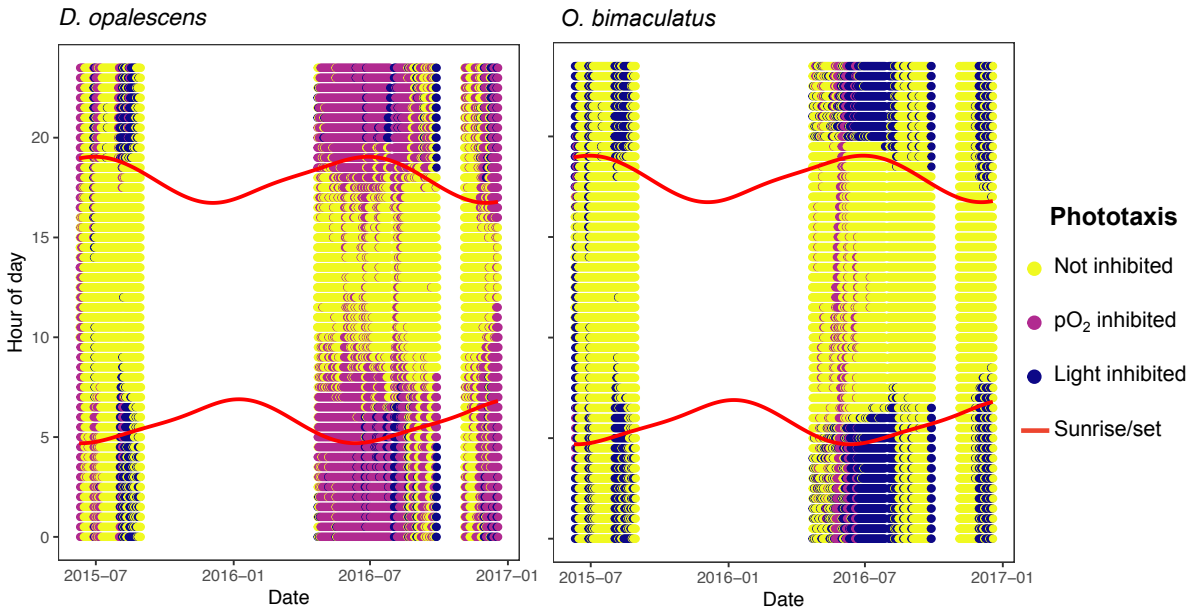

Figure 6.7. The critical luminoxyscape for phototaxis in marine cephalopod paralarvae at 30 m depth in La Jolla between 2015-2017. Using the irradiance and oxygen limits for phototaxis, the times where phototaxis could potentially be oxygen inhibited (navy circles) and light inhibited (magenta circles) are shown in comparison to times when conditions would not inhibit phototaxis (yellow circles) in paralarvae of *D. opalescens* and *O. bimaculatus*. See Table 6.1 for oxygen limits.

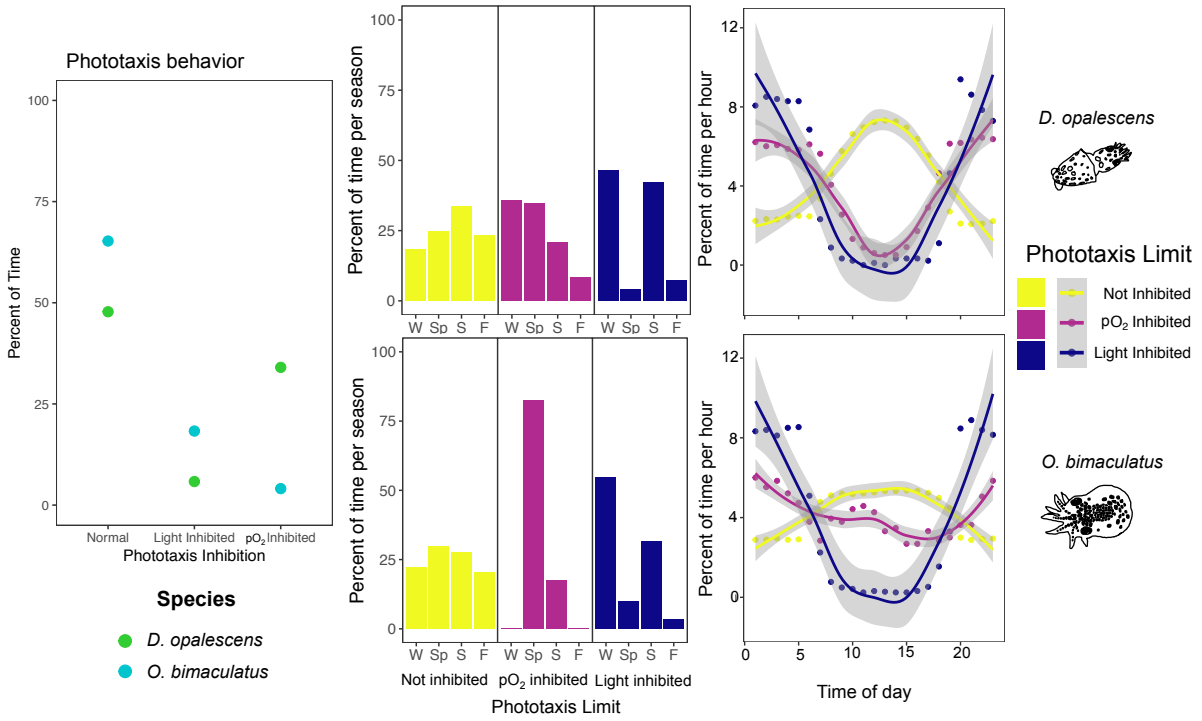

Figure 6.8. The temporal distribution of oxygen-impaired phototaxis for cephalopod paralarvae at 30 m depth in La Jolla, CA during 2015-2017. Left: The percentage of time the oxygen and irradiance were suitable for normal phototaxis (not inhibited), would cause light inhibited phototaxis, or oxygen inhibited phototaxis were calculated for *D. opalescens* (green circles) and *O. bimaculatus* (teal circles). Right: The distribution of oxygen conditions causing no impairment to phototaxis (yellow bars, circles, and lines), oxygen-inhibited phototaxis (magenta bars, circles, and lines), and light-inhibited phototaxis (navy bars, circles, and lines) by season Winter, Spring, Summer, and Fall) and by hour. Lines are a smoothing function for visibility of the data and gray shading in the time of day plots shows the 95% confidence intervals.

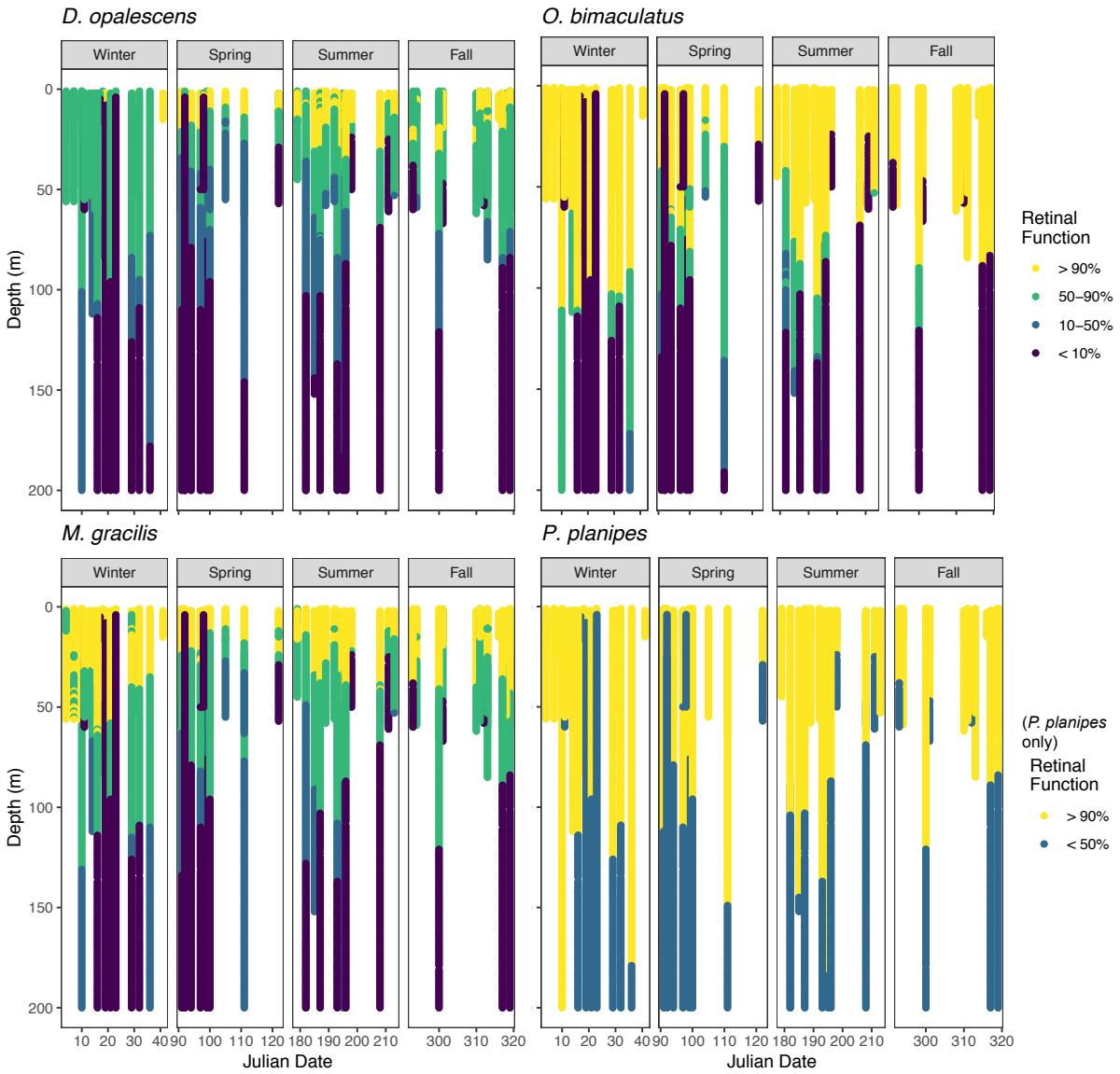

Figure 6.9. Potential vertical changes in luminoxyscapes are shown over time for retinal function in marine invertebrate larvae in the SCB based on CTD cast data averaged across CalCOFI lines 93.3-86.7. The depths with pO_2 that is sufficient for >90% retinal function (V_{90}, yellow), 50-90% (V_{50}-V_{90}; green), 10-50% (V_{10}-V_{50}; blue), and that would impair visual function below 10% (<10%; purple) are given for larvae of *D. opalescens*, *O. bimaculatus*, and *M. gracilis*. Visual function for *P. planipes* larvae were split into depths where there would be 50% or greater retinal function (V50; yellow) and below 50% function (<50%; blue). Data were obtained from nearshore (within 30 km of land), southern California stations (32.8- 33.8 °N) on the CalCOFI long-term ecological monitoring program between 2003-2017. Data are shown for all years, with time as Julian day. Oxygen limits for visual function are from Table 6.1. Casts that do not extend to 200 m depth were from shallower stations; only full casts are shown.

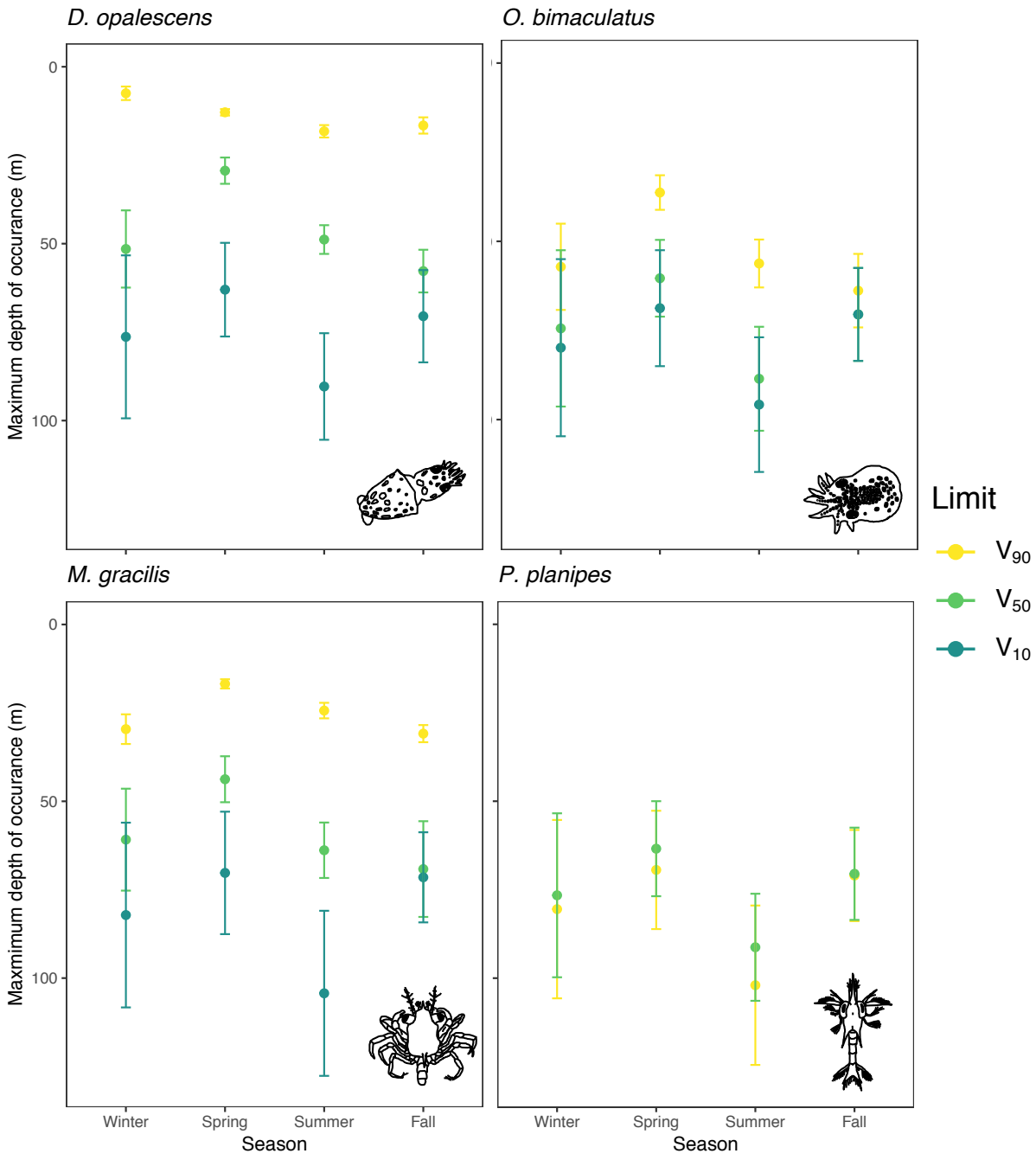

Figure 6.10. Potential seasonal changes in the maximum depth of the critical luminoxyscape calculated for oxygen metrics for vision in marine invertebrate larvae species in the nearshore, southern SCB. The maximum depth (m) at which oxygen limits for vision occurred were calculated by the critical luminoxyscape for 90% (V_{90}, purple), 50% (V_{50}; blue), and 10% (V_{10}, yellow) retinal function for larvae of *D. opalescens*, *O. bimaculatus*, *M. gracilis*, and *P. planipes*. Circles and error bars show means and standard error. Results were calculated from CalCOFI hydrographic data from southern lines (32.8- 33.8 °N) and nearshore stations (within 30 km from shore). Oxygen limits are from Table 6.1.

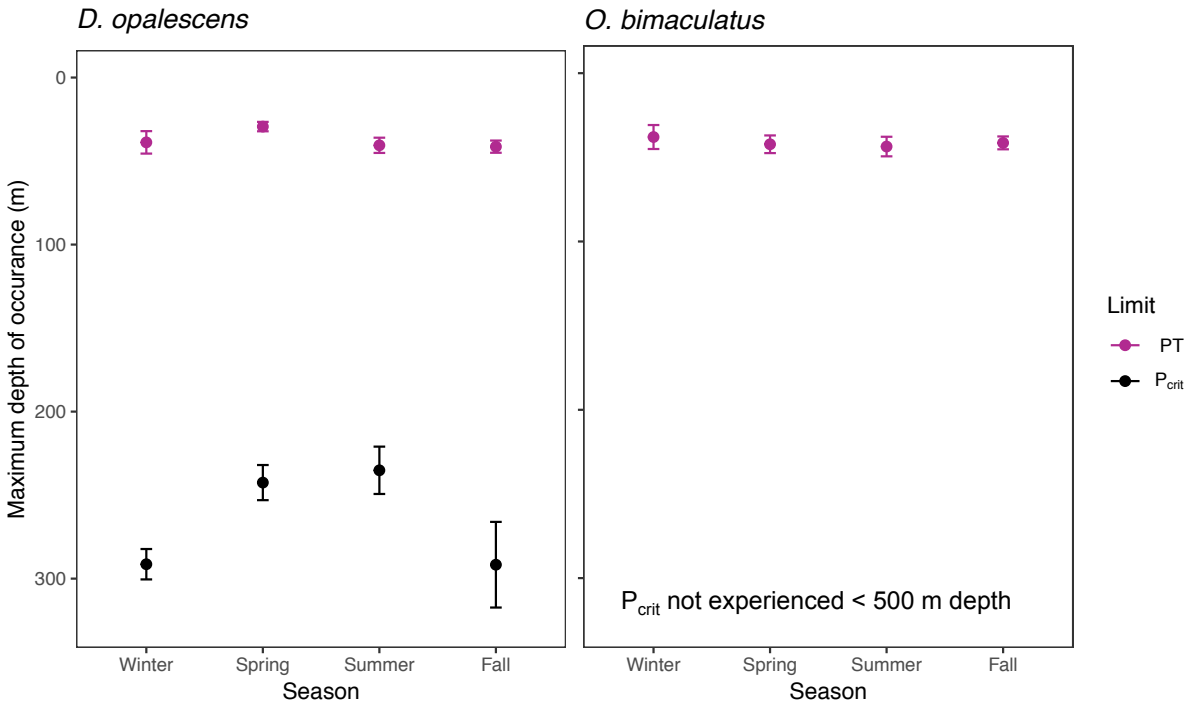

Figure 6.11. Potential seasonal changes in the maximum depth of the critical luminoxyscape calculated for phototaxis and metabolism in marine invertebrate larvae species in the SCB. The maximum depth (m) at which oxygen limits for vision and metabolism occurred were calculated by determining the lower depth of the critical luminoxyscape for uninhibited phototaxis (PT, magenta circles) and where the pO_2 was greater than the P_{crit} (black circles) for larvae of *D. opalescens* and *O. bimaculatus*. Circles and error bars show means and standard error. Results were calculated from CalCOFI hydrographic data from southern lines (32.8- 33.8 °N) and nearshore stations (within 30 km from shore). Oxygen limits for phototaxis and metabolism are in Table 6.1.

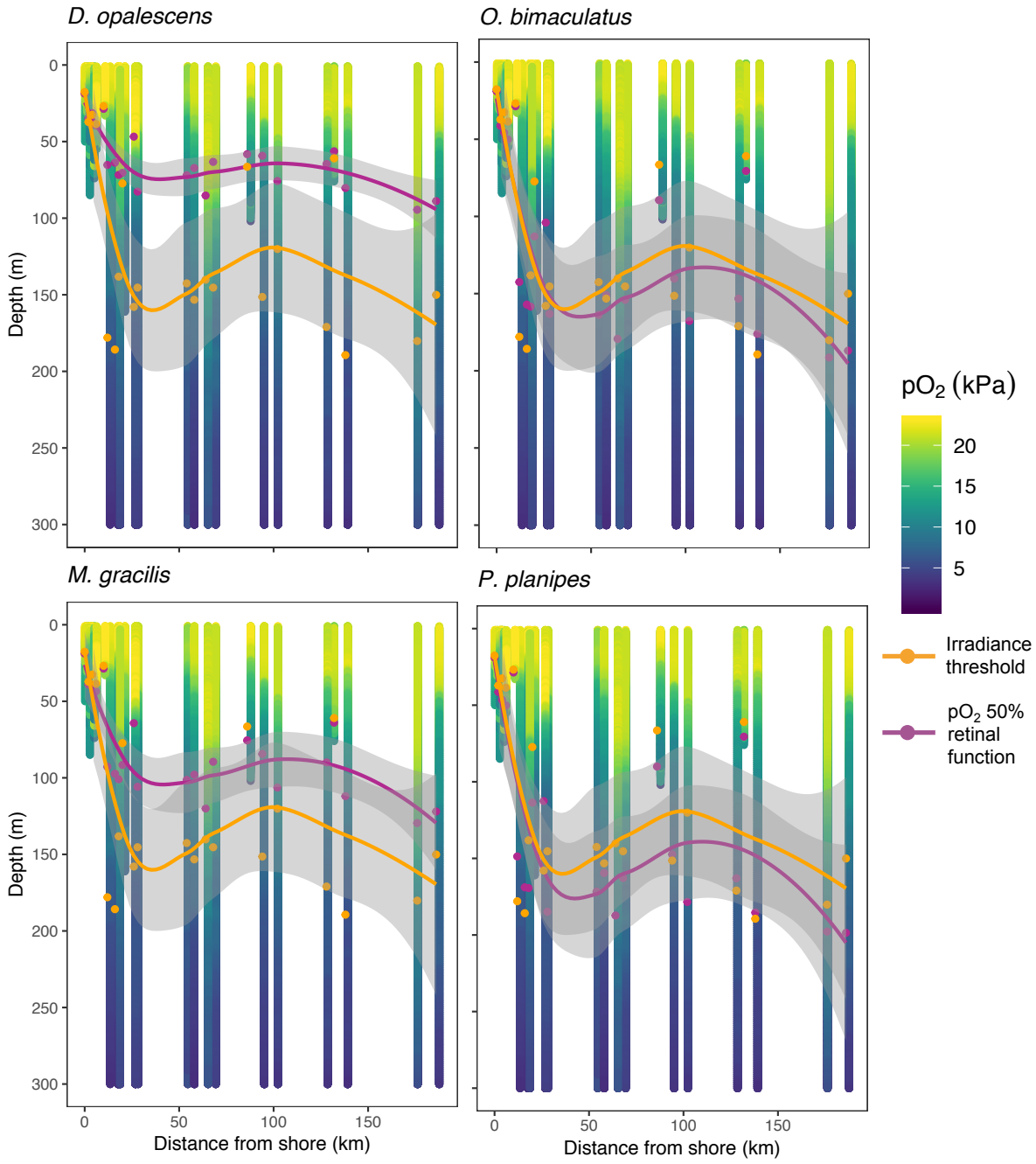

Figure 6.12. Changes in the maximum depth of the critical luminoxyscape for phototaxis with distance from shore in the SCB for marine invertebrate larvae. Using the partial pressure of oxygen (pO_2, kPa; color scale) and irradiance (data not shown), the depths at which the pO_2 (magenta circles and line) and irradiance (orange circles and line) could potentially facilitate at least 50% retinal function are shown as a function of the distance from shore (km). Gray shading indicates the 95% confidence interval of the loess smoothing function (lines). Data from the CalCOFI monitoring program stations between 32.17-34.45 °N and within 190 km from shore are shown.

CHAPTER 7

Conclusions

Lillian R. McCormick

Chapter 7.1 Conclusions of the dissertation

Ocean conditions are changing more rapidly than ever before, with multiple parameters reaching values that can stress marine life. Thus, it is crucial to understand the subtleties of the interactions of different species with a variety of stressors. This dissertation explores the effects of reduced oxygen on vision in several species of marine larvae, beginning with physiological effects to retinal function and metabolism and then testing the manifestation of physiological impairment in visual behavior. Oxygen and irradiance thresholds for visual physiology and behavior were then used to determine when and where marine larvae have the potential to experience visual impairment within their habitat. Three main conclusions emerged from this research: 1) vision in cephalopod and arthropod larvae is very sensitive to oxygen loss, 2) there are species-specific trends of oxygen sensitivity that are consistent across all thresholds tested, and 3) a multi-tiered approach to addressing biological response is advantageous to understanding ocean change scenarios.

The effects of oxygen and light on vision

This research offers substantial evidence that vision in marine invertebrate larvae is impaired by reduced partial pressure of oxygen (pO_2; Fig. 1). The effects of reduced oxygen on various aspects of vision has been tested in fish (Johansson et al. 1997, Robinson et al. 2013), and despite brief consideration (Pinto and Brown 1977), has never been directly measured in marine invertebrates. The effects of reduced oxygen on vision occur at multiple levels of function, beginning with a reduction in retinal responses in all four species tested (McCormick et al. 2019). Retinal responses begin decreasing at very high oxygen levels, starting at 22.2 kPa, 11.5 kPa, 19.4 kPa, and 5.7 kPa for larvae of *D. opalescens*, *O.*

bimaculatus, *M. gracilis*, and *P. planipes*, respectively (McCormick et al. 2019). Oxygen metrics for retinal function in *D. opalescens* and *O. bimaculatus* paralarvae are higher than P_{crit} (2.47 and 0.48 kPa, respectively; Chapter 4). In these experiments, reduced oxygen only significantly affects phototaxis behavior at pO_2 that would cause ~50% retinal function (Chapter 5). This trend is consistent across paralarvae of both *D. opalescens* and *O. bimaculatus*, despite the difference in oxygen sensitivity between species (Chapter 4, 5). Thus cephalopod paralarvae are able to withstand some level of visual deficit before phototaxis behavior is impaired. Phototaxis is a complicated behavior that involves more than just vision, and these results suggest that there is a neurological response threshold, either in the eye, optic lobe, or brain, where the reaction to the stimulus must exceed a specific threshold response prior to the signal manifesting as a mechanical reaction.

Most descriptions of habitat compression (Gilly et al. 2013) or the ecological interactions and changes in distribution in the marine water column (Ekau et al. 2010, Bertrand et al. 2011, Netburn and Koslow 2015) attributed to oxygen limitation in marine organisms discuss metabolic thresholds as the key constraint. However, based on results of this dissertation, paralarvae of *D. opalescens* and *O. bimaculatus* could potentially experience a complete loss of retinal function at the pO_2 corresponding to their P_{crit} (2.47 kPa and 0.48 kPa, respectively; Chapter 4). Accordingly, long-term records of oxygen and light on the southern California shelf reveal that oxygen levels in the marine environment could cause visual impairment within the upper 50-m of water; the P_{crit} of *O. bimaculatus* paralarvae was never measured within 500 m depth in the SCB between 1999-2017, and paralarvae of *D. opalescens* would have only potentially been exposed to pO_2 at the level of their P_{crit} at ~300 m depth, which is far greater than the reported depth range of the paralarvae (Chapter 6;

Zeidberg and Hamner 2002). Additionally, pO_2 at or below the P_{crit} for both cephalopods was never recorded with the SeapHOx deLUX at 30-m depth in La Jolla for the duration of the deployment (2015-2017; Chapter 6). These results suggest that larvae of the study species could potentially experience oxygen-impaired vision as a sub-lethal and sub-metabolic effect, and that this should be considered as an additional explanation for changing distributions in highly visual marine organisms (Koslow et al. 2011).

Species-specific oxygen sensitivity

This dissertation reveals very obvious differences in oxygen sensitivity among species. Larvae of *D. opalescens* and *M. gracilis* are the most sensitive and show retinal impairment at pO_2 just under that of surface-saturated seawater (McCormick et al. 2019). In contrast, larvae of *O. bimaculatus* only show changes in retinal function at moderate pO_2. Larvae of *P. planipes* were the least sensitive and only show small reductions in retinal function at oxygen levels where the three other species already had <10% retinal function remaining (McCormick et al. 2019). This exposes the differential vulnerabilities of species to changing ocean conditions, which may have interesting implications for species interactions. Adult *P. planipes* are normally found at the northern end of their range (SCB) during El Niño years (Boyd 1960, Longhurst 1968, Gomez-Gutierrez and Sanchez-Ortiz 1997) and this species has shown a recent increase in abundance in the SCB (McClatchie et al. 2016). Adult *P. planipes* occur in the same location as developing *D. opalescens*, and are voracious predators on their egg capsules and embryos (Fig. 2). The larvae of *P. planipes* are highly tolerant of low oxygen, with a critical luminoxyscape potentially extending well beyond the 60 m depth range, in contrast to paralarvae of *D. opalescens*, which were very sensitive to reduced pO_2

and show a critical luminoxyscape shallower than their 30-m habitat range (Chapter 6). It is unclear how larvae of the two species interact, but the recent expansion of *P. planipes* may have severe consequences for *D. opalescens* populations in the SCB.

A very interesting result is that general species trends in oxygen sensitivity span across all of the thresholds studied. Paralarvae of *D. opalescens* show oxygen thresholds for retinal function (McCormick et al. 2019), metabolism (Chapter 4), and phototaxis (Chapter 5) that were always at higher pO_2 than the respective thresholds for retinal function (McCormick et al. 2019), metabolism (Chapter 4), and phototaxis (Chapter 5) in paralarvae of *O. bimaculatus*. As a result, if one oxygen threshold was measured (e.g., phototaxis) informed hypotheses could be made about relative pO_2 levels for another threshold (e.g., metabolism). Oxygen tolerance in marine organisms is traditionally measured by calculating the P_{crit} (Seibel 2011), but using oxygen limits for vision may be a more conservative, and more practical estimate for oxygen tolerance in marine species. A functional approach may be a more realistic view of when conditions become sub-optimal and cause the animals to deviate from normal behavior, rather than almost lethal exposures of pO_2.

Conducting science on multiple levels

A multi-tiered approach to understanding biological response to ocean stressors allows a stable foundation of knowledge to be built, which is more robust and may be more easily conveyed to management than studies examining only one facet. Marine organisms are affected by stressors at a physiological level, and laboratory studies are crucial to determine the hard thresholds for tolerance. It is also important to measure the changes in behavior resulting from physiological impairment, and to determine whether the conditions at which

experiments are conducted are actually relevant for the given species (Seibel 2011, Reum et al. 2015). Multi-faceted laboratory studies can then be used to make predictions about changes in distribution, trophic interactions, etc., that may occur under exposure to marine stressors. These predictions come with their own set of caveats, though, as they rely on the assumption that physiological thresholds and behaviors determined in the laboratory using a very specific set of conditions and stimuli are the same in the wild. However, fine-scale distributions and behaviors in the field are difficult to measure in animals as small and hard to identify as invertebrate larvae. While a small tag has been developed for use in soft-bodied marine invertebrates (Mooney et al. 2015), it is not yet possible to readily track individual marine larvae. Therefore, testing hypotheses on multiple levels (e.g., behavior, physiology, ecology) should be a strategy adopted by scientists examining global change. For example, the critical thresholds for metabolism and temperature can be combined with environmental data and used to calculate the metabolic index, which defines areas of the ocean where marine organisms would have suitable conditions for metabolic function (Deutsch et al. 2015). The critical luminoxyscape was developed for this purpose, in order to describe the available habitat suitable for visual function. For example, the laboratory results of retinal function and phototaxis in paralarvae of *D. opalescens* and *O. bimaculatus* show similar irradiance thresholds and very different oxygen thresholds (McCormick et al. 2019; Chapter 5). When combined with environmental data, it is clear that while paralarvae of *D. opalescens* would largely have the potential to be oxygen-limited in their habitat, paralarvae of *O. bimaculatus* would be most likely be light-limited (Chapter 6); these results are very important in comparing the potential survival of each species, but would not have been apparent from the laboratory results only. It is often a challenge to adapt scientific research into policy, and

perhaps mechanisms that relate thresholds to actual distributions in the field would be more useful to policy-makers. With that in mind, one challenge of this type of research is the ability to translate laboratory studies (e.g., 1-second light stimuli) to environmental conditions (e.g., a diffuse, more even light field) realistically. Future work on this topic can improve methods of laboratory experiments so that it correctly mimics the conditions and visual signals experienced in the natural habitat, such as by testing contrast, feeding behavior, or reactions to gradual light stimuli.

Additional steps for this research would be to determine the effects chronic exposures to reduced pO_2 in developing embryos or larvae of these species. Acute exposures of reduced pO_2 in the environment are a realistic scenario (e.g., over a diurnal scale), but oxygen fluctuations also happen over 1-2 week and month to seasonal time scales (Send and Nam 2012, Nam et al. 2015). Larvae are able to recover retinal function after ~30 minute-exposures to reduced pO_2 (McCormick et al. 2019), and it would be valuable to determine whether this would be true for longer duration exposures. It was necessary to isolate oxygen as a variable to determine its effects on light sensitivity in marine larvae, but this is an unrealistic scenario; in the environment, oxygen always co-varies with temperature and pH (Alin et al. 2012, Frieder et al. 2012, Baumann and Smith 2018). The predicted critical luminoxyscapes could be greatly improved if the temperature and pH sensitivity of the oxygen and light thresholds were evaluated. Despite the challenges of determining fine-scale vertical distributions of larvae in the marine environment, new technology, such as the *Zooglider* (Ohman et al. 2019) may supplement more traditional net methods to show actual distributions of larvae in relation to environmental variation.

In conclusion, this thesis research documented for the first time that marine invertebrate larvae experience severe physiological and behavioral impairment from reduced oxygen, and that this has the potential to significantly constrain the habitat suitable for vision under recent and current ocean conditions. Species displayed very specific oxygen tolerances that were manifested in physiological, metabolic, and behavioral thresholds; these thresholds reveal species-specific vulnerabilities to low oxygen. Testing hypotheses with a multi-tiered approach may be advantageous in determining the ecological effects of multiple stressors and may facilitate translation into management in a future of ocean change.

Literature Cited

Alin, S. R., R. A. Feely, A. G. Dickson, J. M. Hernández-ayón, L. W. Juranek, M. D. Ohman, and R. Goericke. 2012. Robust empirical relationships for estimating the carbonate system in the southern California Current System and application to CalCOFI hydrographic cruise data (2005 – 2011). Journal of Geophysical Research 117.

Baumann, H., and E. M. Smith. 2018. Quantifying metabolically driven pH and oxygen fluctuations in US nearshore habitats at diel to interannual time scales. Estuaries and Coasts 41:1102–1117.

Bertrand, A., A. Chaigneau, S. Peraltilla, J. Ledesma, M. Graco, F. Monetti, and F. P. Chavez. 2011. Oxygen: A fundamental property regulating pelagic ecosystem structure in the coastal southeastern tropical pacific. PLoS ONE 6:2–9.

Boyd, C. M. 1960. The larval stages of *Pleuroncodes planipes* Stimson (Crustacea, Decapoda, Galatheidae). Biological Bulletin 118:17–30.

Deutsch, C., A. Ferrel, B. Seibel, H.-O. Pörtner, and R. B. Huey. 2015. Climate change tightens a metabolic constraint on marine habitats. Science 348:1132–1136.

Ekau, W., H. Auel, H. O. P̈ortner, and D. Gilbert. 2010. Impacts of hypoxia on the structure and processes in pelagic communities (zooplankton, macro-invertebrates and fish). Biogeosciences 7:1669–1699.

Frieder, C. A., S. Nam, T. R. Martz, and L. A. Levin. 2012. High temporal and spatial variability of dissolved oxygen and pH in a nearshore California kelp forest. Biogeosciences 9:1–14.

Gilly, W. F., J. M. Beman, S. Y. Litvin, and B. H. Robison. 2013. Oceanographic and biological effects of shoaling of the oxygen minimum zone. Annual Review of Marine Science 5:393–420.

Gomez-Gutierrez, J., and C. A. Sanchez-Ortiz. 1997. Larval drift and population structure of the pelagic phase of *Pleuroncodes planipes* (Stimson) (Crustacea: Galatheidae) off the southwest coast of Baja California, Mexico. Bulletin of Marine Science 61:305–325.

Johansson, D., G. E. Nilsson, and K. B. Døving. 1997. Anoxic depression of light-evoked potentials in retina and optic tectum of crucian carp. Neuroscience letters 237:73–6.

Koslow, J. A., R. Goericke, A. Lara-Lopez, and W. Watson. 2011. Impact of declining intermediate-water oxygen on deepwater fishes in the California Current. Marine Ecology Progress Series 436:207–218.

Longhurst, A. R. 1968. Distribution of the larvae of *Pleuroncodes planipes* in the California Current. Limnology and Oceanography 13:143–155.

McCormick, L. R., L. A. Levin, and N. W. Oesch. 2019. Vision is highly sensitive to oxygen availability in marine invertebrate larvae. Journal of Experimental Biology 222:1–11.

Mooney, T. A., K. Katija, K. A. Shorter, T. Hurst, J. Fontes, and P. Afonso. 2015. ITAG: An eco-sensor for fine-scale behavioral measurements of soft-bodied marine invertebrates. Animal Biotelemetry 3:1–14.

Nam, S., Y. Takeshita, C. A. Frieder, T. Martz, and J. Ballard. 2015. Seasonal advection of Pacific Equatorial Water alters oxygen and pH in the Southern California Bight. Journal of Geophysical Research: Oceans 120:2331–2349.

Netburn, A. N., and J. A. Koslow. 2015. Dissolved oxygen as a constraint on daytime deep scattering layer depth in the southern California current ecosystem. Deep Sea Research Part I: Oceanographic Research Papers 104:149–158.

Ohman, M. D., R. E. Davis, J. T. Sherman, K. R. Grindley, B. M. Whitmore, C. F. Nickels, and J. S. Ellen. 2019. Zooglider: An autonomous vehicle for optical and acoustic sensing of zooplankton. Limnology and Oceanography: Methods 17:69–86.

Pinto, L. H., and J. E. Brown. 1977. Intracellular recordings from photoreceptors of the squid (*Loligo pealii*). Journal of Comparative Physiology A 122:241–250.

Reum, J. C. P., S. R. Alin, C. J. Harvey, N. Bednarsek, W. Evans, R. A. Feely, B. Hales, N. Lucey, J. T. Mathis, P. McElhany, J. Newton, and C. L. Sabine. 2015. Interpretation and design of ocean acidification experiments in upwelling systems in the context of

carbonate chemistry co-variation with temperature and oxygen. ICES Journal of Marine Science 73:582–595.

Robinson, E., A. Jerrett, S. Black, and W. Davison. 2013. Hypoxia impairs visual acuity in snapper (*Pagurus auratus*). Journal of comparative physiology. A, Neuroethology, sensory, neural, and behavioral physiology 199:611–7.

Seibel, B. A. 2011. Critical oxygen levels and metabolic suppression in oceanic oxygen minimum zones. The Journal of experimental biology 214:326–336.

Send, U., and S. Nam. 2012. Relaxation from upwelling: The effect on dissolved oxygen on the continental shelf. Journal of Geophysical Research: Oceans 117:1–9.

Zeidberg, L. D., and W. M. Hamner. 2002. Distribution of squid paralarvae, *Loligo opalescens* (Cephalopoda: Myopsida), in the Southern California Bight in the three years following the 1997-1998 El Niño. Marine Biology 141:111–122.

Figures

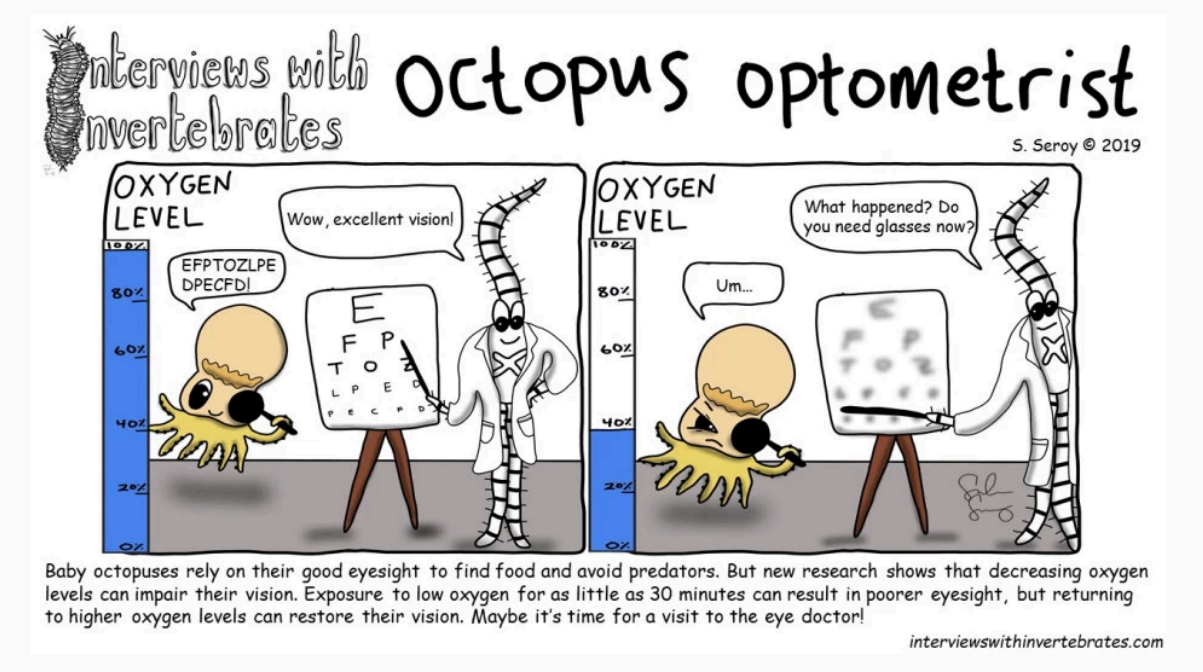

Figure 7.1. A comic synopsis of McCormick et al. (2019) from "Interviews with Invertebrates", created by Sasha Seroy, showing that octopus paralarvae experience impaired vision under exposure to reduced oxygen.

Figure 7.2. Adult *P. planipes* feeding voraciously on *D. opalescens* egg capsules and embryos. Image from 30 m depth in La Jolla, CA at the site the SeapHOx deLUX was deployed (L. McCormick).